TECHNISCHE UNIVERSITÄT MÜNCHEN

Lehrstuhl für Bodenökologie

Enhancement of Degradation of DDT and HCB in Tropical Clay Soils in Model Experiments

Fredrick Orori Kengara

Vollständiger Abdruck der von der Fakultät Wissenschaftszentrum Weihenstephan für Ernährung, Landnutzung und Umwelt der Technischen Universität München zur Erlangung des akademischen Grades eines

Doktors der Naturwissenschaften

genehmigten Dissertation.

Vorsitzender:	Univ.-Prof. Dr. W. Huber
Prüfer der Dissertation:	1. Univ.-Prof. Dr. J. C. Munch
	2. Univ.-Prof. Dr. Dr. K.-W. Schramm

Die Dissertation wurde am 29.03.2010 bei der Technischen Universität München eingereicht und durch die Fakultät Wissenschaftszentrum Weihenstephan für Ernährung, Landnutzung und Umwelt am 28.06.2010 angenommen.

To the persevering mortal, the blessed Immortals are swift (Zoroaster);
Heaven, Water, Earth: the evanescent Truth,
the alpha and the omega.

Abstract

Persistent organic pollutants (POPs) have been banned or restricted in most countries. However, some POPs continue to be released into the environment as industrial by-products e.g. HCB, or through use in vector control especially in the tropics e.g. DDT. POPs have been extensively studied in temperate soils, but information on behaviour in tropical soils is limited. HCB - a highly-chlorinated POP, and DDT – a low-chlorinated POP, were selected as model compounds for the study with two tropical soils in model laboratory experiments.
The aims of the study were
- to investigate the ability of the two agricultural tropical clay soils (a paddy soil and a field soil) to mineralize HCB and DDT under aerobic conditions, and the possibility to enhance the degradation and mineralization of HCB and DDT;
- to understand the processes and soil properties influencing the anaerobic degradation of DDT in the two tropical clay soils; and
- to check the ability of a soil extracted 1,2,4-TCB mineralizing community to degrade a cocktail of organochlorine pesticides (OCPs).
Anaerobic-aerobic cycles were used to enhance degradation. Anaerobic conditions were induced by water-logging the soils in the laboratory, while subsequent aerobic conditions were induced by drying the soils through aeration. Compost was used as a supplementary carbon source. HCB and DDT used for the aerobic and anaerobic-aerobic cycles incubation experiments were ^{14}C ring-labelled.
In the course of the incubation experiments $^{14}CO2$, ^{14}C-volatilization, ^{14}C-extractable residues and ^{14}C-non-extractable residues were monitored. The quality of extractable residues, and changes in concentration of OCPs in the cocktail, were determined and quantified by gas chromatography (GC) and high resolution gas chromatography-high resolution mass spectrometry (HRGC-HRMS) analysis respectively. The following soil properties were analyzed for process parameterization: the cations and anions in the soil solution, reducible Fe, dissolved organic carbon (DOC) in the soil solution, and the quality of DOC by fluorescence analysis.
The results with HCB assays showed that there was hardly any mineralization or degradation of HCB under aerobic conditions, but up to about 4 % of the initially applied DDT was mineralized to CO_2 after 84 days in both soils under aerobic conditions. Compost addition resulted in increased mineralization of aged DDT residues, but had no effect on the mineralization rate of the soils.

The anaerobic-aerobic cycles were successful in inducing and enhancing the degradation and mineralization of HCB in both soils. There was higher mineralization and degradation of HCB in the paddy soil relative to the field soil. However, the increased HCB degradation resulted in increased volatilization due to formation of lower-chlorinated metabolites. . Compost addition resulted in increased degradation and mineralization of HCB in both soils. The results with DDT assays showed that the anaerobic-aerobic cycles were successful in enhancing degradation and mineralization in both soils. There was greater metabolite formation in the paddy soil, but higher DDT dissipation and mineralization in the field soil. Compost addition resulted in increased mineralization of DDT to $^{14}CO_2$ in both soils, but did not cause significant differences on the dissipation rate of DDT.

In the course of the anaerobic degradation of DDT, changes occurred in the soil parameters, namely: salinity, sodicity, reducible Fe, DOC quality, CO_2, N_2O, CH_4, and redox potential. These parameters correlated well with p,p-DDT dissipation and/or p,p-DDD formation. These parameters were also affected by compost amendment. Concerning DOC quality, five fluorophores were identified in the soils and compost and the build up of fluorophore 4 was associated with greater microbial degradation of organic matter. Compost amendment resulted in increased clay dispersion in the field soil but decreased clay dispersion in the paddy soil. Compost addition also resulted in increased CO_2 production but had no significant effect on DDT degradation rate under anaerobic conditions.

The microbial consortium could not degrade most of the compounds in the OCPs cocktail such as the DDTs, Chlordanes and Heptachlors. However, there were indications that the community could be able to degrade mono-aromatic OCPs like pentachloroanisole, pentachlorobenzene and octachlorostyrene.

The results showed that steering ecological conditions is a feasible strategy that can be used to enhance the breakdown of POPs in the two investigated tropical clay soils, and that changes in soil properties affect the fate of pollutants in these upper soils.

Table of content

Acknowledgements

I would like to acknowledge the following:

1. The German Academic Exchange Service (DAAD) for sponsoring my stay in Germany.

2. Prof. Dr J.C. Munch, Director - Institute of Soil Ecology, Helmholtzzentrum München - National Center for Environmental Health, for hosting me in the institute, facilitating my research and guiding me through my work as the main supervisor.

3. Dr Reiner Schroll - in whose working group at the institute of soil ecology I belonged during my doctoral studies - for support in the research and correction of the thesis. I would like to thank other members of the group, namely: Dr Ulrike Doerfler for assistance in the research and correction of the thesis; Dr Roland Fuß for assistance in dissolved organic carbon analysis and providing fluorophore spectra for some standards; Mr Franz Buegger for assistance in elemental C:N analysis; Mr. Rolf Schilling for assistance in CH_4, CO_2 and N_2O analysis; and to all other members of the group who facilitated my work in one way or another.

4. Dr Benhard Ruth of the Institute of Soil Ecology for assistance in the construction of the redox sensor electrodes.

3. Prof Dr Dr Schramm of the Institute of Ecological chemistry for facilitating some of my experiments, reading and evaluating my progress reports for the DAAD. I also wish to thank Mr Henkelmann for assisting in MS analysis and identification of peaks.

4. Mr. Michael Stöckl of the Institute of Ground water Ecology for his assistance in the analysis of ions.

5. Dr Julian Bosch of Institute of Ground water Ecology for assistance in ferrozine analysis and for facilitating my use of the anaerobic nitrogen tent.

6. Dr Welzl Gerhard for his assistance in statistical analysis.

7. Maseno University for granting me study leave.

Acronyms and abbreviations

AEA	Alternative electron acceptor
ANOVA	Analysis of variance
AQDS	Anthraquinone-2,6-disulfonate
ASE	Accelerated solvent extractor
BTEX	Benzene, toluene, ethylbenzene and xylene
C_{dt}	Canonical coefficients
CE	Compost effect
CFU	Colony forming units
CIS	Cold injection system
DCB	Dichlorobenzene
DDA	bis(4'-Chlorophenyl)acetate
DDOH	2,2-bis(4'-Chlorophenyl)ethanol
DDM	bis(4'-Chlorophenyl)methane
DDNU	unsym-bis(4'-Chlorophenyl)ethylene
DDTr	DDT and its metabolites
DOC	Dissolved organic carbon
DOM	Dissolved organic matter
ECD	Electron capture detector
EEM	Excitation emission matrices
EMME	Ethylenemonomethylether
EPA	Environmental Protection Agency
ESP	Exchangeable sodium percentage
F1	Fluorophore 1/Factor 1
F2	Fluorophore 2/Factor 2
F3	Fluorophore 3/Factor 3
F4	Fluorophore 4/Factor 4
F5	Fluorophore 5/Factor 5
FID	Flame Ionization Detector
FS	Field soil
FSC	Field soil + compost
GC	Gas chromatography
GC-FID	Gas chromatography – Flame ionization detector
GC-MS	Gas chromatography-Mass spectroscopy

HCB	Hexachlorobenzene
HCH	Hexachlorocyclohexane
HRGC-HRMS	High resolution gas chromatography-high resolution mass spectrometry
IAEA	International Atomic Energy Agency
K_H	Henry's constant
Kow	Octanol-water partition coefficient
K_p	Sorption coefficient
LME	Linear mixed effects
MW	Molecular weight
NERs	Non-extractable residues
OCP(s)	Organochlorine pesticide(s)
OCS	Octachlorostyrene
OWC	Optimum water content
o,p-DDE	1-chloro-4-[2,2-dichloro-1-(4-chlorophenyl)ethenyl]benzene
o,p-DDD	1-chloro-4-[2,2-dichloro-1-(2-chlorophenyl)ethyl]benzene
o,p-DDT	1-chloro-2-[2,2,2-trichloro-1-(4-chlorophenyl)ethyl]benzene
PCA	Pentachloroanisole
PAH	Polycyclic Aromatic Hydrocarbons
PARAFAC	Parallel Factor Analysis
PCB	Pentachlorobenzene
POP(s)	Persistent Organic Pollutant(s)
p,p-DDD	1-chloro-4-[2,2-dichloro-1-(4-chlorophenyl)ethyl]benzene
p,p-DDE	1-chloro-4-[2,2-dichloro-1-(4-chlorophenyl)ethenyl]benzene
p,p-DDMU	1-chloro-4-[2-chloro-1-(4-chlorophenyl)ethenyl]benzene
p,p-DDM	1,1'-methylene bis(4-chlorobenzene)
p,p-DDT	1,1,1-trichloro-2,2-di(4-chlorophenyl)ethane
PRC	Principle response curve
PS	Paddy soil
PSC	Paddy soil + compost
PTV	Programmable Temperature Vapourizing
SAR	Sodium absorption ratio
SIM	Signal ion monitoring
SPE	Solid phase extraction
TCB	Trichlorobenzene

TCC	Total cation capacity
TEA(s)	Terminal electron acceptor(s)
TEAP(s)	Terminal electron accepting process(es)
TeCB	Tetrachlorobenzene
TOC	Total organic carbon
UNEP	United Nations Environmental Program
UV	Ultraviolet
US EPA	United States (of America) Environmental Protection Agency
VARCOMP	Variance component
WHC	Water holding capacity
WHO	World Health Organization

List of figures

Fig 101: Cell counts during the first and second phases of the OCPs degradation experiment.

List of tables

1.0 Introduction

1.1 The need for soil conservation

Soil is a non-renewable resource that is increasingly becoming degraded (UNEP, 2002). Correlations have already been shown to exist between increased soil degradation and the decreasing food security in the world, especially in the tropics (Stocking, 2003). There is therefore an urgent need to conserve healthy soils and to rehabilitate degraded ones. Soil degradation occurs where both anthropogenic and non-anthropogenic activities cause it to become less vigorous or less healthy (Chisholm and Dumsday, 1987). However, it is anthropogenic activities that are mainly to blame for the increased soil degradation in recent years (UNEP, 2009).

Chemical contamination has gained great importance because of possible entry of the contaminants into the food chain (Aislabie, 1997). Hydrophobic organic compounds in particular have been shown to both bioconcentrate and biomagnify (UNEP, 2009). Therefore research has increasingly focused on remediation of contaminated sites.

Pesticide use has contributed to increased food production. However, it poses an environmental risk because of pesticide residues in soil (Aislabie, 1997), given that soils act as point sources for contamination of other compartments viz: air, water, plants, animals (Wandiga, 2001). There is therefore need to ensure sustainable pesticide use. This can be achieved by activating breakdown of pesticide residues not only at the high concentrations of contaminated soils, but also at the relatively low concentrations found in agricultural soils.

The tropics are characterized by high sunshine radiation throughout the year, a high load of microorganisms, tropical rains, and varied soil types, ecology, and climatological conditions (Bhatnagar and Bhatnagar, 2005; Diabaté et al., 2004; Wandiga, 2001). For instance, whereas the temperate climate is characterized by four seasons including a snow regime, the tropic climate involves a dry and wet (rain) spell. As a result of these conditions, research has now shown that persistent organochlorine pesticides behave differently in the tropics as opposed to the temperate climates (Wandiga, 2001). Therefore results obtained by studies on temperate soils cannot be used to predict pesticide behaviour in tropical soils.

Paddy and field soils represent the two extremes of soils found in tropical climates. The term ‘paddy soils’ is used in this thesis to denote soils characterized by poor drainage. They are used in rice cultivation, and are also found in wetlands in the river and lake basins (Onjala, 2001). The term ‘field soil’ is used in this thesis to denote soils found in higher lands relative to the wetlands. They generally have good drainage and are used for cultivation of crops such

as maize, sugarcane, tea, coffe etc. However, during the rainy season, water-logging could be experienced especially in clay soils.

1.2 Chemical contamination of soils

1.2.1 Persistent Organic Pollutants (POPs)

Organochlorine pesticides continue to be used in the tropics especially for vector control because of their efficacy and affordability. DDT has been re-introduced by the WHO in the fight against malaria (WHO, 2007). Obsolete pesticide stockpiles exist in almost every African country and other tropical countries (UNEP, 2009). In some cases these stockpiles have acted as point sources for extensive environmental contamination of soil and water resources.

1.2.2 The Stockholm convention on POPs

The Stockholm Convention consists of three annexes: A, B and C. Annex A covers those compounds targeted for complete elimination. These are aldrin, dieldrin, endrin, chlordane, heptachlor, mirex, toxaphene, HCB and pentachlorobiphenyls. Annex B is for those compounds whose use is restricted mainly to vector control. At the moment only DDT is under this annex. Annex C includes those compounds that are produced unintentionally, usually from combustion and industrial processes. Therefore the release of these compounds into the environment can only be reduced but not eliminated. The compounds are dioxins, furans, HCB and pentachlorobiphenyls. As can be seen, HCB is included in both annex A and annex C.

Amendments to have more compounds listed were made in August 2009 and will take effect from August 2010 (Stockholm Convention, 2009). The newly listed compounds are alpha hexachlorocyclohexane, beta hexachlorocyclohexane, chlordecone, hexabromobiphenyl, hexabromodiphenyl ether and heptabromodiphenyl ether, lindane, pentachlorobenzene, perfluorooctane sulfonic acid, its salts and perfluorooctane sulfonyl fluoride, tetrabromodiphenyl ether and pentabromodiphenyl ether

1.2.3 DDT and HCB

DDT and HCB belong to a group of organochlorine compounds classified as POPs. (Stockholm convention, 2009). These compounds are highly persistent, semi-volatile and bioaccumulate in the food chain. A number are suspected carcinogens and mutagens while others have been shown to be endocrine disruptors (Aislabie 1997). Some priority

compounds, including DDT and HCB, have been targeted by the Stockholm convention on POPs for restriction or complete phasing out (Stockholm convention, 2009).

The ubiquitous nature of HCB and the continued use of DDT mean that the two compounds will continue to be released into the environment. Secondly, the two compounds represent the two extremes of POPs: DDT is low-chlorinated while HCB is highly chlorinated. The simple structure of HCB makes it a good model compound for high-chlorinated POPs. DDT is also relatively simple, and its use in many tropical countries as the first-line insecticide in mosquito and tsetse fly control (UNEP, 2009) justifies its choice for fate studies in tropical soils.

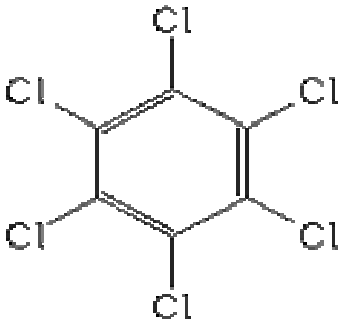

Figure 1: Structure of HCB

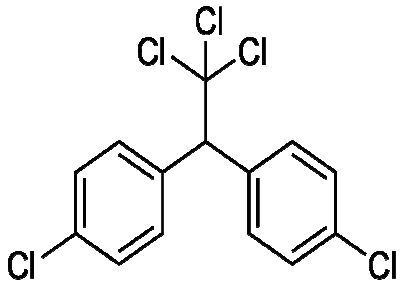

Figure 2: Structure of DDT

1.3 Natural Attenuation for dehalogenation

Given the ubiquitous nature of the POPs, cheap and sustainable approaches for their remediation need to be investigated and developed, more so for the tropics. This is because, given the strained resources of most of the tropical countries, there is little room – if any - for expensive environmental remediation ventures (UNEP, 2009). These ventures should also be sustainable and lead to soil conservation.

The conceptual approach of natural attenuation/intrinsic remediation may be such a measure. Natural attenuation refers to the reliance on natural processes (within the context of a carefully controlled and monitored site cleanup approach) to achieve site-specific remediation objectives within a time frame that is reasonable compared to that offered by other more active methods (US EPA, 2010). It relies on natural subsurface processes rather than traditional engineered procedures to eliminate contaminants in groundwater or soil, and can provide tailored measures for low-risk cases such as found in agricultural soils. The concept of natural attenuation is based on processes such as biological degradation, dispersion,

dilution, sorption, evaporation and/or chemical and bio-chemical stabilisation of pollutants. Toxicity, mobility or amount of pollutants should be reduced to an extent that human health and ecosystems are no more endangered (Nyer & Duffin, 1997).

1.3.1 Anaerobic processes

Apart from traditional aerobic degradation, which is conducted by a wide range of micro-organisms (bacteria, actinomycetes, fungi), there are processes of anaerobic decay, where micro-organisms receive their energy either from the utilisation of oxidised compounds like nitrate, sulfide or Fe(III) as electron acceptors, or by fermentation of organic substances (fermentation: splitting of organic molecules into oxidised and reduced fragments) (Nyer & Duffin, 1997). Laboratory and field studies have indicated that the reduction of organic pollutants may also involve abiotic chemical reactions. Given the abundance and the range of reduction potentials of Fe species that may exist in anoxic environments, it seems likely that - particularly under iron-reducing conditions - such Fe species play a pivotal role as electron donors or electron transfer mediators in redox transformations of organic compounds. Important milieu parameters for estimating natural attenuation are the concentration of oxygen, nitrate, Fe (II), sulfate, methane, and – less significant – manganese, calcium, bicarbonate and pH (Christensen et al., 1994). A recent proposal for standardised testing of applicability of the natural attenuation approach has been based on three criteria:

1. Redox value,
2. Extent of reductive dehalogenation and
3. Dissolved organic carbon (Rijnaarts et al., 1998; Tonnaer et al., 1998).

Each of these is discussed below.

1.3.2 Redox value, Buffer Capacity and anaerobic processes

The general approach for the assessment of the redox status of soils, aquifers and water are platinum electrode measurements or chemical equilibrium calculations based on the chemical analysis of the main redox species (Barcelona et al., 1989; Lindberg & Runnels, 1984; Hostettler, 1984). However, the redox potential value is a capture of current conditions (Bartlett & James, 1995). Therefore to assess and predict the reactions within the soil quantitatively, analysis of the redox species in the system is necessary. This reveals the terminal electron accepting processes (TEAP) responsible for the redox status of the system. Table 1 shows the electron accepting half-reactions of possible TEAPs in the order of decreasing redox-potential (derived from Heron & Christensen, 1994).

Table 1: Electron accepting half-reactions of possible terminal electron accepting processes in the order of decreasing redox-potential

Half-Reaction	
$O_2 + 4H^+ + 4e^- \rightarrow 2H_2O$	(Aerobic)
$NO_3^- + 12H^+ + 10e^- \rightarrow N_2 + 6H_2O$	(Denitrification)
$Mn^{4+} + 2e^- \rightarrow Mn^{2+}$	(Manganese reduction)
$Fe^{3+} + e^- \rightarrow Fe^{2+}$	(Iron reduction)
$SO_4^{2-} + 9H^+ + 8e^- \rightarrow HS^- + 4H_2O$	(Sulphate reduction)
$R\text{-}COOH/CO_2 + 4e^- + 4H^+ \rightarrow CH_4 + H_2O$	(Methanogenesis)

R-COOH = organic acids

Some organochlorines can themselves act as electron acceptors and induce a process known as halorespiration, even at high redox values (Field, 2004)
During reductive dehalogenation, halides are released from natural organohalogens (Gribble, 2004) as well as from xenobiotics. Measurement of chloride content has been used as evidence of dechlorination of xenobiotic organochlorines (Dermietzel and Vieth, 2002).

1.3.3 Role of organic matter in the degradation of organochlorines in soil
There are two major modes for the involvement of humic substances in dechlorination (Field, 2004):
• An oxidative mode in which humic substances accept electrons from the organochlorines, and thus behave as a food source. Humic substances are used by micro-organisms for obtaining energy to support growth, and are themselves oxidised to CO2, e.g.:

$$CH_2{=}CHCl + 4H_2O \rightarrow Cl^- + 2CO_2 + 11H^+ + 10\ e^-$$

• A reductive mode in which humic substances serve as “redox mediators”, taking electrons from the micro-organisms and “dumping” them on the organochlorines, e.g.:

$$CCl_4 + H^+ + 2e^- \rightarrow CHCl_3 + Cl^-$$

1.3.3.1 Oxidative mode – humus as a food source

The first mode is illustrated by the work of Bradley et al. (1998), as shown in Figure 3:

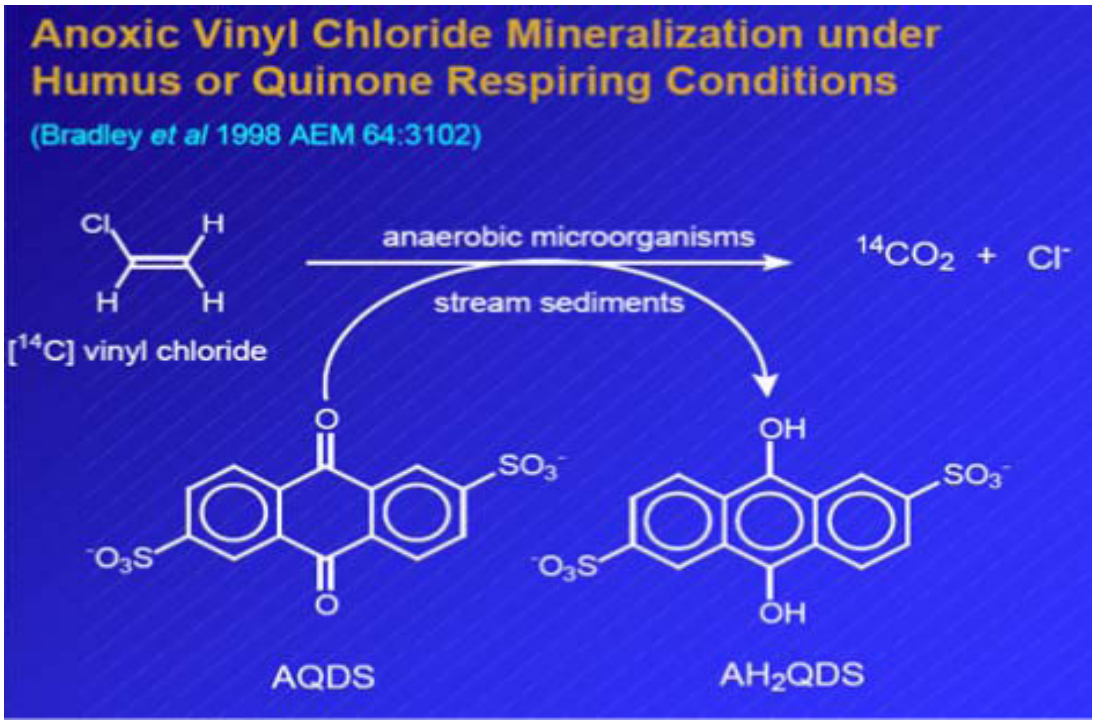

Figure 3: Oxidative mode of dechlorination with humus as food source (from Field, 2004)

Vinyl chloride is oxidised to CO_2 and chloride is released, at the expense of using a quinone as an electron acceptor. In much the same way as humans use oxygen and reduce it to water, these anaerobic micro-organisms take quinones and reduce them to hydroquinones. Bradley et al. (1998) showed that this reaction occurs not only with the model compound AQDS, but also with humus and it is a common metabolism reaction in soils.

1.3.3.2 Reductive mode - humus as a redox mediator

Reductive dehalogenation processes may be both abiotic and biotic (Field, 2004).
In the abiotic pathway, the hydroquinone reduces the organochlorine, being itself oxidised to a quinone (Figure 4). The latter is reduced back to the hydroquinone form by Fe (II), which is oxidised in the process to Fe (III). A similar process exists in which the Fe (II) is replaced by elemental sulphur or H_2S.

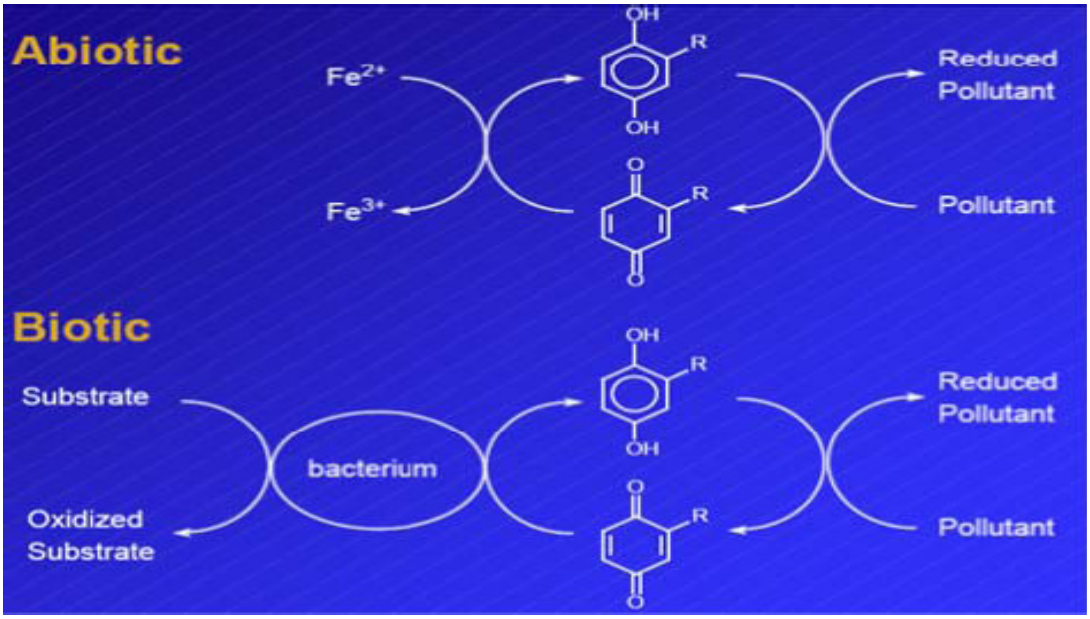

Figure 4: Reductive mode of dehalogenation with humus as redox mediator (from Field, 2004):

In the biotic pathway, also illustrated in Figure 4, a bacterium oxidises a substrate and dumps its electrons on to a sub-stoichiometric amount of humus, which then reduces the organochlorine. In this process, the quinone and hydroquinone present in the humus play the same role as in the abiotic mode.

1.3.4 Bioremediation

An increasingly utilized strategy for decontaminating polluted sites is bioremediation (Iwamoto and Nasu, 2001 and Singh, 2007). The lack of a proper indigenous population of microbial degraders can be overcome by inoculating foreign microorganisms into a system (Edgehill and Finn, 1999). This strategy, usually referred to as "bioaugmentation," is based on the inoculation of a pollutant-degrading microbial strain or a microbial consortium into the contaminated system (Singh, 2007).

In spite of the ability of the diverse bacteria in the environment to degrade many pollutants, a variety of chemical structures of certain pollutants, especially some xenobiotics like POPs, are beyond bacterial biodegradation capabilities (Cao et al., 2009). This is especially the case where single bacterial strains are used for remediation (Diaz, 2004). This has led to the engineering of recombinant bacteria with desirable bioremediation properties (Stephenson and Warnes, 1996; Diaz, 2004). However, this approach is highly controversial because of

biosafety issues associated with the release of such strains into the environment (Diaz, 2004). A less controversial strategy has been to develop syntrophic bacterial consortia whose members are specialized in certain catabolic steps or in the biodegradation of certain pollutants in complex pollutant mixtures, such as the commonly encountered benzene, toluene, ethylbenzene and xylene (BTEX) mixture (Diaz, 2004; Cao et al., 2009). Research work regarding such bacterial consortia is still in its infancy (Cao et al., 2009).

1.4 HCB

HCB is a highly-chlorinated aromatic compound. As such it poses environmental difficulties in so far as degradation is concerned. Indeed, its persistence has earned it a place among the priority compounds targeted by the Stockholm convention (UNEP, 2009). However, its inadvertent industrial production and ubiquitous nature means that it continues to be a compound of environmental concern. Studies have been undertaken to study the fate of HCB in the environment.

1.4.1 Degradation studies of HCB in the soil environment

The half-life for residence of HCB in soil has been estimated to be 970-2100 days (Griffin and Chou, 1981), with the major loss process from soil at the surface being volatilisation. In a study of treated soil stored under aerobic and anaerobic conditions in covered containers to retard volatilisation, no detectable loss of HCB occurred over the one-year experimental period (Isensee *et al*, 1976). In another study, up to 78 % of soil-applied HCB could be recovered in an oxic soil after one year (Beall, 1976). Aerobic and anaerobic biodegradation are the major means of HCB removal at lower soil depths, with half-lives of 2.7-5.7 years (Beck and Hansen, 1974) and 10.6-22.9 years (Howard, 1991), respectively. Meijer et al. (2001) reported a half-life of 11.7 years for sewage-sludge treated soils over the period 1968-1990.

A major problem with these data is that measured ‘disappearance’ from soils includes both volatilisation and degradation. Whereas biodegradation completely removes HCB from the environment, volatilisation leads to continued existence of HCB in a different environmental compartment.

1.4.2 Degradation studies of HCB in soil under anaerobic conditions

Several studies have evaluated the anaerobic bioremediation of chlorinated benzenes in soil (Ramanand et al., 1993; Rosenbrock et al., 1997; Brahushi et al., 2004). In the first study

(Rosenbrock et al., 1997), bioremediation of HCB was evaluated by providing anaerobic conditions to the different soils. In some soils the endogenous organic matter provided electron donors to support HCB dechlorination, whereas in other soils with low organic matter content, organic substrate addition was required. In both cases, dechlorination of radiolabeled [^{36}Cl]HCB (spiked at 30 mg kg^{-1} soil) to $^{36}Cl^-$ was demonstrated accounting for about 40 % dechlorination in 140 days. In the second study (Ramanand et al., 1993), a soil slurry contaminated with a mixture of HCB (0.029 mM), pentachlorobenzene (PCB) (0.074 mM) and 1,2,4-TCB (1.14 mM) was converted almost stoichiometrically to chlorobenzene (CB) (1.01 mM) after 140 days of incubation under methanogenic conditions with H_2 as electron donor. In the third study (Brahushi et al., 2004), HCB in agricultural soil was bioremediated by flooding the soil in laboratory microcosms. After 20 weeks of incubation only 1% of applied [^{14}C]HCB radiolabel could be recovered in the extractable fraction with 1,3,5-TCB as the main metabolite.

HCB has also been shown to degrade anaerobically in sewage sludge, with 1,3,5-trichlorobenzene (1,3,5-TCB) as the main product (Yuan et al, 1999). Zhao et al (2003) investigated the anaerobic degradation of HCB in sediments, and observed a degradation rate of 0.035 month^{-1}, which increased to 0.088 month^{-1} when extra organic carbon was added to the sediment.

The anaerobic degradation pathway of HCB is shown in figure 6.

1.4.3 Degradation studies of HCB in soil under anaerobic/aerobic cycles

The sequential anaerobic-aerobic treatment of HCB was evaluated in one study (Fathepure and Vogel, 1991). A two-stage biological treatment scheme was tested for the biodegradation of HCB (0.075 mg l^{-1}) utilizing laboratory-scale anaerobic and aerobic biofilm reactors (each 0.25 l) operated in series, having hydraulic retention times of 37.5 and 2.24 h, respectively (Fathepure and Vogel, 1991). During the anaerobic stage, acetate was found to be the best electron-donating substrate, supporting 98.7 % removal of HCB, which was recovered mostly as 1,2,3-TCB (60 %) and 1,2-DCB (10 %). Experiments with ^{14}C-HCB revealed that HCB was mineralized to $^{14}CO_2$ by up to 23 % during the sequential anaerobic-aerobic treatment, and the total metabolism to both $^{14}CO_2$ and [^{14}C] in non-volatile intermediates was 94 %.

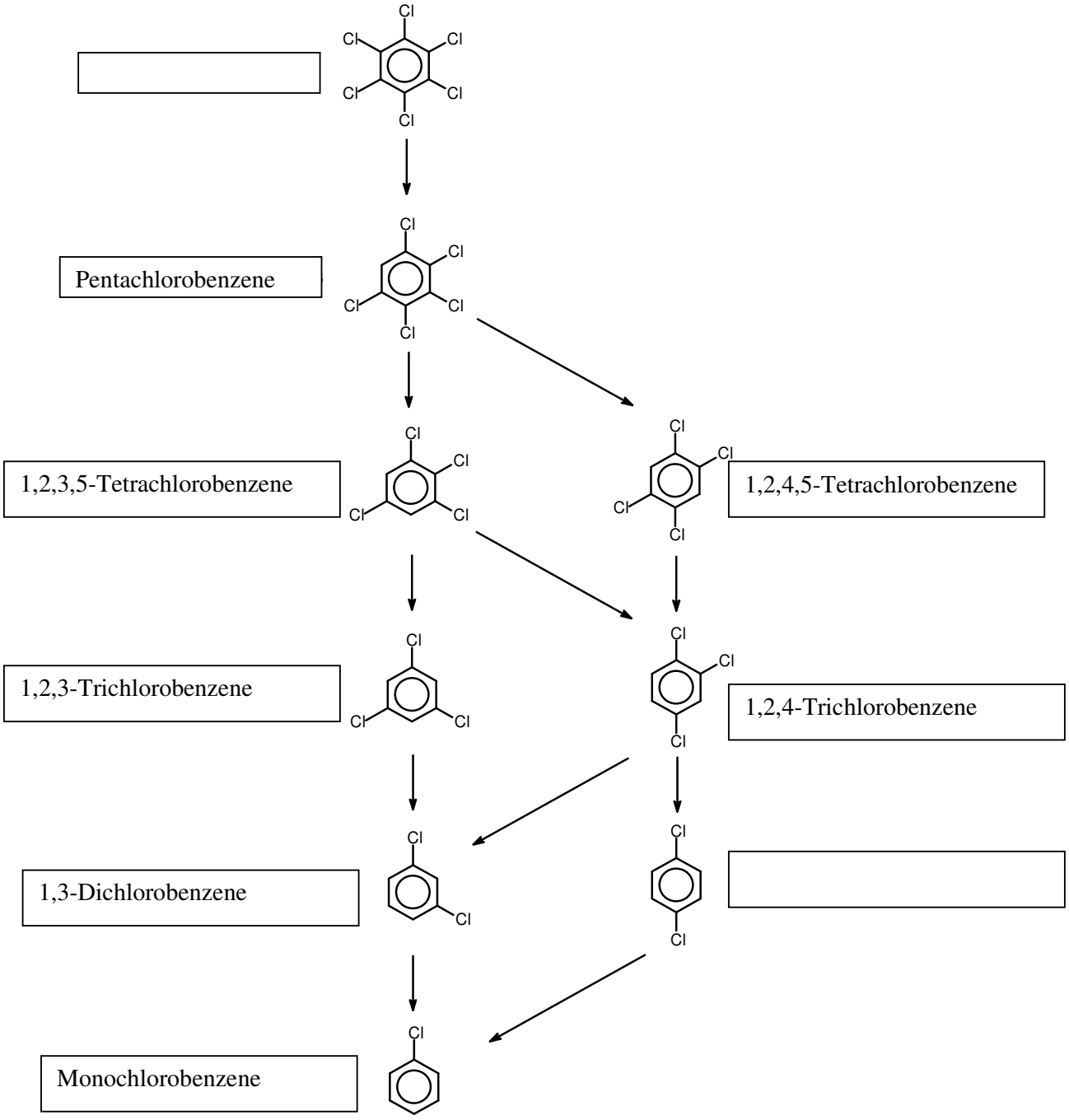

Figure 5: Most common pathways of anaerobic reductive dechlorination of hexachlorobenzene by microbial enrichment cultures and environmental samples (Fathepure et al., 1988; Holliger et al., 1992; Beurskens et al., 1994; Middeldorp et al., 1997; Adrian et al., 1998; Chang et al., 1998; Adrian and Gorisch, 2002; Chen et al., 2002a; Wu et al., 2002).

1.5 DDT

1.5.1 Degradation and transformation of DDT in soil

DDT (1,1,1-trichloro-2,2-bis(4-chlorophenyl ethane) is a persistent environmentally toxic organochlorine insecticide. It has been used extensively since the 1940s for control of agricultural pests, and is still used in many tropical countries for mosquito control (WHO, 2007). Processes such as volatilization, adsorption, run off and plant uptake contribute to the dissipation of DDT residues (DDTr) in soils, often without substantial alteration of the chemical structure (Fishbein 1973). In contrast, biodegradation has the potential to degrade DDTr significantly and reduce soil concentrations in a cost-effective manner (Foght et. al., 2001). Biodegradation may occur under both aerobic and anaerobic conditions due to soil microorganisms including bacteria, fungi, and algae (Arisoy, 1998; EPA 1979c; Lichtenstein and Schulz, 1959; Menzie, 1980; Stewart and Chisholm, 1971; Verma and Pillai, 1991b; Aislabie et al., 1997; Singh et al., 1999). During biodegradation of DDT, both DDE and DDD are formed in soils. Both metabolites may undergo further transformation but the extent and rate are dependent on soil conditions and, possibly, microbial populations present in soil. DDE is often resistant to biodegradation under aerobic and anaerobic conditions (Strompl and Thiele, 1997).The degradation pathways of DDT under aerobic and anaerobic conditions have been reviewed by Zook and Feng (1999) and Aislabie et al. (1997). DDT biodegradation is typically co-metabolic and includes dechlorination and ring cleavage mechanisms. The aerobic and anaerobic degradation pathways are shown in figures 6 and 7

1.5.2 Factors influencing the degradation and transformation of DDT in soil

Factors that influence DDTr biodegradation in soil include the composition and enzymatic activity of the soil microflora, DDTr bioavailability, the presence of soil organic matter as a co-metabolic substrate and (or) inducer, and prevailing soil conditions, including aeration, pH, and temperature (Foght et. al., 2001). Understanding how these factors affect DDTr biodegradation permits rational design of treatments and amendments to stimulate biodegradation in soils.

The rate at which DDT is converted to DDD in flooded soils is dependent on the organic content of the soil (Racke et al., 1997). In a laboratory study, Hitch and Day (1992) found that soils with a low metal content (Al, Ba, Cd, Co, Cr, Fe, and K were the major metals examined) degrade DDT to DDE much more slowly than do soils with high metal content. In microcosm experiments, Boul (1996) found that increasing soil water content enhanced DDT

loss from generally aerobic soil. His results suggested that increased biodegradation contributed to the enhanced DDT dissipation.

In laboratory experiments with marine sediments, DDT has been shown to degrade to DDE and DDD under aerobic and anaerobic conditions, respectively (Kale et al. 1999) and that DDE is dechlorinated to DDMU under methanogenic or sulfidogenic conditions (Quensen et al., 1998). The rate of DDE dechlorination to DDMU was found to be dependent on the presence of sulfate and temperature (Quensen et al., 2001). DDD is also converted to DDMU, but at a much slower rate. DDMU degrades further under anaerobic conditions to DDNU and other subsequent degradation species, such as DDOH and DDA, through chemical action (Heberer and Dünnbier, 1999; Ware et al., 1980).

1.5.3 Field studies on DDT degradation in soil

DDT field studies have been carried out under temperate conditions on agricultural soils (Aigner et al., 1998) and forest soils (Dimond and Owen, 1996), in which DDE was shown to be the major metabolite. A 23 year field study on the effect of land management practices on DDT dissipation showed that flooding increased DDT dissipation while deep ploughing increased DDT persistence (Spencer et al., 1996). Boule et al. (1994) showed that long-term irrigation and superphosphate fertilizer application decreased the levels of DDT residues in pasture soil, especially DDE. The study also indicated that irrigation did not cause increased leaching of the DDT.

^{14}C-DDT degradation studies in soil under tropical and subtropical conditions have been carried out (Wandiga, 2001; Racke et al., 1997), under the auspices of the International Atomic Energy Agency (IAEA). The half-lives of DDT were generally found to be shorter than those in the temperate climate except for one extremely acidic soil (pH 4.5) in Brazil (Racke et al., 1997). The major fate mechanisms under tropical conditions were volatilization, biological and chemical degradation, and to a lesser extent, adsorption. Comparable half-lives have nevertheless been reported in temperate regions (Lichtenstein and Schulz, 1959; Racke et al., 1997; Stewart and Chisholm, 1971).

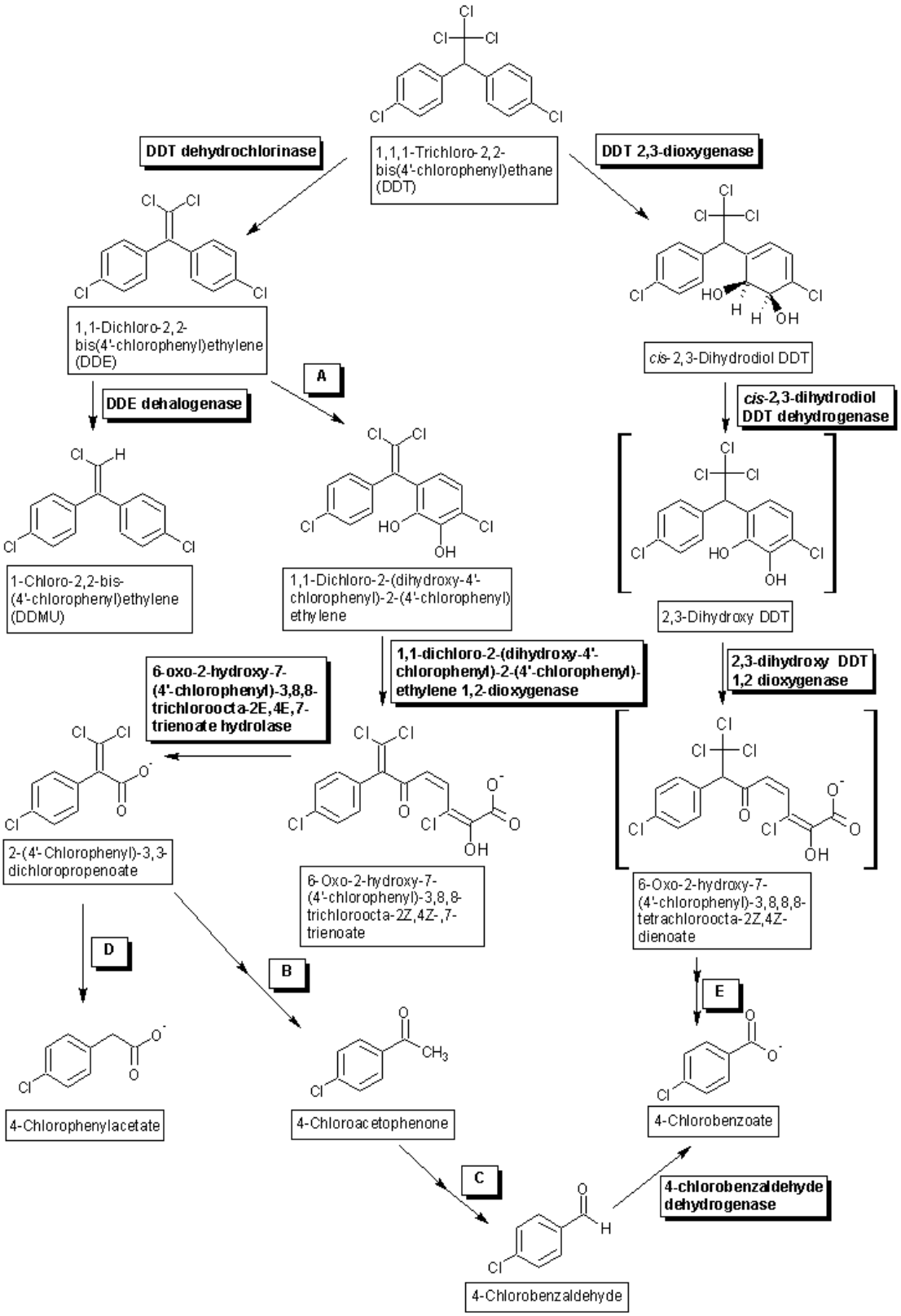

Figure 6: Aerobic degradation pathway of DDT (from Zook and Feng, 2008).

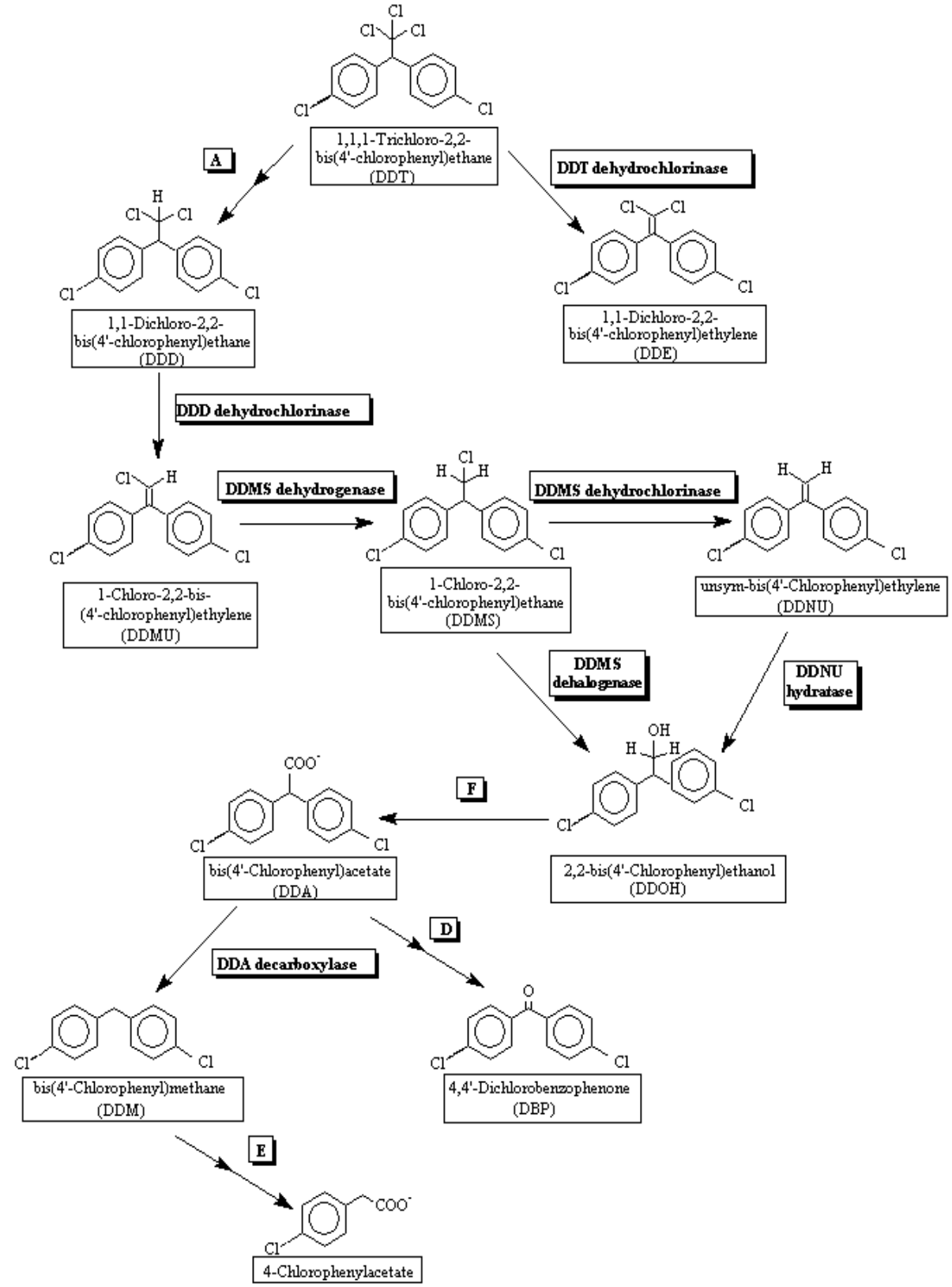

Figure 7: Anaerobic degradation pathway of DDT (from Zook and Feng, 2009)

1.6 Justification and significance of the study

Several works on the fate of POPs in the temperate climate have been reported (UNEP, 2009). Research shows that persistent organochlorine pesticides behave differently in the tropics when compared to the temperate climates (Wandiga, 2001). Therefore results obtained by studies on temperate soils cannot be used to predict behaviour in tropical soils. These facts dictate that studies be carried out on tropical soils so as to understand the fate and behaviour of these pesticides.

1.6.1 Gaps in knowledge on HCB degradation in soil

To the best of my knowledge, the study by Fatherpure and Vogel (1991) is the only one on HCB degradation in soil involving anaerobic-aerobic cycles. While that study was carried out in a bioreactor, the current study simulated natural conditions and induced anaerobic conditions through water logging, because the soils used in the study are susceptible to flooding during the rainy season. In that study (Fatherpure and Vogel, 1991) glucose, methanol and acetate were used as supplementary carbon sources while in the current study compost was used as the supplementary carbon source - a carbon source that can easily and sustainably be used in nature; and while that study involved temperate soils, this study utilized tropical clay soils. There is thus a clear gap that this study seeks to fill, namely: to find out the fate of HCB in tropical clay soils under simulated natural tropical conditions.

1.6.2 Gaps in knowledge on DDT degradation in soil

Several studies have been done to quantify the levels of DDT in the environment (UNEP 2009, Stockholm convention 2009); microbial degradation (Aislabie et al., 1997; Singh, 2007; Foght et al., 2001); field fate studies under temperate and tropical conditions (Aigner et al., 1998; Dimond and Owen, 1996; Wandiga, 2001; Racke et al., 1997; Singh, 2007). A few studies have focused on enhancing in-situ remediation of DDT, mainly in temperate soils (Spencer et al., 1996, Boul et al., 1994), but not on tropical soils. DDT degradation studies utilizing anaerobic–aerobic mixed cultures in bioreactors have been carried out (Coroner-Crutz et. al, 1999, Beunink, 1988), but not under natural conditions.

This work seeks to provide insights on the behaviour of DDT in tropical soils under simulated natural conditions, utilizing a strategy that can be easily replicated in the field (Spencer et al., 1996; Boul et al., 1994). It also seeks to provide an understanding of the soil processes that take place during the anaerobic degradation of DDT in tropical soils. Most studies are focused on the fate of DDT (Racke et. al, 1997; Wandiga, 2001), microbial degradation (Aislabie,

1997; Foght et., al 2001: Diaz, 2004; Cao et. al., 2009); using biofilm reactors for bioremediation of aromatics (DiGioia et al.; 2009; Juang and Kao, 2009; Baraldi et al., 2008; Juang and Wu, 2007; Nicolella et al., 2007) and using recombinant strains for remediation (Diaz, 2004; Cao et. al., 2009) without taking the soil processes into account.

1.6.3 Gaps in knowledge on bioremediation

Research work regarding the use of bacterial consortia for bioremediation is still in its infancy (Cao et al., 2009). This study was designed to add to this nascent field. Few reports exist in literature on degradation of compounds by the genera Bordetella. *Bordetella petrii* has been shown to degrade naphthalene and toluene (Bianchi et al., 2005) while *Bordetella hinzii* has been shown to grow in PAH cultures (Ericksson et al., 2003). The success of this approach would offer a safer bioremediation option relative to the controversial recombinant strains (Diaz, 2004; Cao et al., 2009). To the best of my knowledge, this is the first time that a study testing the capacity of a community - with a species of the Bordetella family as the key degrader - to degrade a complex OCPs mixture, has been carried out. The list of OCPs in the cocktail and some of their characteristics are shown in Table 2.

Table 2: List of OCPs in the cocktail and some physical-chemical properties

Compound	Molecular formula	MW	Solubility mg L^{-1}	Log Kow	*K_H Pa m^3 mol^{-1}
Alpha-HCH (αHCH)	$C_6H_6Cl_6$	290.85	10[c] (28°C)	3.80[c]	0.695[c] (20°C)
beta-HCH (β-HCH)	$C_6H_6Cl_6$	290.85	5[c] (20°C)	3.78[c]	0.046[c] (20°C)
Gamma-HCH (γ-HCH)	$C_6H_6Cl_6$	290.85	17[c] (20°C)	3.71[a]	0.355 [c] (20°C)
delta-HCH (δ-HCH)	$C_6H_6Cl_6$	290.85	10[c] (20°C)	4.14[c]	0.021[c] (20°C)
epsilon-HCH (ε-HCH)	$C_6H_6Cl_6$	290.85			
Pentachlorobenzene (PCB)	C_6HCl_5	250.34	0.68[g] (25°C)	5.19[g]	72.00[g] (25°C)
Pentachloroanisole (PCA)	$C_7H_3Cl_5O$	280.36	0.2[d] (20°C)	5.66[d]	196.57[d] (20°C)
Octachlorostyrene (OCS)	C_8Cl_8	379.7	0.00174[b] (20°C)	6.29[d]	23.30[d] (20°C)
Hexachlorobenzene (HCB)	C_6Cl_6	284.8	0.006[c] (25°C)	5.14[a]	58.77[c] (20°C)
p,p'-DDT	$C_{14}H_9Cl_5$	354.48	0.003[b] (25°C)	6.50[a]	0.841[c] (25°C)
o,p'-DDT	$C_{14}H_9Cl_5$	354.48	0.085[c] (25°C)	6.79[c]	0.060[c] (25°C)
p,p'-DDD	$C_{14}H_{10}Cl_4$	320.1	0.05[b] (25°C)	6.02[a]	2.128[c] (25°C)

o,p'-DDD	$C_{14}H_{10}Cl_4$	320.1	0.10[c] (25°C)	5.87[c]	1.824[c] (25°C)
p,p'-DDE	$C_{14}H_8Cl_4$	318.1	0.065[b] (24°C)	5.50[a]	0.405[c] (25°C)
o,p'-DDE	$C_{14}H_8Cl_4$	318.1	0.0013[b] (20°C)	6.00[c]	0.828[c] (25°C)
trans-Chlordane (trans-CHL)	$C_{10}H_6Cl_8$	409.8	0.014[b] (25°C)	6.07[a]	8.420[c] (25°C)
cis-Chlordane (cis-CHL)	$C_{10}H_6Cl_8$	409.8	0.042[b] (20°C)	6.11[a]	12.92 [a] (25°C)
Oxy-Chlordane (OC)	$C_{10}H_4Cl_8O$	423.8	0.023[f] (20°C)	4.95[a]	7.48 [a] (25°C)
Heptachlor (HC)	$C_{10}H_5Cl_7$	373.3	0.05[c] (25°C)	6.10[c]	29.79 [c] (25°C)
cis-Hexachloroepoxide (cis-HCE)	$C_{10}H_5Cl_7O$	389.4	0.275[c] (25°C)	5.00[e]	1.665[c] (25°C)
trans-Hexachloroepoxide (trans-HCE)	$C_{10}H_5Cl_7O$	389.4	0.275[c] (25°C)	5.40[c]	3.242[d] (25°C)
Aldrin	$C_{12}H_8Cl_6$	364.9	0.011[c] (20°C)	6.50[c]	4.965[c] (20°C)
Dieldrin	$C_{12}H_8Cl_6O$	380.9	0.14[b] (20°C)	3.692-6,20[b]	0.527[c] (20°C)
Endosulfan-I	$C_9H_6Cl_6O_3S_5$	406.9	0.32[b] (22°C)	3.13[b]	1.013[c] (25°C)
Endosulfan-II	$C_9H_6Cl_6O_3S_5$	406.9	0.33[c] (20°C)	3.52[c]	1.935[c] (25°C)
Methoxychlor	$C_{16}H_{15}Cl_3O_2$	345.65	0.10[b] (25°C)	4.68-5.08[c]	1.621 [c] (25°C)
Mirex	$C_{10}Cl_{12}$	545.59	0.0000005[b] (22°C)	5.28[c]	52.284[c] (25°C)

a. Paasivirta et al. (1999)
b. ARS (1995)
c. ATSDR (2009)
d. HSDB (2001).
e. Mackay et al. (1997)
f. PPDB (2009)
g. Shen et al. (2005)

* Some of the K_H values are given in M/atm in the references and have been converted to the SI unit of Pa m^3 mol^{-1} using the relation 1 Pa m^3 mol^{-1} = 9.8692×10^{-6} M/atm

1.7 Objectives of the study

The overall objective of the study was to induce or enhance the degradation and mineralization of HCB and DDT in two tropical clay soils.

The specific objectives were:

i. To study the innate ability of the tropical clay soils to mineralize DDT and HCB under aerobic conditions.

ii. To induce and enhance the degradation and mineralization of HCB in the tropical clay soils using anaerobic/aerobic cycles.

iii. To enhance the degradation and mineralization of DDT in the tropical clay soils using anaerobic/aerobic cycles.

iv. To study the factors and processes involved in the anaerobic degradation of DDT in the tropical clay soils.

v. To study the ability of a 1,2,4-TCB mineralizing community to degrade low concentrations of organochlorine pesticides with a view to using it for bioremediation under aerobic conditions.

1.8 Conceptual framework and experimental basis

1.8.1 Conceptual framework

The general working hypotheses of the study was that steering ecological conditions would enhance the degradation of HCB and DDT in soil. A multi-faceted approach was utilized to activate biotic and abiotic pathways necessary for the degradation of chlorinated compounds, viz

- Anaerobic/aerobic cycles to dehalogenate the primary molecules (under anaerobic conditions) and degrade the less halogenated metabolites (under aerobic conditions).
- Provision of supplementary carbon source to support microbial activity. Microbes generally degrade POPs co-metabolically (Aislabie, 1997). Therefore compost was used because it is a long lasting slow-release carbon source.
- Role and activity of soil inherent redox players in electron transfer processes e.g. Fe (III) could act as an electron acceptor while Fe (II) could act as an electron donor for POPs under changing redox conditions.

1.8.2 Experimental basis

The persistence of HCB, DDT and other POPs is attributed to the chlorine atoms. Dechlorination is difficult under aerobic conditions (Griffin and Chou, 1981; Meijer et al.,

2001). Therefore the water-logging strategy was used to induce reductive dechlorination under anaerobic conditions. The subsequent drying of the soil samples was meant to induce aerobic conditions, under which ring cleavage occurs (Zook and Feng, 1999). Thus anaerobic conditions would enhance dechlorination while aerobic conditions would enhance mineralization (ring cleavage). Compost was used as a slow-release supplementary carbon source because most POPs have been shown to undergo co-metabolic degradation (Aislabie, 1997). It was also expected that a supplementary carbon source would increase microbial activity hence inducing anaerobic conditions. Anaerobic conditions would lead to the activation of several redox players. The electron shuttle of players such as Fe and dissolved organic matter would result in dechlorination (Field, 2004).

2.0: Materials and Methods

2.1 Chemicals, soil samples and compost

2.1.1 Chemicals

Uniformly ^{14}C-ring-labelled HCB (purity >98 %, 185 MBq mmol^{-1} sp. radioactivity, uniformly ^{14}C-ring-labeled 4,4'-DDT (purity >98 %, 12.8 mCi mmol^{-1}sp. radioactivity) and uniformly ^{14}C-ring-labeled 1,2,4-TCB were obtained from International Isotopes (Munich, Germany). ^{13}C labeled internal standards were obtained from Cambridge Isotope Laboratories (Woburn, MA, USA). Scintillation cocktails were obtained from Packard (Dreieich, Germany).

The non-labelled chlorobenzenes - HCB, pentachlorobenzene (PCB), monochlorobenzene (MCB) and the isomers of tetrachlorobenzene (TeCB), trichlorobenzene (TCB) and dichlorobenzene (DCB), purity >99.5% - and the non-labeled 4,4'-DDT, 2,4'-DDT, 4,4'-DDD, 2,4'-DDD, 4,4'-DDE, 2,4'-DDE, 4,4'-DDMU and 4,4'-DDM, purity >99.5% were all purchased from Dr. Ehrenstorfer Laboratories (Augsburg, Germany).

Picograde n-Hexane, Silica gel 60 and florisil columns were obtained from Promochem (Wesel, Germany), diatomaceous earth and 3-(2-Pyridyl)-5,6-diphenyl-1,2,4-triazine-4',4''-disulfonic acid sodium salt (ferrozine) from Sigma Aldrich (Germany), sodium sulphate from Neolab (Munich, Germany), sea sand from Merck (Darmstadt, Germany), scintillation cocktails from Packard (Dreieich, Germany) .

All other chemicals and solvents were of analytical grade and were purchased from Sigma-Aldrich (Germany).

2.1.2 Soil samples and compost

The paddy soil material was taken from the Mwea irrigation scheme in Kenya (00^{o} 42' 00'' N and 37^{o} 22' 00'' E). Farming in the scheme started in 1956, and rice has been the predominant crop. The scheme has a gazetted area of 30,350 acres (NIB, 2009). A total of 16,000 acres has been developed for paddy production. The rest of the scheme is used for settlement, public utilities, subsistence and horticultural crops farming. The scheme is served by two main rivers viz Nyamindi and Thiba rivers. Irrigation water is abstracted from the rivers by gravity, by the help of fixed intake weirs, conveyed and distributed in the scheme via unlined open channels. Land preparation is carried out by flooding the fields to a depth of 4 inches and paddling them by use of tractors equipped with rotavators (Onjala, 2001). Irrigation water is maintained at about 1/3 of the plant height during the growth period (about 4 months). About 3 weeks before cutting the crop, the fields are drained to enable harvesting to be done on dry fields.

The field soil material was taken from a sugarcane farm in the neighbourhood of Chemelil Sugar company (00 ^{o} 05' 04.77'' S and 35 ^{o} 07' 57.51'' E) in the Lake Victoria Catchment area of Kenya. Sugar cane is the only crop grown in the company land (5054 hectares) and in adjacent farms (16171 hectares), and is therefore the economic mainstay of this region (Wawire et al., 2006). The soils were air-dried in the shade for two weeks, crushed and sieved using a 2 mm sieve. The sieved soils were then packed in polythene bags, transported from Kenya and stored in the laboratory at room temperature (20 °C). The soil properties are shown in table 2, fig.8 and fig. 9.

Table 3: Soils and compost characterization

	Paddy soil (Mwea)	Field soil (Chemelil)	Compost
Texture	Clay	Clay	
Organic Carbon (% TM)	2.07	2.25	
DOM (H2O) mg/g	0.3	0.431	4.738
Total carbon (% TM)	2.9	2.34	18.52
Total Nitrogen (% TM)	0.14	0.13	1.414
C:N (Total C:total N) ratio	14.004	18.725	13.10
NO_3^- ($CaCl_2$) mg/100g	3.04	1.48	
NH_4^+($CaCl_2$) mg/100g	0.28	0.06	
NH_4^+ (H_2O) µg/g soil	0	0	2.979
NO_3^- (H_2O) µg/g soil	89.229	3.712	84.135
NO_2^- (H_2O) µg/g soil	3.41	0.066	1.272
SO_4^{2-} (H_2O) µg/g soil	70.194	9.01	17.796
P (P_2O_5 CAL m) mg/100g	6	6	
HPO_4^- µg/g soil	0.117	0.023	0.925
Cl^- (H_2O) µg/g soil	29.443	1.923	41.267
Br^- (H_2O) µg/g soil	0.446	0.224	1.526
K^+ (K_2O_5-CAL m) mg/100g	42	11	
K^+ (H_2O) µg/g soil	4.608	2.884	158.025
Na^+ (H_2O) µg/g soil	134.656	26.259	6.785
Li^+ (H_2O) µg/g soil	0.023	0.006	0.13
CaCO3 (% TM)	< 0.2	4.5	
Ca^{2+} (H_2O) µg/g soil	36.498	3.445	0.617
Mg^{2+} (H_2O) µg/g soil	20.884	0.978	0.671
Cr (KWA) mg/kg	67	44	
Cu (KWA) mg/kg	27	10	
Ni (KWA) mg/kg	39.7	23.6	
Co (KWA) mg/kg	26.9	18.7	
pH (water)	7.88	8.02	7.58
pH ($CaCl_2$)	5.7	7.7	
WHC (oven-dry mass basis) %	91.47	58.07	64.32
OWC (oven-dry mass basis) %	63.17	35.30	52.02
WHC (compost-amended soil) %	94.37	57.37	

The compost was obtained from a composting site near Freising (Kompostieranlage Eggertshof, Eggertshofen, Germany). The compost was sieved through a 2 mm sieve and stored in a cool room at 4 °C. The water content of the stored compost was 33%. The characterization of some of the compost properties is shown in table 2 and fig. 9.

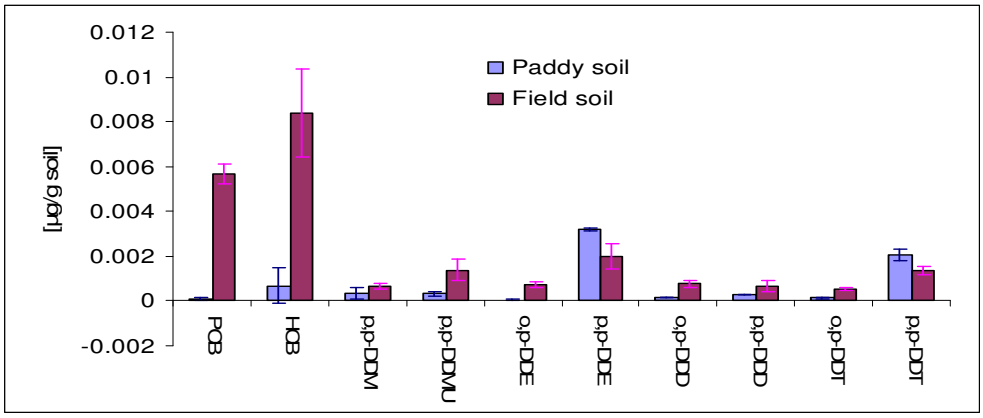

Fig. 8: Contamination levels in the paddy and field soils used for the experiments

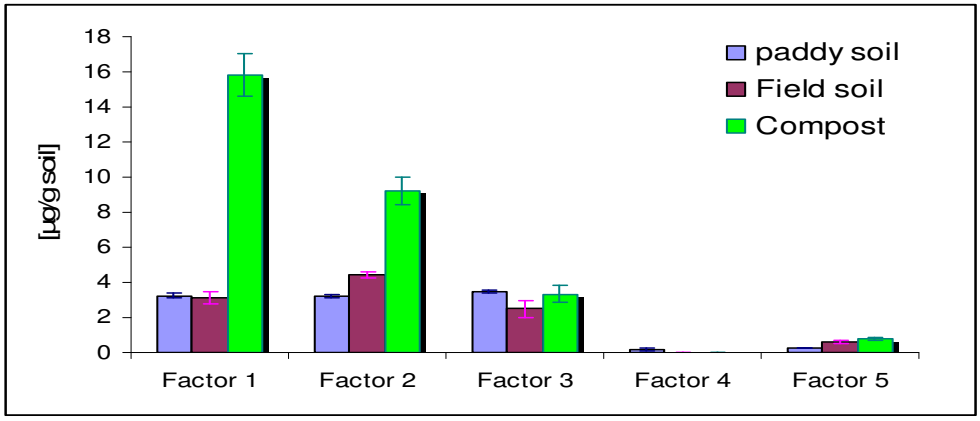

Fig. 9: Organic matter quality in the soils and compost used in the study

Factor 1: Humic-like authochthonous substances

Factor 2: Fulvic-like authochthonous substances

Factor 3: Humic-like anthropogenic substances

Factor 4: Tryptophan/tyrosine/phenolic-like authochthonous substances

Factor 5: Microbial derived authochthonous substances

2.2 Experimental set-up

There were four experimental set-ups in line with the objectives of this study, namely:

i). Incubation of ^{14}C-HCB and ^{14}C-DDT in soil under aerobic cycles conditions

ii). Incubation of ^{14}C-HCB and ^{14}C-DDT in soil under anaerobic-aerobic cycles conditions

iii). Incubation of non-labeled DDT in soil under anaerobic conditions.

iv). Incubation of a 27 OCPs cocktail in liquid culture spiked with a 1,2,4-TCB degrading community, under aerobic conditions.

2.3 Incubation of ^{14}C-HCB and ^{14}C-DDT under aerobic conditions.

This experiment was done to study the innate ability of the two clay soils to mineralize DDT and HCB under aerobic conditions.

2.3.1 Application of ^{14}C-HCB and ^{14}C-DDT, and initiation of experiment

^{14}C-HCB (sp. radioactivity = 649.55 Bq μg^{-1}) was mixed with non-labeled HCB (10 $\mu g/\mu l^{-1}$) dissolved in cyclohexane to prepare the application standard (sp. radioactivity = 11.78 Bq μg^{-1}). The application standard was applied to an aliquot of 5 g dried and pulverised soil sample in a 50 ml beaker glass to give a starting concentration of 30 $\mu g g^{-1}$ corresponding to 25.13 kBq. After evaporation of cyclohexane, the soil aliquot was carefully stirred with a spatula and then transferred to a 250 ml glass beaker where it was mixed with 45 g (dry weight equivalent) of equilibrated soil. The soil was equilibrated at 40 % of OWC at 20°C for two weeks prior to the application.

^{14}C-DDT (sp. radioactivity = 1.3336 KBq μg^{-1} in toluene) was similarly prepared as HCB, using n-hexane. The amount of ^{14}C-DDT (sp. radioactivity = 14.03 Bq μg^{-1}) added to each soil sample gave an initial concentration of 30 $\mu g g^{-1}$ soil (dry weight) corresponding to 33.95 kBq.

The spiked soil samples for both HCB and DDT were transferred to the incubation flasks (Fig. 10), compacted to a density 1.3 gcm^{-3}, water content adjusted to OWC and the flasks incubated at 30 ^{o}C in the dark

2.3.2 Aeration and trapping of $^{14}CO_2$ and ^{14}C-volatiles

The flasks were aerated for 1 hour twice every week. The $^{14}CO_2$ and ^{14}C-volatile compounds were trapped in a closed laboratory aeration system consisting of three traps (Fig. 11). The first trap contained 10 ml EMME for trapping the ^{14}C-volatile compounds and the last two traps each contained 10 ml NaOH for trapping $^{14}CO_2$. Generally, minimal if any radioactivity was detected in the 3rd trap.

2.3.3 Effect of compost on ^{14}C-DDT aged residues

The HCB aerobic experiment was stopped after 84 days because of lack of appreciable mineralization. To test the effect of supplementary carbon sources on the mineralization of DDT aged residues, compost (1.25 %) was added on day 84 to the ^{14}C-DDT spiked soil. The compost had been stored at 4°C at a water content of 33 %. The compost was mixed with the soil, after which the compost-amended soil was compacted once more to a density of 1.3 gcm^{-3} and re-incubated at 30 °C. Aeration and trapping of $^{14}CO_2$ and ^{14}C-volatiles was done twice a week. The experiment ran for another 87 days (total 171 days). After stopping both the HCB and DDT experiments, the soils were frozen at -20 ^{o}C for subsequent ASE extraction.

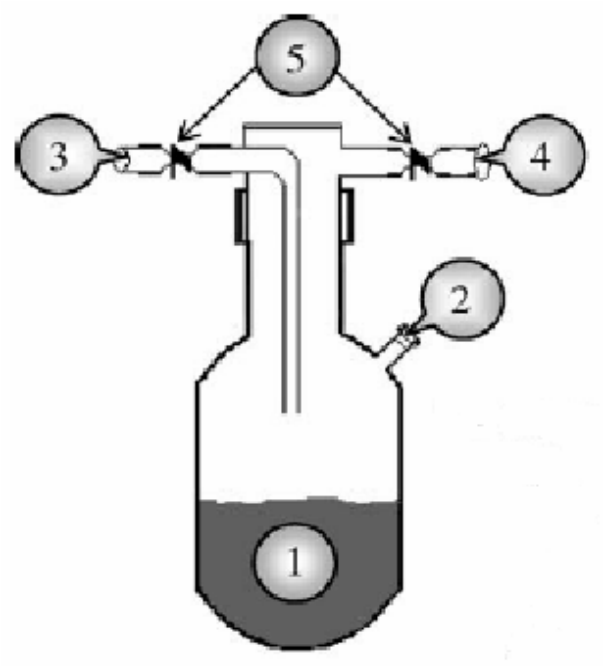

1 = Soil sample
2 = Inlet for gas sampling and application of 1,2,4-TCB
3 = Air inlet during aeration
4 = Air outlet (connected to trapping system during aeration)
5 = Hose clip and viton tube (for closing the system during incubation)

Figure 10: Test system used for incubation

2.4 ^{14}C-HCB and ^{14}C-DDT anaerobic-aerobic cycles incubation experiments

The aim of these experiments was to induce and enhance the degradation and mineralization of ^{14}C-HCB and ^{14}C-DDT respectively, in the tropical clay soils using anaerobic/aerobic cycles.

2.4.1 Experimental set-up

Two different experiments were done to study the effect of anaerobic-aerobic cycles on the degradation, mineralization and volatilization of HCB and DDT in soil. Two soils were used

for each compound and, to study the influence of supplementary carbon sources on the degradation and mineralization of the two compounds, a second set was amended with compost (1.25 %). Compost amendment did not affect the WHC and OWC of the soils (Table 2). The experiments were done in replicates of four in the incubation flasks (Fig. 10). To induce anaerobic conditions, the soils were water-logged, and to achieve aerobic conditions the soils were dried by continuous aeration in a closed aeration system (Fig. 11). Two anaerobic-aerobic cycles were achieved as shown in Table 4.
$^{14}CO_2$, ^{14}C-volatiles, metabolite pattern and redox potential were monitored over the experimental period.

Table 4: Experimental set-up for the anaerobic/aerobic phase experiments

	1st anaerobic phase		Changing from anaerobic to aerobic	1st aerobic phase	1st anaerobic phase	Changing from anaerobic to aerobic	2nd aerobic phase
Action	Water-logging soil samples	Air-tight water-logged conditions	Drying to the OWC	Periodic aeration.	Water-logging soil samples	Drying to the OWC	Periodic aeration.
Aim	Lowering of soil redox status to induce anoxic conditions	Maintain-ing anoxic conditions	Increasing soil redox status to create aerobic conditions	Minerali-zation of the reduced metabo-lites	Lowering of soil redox status to induce anoxic conditions	Increasing soil redox status to create aerobic conditions	Mineraliza-tion of the reduced metabolites
Samp-ling points	1st After about 4 weeks	2nd End of 1st anaerobic phase	3rd After about 4 weeks of aeration	4th End of 1st aerobic phase	End of 2nd anaerobic phase	After about 4 weeks of aeration	End of 2nd aerobic phase

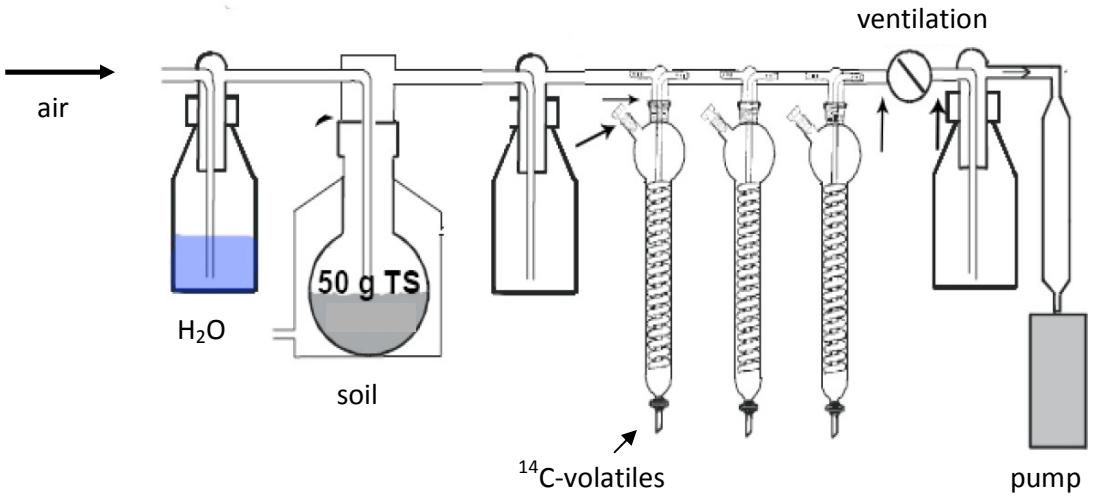

Figure 11: Biodegradation aeration system

2.4.2 Application of 14C-HCB and ^{14}C-DDT and initiation of the anaerobic-aerobic cycles experiments

^{14}C-HCB (sp. radioactivity = 649.55 Bq μg^{-1}) in cyclohexane was mixed with unlabelled HCB (10 µg/µL) to make the application standard (specific radioactivity = 108.09 Bq μg^{-1}). 420 µl of the application standard was applied to an aliquot of 5 g dried and pulverised soil sample in a 50 ml glass beaker. After evaporation of the solvent, the soil aliquot was carefully stirred with a spatula and then transferred to a 250 ml glass beaker where it was mixed with 95 g (dry weight equivalent) of air-dried soil. The spiked soil samples were transferred to 130 ml incubation flasks, compacted to a density of 1.3 g cm^{-3}, water content adjusted to WHC (for determination of WHC, see section 2.18) and an excess of water was added up to 2 ml above the soil surface to ensure that the soils were water-logged. The incubation flasks were then tightly closed. The amount of ^{14}C-HCB added to each soil sample gave an initial concentration of 30 µg g^{-1} soil (dry weight), corresponding to 295 kBq.

^{14}C- DDT (sp. Radioactivity = 1.3336 KBq μg^{-1}) in toluene was mixed with unlabelled p,p-DDT (10 µg/µL) in n-hexane to make the application standard (sp. radioactivity = 64.36 Bq μg^{-1}), of which 600 µl was applied as for HCB above. The amount of ^{14}C-DDT added to each soil sample also gave an initial concentration of 30 $\mu g g^{-1}$ soil (dry weight), corresponding to 97.723 kBq.

After application of the HCB and DDT ^{14}C-labeled standards, the spiked soil samples in the flasks were incubated at 30 ^{o}C in the dark.

2.4.3. Drying, mineralization, volatilisation and soil sampling in the ^{14}C-HCB and ^{14}C-DDT anaerobic-aerobic cycles experiments

Drying was done by aerating the soils continuously at a flow rate of about 1 Lmin^{-1} until a weight equivalent to the OWC (for determination of OWC, see section 2.18) was reached. The flasks were closed and thereafter aerated for 1 hour twice every week. The CO_2 and volatile compounds were trapped in a closed laboratory system (Fig. 10).

Sampling of soil aliquots was done periodically as shown in table 5. Before sampling, the test system was aerated for 1 hour. To facilitate the first soil sampling, a second set of 16 replicates for each compound was prepared and sacrificed after 4 weeks. This was so as to ensure that anaerobic conditions were maintained in the main experiment. The amount of ^{14}C-labeled standards added to each soil (sp. radioactivity of 6.68 Bq µg^{-1} for DDT and 9.27 68 Bq µg^{-1} for HCB) gave final concentrations 30 µgg^{-1} soil (dry weight), corresponding to 25.127 kBq for HCB and 10.081 kBq for DDT.

Table 5: Sampling plan

1st anaerobic phase		1st anaerobic phase		2nd anaerobic phase	2nd anaerobic phase	
After about 4 weeks	End of anaerobic /beginning of aerobic phase	After about 4 weeks of aeration	End of aerobic/beg-inning of anaerobic phase	End of anaerobic/ beginning of aerobic phase	After about 4 weeks of aeration	End of experiment

At the end of each incubation time interval, ^{14}C-volatile compounds, $^{14}CO_2$, extractable ^{14}C-residues, non-extractable ^{14}C-residues and the metabolite pattern were determined. During the aerobic phase, the water content was maintained at OWC. There were a total of 7 sampling points for soil aliquots.

2.5 DDT anaerobic experiment

The aim of this experiment was to study the factors and processes involved in the anaerobic degradation of DDT in tropical clay soils.

2.5.1 Experimental set-up

The two tropical clay soils - field soil and paddy soil - were used for the study.
Non-labeled 4,4'-DDT dissolved in picograde n-hexane was applied to an aliquot of 5 g dried and pulverised soil sample in a 50 ml beaker glass. After evaporation of the solvent the soil aliquot was carefully stirred with a spatula and then transferred to a 250 ml glass beaker where it was mixed with 165 g (dry weight equivalent) of air-dried soil. The spiked soil samples were transferred to 250 ml incubation brown open flasks, compacted to a density of 1.3 g cm^{-3}, water-logged and then covered with silicon corks in which redox electrodes (for details on redox sensors, see 2.10) had been inserted. The flasks were then incubated at 30 ^{o}C in the dark for 8 weeks. In the first 6 weeks, methane and soil sampling was done weekly. The last sampling was done on the 8th week. The redox status of the soil was measured throughout the experimental period. The soil aliquots were sampled under a nitrogen tent (Toepffer Lab Systems, Goeppingen Germany) to ensure anaerobic conditions. Other parameters measured were pH, reducible Fe, dissolved organic carbon (DOC), ions, metabolite pattern, methane, CO_2 and N_2O production.

2.6 Extraction of the soil samples for GC analysis

Accelerated solvent extraction (ASE) was used for the extraction of chlorobenzenes and DDTs from soil. Prior to extraction soils were defrosted at 20 °C, homogenized and aliquots of the soil samples (approximately 5 g dry weight) mixed with diatomaceous earth (DE) – a drying and dispersive agent - in different DE:soil ratios depending on the wetness of the samples. The extraction was performed in an ASE-200 (Dionex, Idstein, Germany) at a temperature of 90 ^{o}C, a pressure of 100 bar and 5 extraction cycles. Hexane/acetone (3:1 v/v) of analytical grade, were used as extraction solvents. For determination of radioactivity in liquid samples, 0.5 ml aliquots of the extract were mixed with 4.5 ml of Ultima Gold XR scintillation cocktail and measured in a Tricarb 1900 TR liquid scintillation counter (Packard, Dreieich, Germany).

2.7. Drying, concentration and clean-up of the extracts

2.7.1 Drying, concentration and clean-up of HCB extracts

For drying and clean-up, the method used by Brahushi et al. (2004) was adopted. The procedure consists of liquid–liquid separation to get rid of the water followed by drying with Na_2SO_4 (pre-heated at 600 °C). Kuderna–Danish concentration of the dried extract was done to about 2 ml, followed by clean-up with 2 g Chromaband florisil SPE columns (Machery-Nagel, Dueren, Germany) pre-conditioned with 10 ml picograde hexane. Elution was done

with picograde n-hexane to give a final volume of 15 ml. The cleaned samples were stored at -20 °C prior to GC analysis. For each chlorobenzene the losses during extraction and clean up were measured and the results corrected by the respective recovery correction factors. The recoveries of the various standards are shown in figure 12.

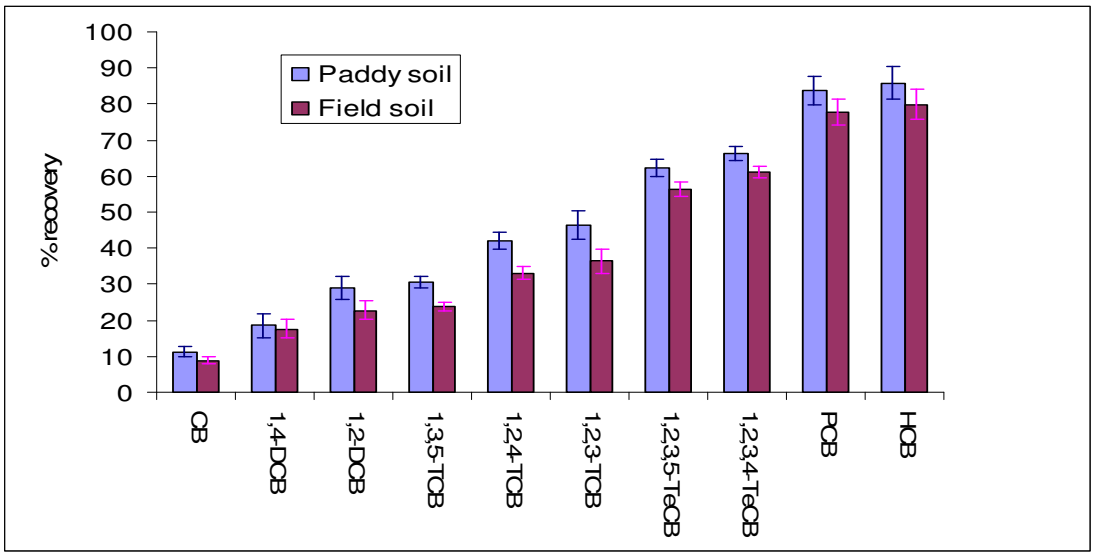

Figure 12: Percentage recoveries of chlorobenzenes in the paddy and field soils

2.7.2 Drying, concentration and clean-up of DDT extracts

The crude ASE extracts were dried with Na_2SO_4 (pre-heated at 600 °C) and rotary evaporated at 40 ^oC and a rotation speed of 100 rpm, to a final volume of about 1 ml. To remove interferences, the concentrated crude extracts were cleaned-up by column chromatography. The solvents used were of residue quality. The glass columns were 250 mm long with an inner diameter of 24 mm. Elution flow rates were about 0.1 ml/s. The clean-up column stationary phase consisted of: 5 g silica gel, 2.5 g alumina (basic, super active) + 3% H_2O, followed by topping with Na_2SO_4. The silica gel, alumina and Na_2SO_4 had been pre-heated at 600 ^oC for 24 hours. The columns were conditioned with 30 ml hexane:dichloromethane (1:1). The crude extract was then introduced into the column and eluted with 60 ml hexane:dichloromethane (1:1). The cleaned extract was rotary evaporated to a final volume of about 1 ml. It was then reconstituted to 5 ml in picograde hexane in volumetric flasks (5 ml) and transferred into 5 ml brown vials which were then stoppered with caps having Teflon septa. The brown vials were stored at -20 ^oC for subsequent gas chromatography. For each available standard the losses during extraction and clean up were measured and the results corrected by the respective recovery correction factors. The recoveries of the various standards are shown in figure 13.

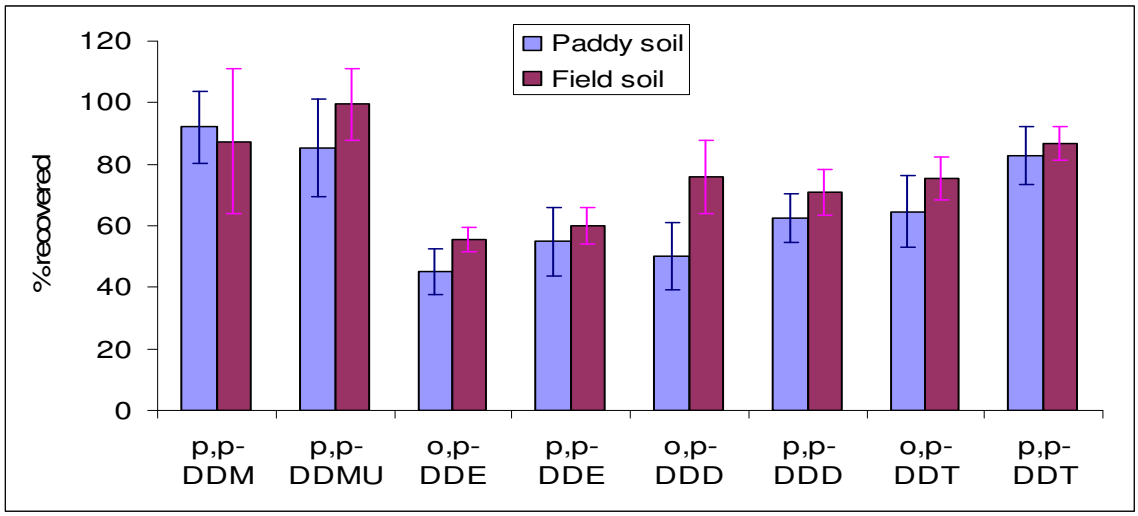

Figure 13: Percentage recoveries of DDT and its metabolites

2.8. GC analysis

The analysis of the chlorobenzenes and DDTs was carried out on a GC-ECD system (Trace GC, 2000 Series, ThermoQuest, Egelsbach, Germany) equipped with a DB-5 capillary column (30 m length, 0.32 mm ID and 0.25 µm film thickness, J&W Scientific, USA) and an AS 2000 autosampler. Detector temperature: 290 ^{o}C, base temperature of 280 ^{o}C, reference current of 1 nA, pulse amplitude of 50 V and pulse width of 1µs. Helium was used as carrier gas (70 kPa in constant pressure flow mode) with a flow rate of 20 ml min^{-}1 and nitrogen as make-up gas (30 ml min^{-}1). The injection volume was 1 µl in the PTV mode (1 min) with a split flow of 50ml/min.

2.8.1 Identification and quantification of chlorobenzenes

The GC parameters were: temperature program of 60^{o}C for 2 min, 10^{o}C min^{-}1 to 220 ^{o}C; Injector (PTV) temperature: 50 ^{o}C to a maximum of 300^{o}C in 3 minutes. The chlorobenzenes were identified by comparing their retention times with reference standards and quantification was performed by using linear calibration curves (r^2 = 0.99) of the individual chlorobenzenes. The method detection limits were: 100 ng µl^{-1} for CB, 100 pg µl^{-}1 for DCBs, 10 pg µl^{-}1 for TCBs, 5 pg µl^{-}1 for TeCBs and 1 pg µl^{-}1 for PCB and HCB.

2.8.2 Identification and quantification of DDTs

The GC parameters were: temperature program of 50^{o}C for 1 min, 30 ^{o}C min^{-}1 to 220 ^{o}C with a hold time of 2 minutes, 2 ^{o}C min^{-}1 to 220 ^{o}C and 10 ^{o}C to 270 ^{o}C; Injector (PTV) temperature: 50 ^{o}C to a maximum of 300^{o}C in 3 minutes. The DDTs were identified by

comparing their retention times with reference standards and quantification was performed by using linear calibration curves ($r^2 = 0.99$) of the individual DDTs. The method detection limits were 200 pg μl^{-1} for p,p-DDM, 10 pg μl^{-1} for p,p-DDMU, 5 pg μl^{-1} for o,p-DDT, o,p-DDD, p,p-DDE, p,p-DDT, p,p-DDD and 1 pg μl^{-1} for o,p-DDE.

2.8.3 Quality assurance

Prior to GC analysis, p,p-DDT standard was injected to check for degradation in the injection pot. Analysis was undertaken only when degradation of DDT was below 15%. This standard was also injected after every 20 samples. Whenever degradation was found to be higher than 15 %, remedial action was undertaken and the affected samples analyzed again. The highest and lowest concentration standard mixtures were analyzed after every 20 samples to confirm the integrity of the calibration curve.

Apart from correcting for the losses of each metabolite (2.8.1 and 2.8.2) further measures were taken to ensure the accuracy of the results. For ^{14}C-spiked soil samples, the radioactivity losses at each preparation step were monitored. For the non-labelled DDT samples, HCB was used as an internal standard for the sample preparation process. High resolution gas chromatography-high resolution mass spectrometry (HRGC-HRMS) analysis was used to confirm the identity of the peaks (Table 6).

2.9. Non-extractable residues and mass balance

The residual radioactivity in the soil after extraction (non-extractable residues) was determined by combusting aliquots of the soil samples with a sample oxidizer (Oxidizer 306, Packard, Dreieich, Germany), automatically trapping the evolved $^{14}CO_2$ in Carbo-Sorb E (Packard, Dreieich, Germany) and mixing it with Permafluor E (Packard, Dreieich, Germany) prior to liquid scintillation counting (Tricarb 1900 TR, Packard, Dreieich, Germany). Addition of the measured radioactivity of the ^{14}C-volatile compounds, $^{14}CO_2$, extractable and non-extractable ^{14}C-residues, was done to establish the ^{14}C-mass balance.

2.10. Determination of redox potential

The redox sensors used to monitor the redox potential were prepared in the laboratory. The platinum and silver wires, used for the platinum and reference electrodes respectively, were obtained from VWR International GmbH, Munich Germany. The wires were fitted into capillary tubes. A porous ceramic plate (0.5 inches diameter, 15 bar) was used instead of a semi-permeable membrane in the reference electrode, and was obtained from Geotechnik

Hans Herbert Mennerich, Hannover Germany. The glue used to hold the electrode components together was obtained from Wevo-Chemie GmbH, Ostfildern-Kemnat, Germany. The electrodes were fitted into the incubation flasks (Fig. 10), but with openings for insertion of the electrodes on opposite ends. 50 g soil was mixed with non-labeled pesticide to give a final concentration of 30 µg $g^{-}1$ of soil. The soil was then added into the flasks and carefully compacted to avoid damaging the electrodes. Water was added up to 2 ml above the soil level followed by closing of the flasks. The redox potential (Eh) was measured using a high-input impedance voltmeter and the readings were corrected viz

Eh = Voltmeter reading (V) + 0.2 V or Voltmeter reading (mV) + 200 mV

2.11 Methane, CO_2 and N_2O sampling and analysis in the DDT anaerobic experiment

The production of methane, CO_2 and N_2O was quantified by sampling periodically (Table 4). 1 cm^3 of gas in the headspace above the soil surface with a gas tight Hamilton syringe which was fixed to a needle inserted through the silicon cork into the headspace of the incubation flask. The gas samples were then injected into helium-filled 100 ml flasks. The gas samples were analysed by a GC-FID (GC 14A, Shimadzu, Duisburg, Germany), according to the analytical procedure published by Loftfield et al. (1992). The computer-controlled analytical system consists of a gas chromatograph equipped with a flame ionization detector (FID), an electron capture detector (ECD), and pressure-controlled inlets for up to 64 sample containers. The system automates sample injection, the analysis of CH_4, CO_2, and N_2O in each sample and the subsequent evacuation of the sample containers. The oven temperature was kept constant at 60 °C, while the detector temperature was 280 °C. Nitrogen was used as the carrier and make-up gas. Whenever the concentration was above the detection limit, dilution of the gas samples was done by measuring out a 1 ml sample into 100 ml helium filled flasks.

2.12 Analysis of reducible Fe in the DDT anaerobic experiment

Approximately 0.1 g soil aliquots (oven dry mass) in 2 ml Eppendorf tubes were extracted with 1 ml of 1M HCl for reduced Fe and with 1 ml of 10% $NH_3OH.HCl$ in 1M HCl for total reducible Fe. $NH_3OH.HCl$ is a reducing agent and reduces all the reducible Fe to Fe (II). Shaking was done for 24 hours followed by centrifugation at 6000 g for 10 minutes in a Biofuge Pico centrifuge (Heraeus Instruments, Osterode Germany). 100 µl of the supernatant was pipetted for spectrophotometric analysis. Dilutions for both reduced and reducible Fe extracts were done using 1M HCl.

A Varian Cary 50 UV-Visible dual beam spectrophotometer (Australia) was used for analysis using the method of Stookey (1971) that measures Fe^{2+} only. 100 µl of the sample was pipetted into a disposable cuvette and 900 µl of ferrozine reagent added (ratio of 1:9). Absorbance was measured at 562 nm. The ferrozine reagent was prepared by dissolving 1 g of ferrozine (3-(2-Pyridyl)-5,6-diphenyl-1,2,4-triazine-4',4''-disulfonic acid sodium salt, Sigma-Aldrich.) and 500 g of ammonium acetate (Sigma-Aldrich) in 1L of distilled water.
Fe^{3+} was determined indirectly by getting the difference between the total reducible Fe and the reduced Fe.

2.13 Measurement of total carbon and nitrogen in soils and compost

Approximately 20 mg of oven-dried soil samples were ground and their total organic carbon and total nitrogen were analyzed with catalytic combustion under oxygen using an elemental analyzer (Euro EA, Eurovector, Milano, Italy).

2.14. Extraction of dissolved organic carbon (DOC) and ions in the DDT anaerobic experiment

The soil and compost samples were extracted by a variation of the method used by Junko and Zsolany (2008). Whereas Junko and Zsolany (2008) used $CaCl_2$ for extraction of the soils, double-distilled water was used for extraction in this experiment. Double distilled water was added to the samples to give a final soil:water ratio of 1:2 (oven-dry mass:v), followed by shaking the tubes on an overhead shaker for 1 hour. Centrifugation was done at 5000 g for 20 minutes on a Beckmann Coulter J2-21 Centrifuge (Krefeld, Germany) before filtering the supernatant with 0.4 µm polycarbonate membranes (Whatman, Germany). The filtrate was used for the characterization of DOM (section 2.15) and analysis of inorganic ions (section 2.17)

2.15 Characterization and quantification of DOC in the DDT anaerobic experiment

Characterization of the DOC was done using spectrophotometric analysis followed by parallel factor analysis (PARAFAC) of the data. Quantification of DOC was done by total organic carbon (TOC) analysis.

2.15.1 Spectroscopic analysis

Fluorescence excitation emission matrix spectroscopy was used to qualitatively assess different DOC fractions (Coble et al., 1990). An aliquot of the filtrate (section 2.13) was put

into a 1 cm quartz cell and the absorbance at 240 nm was measured in a Varian Bio Cary 50 UV-Visible spectrophotometer (Australia). Dilution with double distilled water was done to give a final absorbance of 0.1 cm^{-1} or less so as to avoid concentration effects (Zsolany, 2003). 2M HCl was added to an aliquot of the diluted filtrate to give an acid:filtrate ratio of 1:100 which resulted in a final pH of 2. This was done to get rid of carbonates and other inorganic forms of carbon. The acidified filtrate was transferred into a 1 cm quartz cell and scanned in the UV-Visible spectrophotometer. The scan was from 600 nm to 240 nm (in dual beam mode). The set-up parameters were average scan time of 0.0125 s, data interval of 5 nm and a scan rate of 24000 nm min^{-1}. This yielded the absorbance spectra.

The cell was then scanned in 3-D mode for fluorescence in a Varian Cary Eclipse Fluorescence Spectrophotometer (Australia). The excitation wavelength (λex) was 240 nm, the emission wavelength 300-600 nm and an excitation increment of 5 nm. The excitation slit was 10 nm while the emission slit was 20 nm. The scan rate was 6000 nm/min with averaging times of 0.05 s. This resulted in excitation emission matrices (EEM). These EEM were corrected for instrument bias as suggested by the instrument manufacturer. Subsequently, the fluorescence spectra were corrected for the inner filter effect with the absorbance spectra (McKnight et al., 2001). The resulting corrected EEM were normalised by dividing with the integral of the Raman scatter peak (excitation wavelength 350 nm) of a corrected blank water spectrum measured along with the samples Afterwards, water spectra, which had been corrected in the same way as the sample spectra, were subtracted. This resulted in fluorescence spectra, which were in Raman units (R.u.) (Stedmon et al., 2003). Finally the Rayleigh scatter peaks were removed and any missing data interpolated (Bahram et al., 2006).

The parallel factor analysis (PARAFAC) model (Carroll & Chang, 1970; Harshman, 1970; Bro, 1998) as implemented in the N-way toolbox (Andersson & Bro, 2000) for Matlab (The Mathworks, USA) was applied for further evaluation of the fluorescence spectra. The model separates and quantifies the factors contributing to fluorescence spectra, e.g. groups of fluorophores or even single fluorophores. The model was run with an increasing number of factors. Non-negativity constraints were applied to the models as fluorescence intensities are always positive. Several model quality parameters such as sum of squared errors, residue plots, and core consistency (Bro & Kiers, 2003) were used to decide on the number of factors best suited to explain the spectra. Core consistency describes the degree of trilinearity of the variation within a PARAFAC model. It is close to 100 % for (mathematically) excellent models. PARAFAC models with a core consistency close to 50 % are mathematically

problematic, but may be acceptable (based on other quality measures). Models with a very low or negative core consistency are invalid.

2.15.2 Quantification of DOC

The acidified filtrates (section 2.13.1) were analyzed for DOC with a Total Organic Carbon analyzer (DIMATEC, Germany). Potassium hydrogen phthalate solutions were used as calibration standards. The concentrations of standards used were 1 µg ml^{-1}, 6 µg ml^{-1}, 11 µg ml^{-1}, 16µg ml^{-1}, 21 µg ml^{-1}, 26 µg ml^{-1} and 31 µg ml^{-1}. The standards were measured before and after the sample analysis. The samples were purged with oxygen for 2 min prior to analysis to ensure complete removal of carbonates. The carrier gas (O_2) had a flow rate of 150 ml min^{-1} while oxygen pressure was set at 4 bar.

2.16 pH measurement

5 g soil (oven- dry weight equivalent) was weighed into 50 ml falcon tubes and double distilled water added to give a final soil:water ratio of 1:2. The tubes were shaken on an overhead shaker for 1 hour. They were then allowed to stand for 1 hour after which they were shaken vigorously for 1 minute, followed by pH measurement on an Inolab pH meter (Wissenschaftlich Technische Werkstätten, Weilheim Germany).

2.17 Analysis of Ions in the DDT anaerobic experiment

The ions were measured to monitor the changes in soil chemistry with reducing redox potential. The soil filtrate (section 2.12 above) was analyzed for anions (Cl^-, NO_2^-, Br^-, NO_3^-, HPO_4^-, SO_4^{2-}) and cations (Li^+, Na^+, NH_4^+, K^+, Ca^{2+}, Mg^{2+}) using a Dionex DX-100 Ion Chromatograph (Germany), with a Dionex AS40 autosampler (Germany) and a Dionex UCI-50 Universal Chromatography Interface (Germany). The analytical columns and column guards were all from Dionex (RFIC™ Ionpack®), Germany): AS4A 4x250 mm column fitted with a AG4A 4x250 mm column guard for anions, and CS12A 4x250 mm column fitted with a CG12A 4x250 mm column guard for the cations. The elution solvents were aqueous H_2SO_4 for cations and a Na_2CO_4/Na_2HCO_3 solution mixture for anions.

2.18 Determination of WHC and OWC

Air-dried and sieved soil and compost samples (2 mm) were pressed into small metal rings (9.4 cm^3) to achieve a soil density of 1.3 g cm^{-3} for the soil (Schroll et al., 2006) and 1.0 g cm^{-3} for the compost. The compacted samples were left to stand in water until they were

saturated. They were then removed from the water and any excess water was allowed to drain off. Gravimetric water content was then determined and taken as the WHC. The saturated samples were put in a sand/kaolinbox (Eijkelkamp, Netherlands) and allowed to equilibrate under a pressure of -1.5 KPa. Gravimetric measurements were done periodically, and when the mass was constant, gravimetric water content was determined and taken as the OWC. ,

2.19 Potential of a 1,2,4-TCB mineralizing community to degrade organochlorine pesticides (OCPs)

This experiment was perfomed to test if the 1,2,4-TCB degrading microbial community had the ability to degrade higher-chlorinated OCPs, with a view to applying it for in-situ remediation. As a first step, the experiment was perfomed in a liquid culture spiked with a cocktail of 27 OCPs that are usually detected in the environment (Shen et al., 2009).

2.19.1 Degrading bacterial community

The soil-borne degrading bacterial community, used in this study, was enriched from a site in Hungary which had been polluted with chlorobenzenes for 25 years (Schroll et al., 2004). From this community, Bordetella sp. F2 was isolated and identified as the key degrading organism able to use 1,2,4-TCB as the sole energy and C source (Wang et al., 2007). The phylogenetic description of the enriched microbial community is found in Wang et al., 2009 (submitted). The active degrading bacterial community which was stored at -80°C, was thawed and after thawing, its 1,2,4-TCB mineralization ability was confirmed by biomineralization experiments.

2.19.2. Biomineralization experiments

Beside the confirmation of the mineralizing capacity, the biodegradation experiments served as a measure to find out whether the microbial community could remain active over the entire 30 weeks study period, without changing the liquid culture media. The microbial community ($1.71x10^6$ CFU) was spiked into 50 mL of liquid media (see section 2.16.3) in special incubation flasks (Brahushi et al., 2004). The starting concentration was similar to that in the cocktail culture ($1.23x10^6$ CFU). After applying 25 µL ^{14}C-1,2,4-TCB to give a final concentration of 15 µg mL^{-1}, the samples were incubated on a shaker (120 rpm) in the dark at 20 ± 1°C (Wang et. al., 2007). Filters (0.20 µm, Sartorius, Göttingen, Germany) were installed at the air inlet and outlet of the flasks. The flasks were connected to a closed laboratory trapping system and aerated twice per week for one hour at an air exchange rate of

1 L/h to trap $^{14}CO_2$ and volatile ^{14}C-substances separately. The trapping system and sampling of the trapping solutions is described in Schroll et al. (2004). In order to keep the TCB concentration in the liquid culture nearly constant, 25 µL ^{14}C-1,2,4-TCB was reapplied after each aeration (Wang et al., 2007). All radioactivity measurements were done in a liquid scintillation counter (Tricarb 1900 TR, Packard, Dreieich, Germany).

2.19.3 OCPs degradation experiment: design, sampling and cell counting

Microbial degradation experiments were performed in a mineral medium (van der Meer et al., 1987) which contained 2.9 g $Na_2HPO_4 \bullet 2H_2O$, 1.5 g KH_2PO_4, 1 g NH_4NO_3, 100 mg $MgSO_4 \bullet 7H_2O$, 50 mg $Ca(NO_3)_2 \bullet 4H_2O$ and 1 mL trace metal solution (Zehnder et al., 1980) per liter of double distilled water. 100 mL of the autoclaved mineral medium was put into each of 10 smooth-necked 250 mL autoclaved conical flasks, under sterile conditions under a flow bank. 100 µL of the OCPs cocktail was added into each of the 10 flasks, resulting in a final concentration of 10 ng mL^{-1} medium for each compound. 0.5 mL of the microbial consortium was spiked into 5 of these incubation flasks to give a starting microbial concentration of 1.23×10^6 CFU. The other 5 flasks served as controls. The flasks were stoppered with autoclaved corks that allow air flow into the flasks while maintaining sterile conditions. The flasks were shaken for one hour on an orbital shaker (120 rpm) to mix the OCPs and the mineral media. The first sampling was then done and thereafter the flasks were returned on the shaker (120 rpm) and shaken continuously in the dark at 20 ± 1°C. Subsequent sampling was conducted on days 2, 5, 8, 16, 32, 64, 97, 164 and 186 during the first phase.

On day 186 the cocktail was reapplied to the liquid media. The microbial culture (1.71×10^6 CFU) was also respiked into the five microbial flasks. This marked the beginning of the second phase of the experiment which lasted for four weeks. Its purpose was to confirm the results of the first experiment. Like in the first phase, the first sampling was done after one hour of shaking. Subsequent samplings were done after one week intervals.

Sampling was always done under sterile conditions under a flow bank. 1 mL was sampled for ultimate GC-MS analysis of OCPs while 100 µL was sampled for determination of colony forming units (CFU). Cell counting was performed by spreading serial dilutions of the liquid culture on Nutrient Broth (Sigma-Aldrich, Taufkirchen, Germany) agar plates and incubating them at 30°C. CFU were determined after 48 h.

2.19.4. Extraction of OCPs, Clean-up, analysis and quantification

10 µL of ^{13}C-OCP internal standard was added to 10 g of Isolute HM-N (diatomaceous earth) in 250 mm long columns with an inner diameter of 24 mm, followed by 1 mL of the liquid culture sample. The columns were allowed to stand undisturbed for one hour and then extracted with 50 mL of acetone:hexane (1:3) at a flow rate of about 0.1 mL sec^{-1}. The extract was rotary evaporated at 50°C and a rotation speed of 100 rpm, to a final volume of about 1 mL.

Table 6: GC-MS parameters for the isomer specific detection of OCPs

GC	MS
Type: Agilent 6890; Column: Rtx-Dioxin2, 40 m, 0.18 mm ID, 0.18 µm film thickness (Restek); Temperature program: 60°C, 1.5 min, 25°C min^{-1}, 140°C, 8°C min^{-1}, 300°C, 20 min; Carrier gas: helium, constant flow: 1.3 ml/min; Injector: Cold injection system CIS 4 (Gerstel); Temperature program injector: 120°C, 12°C s^{-1}, 280°C, 5 min; Temperature transfer line: 300°C; Autosampler: A200S (CTC); Injection volume: 0.5 µl pulsed splitless	Type: MAT 95S (Thermo); Ionisation mode: EI, 50 eV, 260°C ; Resolution: > 9000; Detection: SIM mode

To remove interferences, the concentrated crude extracts were cleaned-up by column chromatography. The solvents used were of residue quality. The glass columns were 250 mm long with an inner diameter of 24 mm. Elution flow rates were about 0.1 mL sec^{-1}. The clean-up column stationary phase consisted of 5 g silica gel, 2.5 g alumina (basic, super active) + 3% H_2O, followed by topping with Na_2SO_4. The silica gel, alumina and Na_2SO_4 had been pre-heated at 600°C for 24 hours. The columns were conditioned with 30 mL hexane:dichloromethane (1:1). The crude extract was introduced into the column and eluted with 60 mL hexane:dichloromethane (1:1). The cleaned extract was rotary evaporated at 50°C and a rotation speed of 100 rpm, to a final volume of about 1 mL. Then it was put into brown vials (placed in a Barkey evaporator at 30°C) to which ^{13}C internal standards of the 27 compounds had been added to establish the method efficiency, and evaporated to 50 µL under a gentle flow of nitrogen. The vials were sealed with caps having Teflon septa. The sealed

vials were stored at -20°C for subsequent high resolution gas chromatography-high resolution mass spectrometry (HRGC-HRMS) analysis. The instrumental parameters are listed in Table 6. The MS was operated in SIM mode and the two most intense ions of the molecular ion cluster or of an abundant fragment ion cluster were monitored for the unlabeled and labeled isomers. Identification and quantification were carried out by applying the isotope dilution method.

2.20. Data analysis

Both univariate and multivariate statistical methods were used to evaluate and analyze the data. Simple computations and graphics were perfomed in Excel, while robust statistical treatment of the data was perfomed in the R program. Where trend analysis over time was necessary, the data were fitted into the linear mixed effects model. To appreciate the differences between and within groups, the data were subjected to multivariate analysis.

2.20.1 Linear mixed-effects model

The linear mixed-effects (LME) model may be viewed as a generalization of the analysis of variance (ANOVA), variance component (VARCOMP) and regression analysis models (Demidenko, 2004). In contrast to classical statistics, which assumes that observations are independent and identically distributed, the mixed-effects model treats clustered data adequately and assumes two sources of variation - within the cluster/group and between the clusters/groups. Two types of coefficients are distinguished in the mixed model: group-averaged and group (or subject) - specific. The LME model was fitted assuming a linear or monotone trend in the period where an effect was analyzed. The model allows for grouping of data and model assumptions—normal distributed residuals and variance homogeneity—were tested (Schramm et al., 2008).

2.20.1.1 Interpreting the ANOVA (significant test p-value) tables

The ANOVA results were used to select the right LME model. In generating the tables, the un-amended field soil (FS) was used as the control. The rows of the generated ANOVA tables are labeled as Intercept (FS), Slope (FS), Intercept (PS), Intercept (CE), Slope (PS) and Slope (CE). Intercept (FS) shows the significance of the intercept of the field soil with respect to zero: a significant p-value simply indicates that the intercept is not zero. The second row shows the significance of the slope of the field soil: a significant p-value indicates that there is a change in slope i.e. the line is not parallel to the x-axis. Intercept (PS) shows if there are

significant differences between the intercepts of the paddy and field soils. Intercept (CE) shows whether or not compost caused significant differences between the intercepts of the soils. Slope (PS) shows if there are significant differences between the slopes of the paddy and field soils. Slope (CE) shows whether or not compost caused significant differences between the slopes of the soils. In one case, the table contains Slope (soil:CE). This tests whether there is a significant effect of both soil type and compost on the slope.
In selecting the appropriate model, the ANOVA table is read from the bottom upwards. For instance, a significant slope (CE) value would mean a LME model taking compost effect on the slopes into account would be selected.

2.20.2 Multivariate analysis

A multivariate analysis of the data (log transformed if necessary for linearity) centred over time was performed. Values below the detection limit were substituted for by uniformly distributed random values between zero and the minimum analyzed value. To analyse the differences in the chemical concentrations between the controls and treated samples, a derivation of the principal response curve method was used - an ordination method based on redundancy analysis (RDA), (Van den Brink and Ter Braak, 1998). Principal response curve analysis is a multivariate technique which is suitable to investigate the effects of species (e.g. chemicals) and their changes over time (Moser et al., 2007), and is increasingly being used in data analysis (Cuppen et al., 2000; Hense et al., 2005; Hense et al., 2008; Schramm et al., 2008). The method makes it possible to summarize the effects of all the species and to display them in a single diagram. The environmental variable is the concentration of the samples, with sampling time as the co-variable (Van den Brink and Ter Braak, 1999). The focus is on the deviation of the concentrations of the species in the treated samples from those in the controls (Moser et al., 2007). For the experimental design, this method is equivalent to a two-step procedure which involves the transformation of the data (centering with respect to sampling days) and a principal component analysis (Van den Brink and Ter Braak, 1999).
In contrast to the principal response curve method, the groups (controls and treatments) were not averaged. This enabled a better visibility of differences within each group. A linear combination of variables (changes in the abundance of chemical concentrations) was calculated to determine the strength of the differences in the chemical composition between the samples at each sampling date, expressed as canonical coefficients (c_{dt}) (Hense et al., 2005). The curves were derived by plotting the c_{dt}-values against time. The line at y=0

represents the mean of both the controls and treatments, while the c_{dt}'s represent the deviation of the controls and treatments from this mean, for each sampling date.

Loadings indicate the direction and strength of the change in concentration for each chemical (Hense et al., 2005). For samples with positive c_{dt}-values, chemicals with positive loadings tend to have higher concentrations, while chemicals with lower loadings tend to have lower concentrations (Moser et al., 2007). The concentrations of chemicals (for samples with positive c_{dt}-values) increase with increasing loading and c_{dt}-values. For samples with negative c_{dt}-values, chemicals with positive loadings tend to have lower concentrations, while chemicals with negative loadings tend to have higher concentrations. The concentrations of chemicals (for samples with negative c_{dt}-values) increase with decreasing loading and c_{dt}-values (or increasing negative absolute values).

Apart from the PRC, a PRC statistic (declared variance) is given (Moser et al., 2007). Several canonical axes (also referred to as components) can be used to discriminate between the groups, but usually the first canonical axis (first component) is the most important. The power of a canonical axis (component) to explain the data is reported as a percentage (declared variance), and shows the percentage contribution of the axis to the sum of all axes. If the declared variance of the first component is high (e.g. 70 %), then it is sufficient in explaining the data and no other axis is needed. However, if the declared variance of the first component is low (e.g. 30 %), a second component is needed to explain the data (For details see Van den Brink and Ter Braak, 1998 and 1999). Lastly, the significance of the differences between the groups in the PRC curve is also reported. Significance is tested for by a Monte–Carlo permutation test (Hense et al., 2008; Moser et al., 2007), and the same method was used for these data.

In terms of interpretation, in a PRC of treatments and controls - with the controls having positive c_{dt}-values and the treatments having negative c_{dt}-values - chemicals with positive loadings will have higher concentrations in the controls, while chemicals with negative loadings will have higher concentrations in the treatments (Hense et al., 2005; Moser et al., 2007). Chemicals with loadings of zero will either be present in equal concentrations in both controls and treatments, or will be absent from both controls and treatments. Therefore a zero loading means that these chemicals do not contribute to the differences between the controls and treatments.

3.0 Results

3.1 Mineralization, volatilization and degradation of ^{14}C-DDT and ^{14}C-HCB under aerobic conditions

3.1.1 Mineralization and volatilization of HCB and DDT in field and paddy soils

The objective of the experiment was to determine the natural capability of the paddy and field soils to mineralize HCB and DDT. The null hypothesis was that there would be no differences in capability of the soils to mineralize either DDT or HCB. Figure 14 shows the cumulative $^{14}CO_2$ released with time from the mineralization of DDT and HCB in the field and paddy soils. As can be seen, the soils had a higher capacity of mineralizing DDT relative to HCB. About 3 % and 0.14 % cumulative mineralization of ^{14}C-DDT and ^{14}C-HCB respectively, was achieved in both soils after 84 days. There was very low volatilization in both soils and for both compounds at below 0.6 % (Figure 15). However, there was higher volatilization of DDT relative to HCB.

Table 7: Significant test *p*-values for the ^{14}C mineralization and volatilization of DDT and HCB in the paddy and field soils under aerobic conditions

Group	CO_2 - DDT	Volatiles - DDT	CO_2 - HCB	Volatiles - HCB
Intercept (FS)	<0.0001	<0.0001	<0.0001	<0.0001
Slope (FS)	<0.0001	0.3097	0.0012	0.9559
Intercept (PS)	0.0832	0.7146	0.6353	0.0493
Slope (PS)	0.5860	0.1252	<0.0001	<0.0001

To appreciate the differences in the mineralization and volatilization of each of the two compounds in the two soils, the non-cumulative $^{14}CO_2$ and ^{14}C-volatilization data were linearized by log-transformation and tested for significance (Table 7). The data were then fitted into the linear mixed-effects model (Figures 16, 17, 18 and 19). There was a decrease in mineralization of ^{14}C-DDT over time in both soils (Fig. 16). However, there were no significant differences ($p = 0.05$) in the mineralization rate (slope) of ^{14}C-DDT between the two soils (Table 8 and Fig. 16). There were also no significant differences in volatilization of ^{14}C-DDT between the two soils (Table 8 and Fig. 17).

$^{14}CO_2$ production from the mineralization of ^{14}C-HCB increased over time in the paddy soil as indicated by a positive slope (Fig. 18 and Table 8). $^{14}CO_2$ production decreased in the field soil as indicated by a negative slope (Fig. 17 and Table 8). This shows that there were higher amounts of $^{14}CO_2$ produced in the paddy soil relative to the field soil. The differences in

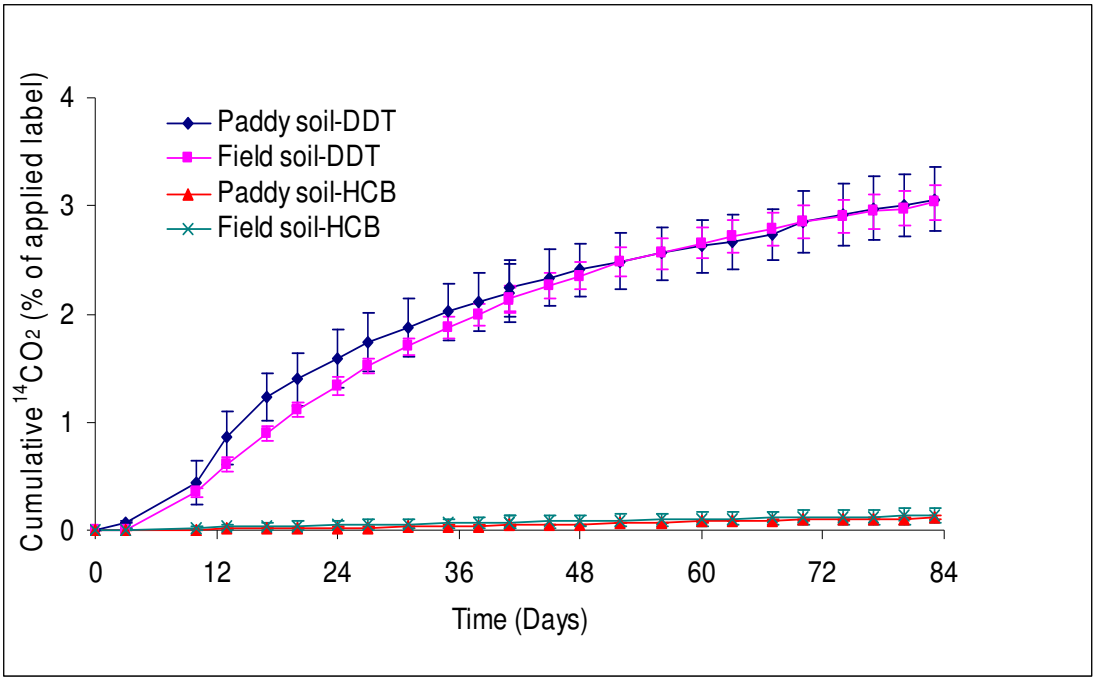

Figure 14: Cumulative ^{14}C mineralization of ^{14}C-DDT and ^{14}C-HCB with time in the paddy and field soils under aerobic conditions

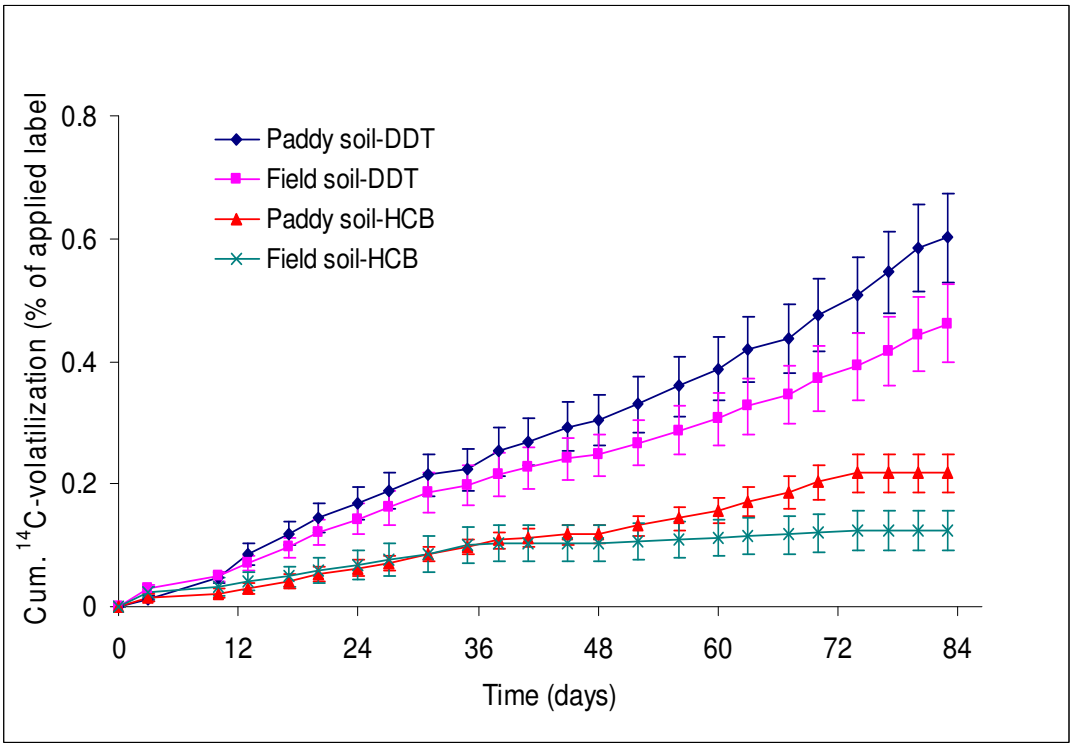

Figure 15: Cumulative volatilization of ^{14}C-DDT and ^{14}C-HCB with time in the paddy and field soils under aerobic conditions

$^{14}CO_2$ production from ^{14}C-HCB mineralization between the two soils were significant (Table 7).

The volatilization of ^{14}C-HCB increased over time in the paddy soil, as indicated by a positive slope (Fig. 19 and Table 8), but decreased in the field soil as indicated by a negative slope (Fig. 19 and Table 8). This shows that there was higher volatilization in the paddy soil relative to the field soil. The differences in the volatilization of ^{14}C-HCB between the two soils were significant (Table 7).

Table 8: Slopes {Log(µg/g soil)/day} and intercepts {Log(µg/g soil)} of LME model fitting of Log^{14}C-HCB mineralization and volatilization in the field and paddy soils under aerobic conditions.

	HCB mineralization		HCB volatilization		DDT mineralization		DDT volatilization	
	Intercept	Slope	Intercept	Slope	Intercept	Slope	Intercept	Slope
FS	-6.25	-0.0025	-6.32	-0.01	-0.396	-0.0036	-8.9141	-0.00001
PS	-7.02	0.0125	-6.15	0.01	-0.396	-0.0036	-8.9141	-0.00001

3.1.2 Degradation of HCB and ^{14}C-HCB mass balance in the field and paddy soils

GC analysis showed that the applied HCB (30 µg/g soil) was quantitatively recovered and only traces of PCB could be detected (Table 9). There was a significantly higher build-up of HCB non-extractable residues in the paddy soil relative to field soil, but the extractable residues were comparable between the two soils (Fig. 17). Owing to the negligible mineralization, the HCB experiment was stopped on day 84. The ^{14}C-radioactivity mass balance is shown in Fig. 20.

Table 9: Concentrations of HCB extractable residues quality in µg/g soil at the end of the aerobic incubation experiment

Compound	Paddy soil	Field soil
PCB	0.0163±0.0033	0.0202±0.0059
HCB	27.328±4.6045	28.273±3.1929

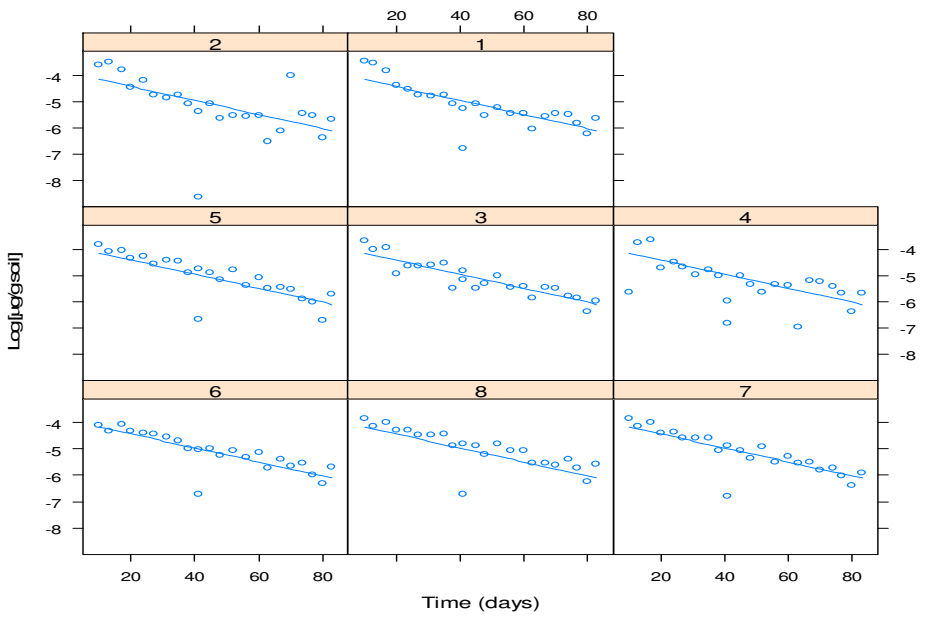

Fig. 16: LME model fitting for log-transformed $^{14}CO_2$ data of ^{14}C-DDT mineralization (**y-axis = Log $^{14}CO_2$ produced**) in the paddy and field soils under aerobic conditions.

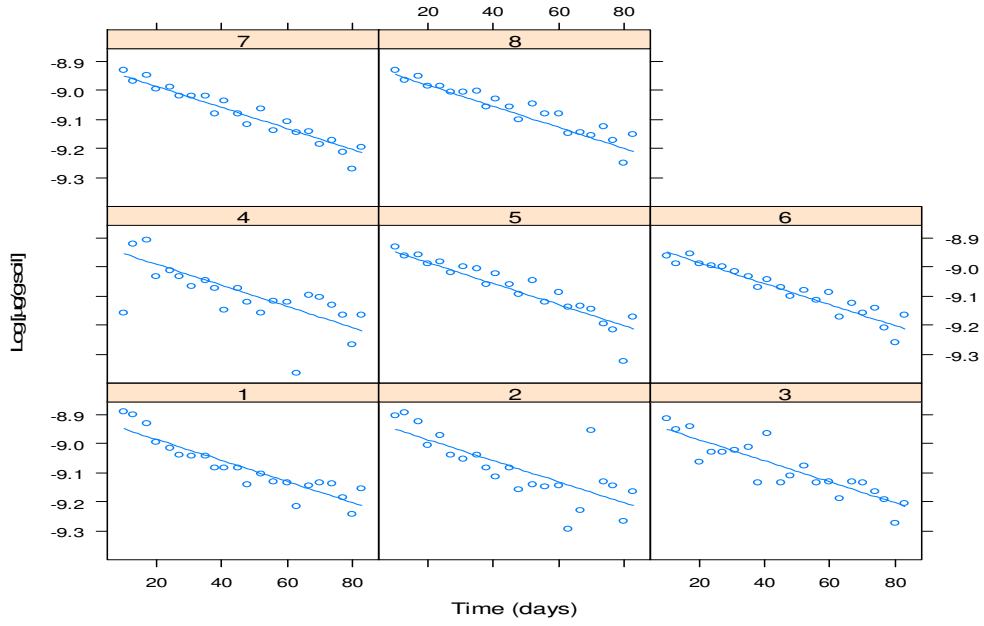

Fig. 17: LME model fitting for log-transformed ^{14}C-volatilization data of ^{14}C-DDT mineralization (**y-axis = Log ^{14}C-volatiles**) in the paddy and field soils under aerobic conditions.

1-4 = Paddy soil replicates; 5-8 = Field soil replicates

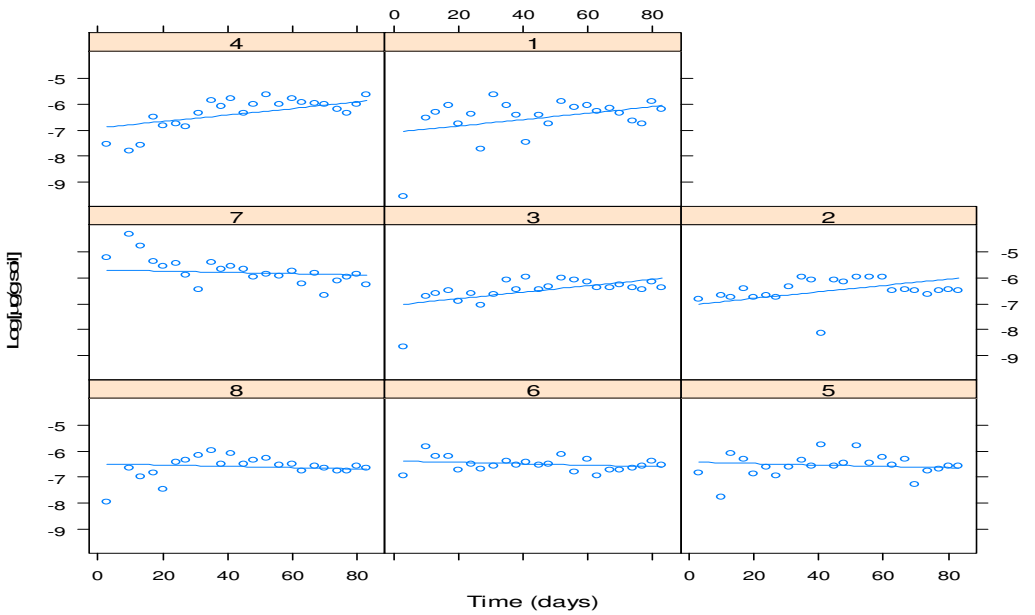

Fig 18: LME model fitting for log-transformed $^{14}CO_2$ data of ^{14}C-HCB mineralization (**y-axis = Log $^{14}CO_2$ produced**) in the paddy and field soils under aerobic conditions.

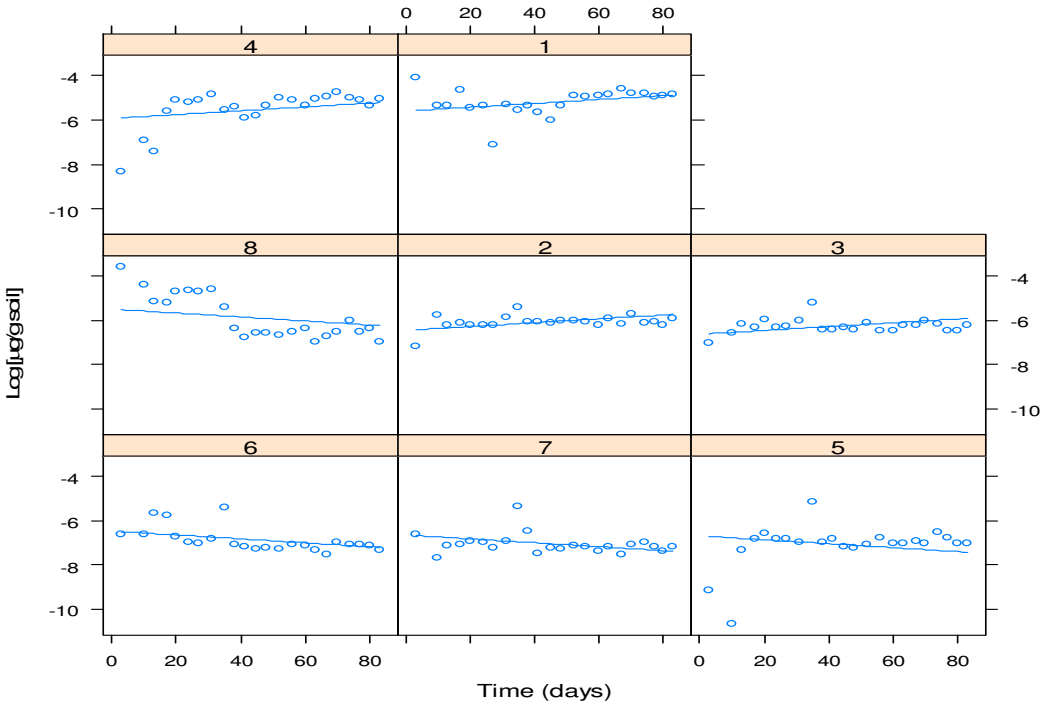

Fig 19: LME model fitting for log-transformed ^{14}C-volatilization data of ^{14}C-HCB (**y-axis = Log ^{14}C-volatiles released**) in the paddy and field soils under aerobic conditions

1-4 = Paddy soil replicates; 5-8 = Field soil replicates

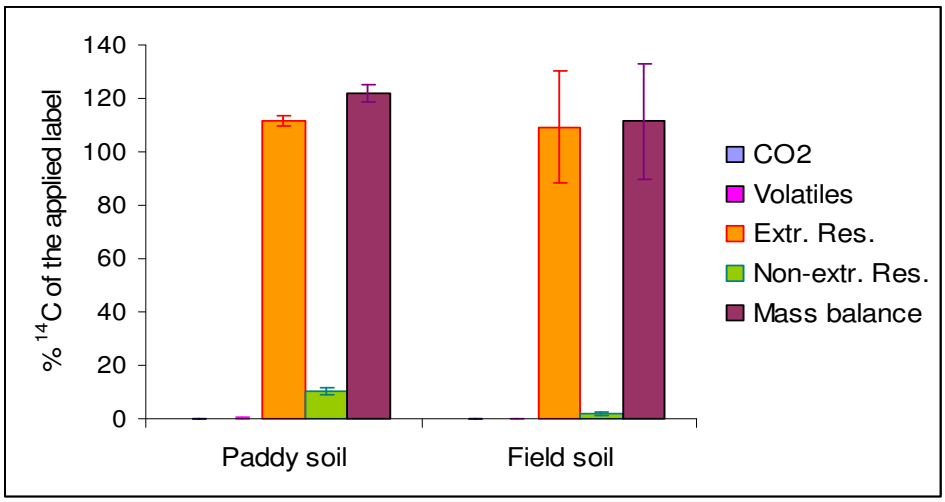

Figure 20: HCB ^{14}C- mass balance as percentage of the applied radioactivity at the end of the aerobic incubation experiment.

3.1.3 Effect of compost on the mineralization and volatilization of aged DDT residues

On day 84, compost was added to the DDT-spiked soils. The purpose of this experiment was to study the effect of an additional carbon source on the mineralization of DDT residues, which were assumed to be aged. The hypothesis was that the supplementary carbon source would lead to increased mineralization because DDT is usually degraded co-metabolically (Aislabie, 1997).

The data (non-cumulative) after day 84 was linearized by log-transformation, and analyzed for significant differences (Table 10). The mineralization and volatilization data were then fitted into the linear mixed-effects model (Fig. 21 and Fig. 22). Mineralization decreased over time in both soils as indicated by negative slopes (Fig. 21). The paddy soil had a higher negative slope compared to the field soil (Fig. 21, Fig. 22 and Table 11).This indicates that there was a higher rate of decrease in $^{14}CO_2$ production in the paddy soil. This therefore means that there were higher amounts of $^{14}CO_2$ produced in the field soil relative to the paddy soil.

Compost did not have a significant effect on the rate of $^{14}CO_2$ production (Tables 10, 11 and Fig. 21). However, there were higher amounts of $^{14}CO_2$ in the compost-amended samples in both soils as indicated by the higher intercept values (Fig. 21 and Table 11). This means that compost resulted in an overall increase in the amounts of $^{14}CO_2$ without affecting the rate of production.

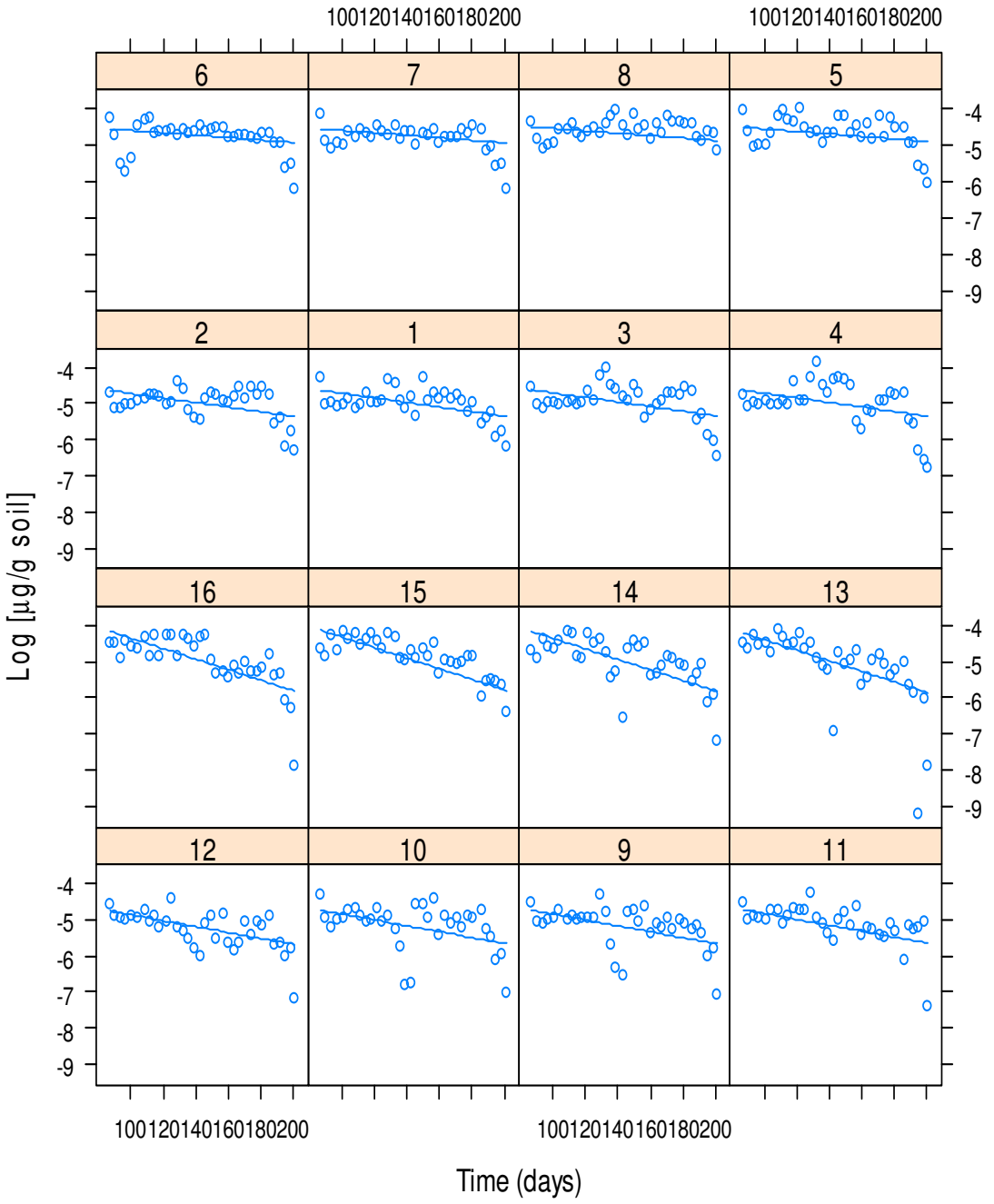

Fig. 21: LME model fitting for log-transformed $^{14}CO_2$ data of ^{14}C-DDT mineralization (**y-axis = Log $^{14}CO_2$ produced**) in the paddy and field soils under aerobic conditions after compost amendment

1-4 = Paddy soil replicates; 5-8 = Paddy soil+compost replicates; 9-12 = Field soil replicates; Field soil+compost replicates

Volatilization also decreased over time in both soils as indicated by negative slopes (Fig. 22 and Table 11). There were significant differences in volatilization between the soils (Table 10). The field soil had a higher negative slope relative to the paddy soil (Fig. 22 and Table 11). This indicates that there was higher rate of decrease in volatilization in the field soil. This means that there was higher volatilization in the paddy soil compared to the field soil. Compost did not have a significant effect on volatilization in both soils (Tables 10 and 11).

Table 10: Significant test p-values (p = 0.05) for the mineralization and volatilization of ^{14}C-DDT after compost amendment under aerobic conditions

Group	CO2	Volatiles
Intercept (FS)	<0.0001	<0.0001
Slope (FS)	<0.0001	<0.0001
Intercept (PS)	0.0001	0.2238
Intercept (CE)	0.0002	0.4272
Slope (PS)	<0.0001	0.0004
Slope (CE)	0.1608	0.9968
Slope(soil:CE)	0.0001	

Table 11: Slopes {Log(µg/g soil)/day}and intercepts {Log(µg/g soil)} for the LME model fitting of ^{14}C-DDT mineralization and volatilization

	DDT mineralization		DDT volatilization	
	Intercept	Slope	Intercept	Slope
Field soil	-4.04	-0.011	-4.34	-0.014
Field soil + compost	-3.11	-0.011	-4.34	-0.014
Paddy soil	-4.09	-0.048	-5.13	-0.0098
Paddy soil + compost	-2.96	-0.048	-5.13	-0.0098

3.1.4 Degradation of DDT and ^{14}C-DDT mass balance in the field and paddy soils

The metabolite pattern showed that p,p-DDD, p,p-DDE and p,p-DDMU were formed in equal amounts in the compost-amended and un-amended paddy soil (Fig. 23). A similar pattern was noted in the field soil samples. However there were significant differences in the amounts of p,p-DDD and p,p-DDE formed in the two soils (Fig. 23). The paddy soil had higher amounts of p,p-DDD while the field soil had higher amounts of p,p-DDE.

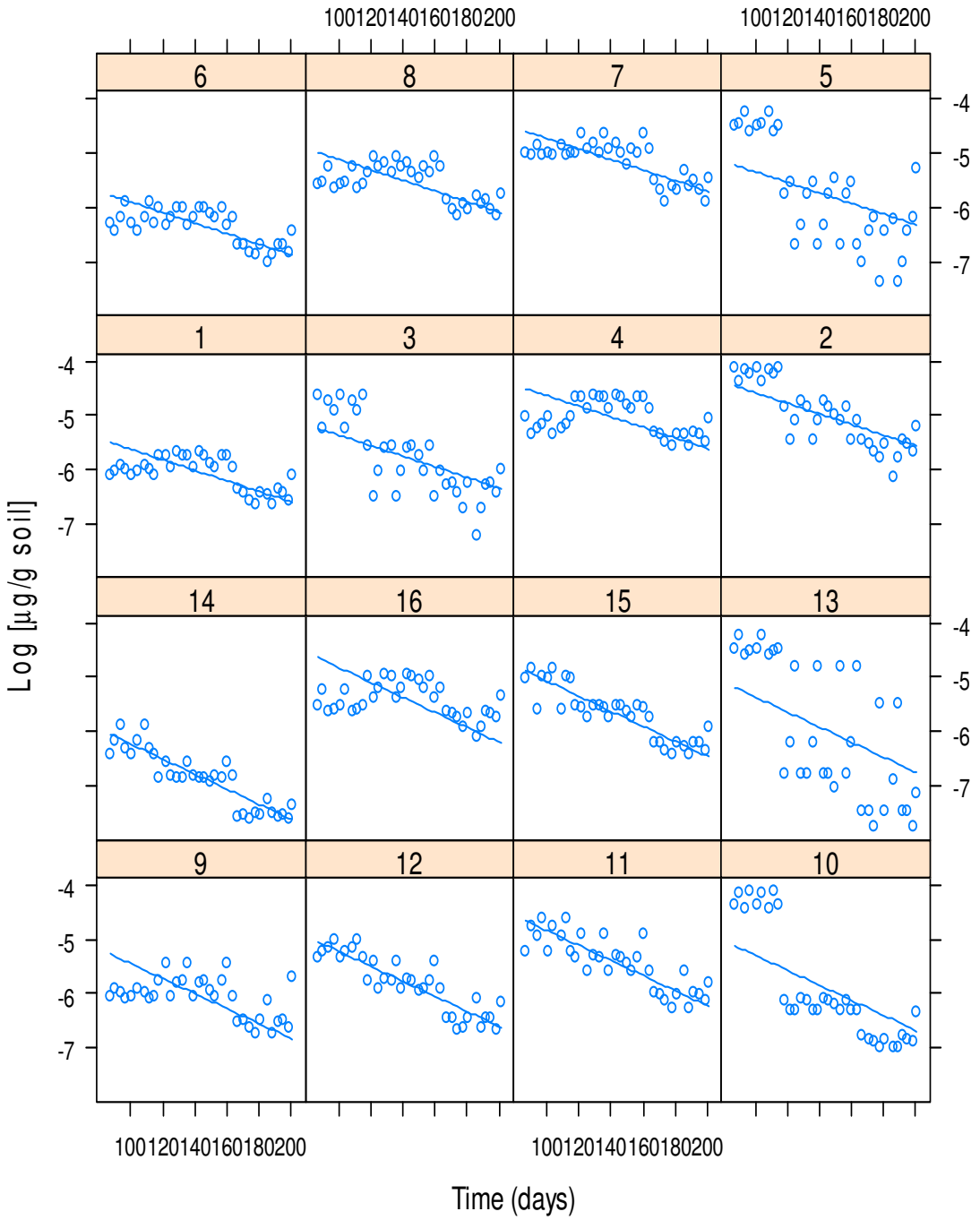

Fig 22: LME model fitting for log-transformed ^{14}C-volatilization data of ^{14}C-DDT (**y-axis = Log ^{14}C-volatiles released**) in the paddy and field soils under aerobic conditions after compost amendment

1-4 = Paddy soil replicates; 5-8 = Paddy soil+compost replicates; 9-12 = Field soil replicates; Field soil+compost replicates

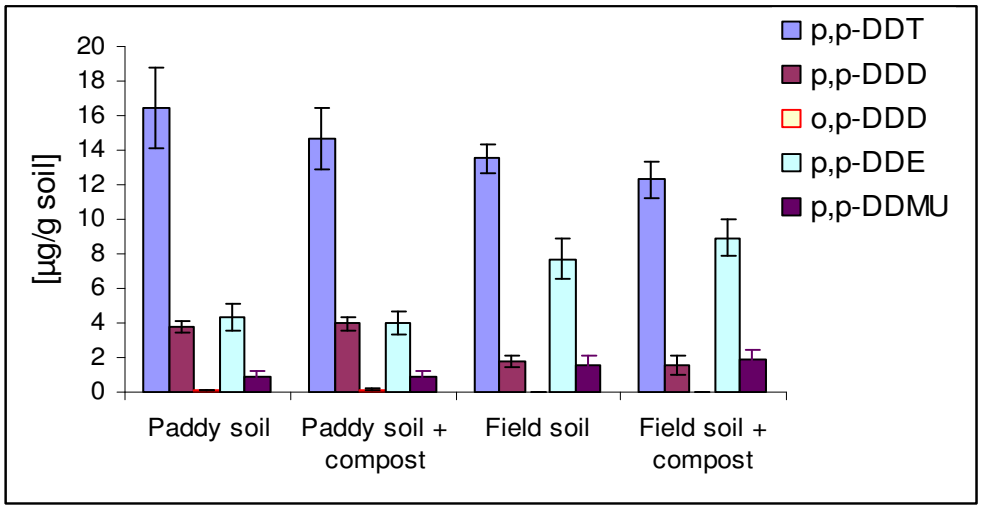

Figure 23: Metabolite pattern of DDT degradation in the paddy and field soils at the end of the aerobic incubation experiment.

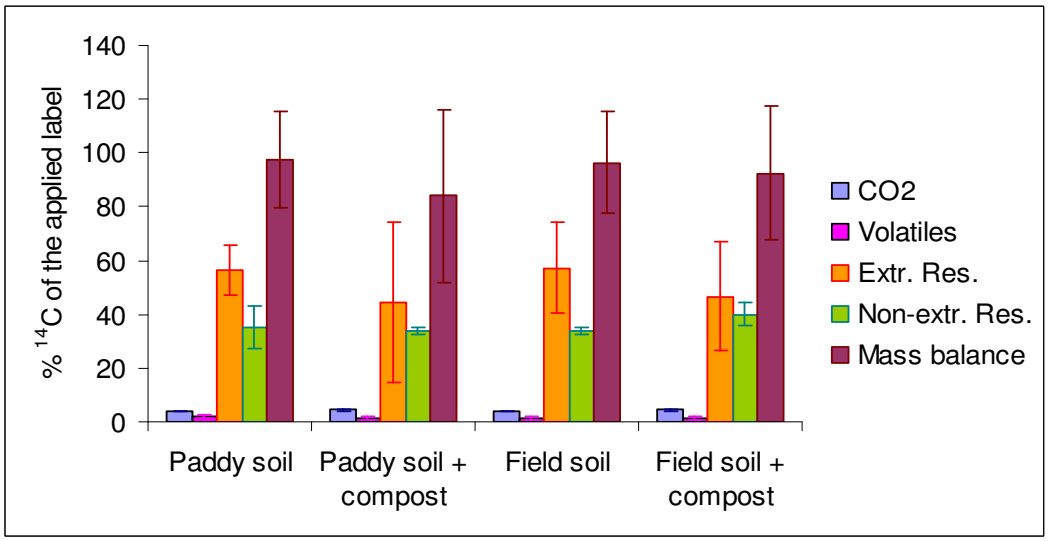

Fig 24: DDT residues and mass balance as percentage of the applied radioactivity at the end of the aerobic incubation experiment.

The extractable, non-extractable residues and mass balances of the radioactivity were comparable in both soils (Fig 24). There were no significant differences ($p = 0.05$) between the extractable and non-extractable residues of ^{14}C-DDT in the two soils.

3.2 Mineralization, volatilization and degradation of ^{14}C-HCB under anaerobic-aerobic cycles

3.2.1 Mineralization and volatilization of HCB

The purpose of this study was to induce degradation and mineralization of HCB in the paddy and field soils. The hypothesis was that anaerobic conditions would cause dechlorination and that the subsequent lower-chlorinated products would be amenable to mineralization under aerobic conditions. Figure 25 shows the cumulative mineralization of HCB over the entire experimental period. There was higher mineralization in the paddy soil relative to the field soil. The mineralization was higher in the paddy soil relative to the compost-treated paddy soil during the first aerobic phase. However, this changed in the second aerobic phase where the compost-treated samples had higher mineralization. This effect was not noted in the field soil samples.

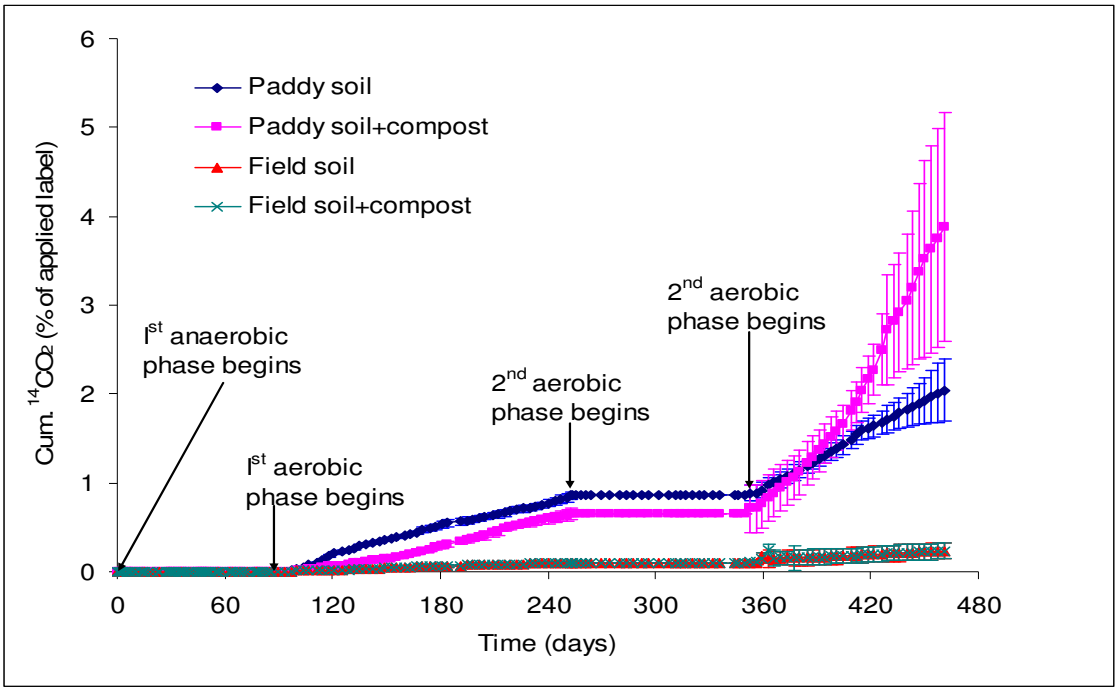

Figure 25: Cumulative $^{14}CO_2$ produced by ^{14}C -HCB mineralization in the paddy and field soils under anaerobic-aerobic cycles conditions.

To better appreciate the results, separate statistical analysis was done on the data (non-cumulative) of the two aerobic phases. The data for the first and second aerobic phases were linearized by log-transformation and tested for significance (Table 12). As can be seen there were significant differences ($p = 0.05$) between the groups in both phases, except for the soils in the second aerobic phase. The log-transformed data was fitted into the linear mixed-effects model (Fig. 26 for the first aerobic phase and Fig. 27 for the second aerobic phase) and the

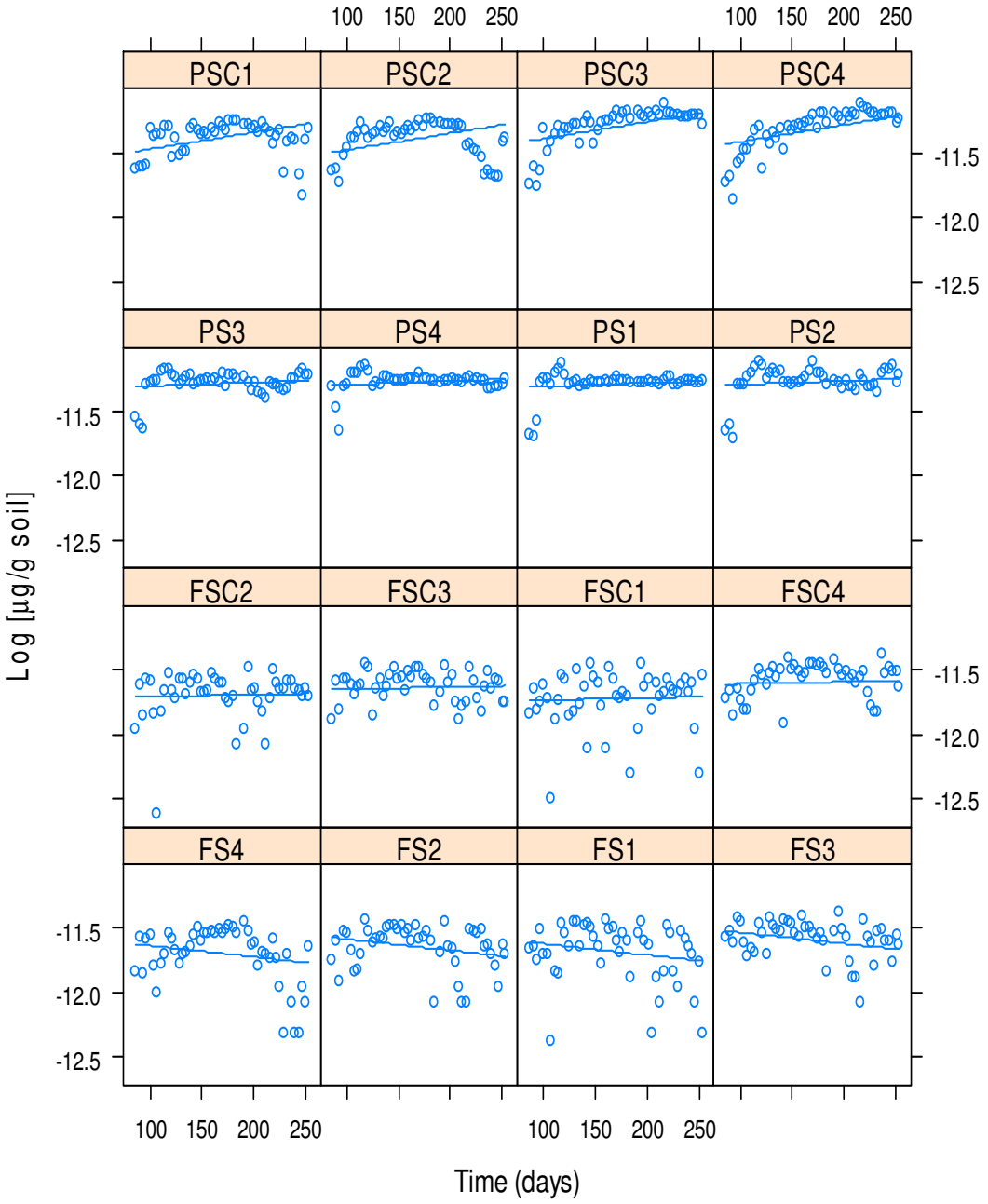

Figure 26: LME model fitting for log-transformed $^{14}CO_2$ data of ^{14}C-HCB mineralization (**y-axis = Log $^{14}CO_2$** produced) in the paddy and field soils during the first aerobic phase of the anaerobic-aerobic cycles experiment.

PS1-PS4 = Paddy soil replicates; PSC1-PSC4 = Paddy soil+compost replicates; FS1-FS4 = Field soil replicates; FSC1-FSC4 Field soil+compost replicates

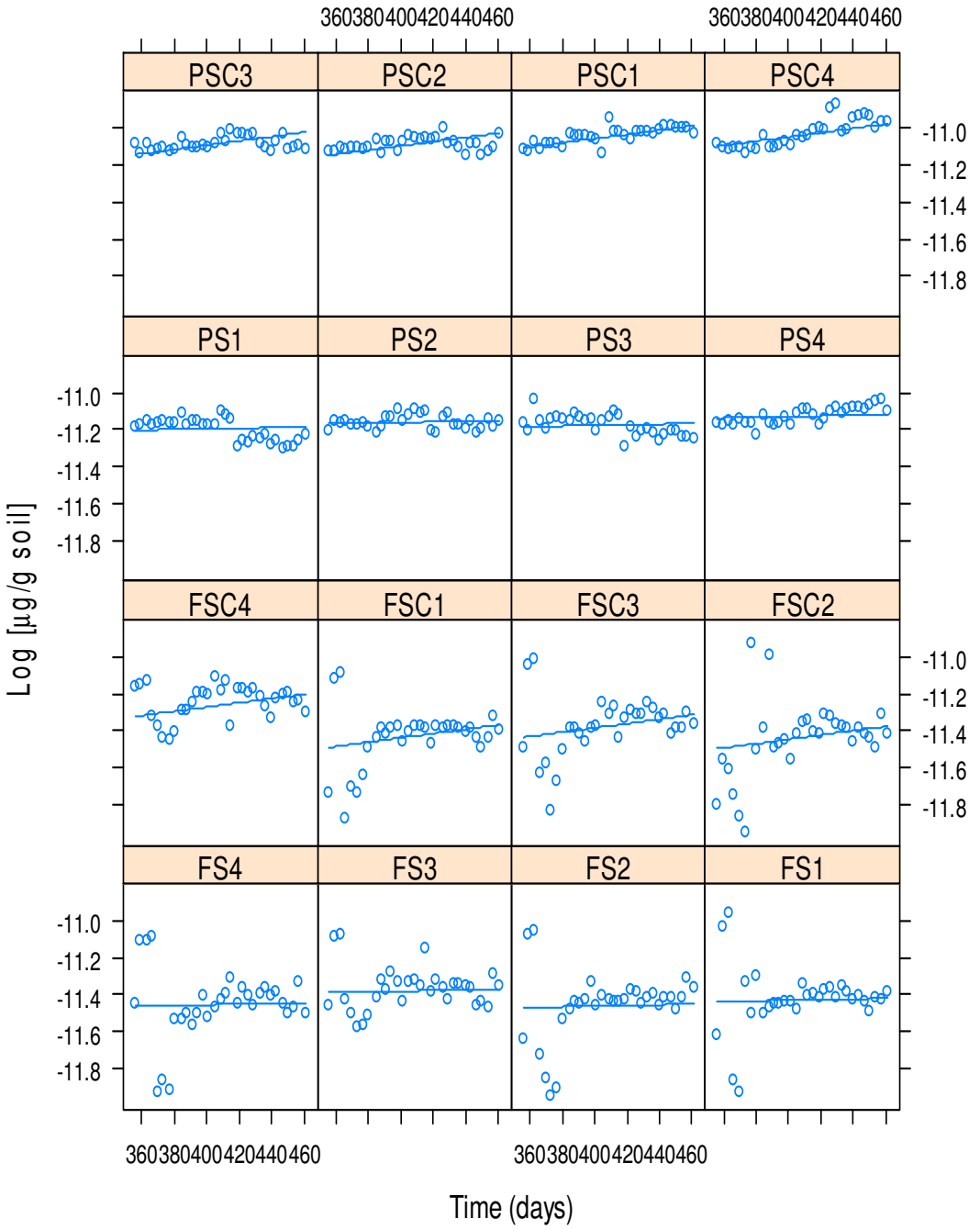

Figure 27: LME model fitting for log-transformed $^{14}CO_2$ data of ^{14}C-HCB mineralization (**y-axis = Log $^{14}CO_2$ produced**) in the paddy and field soils during the second phase of the anaerobic-aerobic cycles experiment.

PS1-PS4 = Paddy soil replicates; PSC1-PSC4 = Paddy soil+compost replicates; FS1-FS4 = Field soil replicates; FSC1-FSC4 Field soil+compost replicates

graph parameters are shown in table 13. There were higher slopes in the paddy soil samples relative to the field soil samples (Table 13). The compost-treated samples had higher mineralization rates in both soils relative to the untreated samples, indicated by higher positive slopes (Fig. 26 and Table 13). Indeed, the un-amended field soil had a negative slope indicating a decrease in mineralization with time (Fig. 26). The same effect (higher mineralization in compost-amended soils) was noted in the second aerobic phase where the amended soils had positive slopes – indicating an increase in mineralization, while the untreated ones had negative slopes – indicating a decrease in mineralization with time (Fig. 27 and Table 13).

Table 12: Significant test p-values (p = 0.05) for ^{14}C-HCB mineralization and volatilization in the field and paddy soils during the first and second aerobic phases of the anaerobic-aerobic incubation experiment.

group	$^{14}CO_2$ mineralization		^{14}C-volatilization	
	Phase 1	Phase 2	*Phase 1	Phase 2
Intercept (FS)	<0.0001	<0.0001	<0.0001	<0.0001
Slope (FS)	0.0014	0.0032	<0.0001	<0.0001
Intercept (PS)	<0.0001	<0.0001	<0.0001	0.1132
Intercept (CE)	0.0933	0.0060	0.0325	0.9689
Slope (PS)	<0.0001	0.7347	<0.0001	0.0001
Slope (CE)	<0.0001	0.0003	0.0267	0.5562

*Excluding first time period (up to day 139)

Table 13: Slopes {Log(µg/g soil)/day} and intercepts {Log(µg/g soil)} for the LME model fitting of Log$^{14}CO_2$ produced from ^{14}C-HCB mineralization in the paddy and field soils during the anaerobic-aerobic cycles incubation experiment.

Group	Phase 1		Phase 2	
	Intercept	Slope	Intercept	Slope
Field soil (FS)	-5.33	-0.004303	-4.62	-0.000745
Field soil+compost (FSC)	-6.05	+0.001223	-4.41	+0.00753
Paddy soil (PS)	-3.80	+0.002379	-2.49	-0.000745
Paddy soil+compost (PSC)	-4.52	+0.007905	-2.29	+0.00753

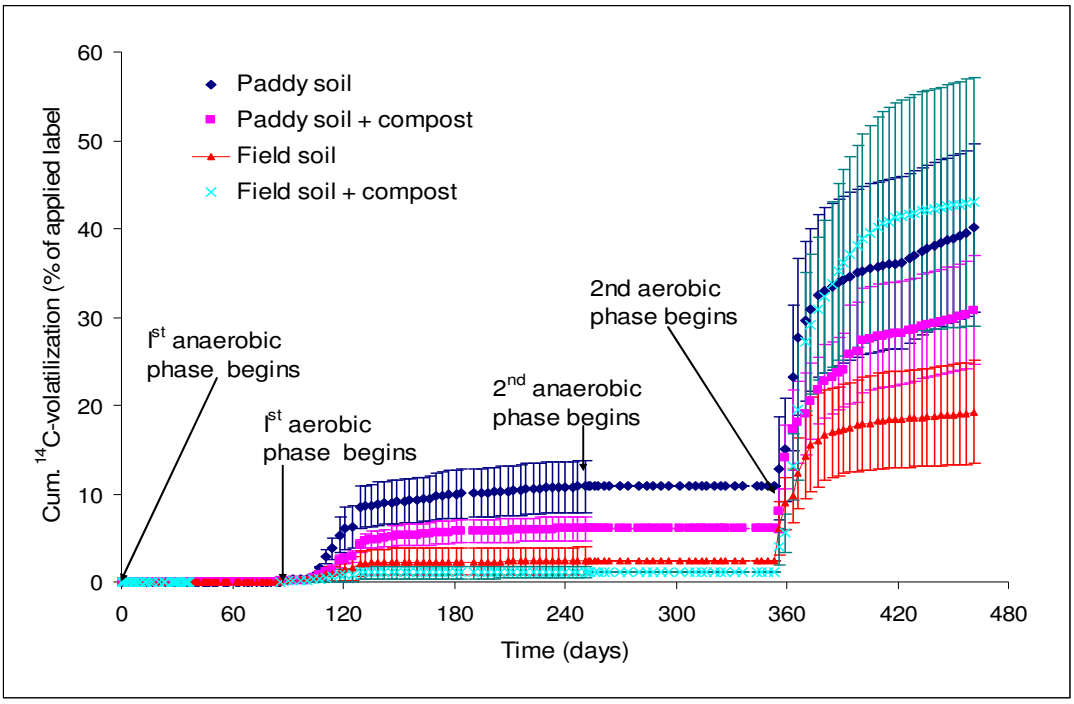

Figure 28: Cumulative ^{14}C-HCB volatilization in the paddy and field soils under anaerobic-aerobic cycles conditions

Figure 28 shows the cumulative volatilization of HCB over the entire experimental period. There was higher volatilization in the paddy soil relative to the field soil. The volatilization was higher in the paddy soil relative to the compost-treated paddy soil during the first and second aerobic phases. However, in the field soil, the volatilization was higher in the soil samples during the first aerobic phase and higher in the compost-treated samples in the second aerobic phase.

The log-transformed data for the volatilization rates in the first and second aerobic phases were tested for significant differences (Table 12). As can be seen, there were significant differences ($p = 0.05$) in slopes of all groups in both phases, except for the compost effect in the second aerobic phase (Table 12). The linearized data was fitted into the linear mixed-effects model (Fig. 29 and Fig. 30). The volatilization slopes were negative for all sets indicating decreasing volatilization rates, with the compost-treated samples having higher absolute slopes in both sets during the first aerobic phase (Fig. 29 and Table 12). This means that the decrease in volatilization was faster in the compost-amended samples. The soils and treatments had the same slopes in the second aerobic phase (Fig. 30 and Table 12), indicating similar volatilization rates.

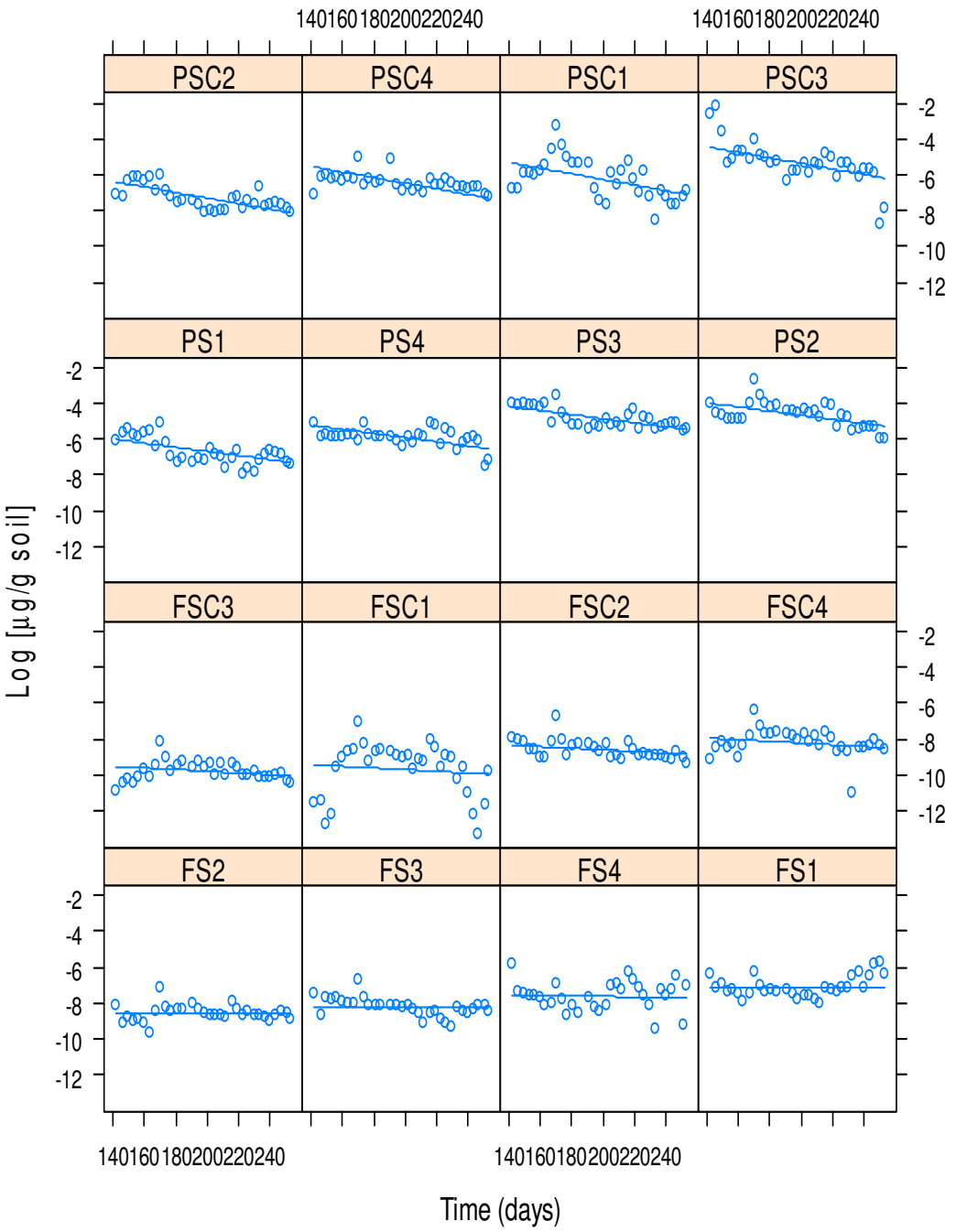

Figure 29: LME model fitting for log-transformed ^{14}C-HCB volatilization data (y-axis = **Log ^{14}C-volatiles** released) in the paddy and field soils during the first aerobic phase of the anaerobic-aerobic cycles experiment.

PS1-PS4 = Paddy soil replicates; PSC1-PSC4 = Paddy soil+compost replicates; FS1-FS4 = Field soil replicates; FSC1-FSC4 Field soil+compost replicates

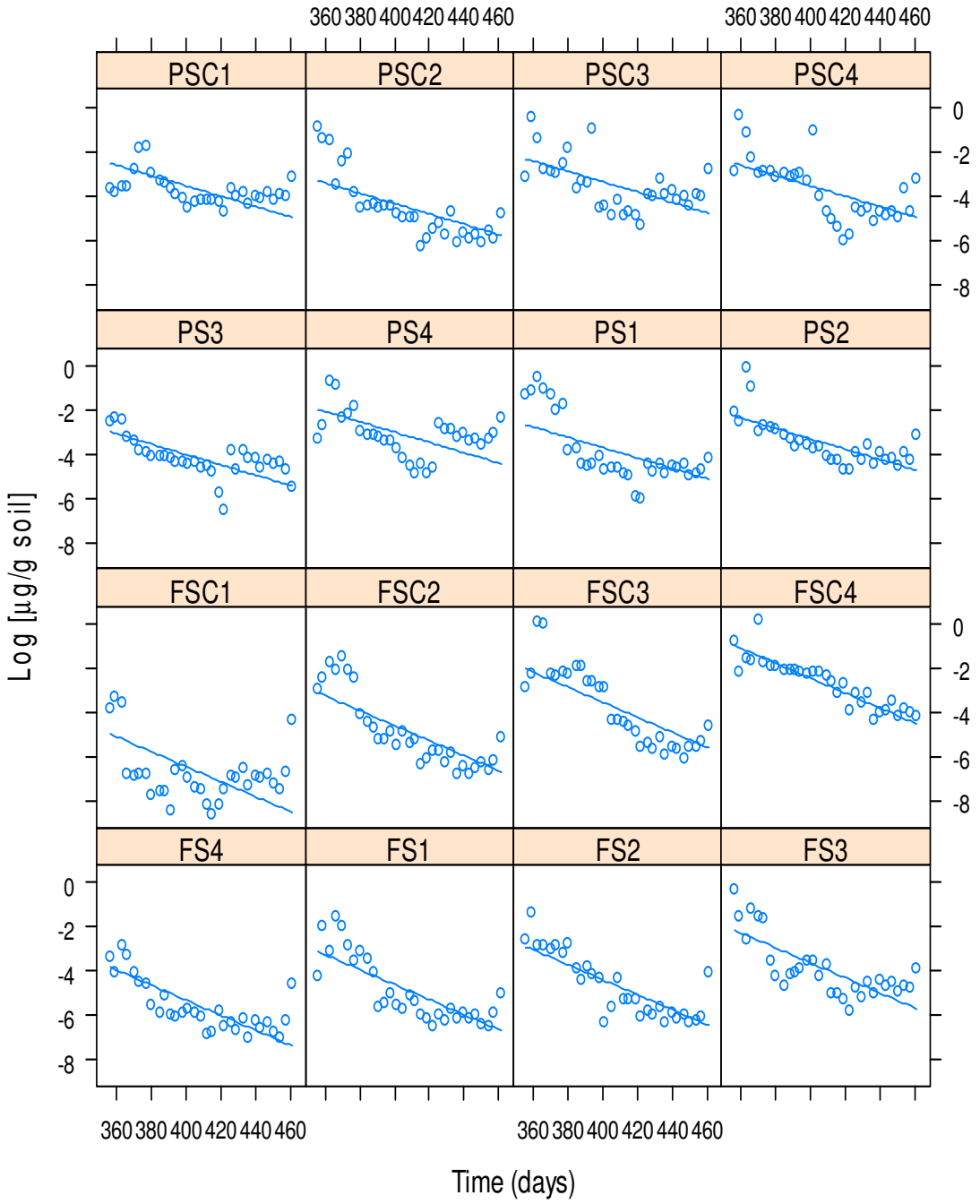

Figure 30: LME model fitting for log-transformed ^{14}C-HCB volatilization data (y-axis = **Log ^{14}C-volatiles** produced) in the paddy and field soils during the first aerobic phase of the anaerobic-aerobic cycles experiment.

PS1-PS4 = Paddy soil replicates; PSC1-PSC4 = Paddy soil+compost replicates; FS1-FS4 = Field soil replicates; FSC1-FSC4 Field soil+compost replicate

Table 14: Slopes {Log(µg/g soil)/day} and intercepts {Log(µg/g soil)} for the LME model fitting of Log^{14}C-volatiles from ^{14}C-HCB volatilization in the paddy and field soils during the anaerobic-aerobic cycles incubation experiment.

Group	Phase 1		Phase 2	
	Intercept	Slope	Intercept	Slope
Field soil (FS)	-5.625	-0.000549	-0.577	-0.033865
Field soil+compost (FSC)	-6.386	-0.004653	-0.577	-0.033865
Paddy soil (PS)	-2.436	-0.011431	-0.276	-0.023309
Paddy soil+compost (PSC)	-3.197	-0.015535	-0.276	-0.023309

3.2.2 HCB degradation, formation of extractable and non-extractable residues

Table 15: Significant test p-values (p = 0.05) for extractable residues formation, non-extractable residues dissipation and HCB degradation during the anaerobic-aerobic cycles incubation experiment.

group	Extractable residues	Non-extractable residues	HCB degradation
Intercept (FS)	<0.0001	<0.0001	<0.0001
Slope (FS)	<0.0001	<0.0001	<0.0001
Intercept (PS)	0.2634	<0.0001	<0.0001
Intercept (CE)	0.0417	0.030	0.0376
Slope (PS)	0.9748	<0.0001	0.1060
Slope (CE)	0.4965	0.018	0.7783

Figure 31 shows the LME model fitting of the ^{14}C-extractable residues data. There were no significant differences (p = 0.05) in slope or intercept between the groups (Fig. 31 and Table 16). Figure 32 shows the LME model fitting of the ^{14}C- non-extractable residues (NERs) data. There were significant differences between all the groups (Table 13). There was higher formation of NERs in the paddy soil samples relative to the field soil samples. There was an overall decrease in the rate of formation of NERs in the field soil, indicated by a negative slope (Fig. 32 and Table 16). The compost-amended field soil had a positive slope (Fig. 32 and Table 16), indicating an increasing rate of formation of NERs. Both the paddy soil sets had positive slopes, with the compost-amended paddy soil having a higher NERs formation rate (Fig. 32 and Table 16).

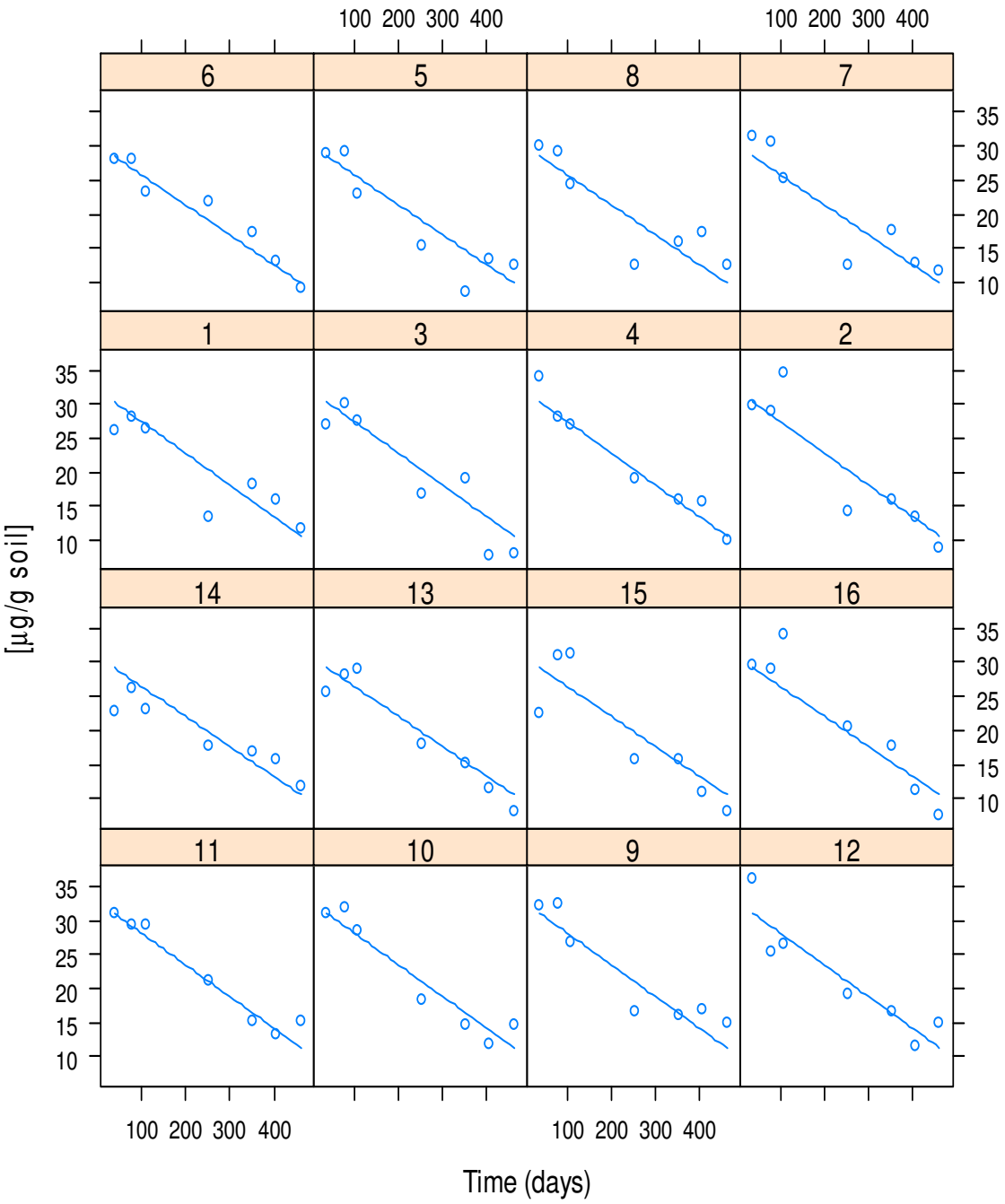

Figure 31: LME model fitting for ^{14}C-HCB extractable residues data (y-axis = **^{14}C-extractable residues**) in the paddy and field soils during the anaerobic-aerobic cycles experiment.

1-4 = Paddy soil replicates; 5-8 = Paddy soil+compost replicates; 9-12 = Field soil replicates; Field soil+compost replicates

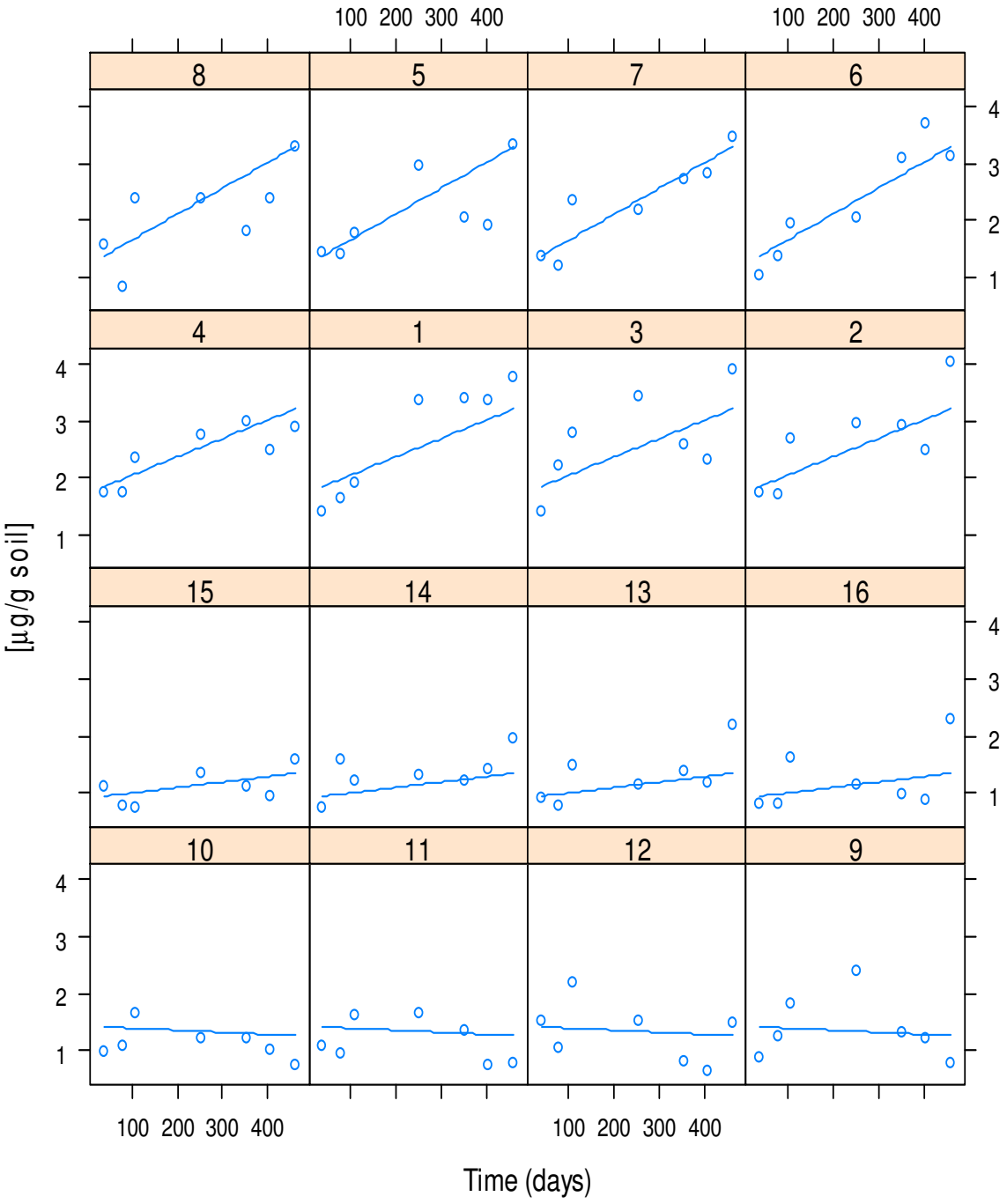

Figure 32: LME model fitting for ^{14}C-HCB non-extractable residues data (y-axis = **^{14}C-non-extractable residues**) in the paddy and field soils during the anaerobic-aerobic cycles experiment.

1-4 = Paddy soil; 5-8 = Paddy soil+compost; 9-12 = Field soil; 13-16 = Field soil+compost

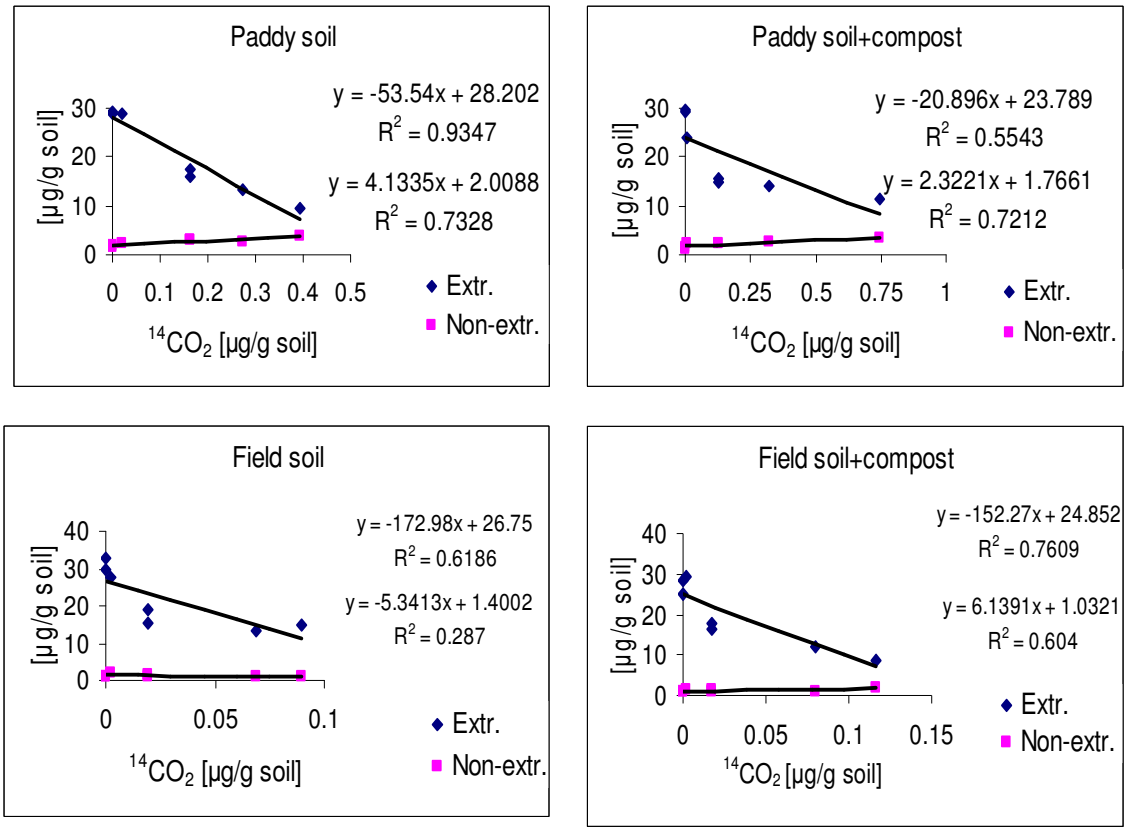

Fig. 33: Correlations of $^{14}CO_2$ with ^{14}C-extractable and ^{14}C-non-extractable residues formed during the degradation of ^{14}C-HCB in the paddy and field soils under anaerobic-aerobic cycles (n = 8, df = 6, Pearson R^2 critical value = 0.3387 (p=0.05))

Table 16: Slopes {(µg/g soil)/day} and intercepts (µg/g soil) for the LME model fitting of ^{14}C-extractable and ^{14}C-non-extractable residues in the paddy and field soils during the anaerobic-aerobic cycles incubation experiment.

Group	HCB extractable residues		HCB non-extractable residues	
	Intercept [µg/g soil]	Intercept [µg/g soil]	Slope [µg/g soil]	Slope [µg/g soil]
Field soil	32.798	-0.0467	1.432	-0.000355
Field soil + compost	32.798	-0.0467	0.9061	0.000955
Paddy soil	32.798	-0.0467	1.729	0.003221
Paddy soil + compost	32.798	-0.0467	1.2029	0.004532

To test whether the extractable and non-extractable residues had an influence on HCB mineralization, cumulative $^{14}CO_2$ values were correlated with ^{14}C-residues (Fig. 33). $^{14}CO_2$

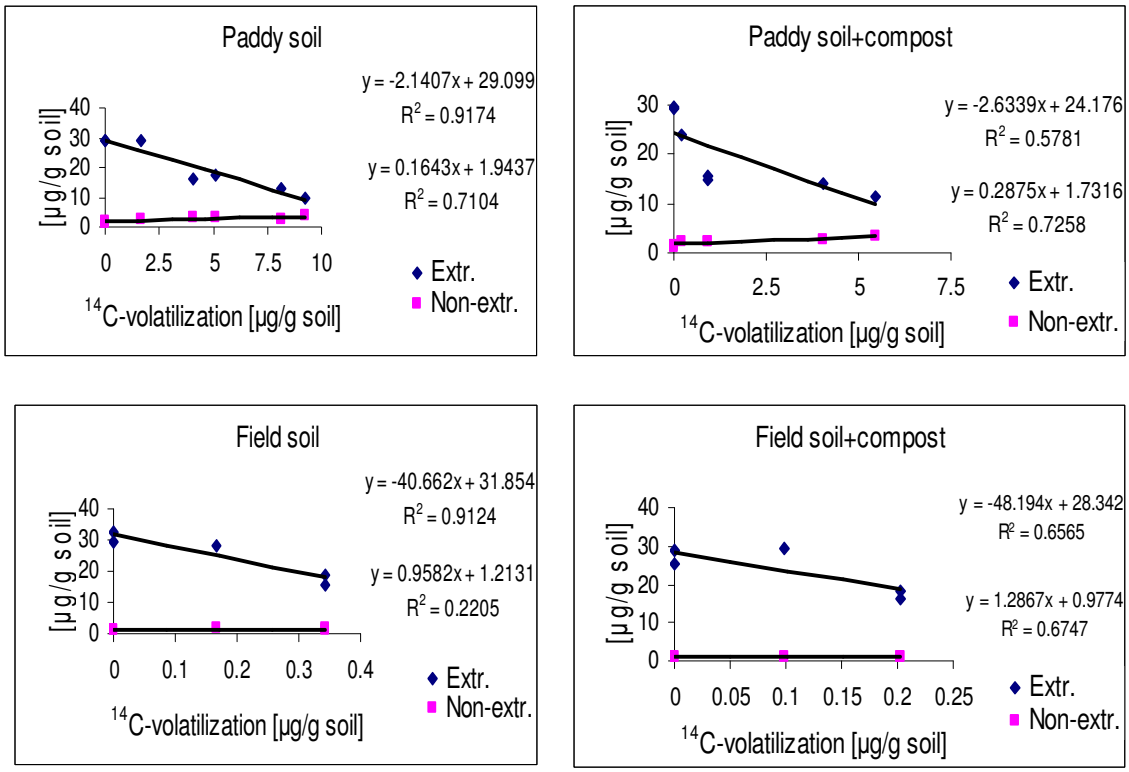

Fig. 34: Correlations of ^{14}C-volatilization with ^{14}C-extractable and ^{14}C-non-extractable residues released during the degradation of ^{14}C-HCB in the paddy and field soils under anaerobic-aerobic cycles (n = 8, df = 6, Pearson's R^2 critical value = 0.3387 (p=0.05) for the paddy soil; n = 5, df = Pearson R^2 critical value = 0.4476 (p=0.05) for the field soil)

had significant negative correlations with extractable residues in all the samples. Apart from the field soil, $^{14}CO_2$ had significant positive correlations with non-extractable residues in all the other samples. In the paddy soil the correlations were stronger in the un-amended soil, while in the field soil the correlations were stronger in the compost-amended soil (Fig. 33). To test whether the extractable and non-extractable residues had an influence on HCB volatilization, cumulative ^{14}C-volatilization values were correlated with ^{14}C-residues (Fig. 34). ^{14}C-volatiles had significant negative correlations with extractable residues in all the samples except for the compost-amended paddy soil. Apart from the field soil, ^{14}C-volatiles had significant positive correlations with non-extractable residues in all the other samples. In the paddy soil the correlations were stronger in the un-amended soil, while in the field soil the correlations were stronger in the compost-amended soil (Fig. 34).

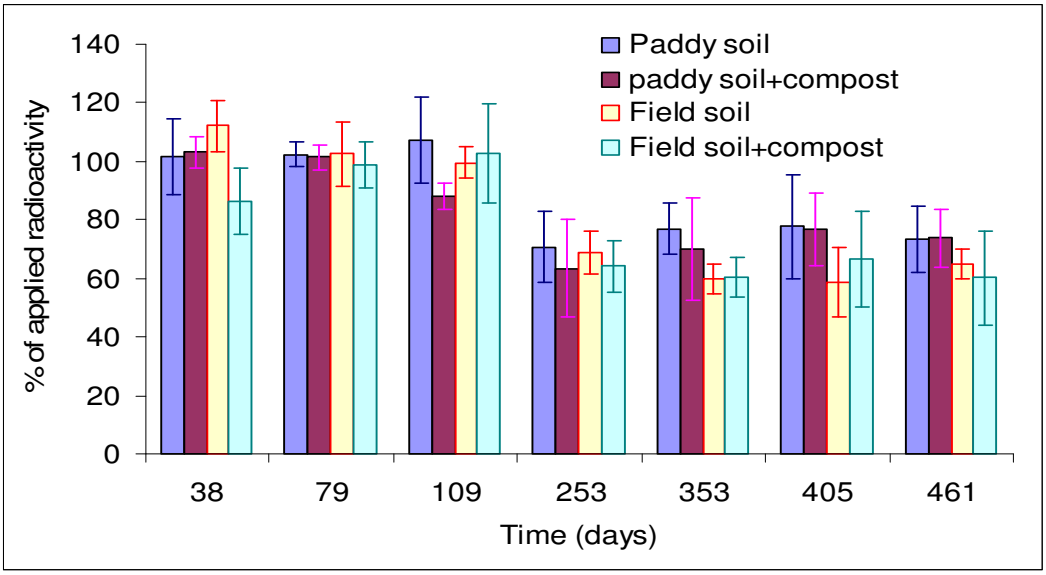

Figure 35: Mass balance of radioactivity at the different sampling points during the anaerobic-aerobic cycles incubation of ^{14}C-HCB-spiked paddy and field soils.

The mass balance of the applied radioactivity at each soil sampling point is shown in figure 35. Most of the radioactivity could be accounted for.

Figure 36 shows the LME model fitting for the HCB degradation data. The sets had similar slopes (Table 17). However, the differences in intercepts (Table 17) mean that the concentrations in the paddy soil were lower than those in the field soil throughout the experimental period. It also means that the concentration of HCB in the composted-amended sets were lower than those in the un-amended sets for both soils (Table 17).

Table 17: Slopes {(µg/g soil)/day} and intercepts (µg/g soil) for the LME model fitting of HCB degradation in the paddy and field soils during the anaerobic-aerobic cycles incubation experiment.

Group	Intercept	Slope (dissipation rate)
Field soil	27.694	-0.048441
Field soil + Compost	26.148	-0.048441
Paddy soil	21.739	-0.048441
Paddy soil + Compost	20.192	-0.048441

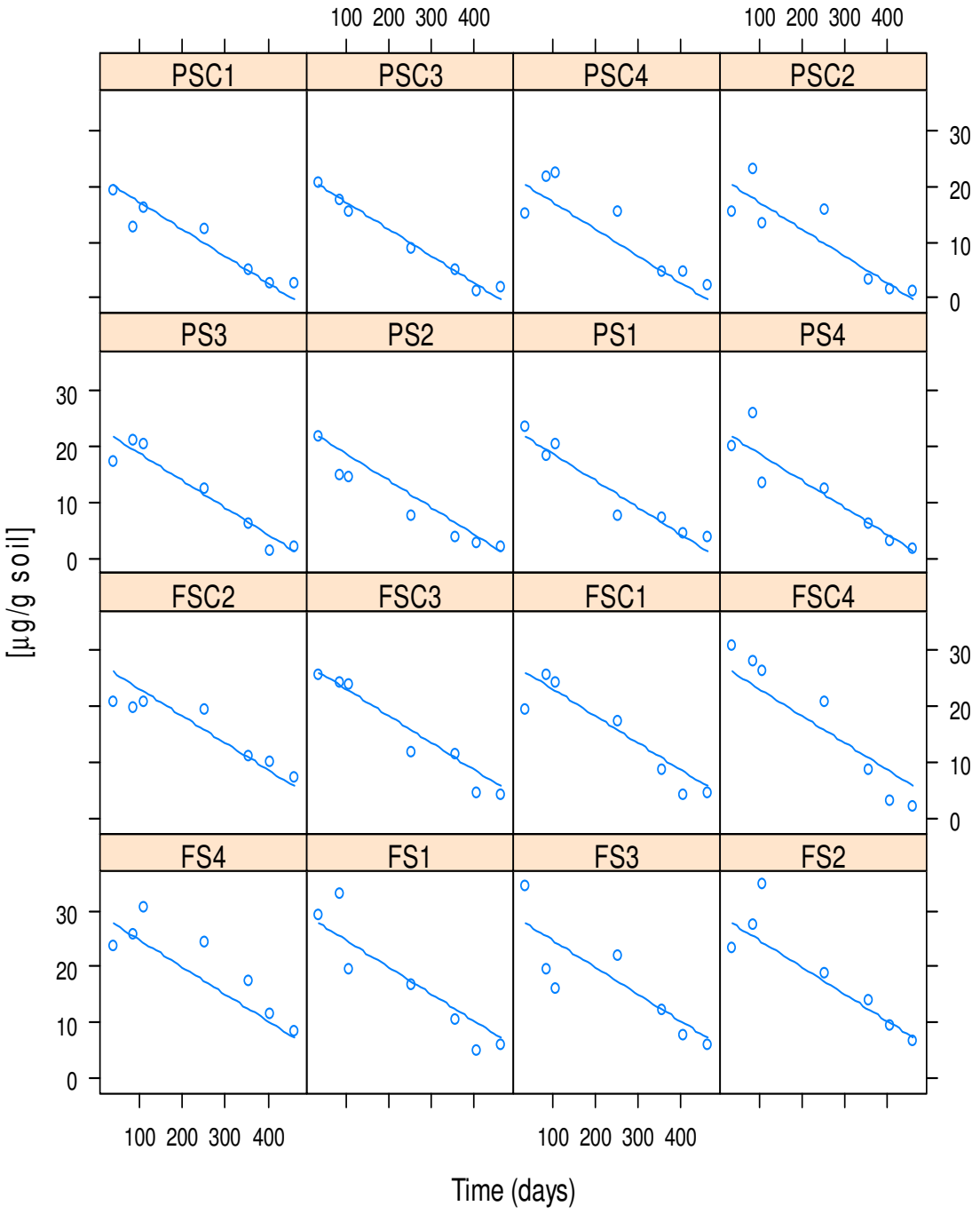

Figure 36: LME model fitting for HCB degradation data (y-axis = **HCB concentration**) in the paddy and field soils during the anaerobic-aerobic cycles experiment.

PS1-PS4 = Paddy soil replicates; PSC1-PSC4 = Paddy soil+compost replicates; FS1-FS4 = Field soil replicates; FSC1-FSC4 Field soil+compost replicate

3.2.3 HCB metabolite formation in the field and paddy soils

3.2.3.1 Influence of soil type on metabolite formation

Figures 37 and 38 show the univariate curves for the concentrations of HCB metabolites in the paddy and field soils respectively. The metabolites were separated with respect to soil because of differences in amounts formed and interaction effects. There was higher metabolite formation in the paddy soil relative to the field soil (Figures 37 and 38). Metabolite formation (especially PCB) began in the first anaerobic/aerobic phase (< day 256) in the paddy soil (Fig. 37), but there was little metabolite formation in the field soil over this period (Fig. 38). PCB and 1,3,5-TCB were the major metabolites formed in the paddy soil (Fig. 37), while 1,4-TCB and 1,3,5-TCB were the main metabolites in the field soil (Fig 38).

To better appreciate the influence of soil type on metabolite formation a principal response curve analysis of the metabolites was done (Fig. 39). There was a clear separation between the soils, with the paddy soil having higher concentrations than the field soil. The loadings indicate that PCB and 1,2,3,5-TeCB were much higher in the paddy soil, while 1,4-DCB was much higher in the field soil. 1,2,3-TCB was also slightly higher in the field soil. The other metabolites had loadings of zero or around zero and were therefore in comparable concentrations in both soils (Fig. 39). Figure 40 shows the analysis of HCB metabolites in the two soils using group information (ade4-package, between function) based on component 1

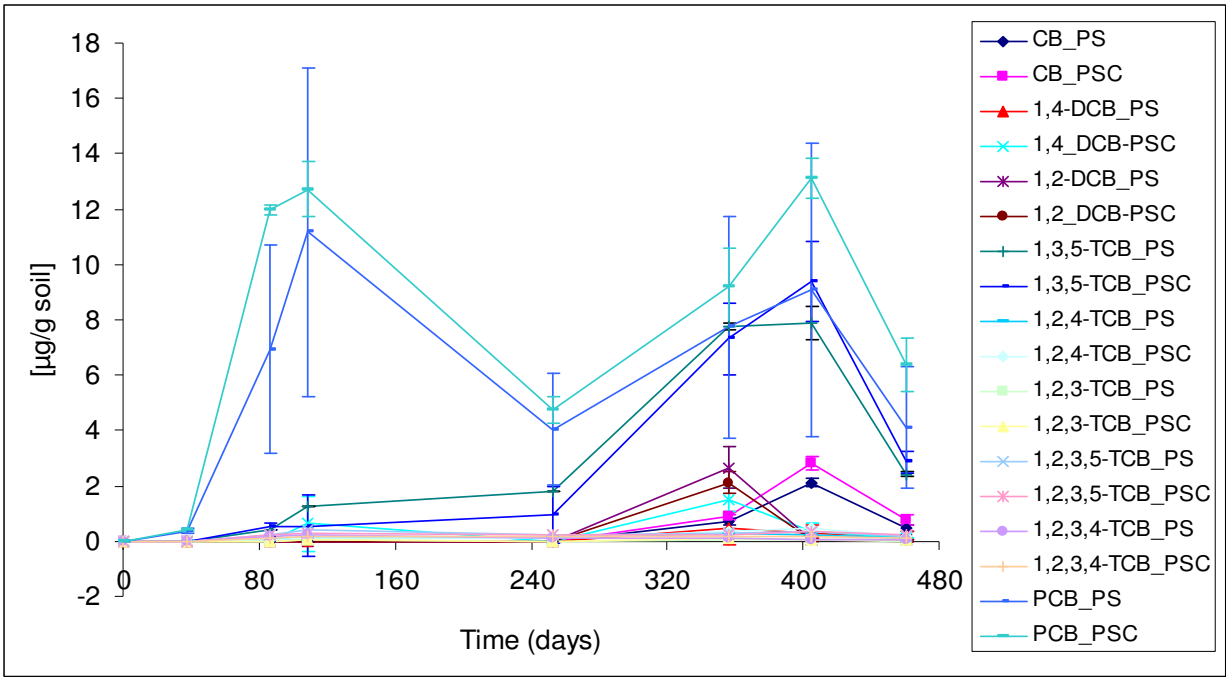

Figure 37: HCB metabolites concentrations in paddy soil samples during the anaerobic-aerobic cycles incubation experiment (Table of data is in the appendix).

PS = Paddy soil, PSC = Paddy soil + compost.

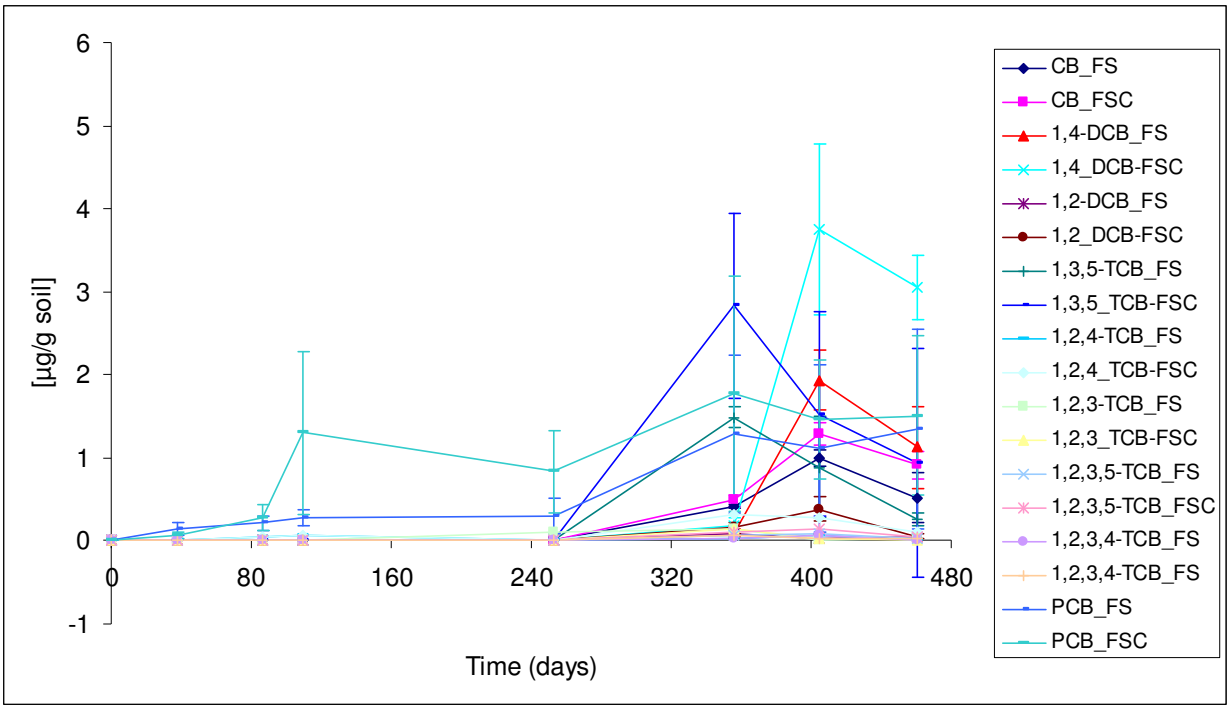

Figure 38: HCB metabolites concentrations in field soil samples during the anaerobic-aerobic cycles incubation experiment (Table of data is in the appendix).
PS = Paddy soil, PSC = Paddy soil + compost.

and 2. The first component divided the groups into two classes according to soil type. 1,4-DCB and 1,2,3-TCB were higher in the field soil, consistent with the loadings of the PRC curve (Fig. 39). However, the analysis showed that all the other metabolites were higher in the paddy soil.

3.2.3.2 Influence of compost on metabolite formation in the paddy and field soils

Figures 41, 42, 43 and 44 show the PRC analysis of the metabolites during the second anaerobic-aerobic phase. The aim of the analysis was to find out if compost had any effect on metabolite formation. To analyse the compost effect, data were separated with respect to soil and restricted to the last three time points. This period was selected because all the analyzed metabolites were present in all the replicates (Fig. 37 and Fig. 38). The separation of the data was because of interaction effects between the soils.

Fig. 41 shows the PRC curve for metabolites in the paddy soil, There was a clear compost effect, with the treated samples having higher concentrations than the untreated ones. The loadings showed that 1,2,3,4-TeCB, PCB, 1,2,4-TCB and CB were higher in the compost-

amended soil, while 1,2-DCB, 1,2,3,5-TeCB and 1,2,3-TCB were higher in the un-amended soil. 1,3,5-TCB had a loading of around zero and was therefore comparable in both treatments. Figure 42 shows the analysis of HCB metabolites in the paddy soil using group information (ade4-package, between function) based on component 1 and 2. The first component divided the groups into two classes according to compost treatment. 1,2-DCB and 1,2,3,5-TCB were higher in the untreated paddy soil, consistent with the loadings of the PRC curve (Fig. 39). However, the analysis showed that all the other metabolites were higher in the compost-treated paddy soil.

Fig. 43 shows the PRC curve for metabolites in the field soil. There was again a clear compost effect, with the treated samples having higher concentrations than the untreated ones. 1,2,4-TeCB, 1,4-DCB and 1,2,3,5-TeCB were higher in the compost-treated field soil, while 1,2,3,4-TCB was higher in the un-amended field soil. 1,2,3-TCB and PCB showed slightly higher loadings in the un-amended soil, but the values were close to zero and therefore the concentrations – along with those of 1,2-DCB, 1,3,5-TCB and CB – were comparable in both treatments. Figure 44 shows the analysis of HCB metabolites in the field soil using group information (ade4-package, between function) based on component 1 and 2. The first component divided the groups into two classes according to compost treatment. Contrary to the PRC loadings, the analysis showed 1,2,3,4-TeCB to be a borderline case, meaning that the concentrations in the two classes were comparable. All the other metabolites were shown to be higher in the compost-treated soil.

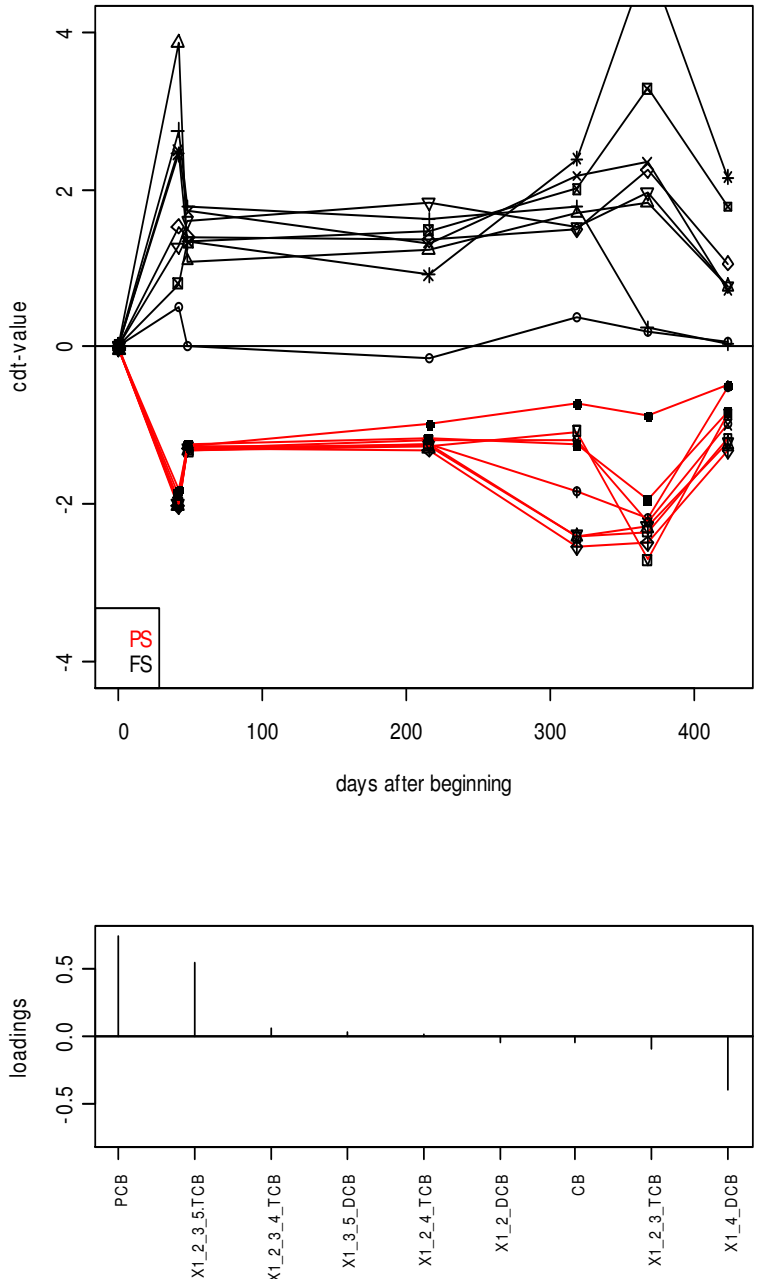

Fig.39: Principal response curve (1st component: declared variance = 49.7%) for the HCB metabolites in the field and paddy soils during the anaerobic-aerobic cycles experiment.

PS = Paddy soil (8 replicates), FS = Field soil (8 replicates)

'x'is used e.g. x123-TCB because the first character in R program (used for data analysis) must be a letter.

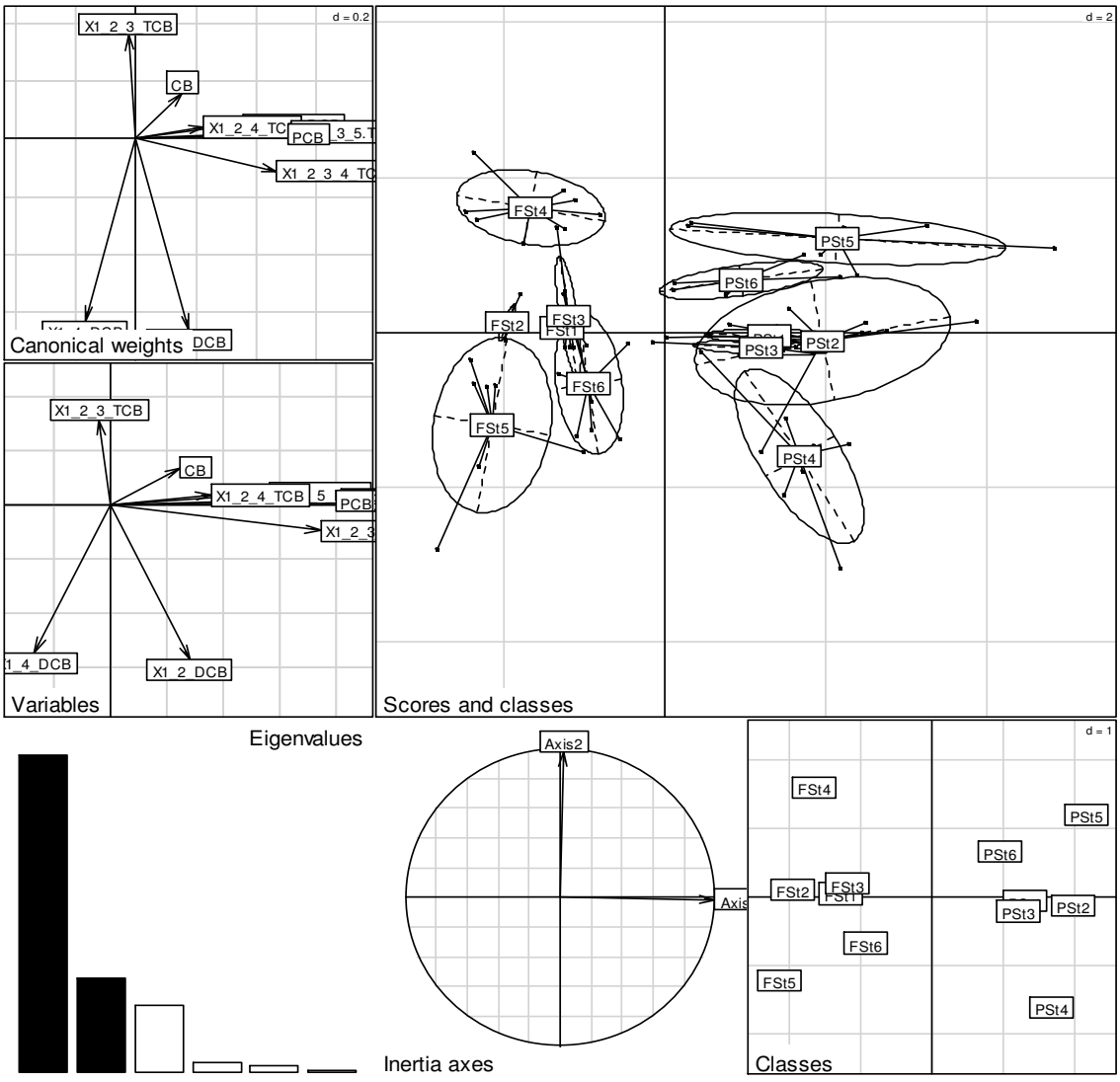

Figure 40: Results of data analysis using group information (ade4-package, between function), based on components 1 and 2, showing the distribution of HCB metabolites in the paddy and field soils during the anaerobic-aerobic incubation experiment. 'Scores and classes' is a 3-D presentation of the data separation by the two components/axes, while 'Classes' is a simple 2-D presentation of the same; 'Canonical weights' shows the loading of each metabolite; 'Variables' shows the extent and direction of each metabolite; 'Eigenvalues' shows the contribution of the components/axes in explaining the data: the two dark axes have been used to separate the groups.

PS = Paddy soil; FS = Field soil. The last 2 digits refer to the sampling time e.g. FSt5 meansfield soil at the 5th sampling. 'x'is used e.g. x123-TCB because the first character in R (used for data analysis) must be a letter.

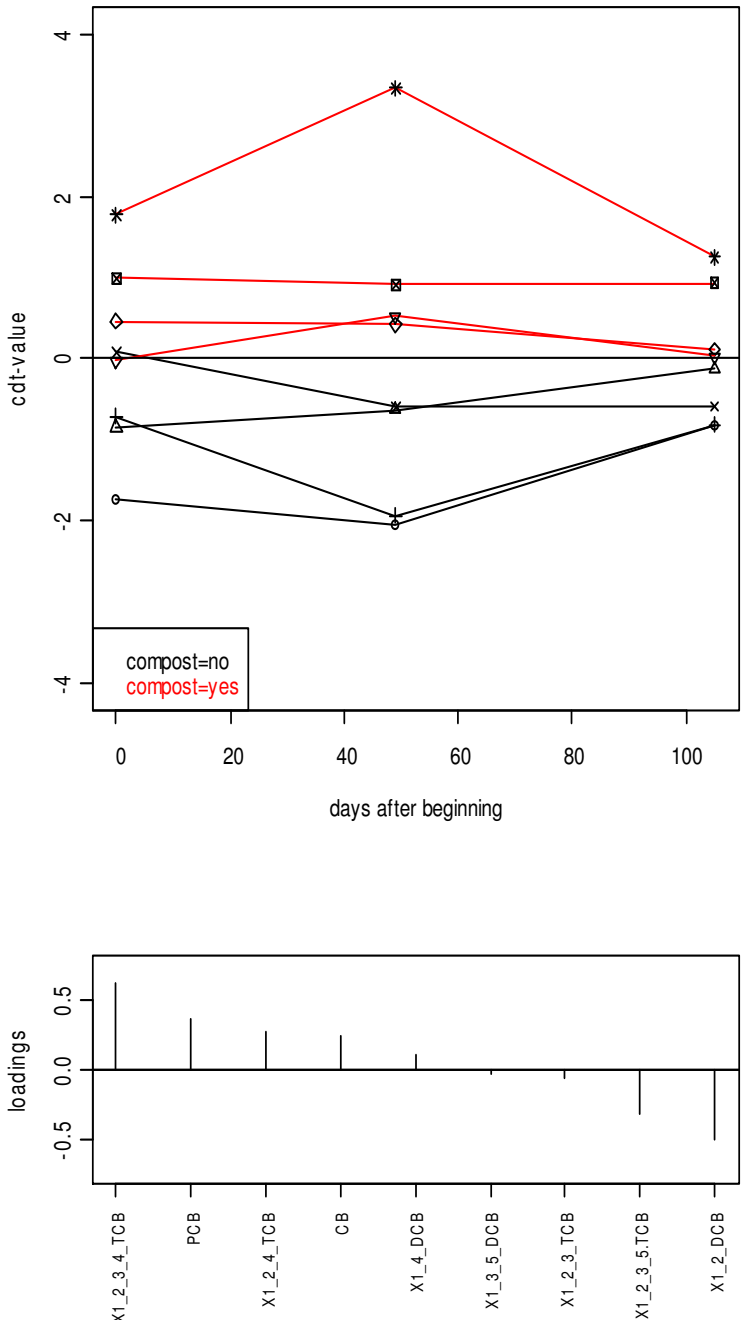

Fig.41: Principal response curve (1st component: declared variance = 47.2%) for HCB metabolites in the last three samplings (second anaerobic-aerobic cycle) in the paddy soil.

'Compost = no' means soil without compost (4 replicates); 'compost = yes' means soil with compost (4 replicates). 'x'is used e.g. x123-TCB because the first character in R (used for data analysis) must be a letter.

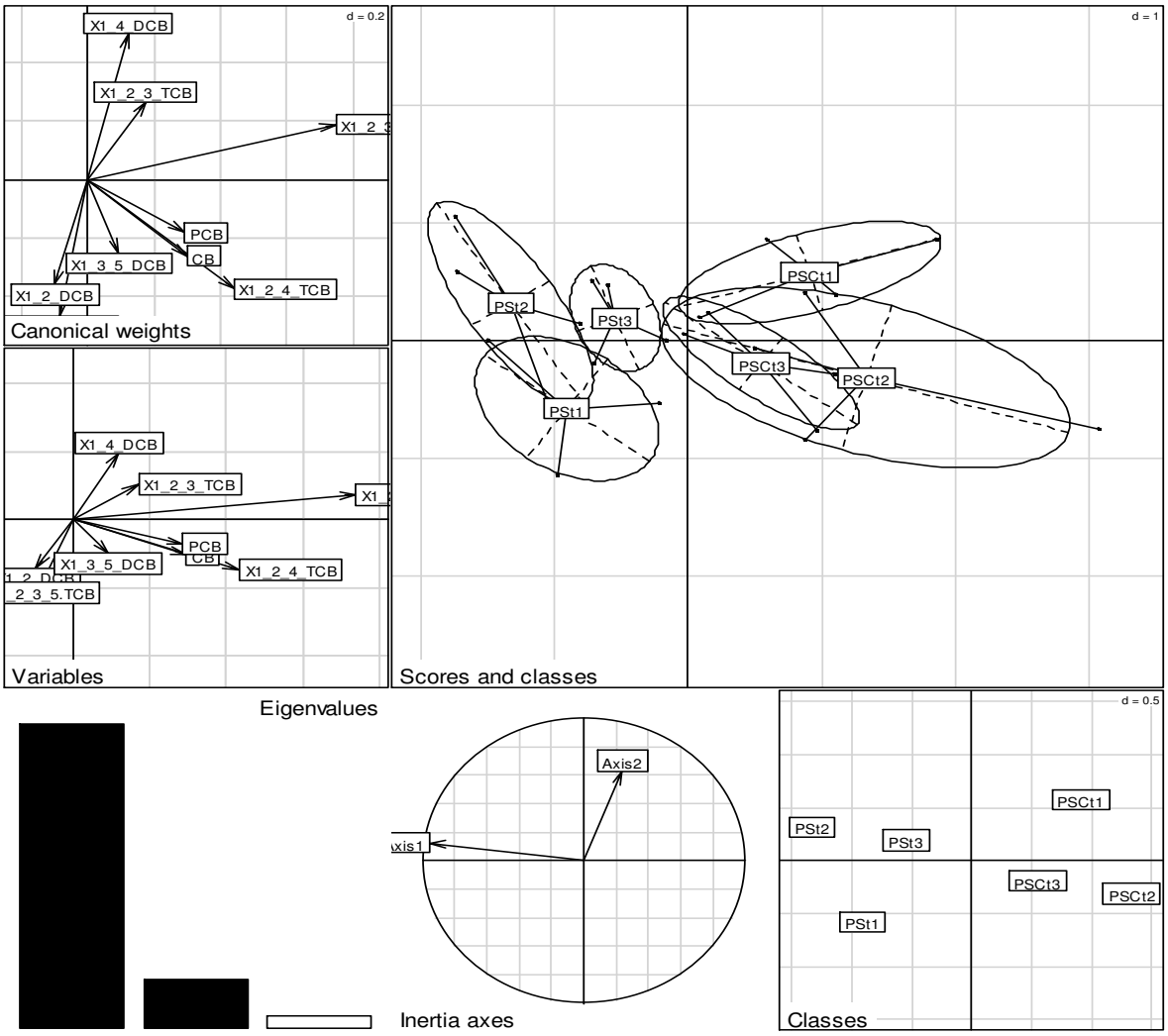

Figure 42: Results of data analysis using group information (ade4-package, between function), based on components 1 and 2, showing the distribution of HCB metabolites in the paddy soil during the second anaerobic-aerobic phase (last three time points). 'Scores and classes' is a 3-D presentation of the data separation by the two components/axes, while 'Classes' is a simple 2-D presentation of the same; 'Canonical weights' shows the loading of each metabolite; 'Variables' shows the extent and direction of each metabolite; 'Eigenvalues' shows the contribution of the components/axes in explaining the data: the two dark axes have been used to separate the groups.

PS=Paddy soil; PSC=Paddy soil+compost. The last 2 digits refer to the sampling time e.g. FSt5 means field soil at the 5th sampling. 'x'is used e.g. x123-TCB because the first character in R (used for data analysis) must be a letter.

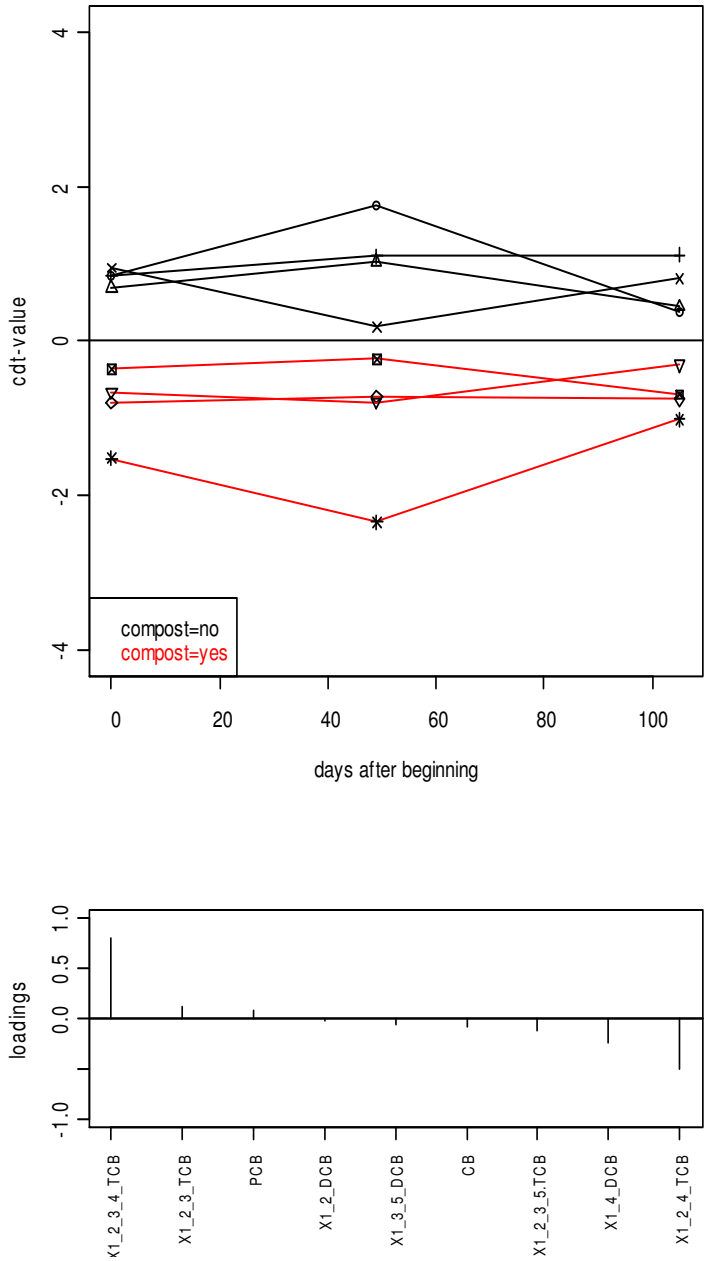

Fig.43: Principal response curve (1st component: declared variance = 46.3) for HCB metabolites in the last three samplings (second anaerobic-aerobic cycle) in the field soil.

'Compost = no' means soil without compost (4 replicates); 'compost = yes' means soil with compost (4 replicates). The last 2 digits refer to the sampling time e.g. FSt5 meansfield soil at the 5th sampling. 'x'is used e.g. x123-TCB because the first character in R (used for data analysis) must be a letter.

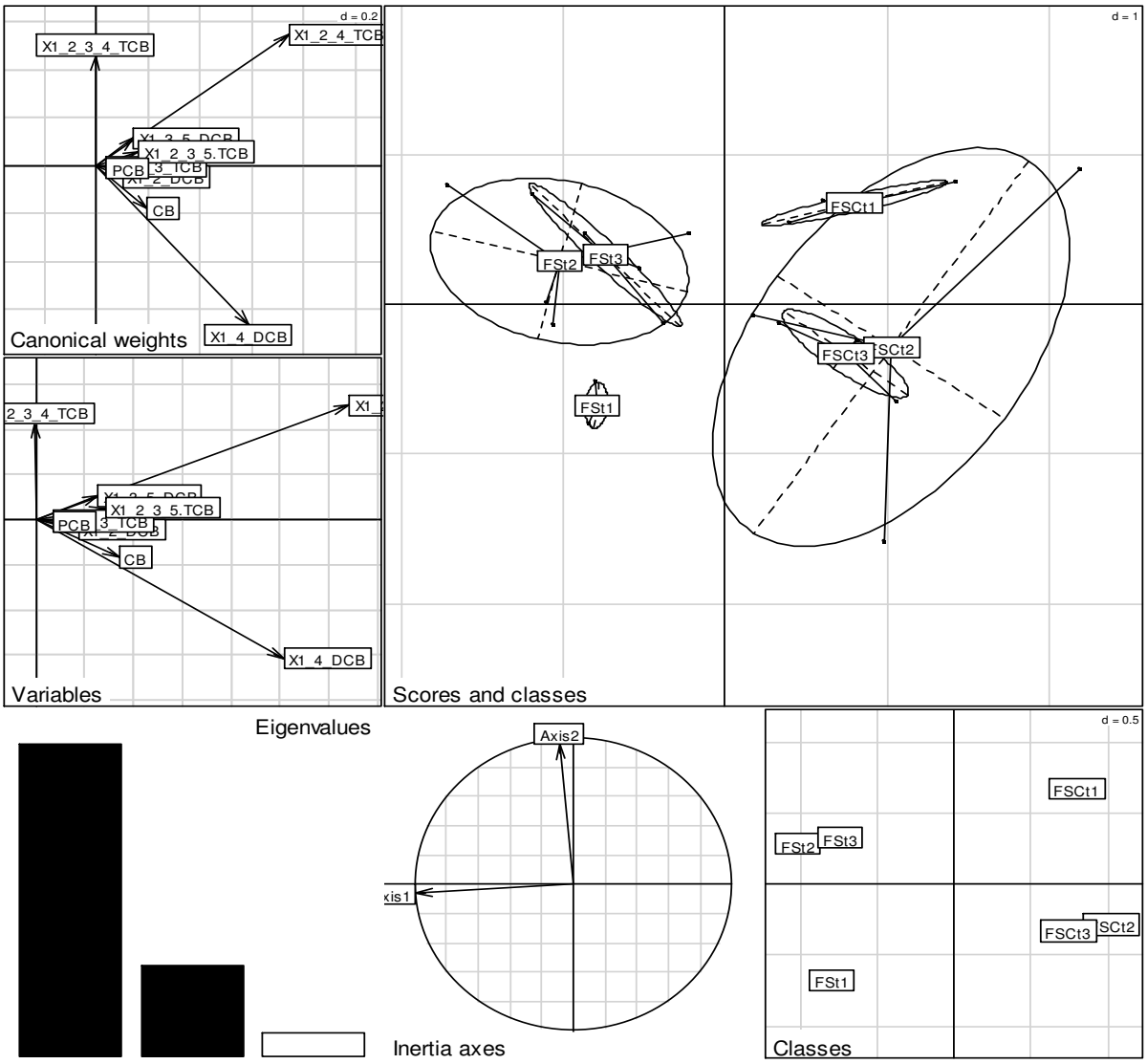

Figure 44: Results of data analysis using group information (ade4-package, between function), based on components 1 and 2, showing the distribution of HCB metabolites in the field soil during the second anaerobic-aerobic phase (last three time points). 'Scores and classes' is a 3-D presentation of the data separation by the two components/axes, while 'Classes' is a simple 2-D presentation of the same; 'Canonical weights' shows the loading of each metabolite; 'Variables' shows the extent and direction of each metabolite; 'Eigenvalues' shows the contribution of the components/axes in explaining the data: the two dark axis have been used to separate the groups.

FS=Field soil; FSC=Field soil+compost. The last 2 digits refer to the sampling time e.g. FSt5 means field soil at the 5th sampling. 'x'is used e.g. x123-TCB because the first character in R (used for data analysis) must be a letter.

3.2.4 Changes in soil redox potential during the aerobic-anaerobic cycles

Figure 45 shows the redox potential of the test systems with time. The measurements were carried out to check and verify that anaerobic conditions were actually achieved. It was expected that water-logging would induce anaerobic conditions, and that compost would cause faster anoxic conditions. As can be seen from figure 45, anaerobic conditions were achieved. At the beginning of the second anaerobic phase, water-logging did not induce anaerobic conditions. This was attributed to a lack of easily degradable energy sources, given the time period that the experiment had lasted. Yeast extract was added and there was an immediate sharp decrease in redox potential on day 256 (Fig. 45).

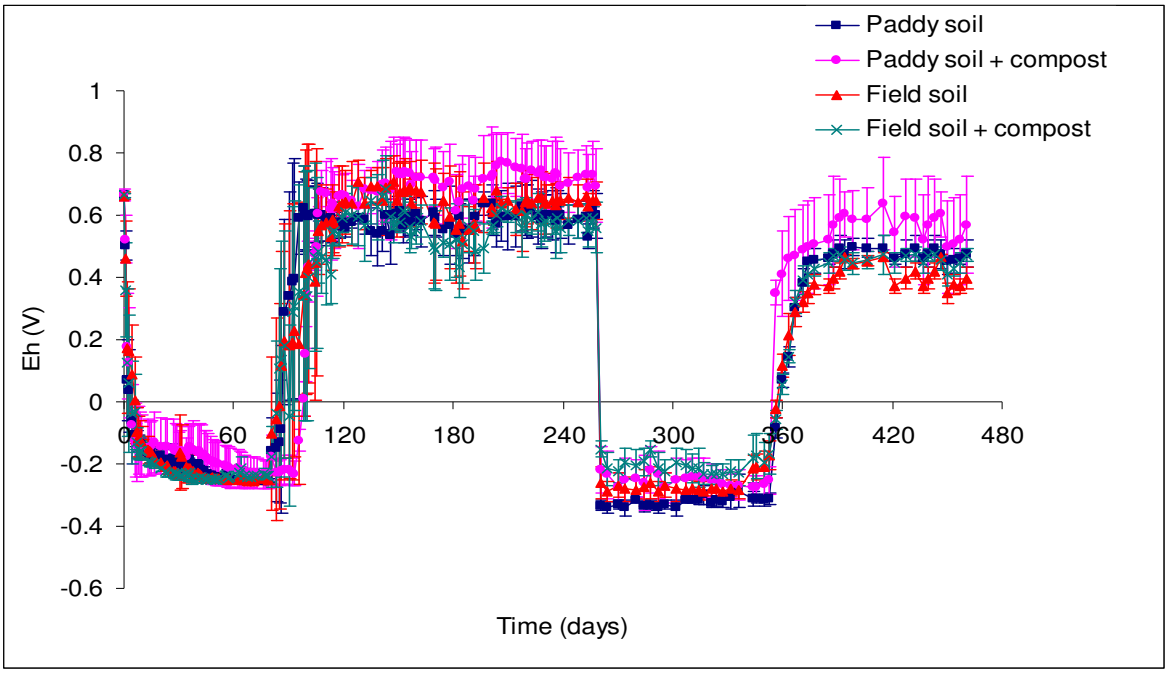

Figure 45: Redox Potential of the HCB-spiked field and paddy soils under anaerobic-aerobic cycles conditions

3.3 Mineralization, volatilization and degradation of ^{14}C-DDT under anaerobic-aerobic cycles conditions

3.3.1 Mineralization and volatilization of DDT

The objective of this experiment was to find out if inducing anaerobic conditions would lead to subsequent increases in mineralization during the aerobic phase. The hypothesis was that reductive dechlorination would occur under anaerobic conditions, while ring cleavage would occur during the aerobic phase hence leading to increased mineralization. Dechlorination has been identified as the limiting step in aerobic degradation (Aislabie, 1997). Figure 46 shows the mineralization with time of ^{14}C-DDT in field and paddy soils under anaerobic/aerobic conditions. There were significant differences between the two soils and also between the soils and treatments, with higher mineralization witnessed in the field soil. Compost clearly increased the mineralization after the first anaerobic phase in both soils. The same effect was, however, not noted in the second phase.

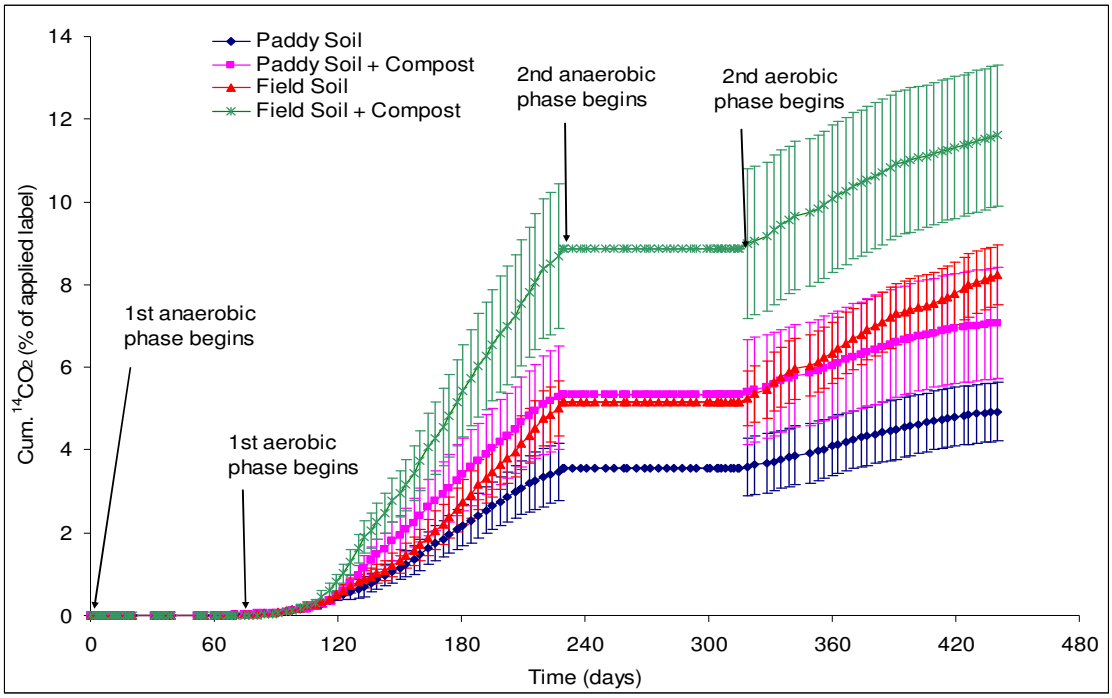

Figure 46: ^{14}C-DDT mineralization with time in field and paddy soils under anaerobic-aerobic cycles conditions

To better appreciate the differences between the 4 groups (Fig. 46), the mineralization data for each time point was centred. This has the effect of removing variability and trend caused by time, so that only differences between the groups are shown. Centering involves taking the average of all the replicates (controls and treatments) and assigning zero to this value. This is the 'centering value', and it is subtracted from each of the replicates. The resulting data is

'centered' and is free from time course effects. It only shows differences between the two groups. The centred data was fitted into the LME model (Fig. 47 and Fig. 48). This treatment of the data revealed significant differences (p = 0.05) between the groups (Table 18).
During the first aerobic phase, mineralization in the field soil increased relative to the paddy soil, with the compost-amended soil having a higher rate (Fig. 47 and Table 19). Conversely, mineralization in the paddy soil decreased relative to the field soil, with the compost-amended paddy soil having a higher rate of decrease. In the second aerobic phase, however, mineralization in the paddy soil increased relative to the field soil, with the paddy soil having a higher rate relative to the compost-amended paddy soil (Fig. 48 and Table 19). The field soil mineralization decreased relative to that of the paddy soil with the compost-amended field soil having a higher rate of decrease.

Table 18: Significant test p-values (p = 0.05) for CO_2, extractable residues, non-extractable residues, and p,p-DDT concentrations in the paddy and field soils during the ^{14}C-DDT anaerobic-aerobic cycles incubation experiment.

	*CO_2	Extr. residues	Non-extr. residues	p,p-DDT
Intercept (FS)	1.0000	<0.0001	<0.0001	<0.0001
Slope (FS)	1.0000	<0.0001	<0.0001	<0.0001
Intercept (PS)	0.0066	0.0207	0.0138	0.0001
Intercept (CE)	0.0041	0.0101	0.0811	0.0958
Slope (PS)	<0.0001	0.1041	0.1873	<0.0001
Slope (CE)	<0.0001	0.8098	0.5237	0.1985

FS = Field soil; PS = Paddy soil; CE = compost effect

*ANOVA of time-centered data

Table 19: Slopes {(µg/g soil)/day} and intercepts (µg/g soil) for the LME model fitting of ^{14}C-DDT mineralization time-centered data in the paddy and field soils during the anaerobic-aerobic cycles experiment.

group	Log $^{14}CO_2$ Phase 1		Log $^{14}CO_2$ Phase 2	
	Intercept	Slope	Intercept	Slope
Field soil	-0.0088	0.000055	0.0115	-0.000014
Field soil + compost	-0.0063	0.00016	0.03005	-0.000063
Paddy soil	0.0063	-0.00016	-0.03005	0.000063
Paddy soil + compost	0.0088	-0.000055	-0.0115	0.000014

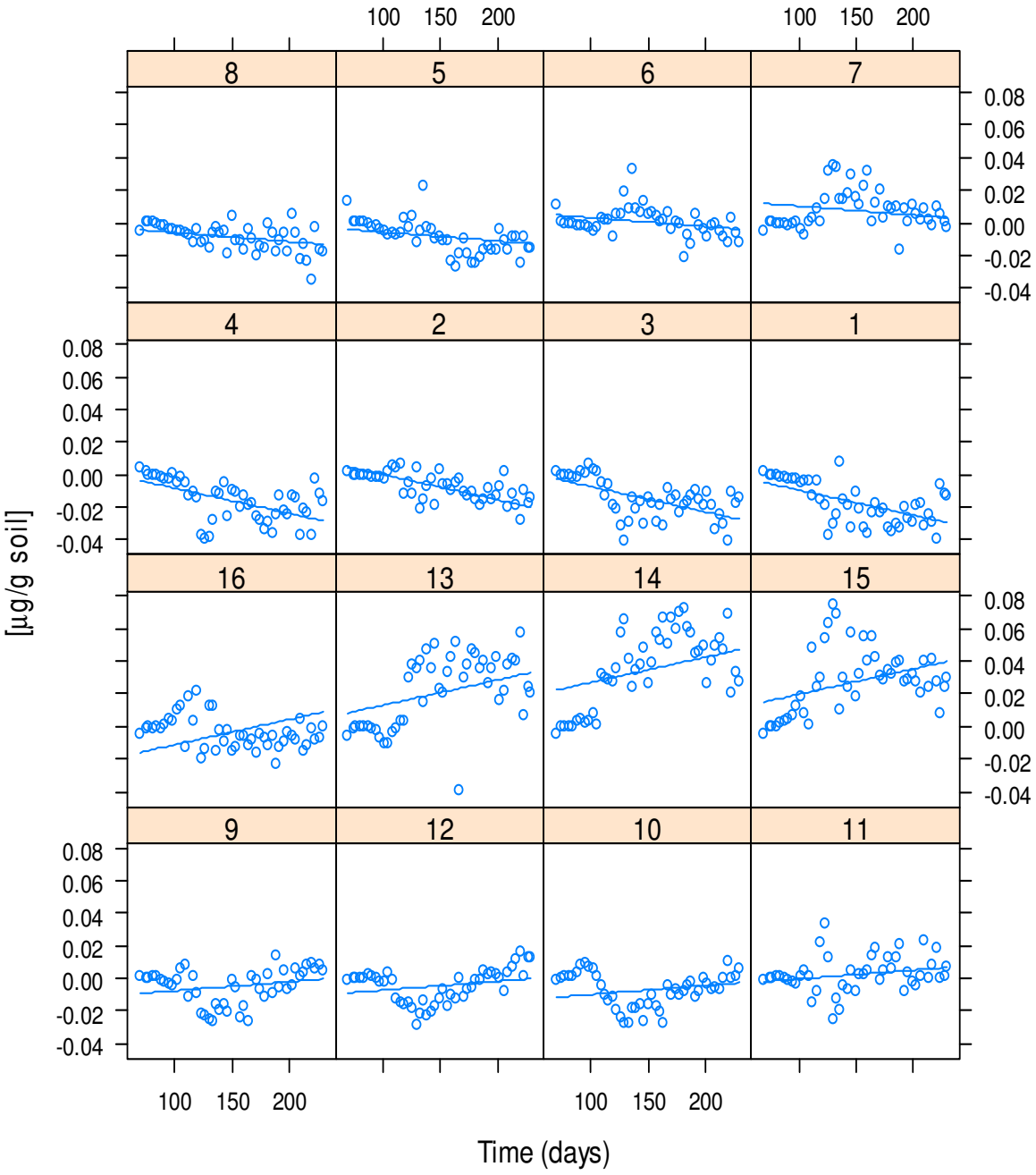

Fig. 47: LME model fitting for the time-centered ^{14}C-DDT mineralization data (y-axis = $^{14}CO_2$) during the first aerobic phase of the anaerobic-aerobic cycles incubation experiment.

1-4 = Paddy soil replicates; 5-8 = Paddy soil+compost replicates; 9-12 = Field soil replicates; 13-16 = Field soil+compost replicates

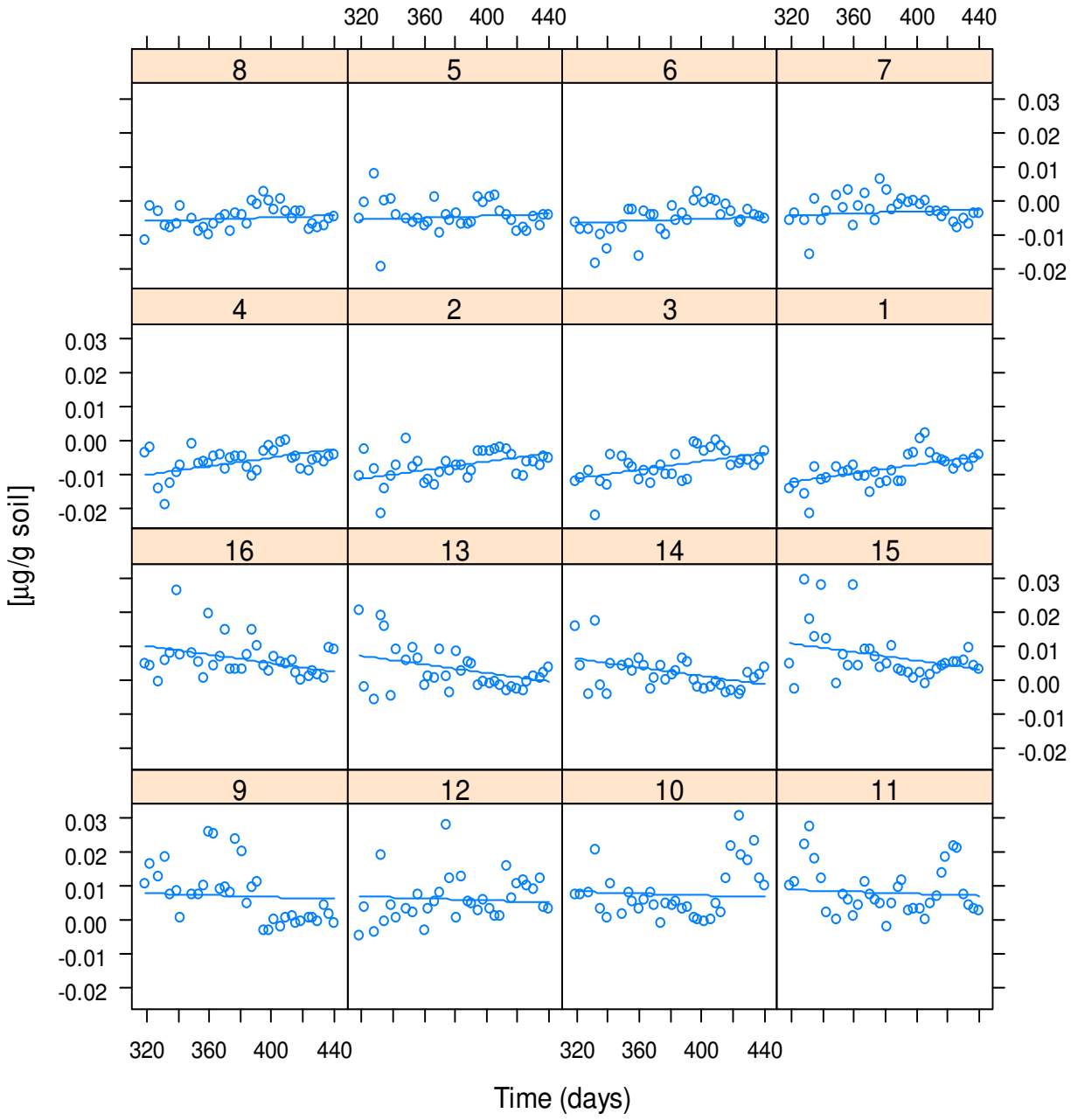

Fig. 48: LME model fitting for ^{14}C-DDT time-centered mineralization data (y-axis = $^{14}CO_2$) during the second aerobic phase of the anaerobic-aerobic cycles incubation experiment.

1-4 = Paddy soil replicates; 5-8 = Paddy soil+compost replicates; 9-12 = Field soil replicates; 13-16 = Field soil+compost replicates

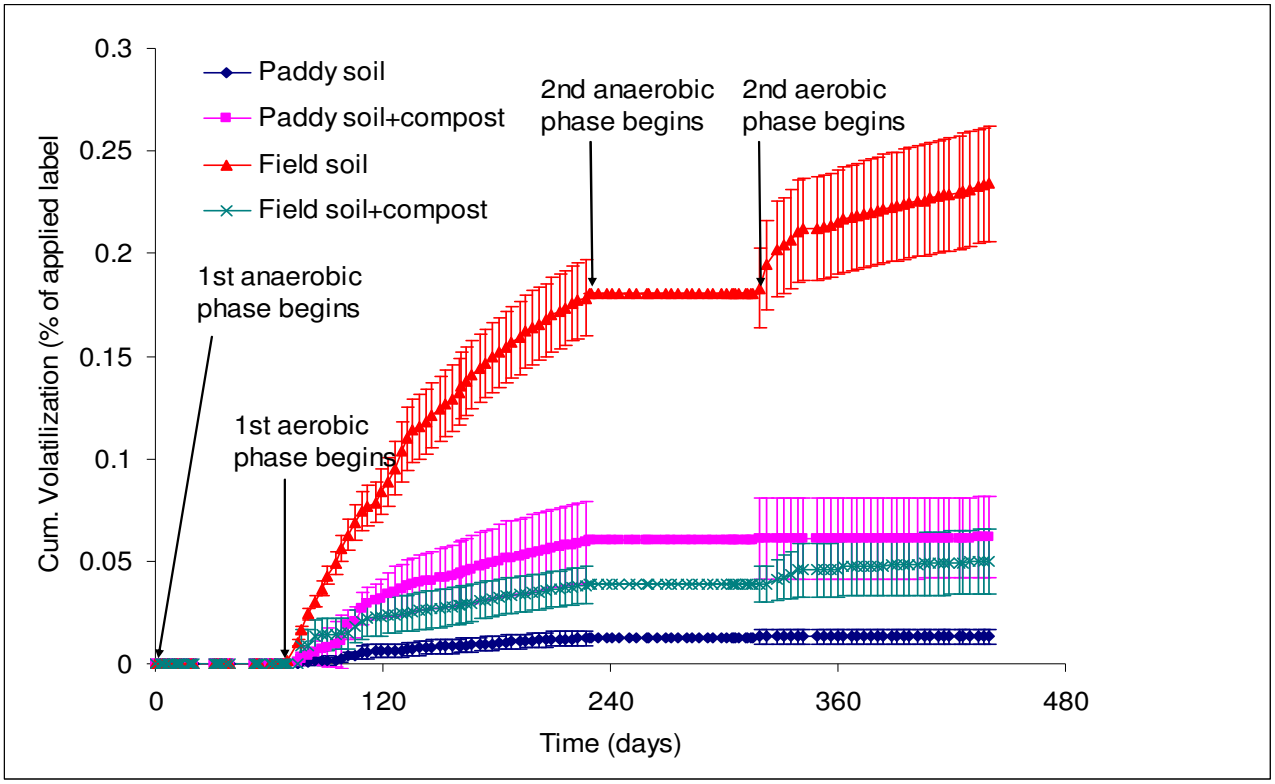

Figure 49: ^{14}C-DDT volatilization in field and paddy soils under anaerobic-aerobic cycles conditions

There was minimal volatilization in both soils (Fig. 49) with high variability in volatilization in the untreated field soil. The volatilization was lower in the compost treated field soil. Conversely, the compost amended paddy soil had higher volatilization relative to the unamended soil.

3.3.2 Formation of extractable and non-extractable residues

The extractable residues of all the sets decreased with time up to day 254 (Fig. 50). This corresponded to the first anaerobic-aerobic phase. The field soil extractable residues decreased up to day 319 after which they remained fairly constant. There was an increase of extractable residues in the amended paddy soil during the second anaerobic phase (between days 254 and 319), after which the concentrations were fairly constant. The extractable residues of the un-amended paddy and amended field soils decreased up to day 319 and then increased thereafter.

The decrease in extractable residues on 319 of the un-amended paddy and amended field soils was accompanied by an increase in non-extractable residues (Fig. 50 and Fig. 51). The non-extractable residues decreased at the next sampling point. The non-extractable residues of the

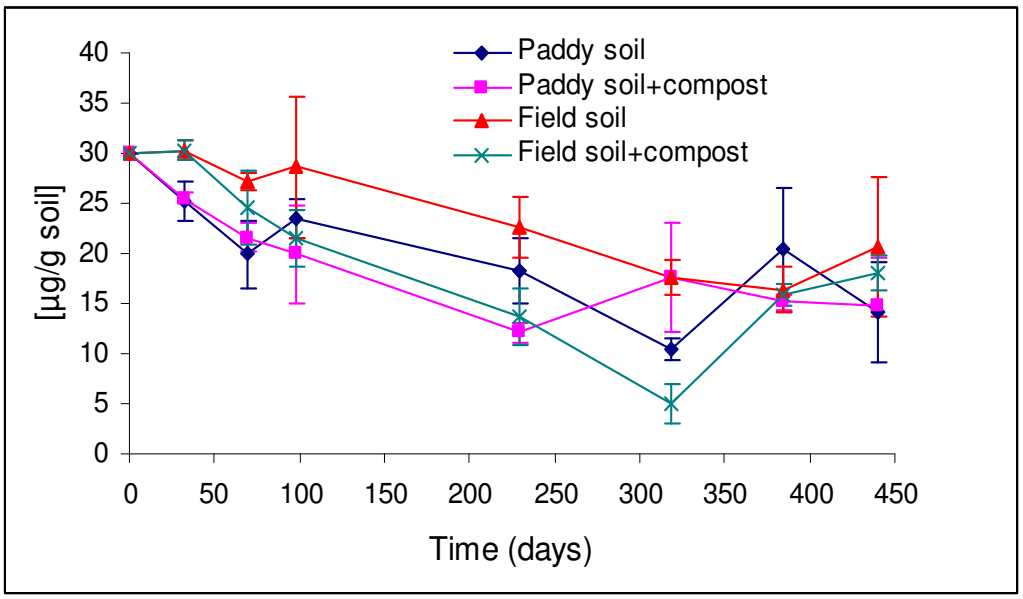

Fig 50: Changes in ^{14}C-DDT extractable residues in the field and paddy soils under anaerobic-aerobic cycles conditions

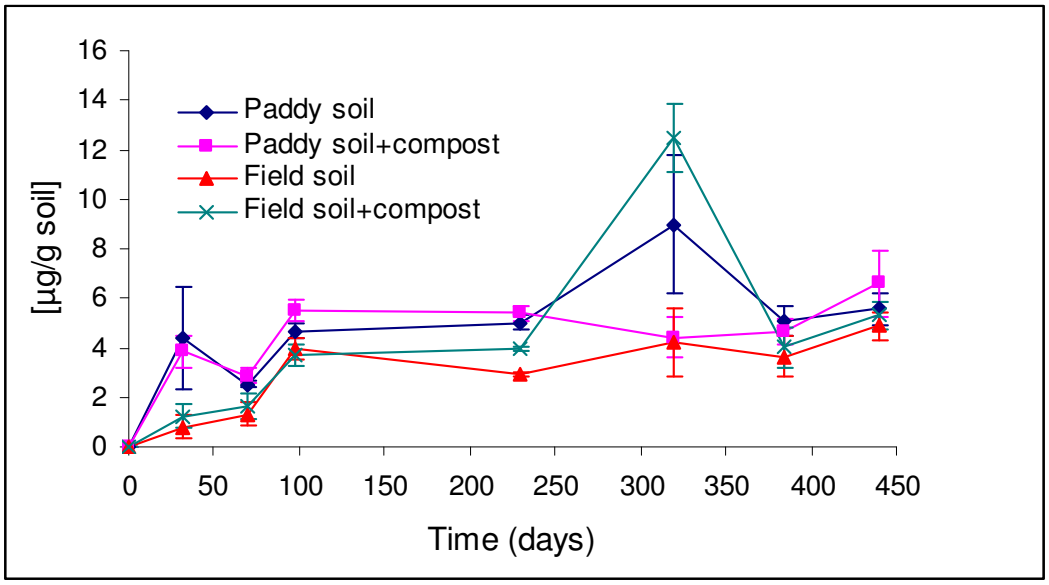

Fig 51: Changes in ^{14}C-DDT non-extractable residues in field and paddy soils under anaerobic-aerobic cycles conditions

field soil and amended paddy soil remained fairly constant after the initial build-up in the first anaerobic phase (Fig. 51). There were no significant differences ($p = 0.05$), however, between the soils in the changes of extractable and non-extractable residues – neither was there a significant compost effect (Table 18).

3.3.3 Multivariate analysis of ^{14}C-radioactivity distribution in the soils

To better appreciate the differences between the groups, PRC analysis of cumulative $^{14}CO_2$, ^{14}C-volatiles, ^{14}C-extractable and ^{14}C-non-extractable residues was done (Figures 52, 53, 54). The first two components did not show differences between the groups (Figs. 52 and 53), though there was a tendency towards separation for the field soil (Fig. 52). The high variability in the field soil C_{dt}-values (Fig. 52) is due to the high variability in volatilization of the field soil (Fig. 49).

The first component (vertical axis in scores and classes/classes sections of Fig. 54) of analysis using group information separated the groups into two classes according to soil type. The only exceptions were FSCt6 and PSCt6 (Compost-treated Field and Paddy soils at sampling point 6 i.e. day 319). PSCt6 had the highest amounts of extractable residues while FSCt6 had the highest amount of non-extractable residues (Canonical weights/variables sections of Fig. 54). The second component (horizontal axis in the scores and classes/classes sections of Fig. 54) of analysis using group information did not show further separation.

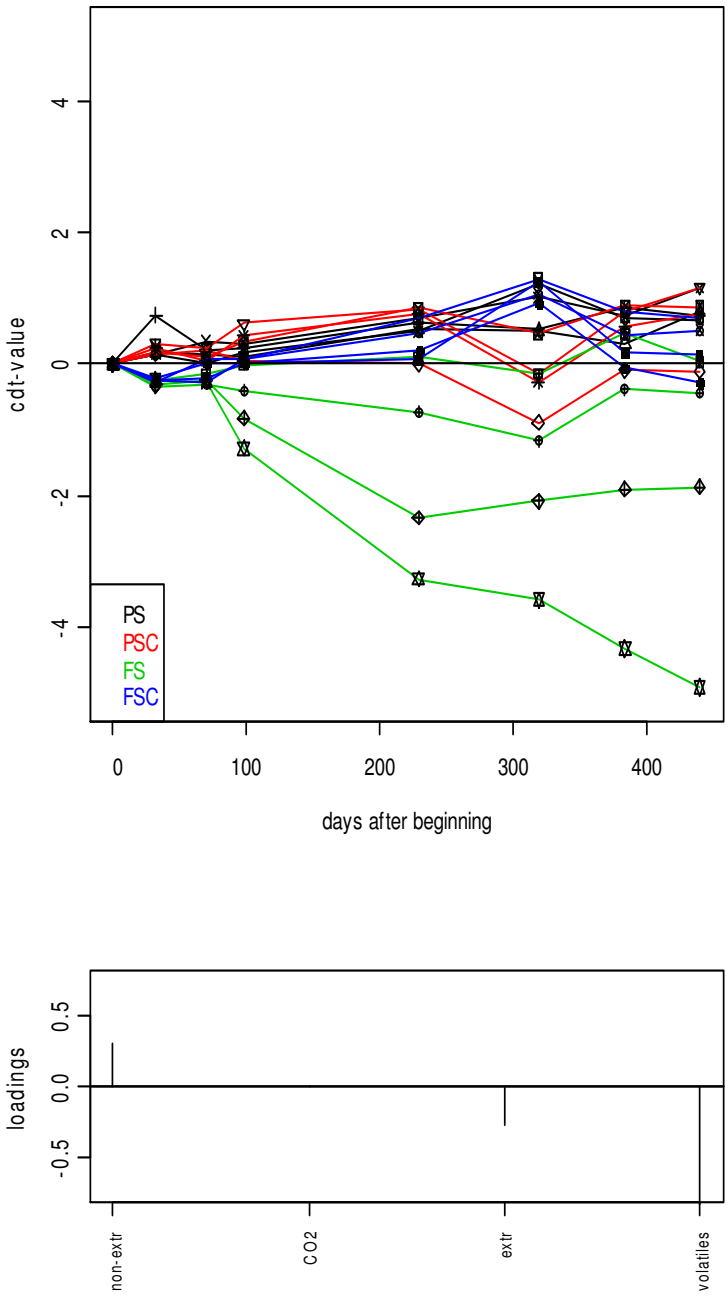

Fig. 52: PRC-curve (component 1: declared variance = 51.2 %) for $^{14}CO_2$, ^{14}C-volatiles, ^{14}C-extractable residues and ^{14}C-non-extractable residues of ^{14}C-DDT in the paddy and field soils during the anaerobic-aerobic cycles incubation experiment.

PS = Paddy soil (4 replicates), PSC=Paddy soil+compost (4 replicates), FS=Field soil (4 replicates), FSC=Field soil+compost (4 replicates).

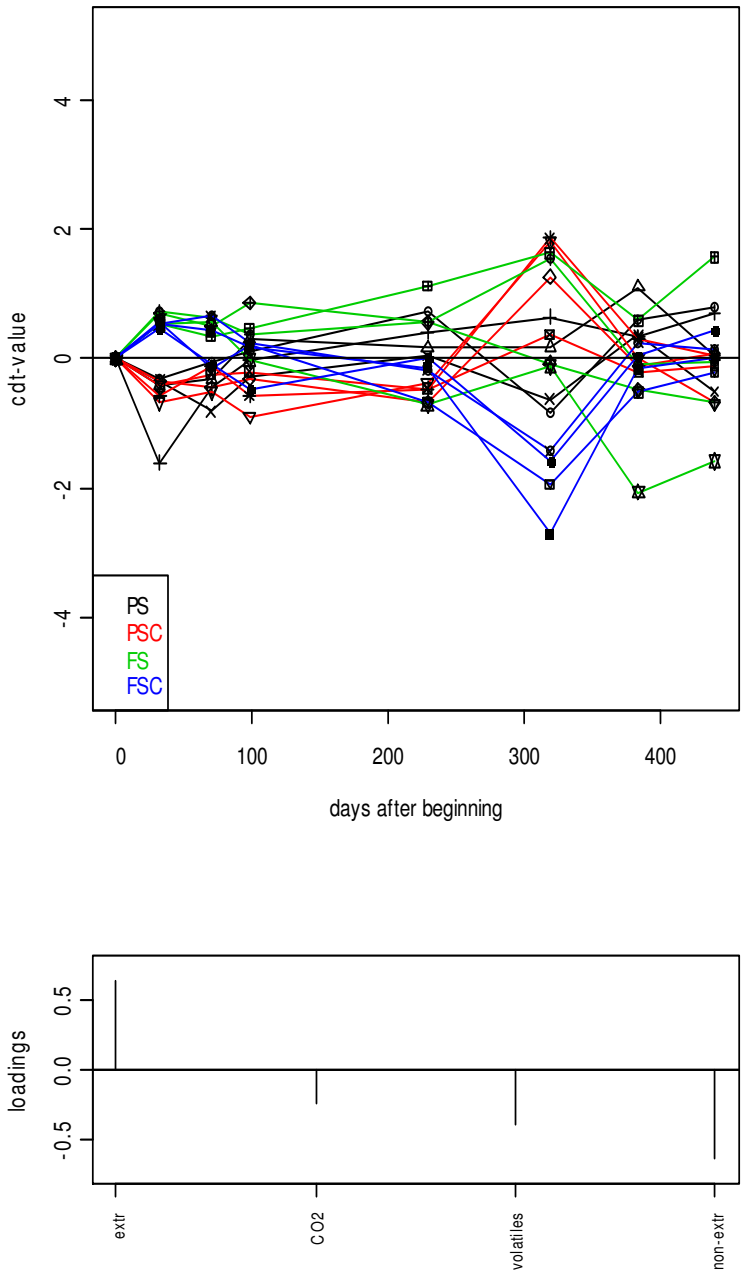

Fig. 53: PRC-curve (component 2: declared variance = 27.9 %); for $^{14}CO_2$, ^{14}C-volatiles, ^{14}C-extractable residues and ^{14}C-non-extractable residues of ^{14}C-DDT in the paddy and field soils during the anaerobic-aerobic cycles incubation experiment.

PS = Paddy soil (4 replicates), PSC=Paddy soil+compost (4 replicates), FS=Field soil (4 replicates), FSC=Field soil+compost (4 replicates)

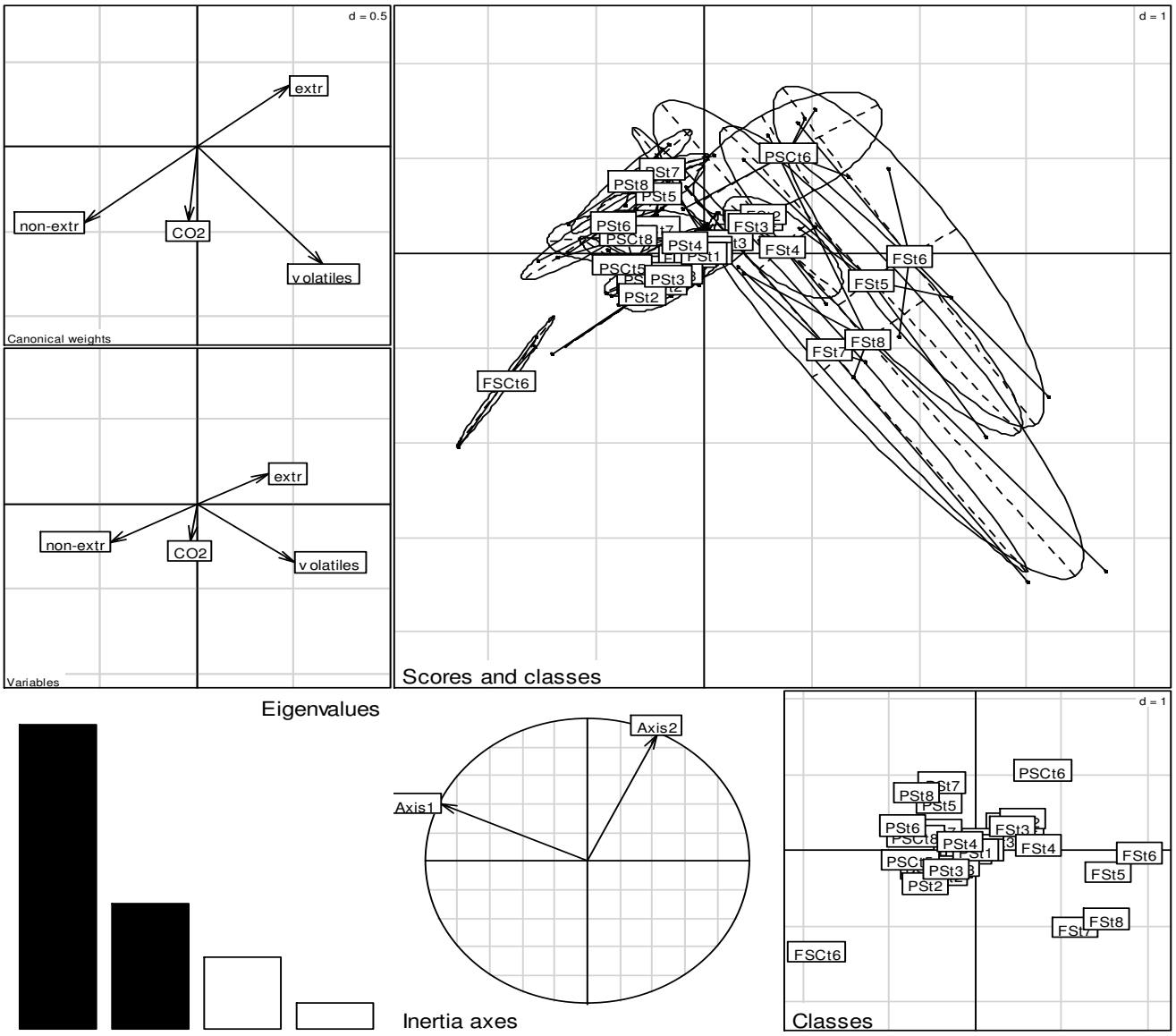

Fig. 54: Results of data analysis using group information (ade4-package, between function), based on components 1 and 2, showing the distribution of $^{14}CO_2$, ^{14}C-volatiles, ^{14}C-extractable residues and ^{14}C-non-extractable residues of ^{14}C-DDT in the paddy and field soils during the anaerobic-aerobic cycles incubation experiment. 'Scores and classes' is a 3-D presentation of the data separation by the two components/axes, while 'Classes' is a simple 2-D presentation of the same; 'Canonical weights' shows the loading of each metabolite; 'Variables' shows the extent and direction of each metabolite; 'Eigenvalues' shows the contribution of the components/axes in explaining the data: the two dark axes have been used to separate the groups.

PS = Paddy soil, PSC=Paddy soil+compost, FS=Field soil, FSC=Field soil+compost.
The last 2 digits refer to the sampling time e.g. FSt5 meansfield soil at the 5th sampling.

3.3.4 DDT degradation and metabolite formation under anaerobic-aerobic cycles conditions

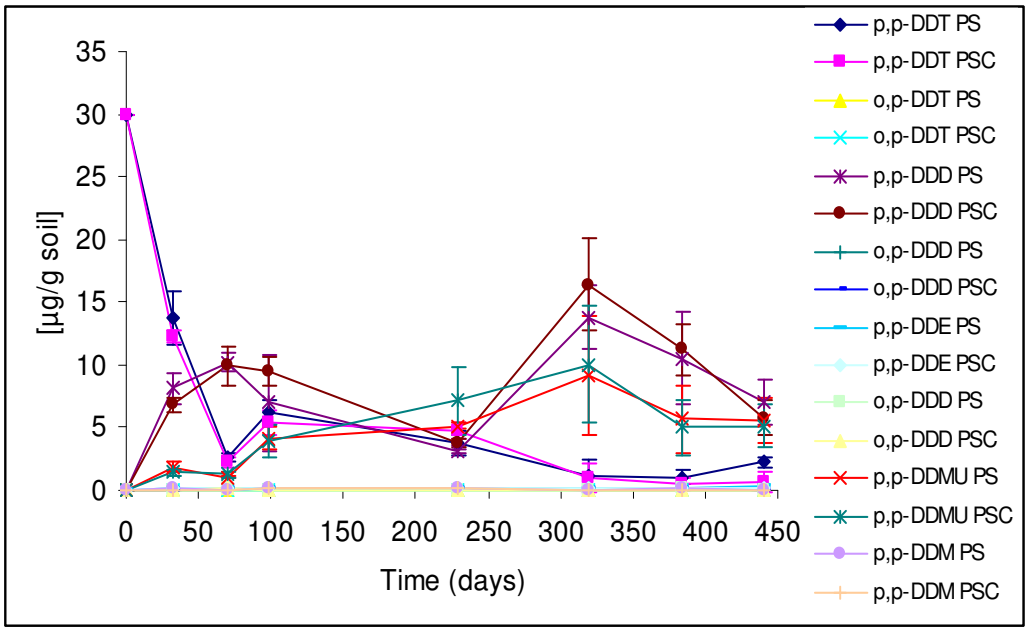

Fig. 55: DDT degradation and metabolite pattern in the paddy soil during the anaerobic-aerobic cycles experiment (Table of data is in the appendix).

PS = Paddy soil, PSC = Paddy soil + compost.

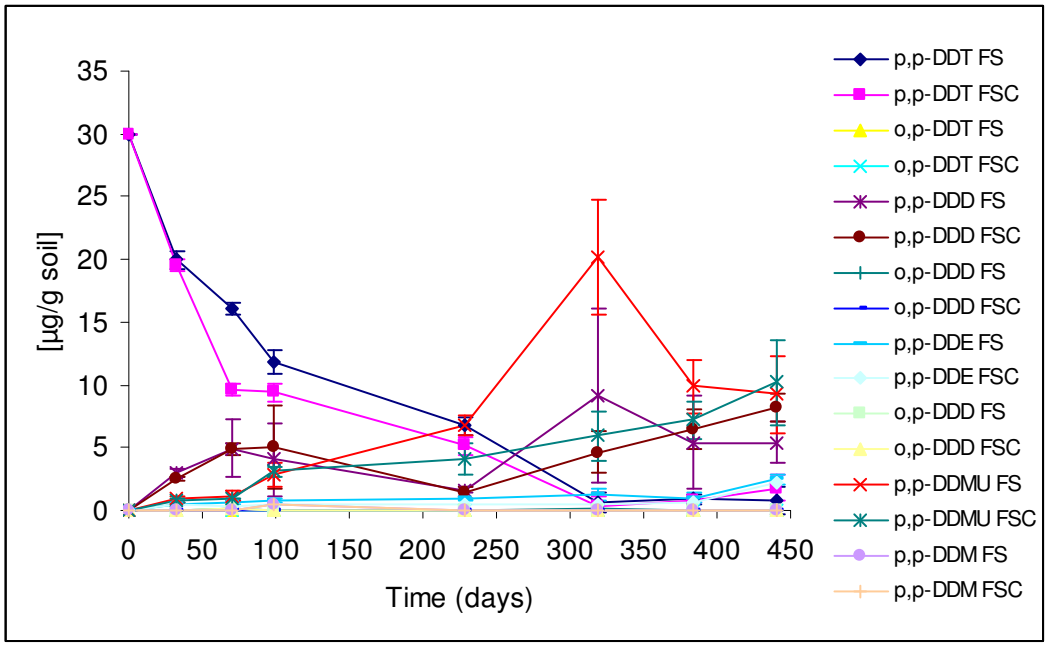

Fig. 56: DDT degradation and metabolite pattern in the field soil during the anaerobic-aerobic cycles incubation experiment (Table of data is in the appendix).

PS = Paddy soil, PSC = Paddy soil + compost.

Table 20: Slopes {(µg/g soil)/day} and intercepts (µg/g soil) for the p,p-DDT LME curve

group	DDT degradation	
	Intercept	Slope
Field soil	16.853	-0.0422
Field soil + compost	16.853	-0.0422
Paddy soil	8.462	-0.0194
Paddy soil + compost	8.462	-0.0194

Figures 55 and 56 show the DDT degradation and metabolite pattern in the paddy and field soils respectively. p,p-DDD and p,p-DDMU were the major metabolites formed in both soils. The p,p-DDT data was fitted into the linear mixed effects model (Fig. 57). The mixed model showed that there were significant differences ($p = 0.05$) between the soils (Table 18), with the degradation rate being higher in the field soil (Fig. 57 and Table 20). Compost had no significant effect on the dissipation rate of DDT in both soils

3.3.5 Multivariate analysis of the DDT degradation and metabolite formation data

To better appreciate the differences in p,p-DDT dissipation and metabolite formation between the groups, a PRC analysis of the data was done. The first principle component showed clear differences between the two soils, but there was no clear separation between the compost-treated and untreated sets of each soil (Fig. 58). There were higher amounts of o,p-DDT, p,p-DDE, p,p-DDM and p,p-DDT in the field soil, while the paddy soil had higher concentrations of o,p-DDD, p,p-DDD, p,p-DDMU and o,p-DDE. The second component showed clear separation between the soils only at the last time point (Fig. 59).

The first component of analysis using group information (vertical axis in the scores and classes/classes sections of Fig. 60) separated the groups into two classes according to soil type..p,p-DDD, o,p-DDD and o,p-DDE were higher in the paddy soil (canonical weights/variables sections of Fig. 60). However, unlike in the PRC curve (Fig. 58), p,p-DDMU was higher in the field soil (canonical weights/variables sections of Fig. 60). The second component (horizontal axis in the scores and classes/classes sections of Fig. 60) of analysis using group information did not show further separation.

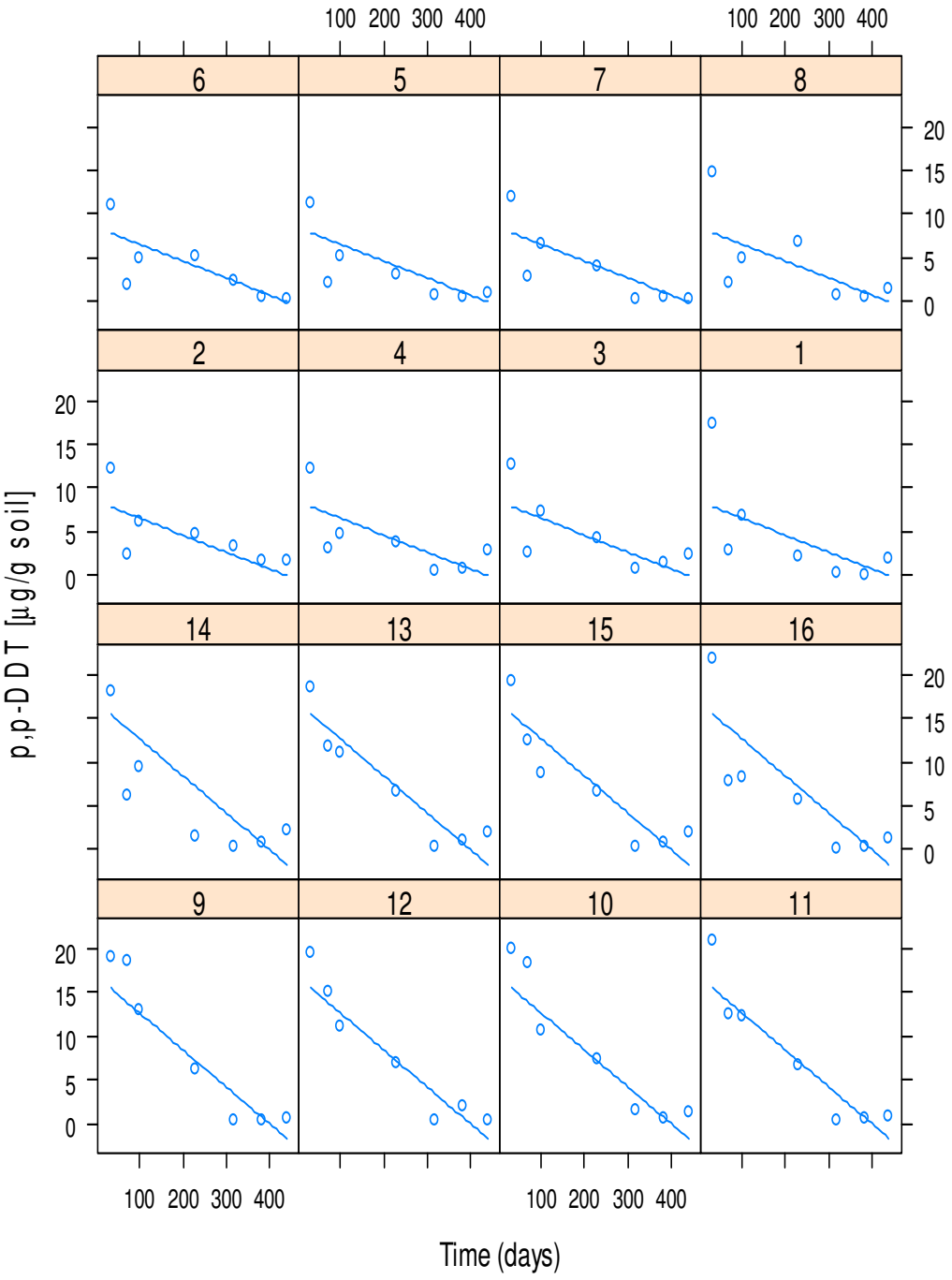

Fig. 57: LME modelling curve for p,p-DDT degradation in the paddy and field soils during the anaerobic-aerobic cycles incubation experiment.

1-4 = Paddy soil replicates; 5-8 = Paddy soil+compost replicates; 9-12 = Field soil replicates; 13-16 = Field soil+compost replicates

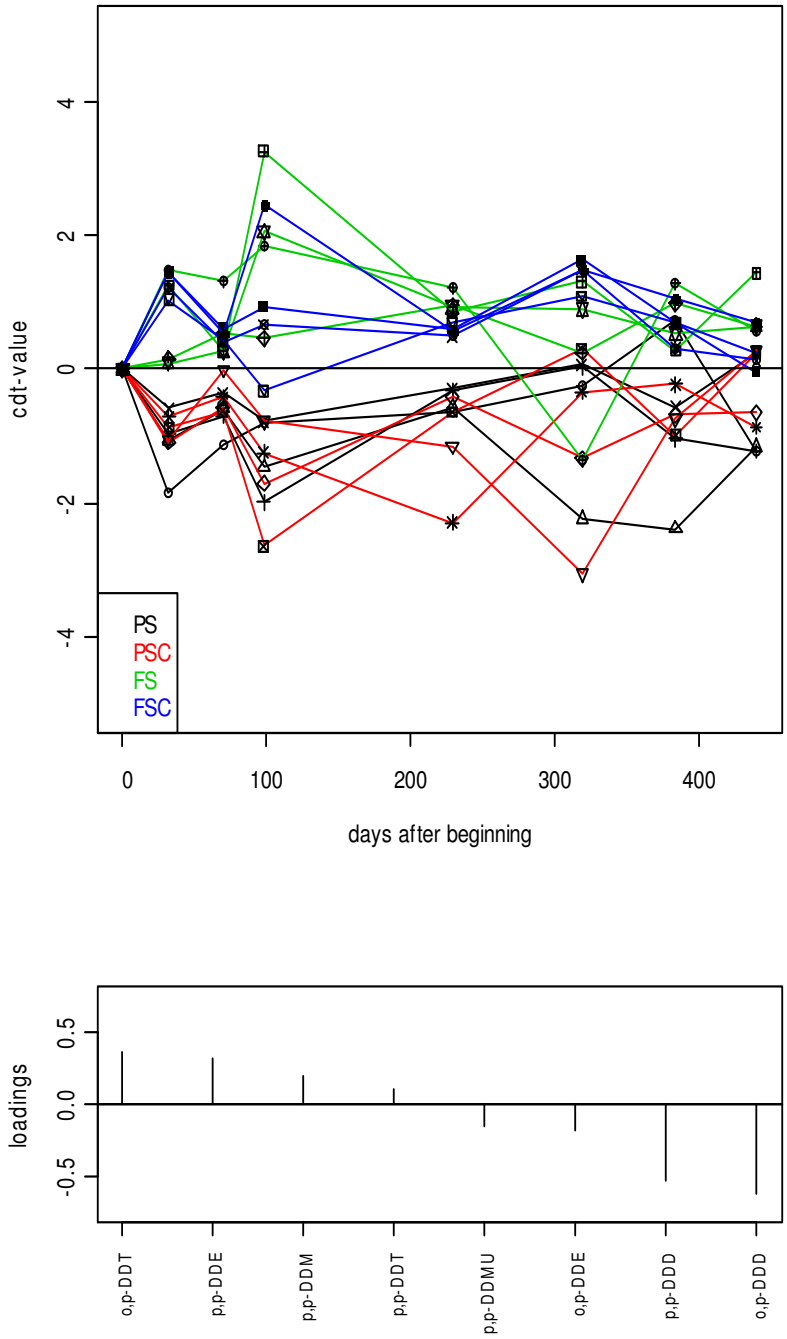

Fig. 58: PRC-curve (component 1**:** declared variance = 30.6 %) for p,p-DDT and its metabolites in the field and paddy soils during the anaerobic-aerobic cycles experiment.

PS = Paddy soil (4 replicates), PSC=Paddy soil+compost (4 replicates), FS=Field soil (4 replicates), FSC=Field soil+compost (4 replicates).

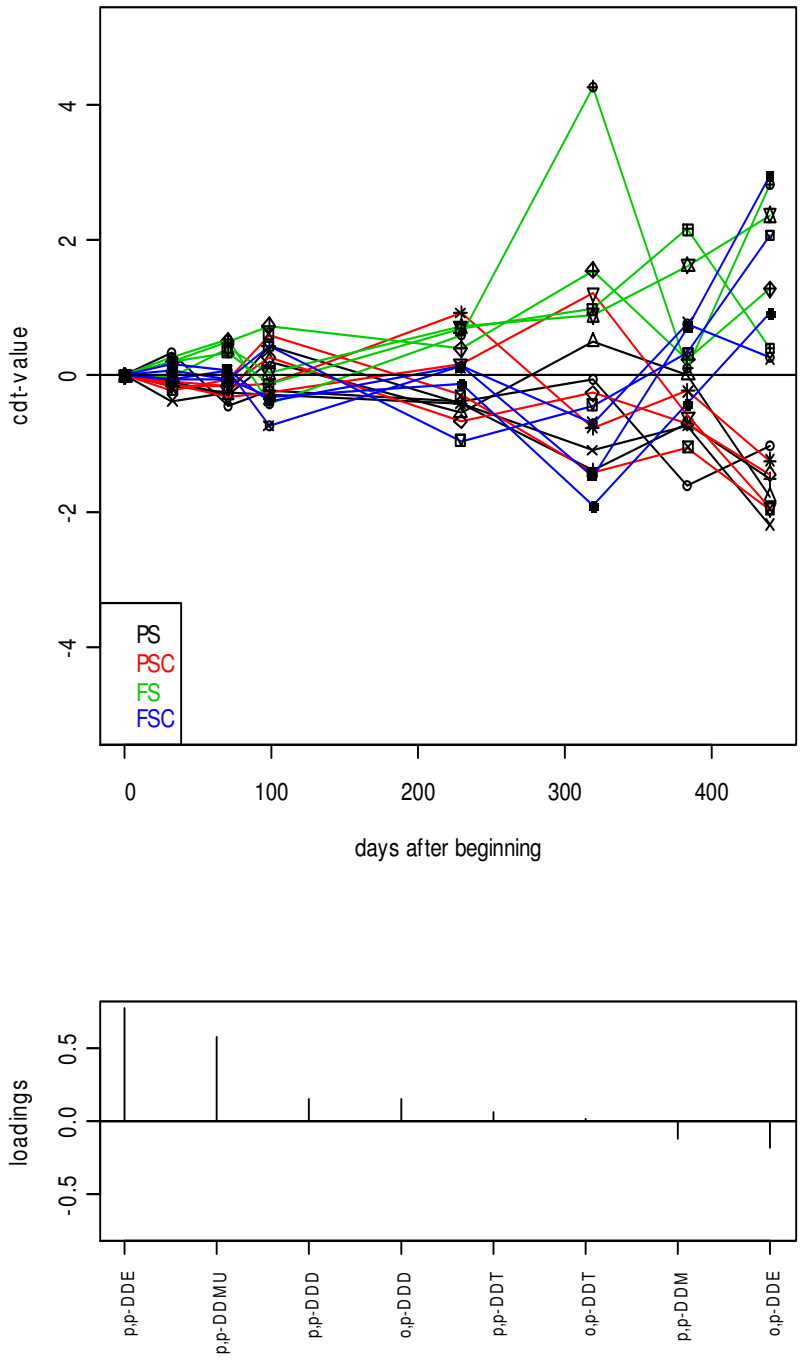

Fig. 59: PRC-curve (component 2) for p,p-DDT and its metabolites in the field and paddy soils during the anaerobic-aerobic cycles experiment (declared variance = 24.7).

PS = Paddy soil (4 replicates), PSC=Paddy soil+compost (4 replicates), FS=Field soil (4 replicates), FSC=Field soil+compost (4 replicates).

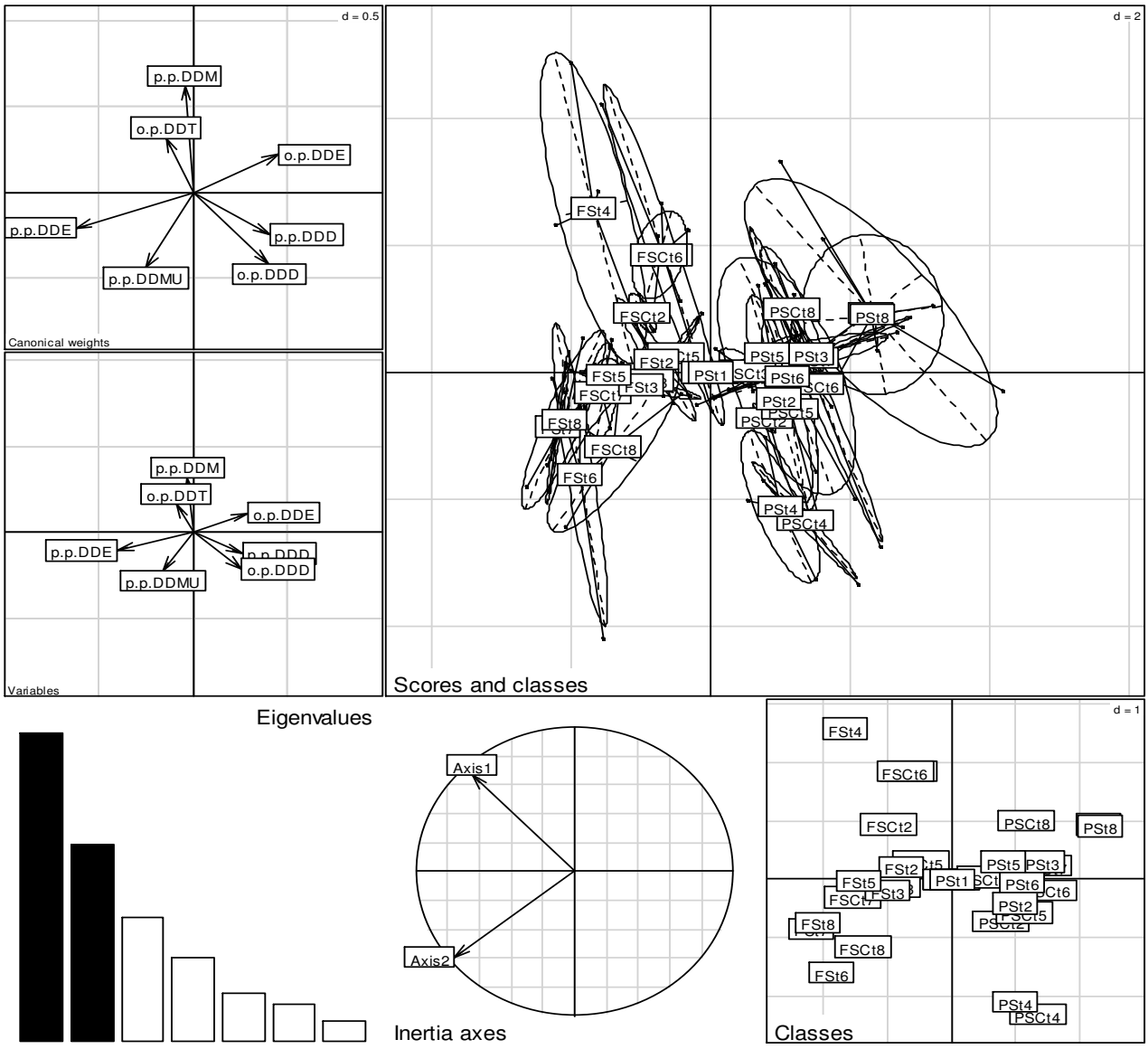

Fig. 60: Results of data analysis using group information (ade4-package, between function), based on components 1 and 2, showing the distribution of p,p-DDT and its metabolites in the field and paddy soils during the anaerobic-aerobic cycles incubation experiment. 'Scores and classes' is a 3-D presentation of the data separation by the two components/axes, while 'Classes' is a simple 2-D presentation of the same; 'Canonical weights' shows the loading of each metabolite; 'Variables' shows the extent and direction of each metabolite; 'Eigenvalues' shows the contribution of the axes in explaining the data: the two dark axes have been used to separate the groups.

PS = Paddy soil, PSC=Paddy soil+compost, FS=Field soil, FSC=Field soil+compost.
The last 2 digits refer to the sampling time e.g. FSt5 meansfield soil at the 5th sampling.

3.3.6 Mass balance and redox potential changes during the anaerobic-aerobic cycles.

Figure 61 shows the mass balance of ^{14}C-radioactivity. Figure 62 shows the redox potential with time of DDT-spiked field and paddy soils under aerobic-anaerobic cycles conditions. The objective of the experiment was to confirm that anaerobic conditions were actually achieved and maintained during water-logging of the soils. Like in the HCB experiment, yeast extract was applied during the second aerobic phase to induce anaerobic conditions.

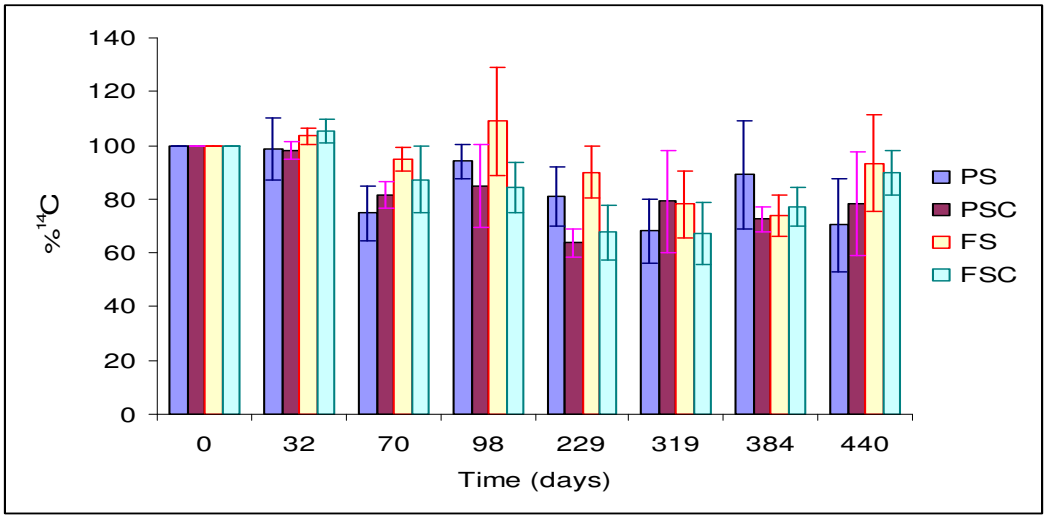

Fig 61: ^{14}C-Mass balance with time during the degradation of ^{14}C-DDT in paddy and field soils under anaerobic-aerobic cycles conditions.

PS = Paddy soil, PSC=Paddy soil+compost, FS=Field soil, FSC=Field soil+compost

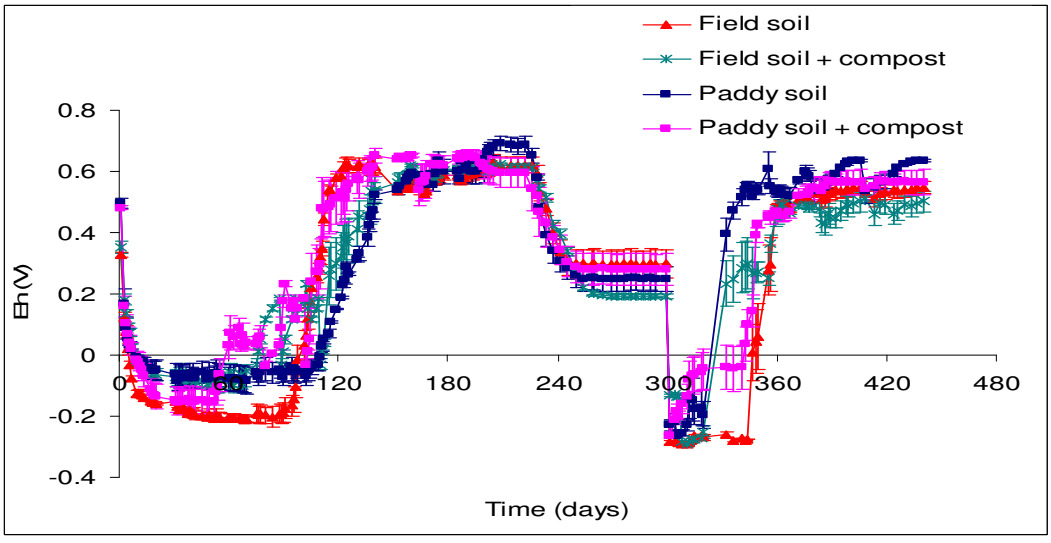

Figure 62: Redox Potential of the field and paddy soils during the degradation of DDT under anaerobic-aerobic cycles conditions

3.4 Factors Influencing the Anaerobic Degradation of DDT in Tropical Clay Soils

The aim of this experiment was to follow and understand the soil processes that take place during the anaerobic degradation of DDT. This was motivated by the fact that there were significant and profound differences between the soils with and without compost in the anaerobic-aerobic cycles experiment. This observation commanded further research with a view to gaining a deeper understanding of the underlying processes.

3.4.1 DDT degradation and metabolite formation under anaerobic conditions

Figures 63 and 64 show the DDT degradation and metabolite formation in the paddy and field soils respectively. p,p-DDD and p,p-DDMU were the major metabolites formed in both soils. There were significant differences (p=0.05) between the two soils in the rate of dissipation of p,p-DDT, and in the rate of formation of o,p-DDE, p,p-DDMU and p,p-DDM (Table 21). However, there were no significant differences between the compost-treated and untreated sets.

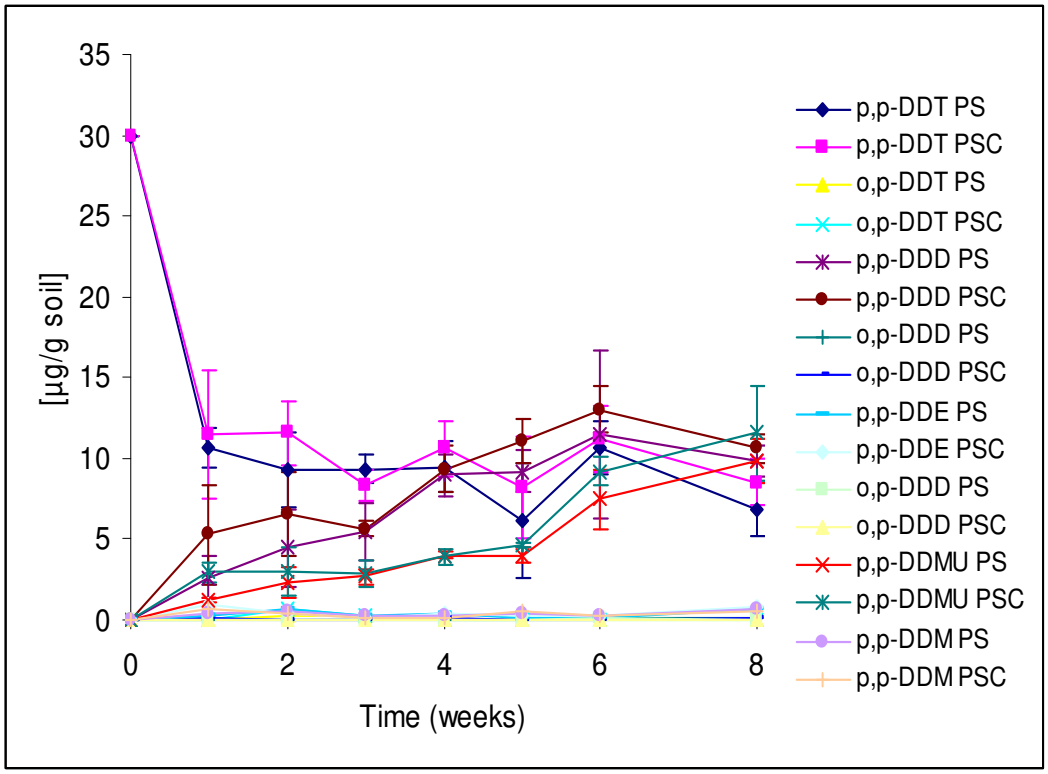

Fig. 63: DDT degradation and metabolite pattern in the paddy soil under anaerobic conditions (Table of data is in the appendix).

PS = Paddy soil, PSC=Paddy soil+compost.

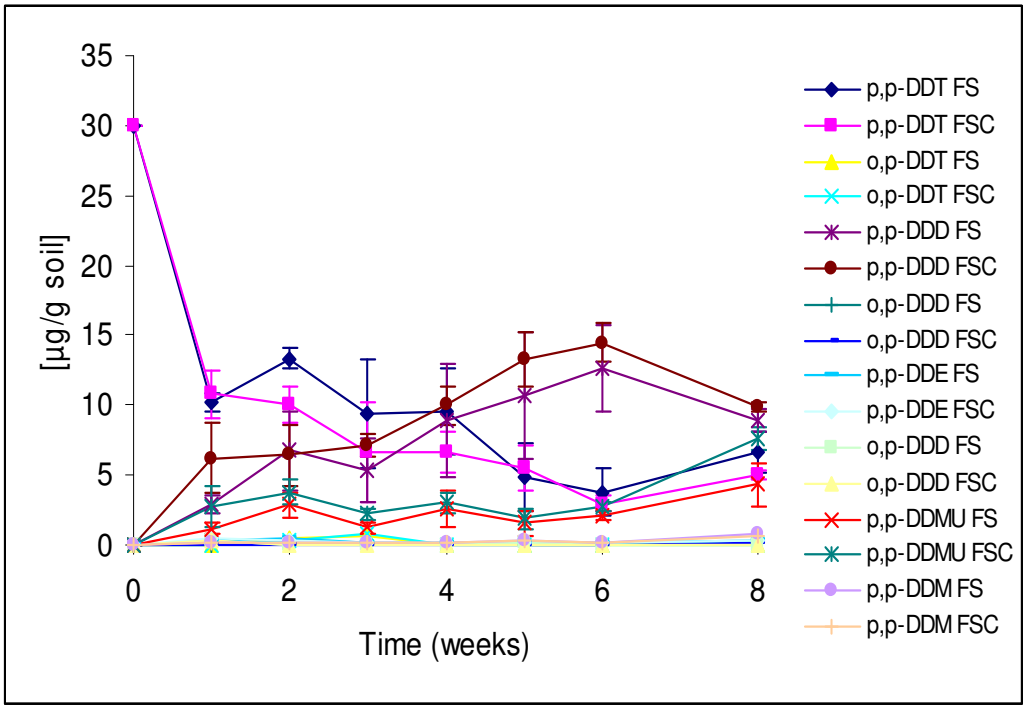

Fig. 64: DDT degradation and metabolite pattern in the field soil under anaerobic conditions (Table of data is in the appendix).

FS=Field soil, FSC=Field soil+compost.

Table 21: Significant test p-values for DDT and its metabolites in the paddy and field soils during the anaerobic degradation of DDT

group	p,p-DDT	o,p-DDT	p,p-DDD	o,p-DDD	p,p-DDE	o,p-DDE	p,p-DDMU	p,p-DDM
Intercept (FS)	<0.0001	<0.0001	<0.0001	<0.0001	<0.0001	0.0008	<0.0001	<0.0001
Slope (FS)	<0.0001	0.0007	<0.0001	<0.0001	0.2995	0.1796	<0.0001	0.0006
Intercept (PS)	0.0094	0.2655	0.3349	0.3349	0.0038	0.0038	0.0016	0.0041
Intercept (CE)	0.7682	0.6751	0.0617	0.5024	0.2759	0.9903	0.2256	0.8540
Slope (PS)	0.0015	0.6458	0.7692	0.3437	0.2564	0.0135	0.0058	0.0005

FS = Field soil; PS = Paddy soil; CE = compost effect

The p,p-DDT data was fitted into the linear mixed effects model (Fig. 65). The mixed model shows that there were differences between the soils with the degradation rate being higher in the field soil (Table 22). Compost had no significant effect on the dissipation rate of DDT in both soils (Fig. 65 and Table 22).

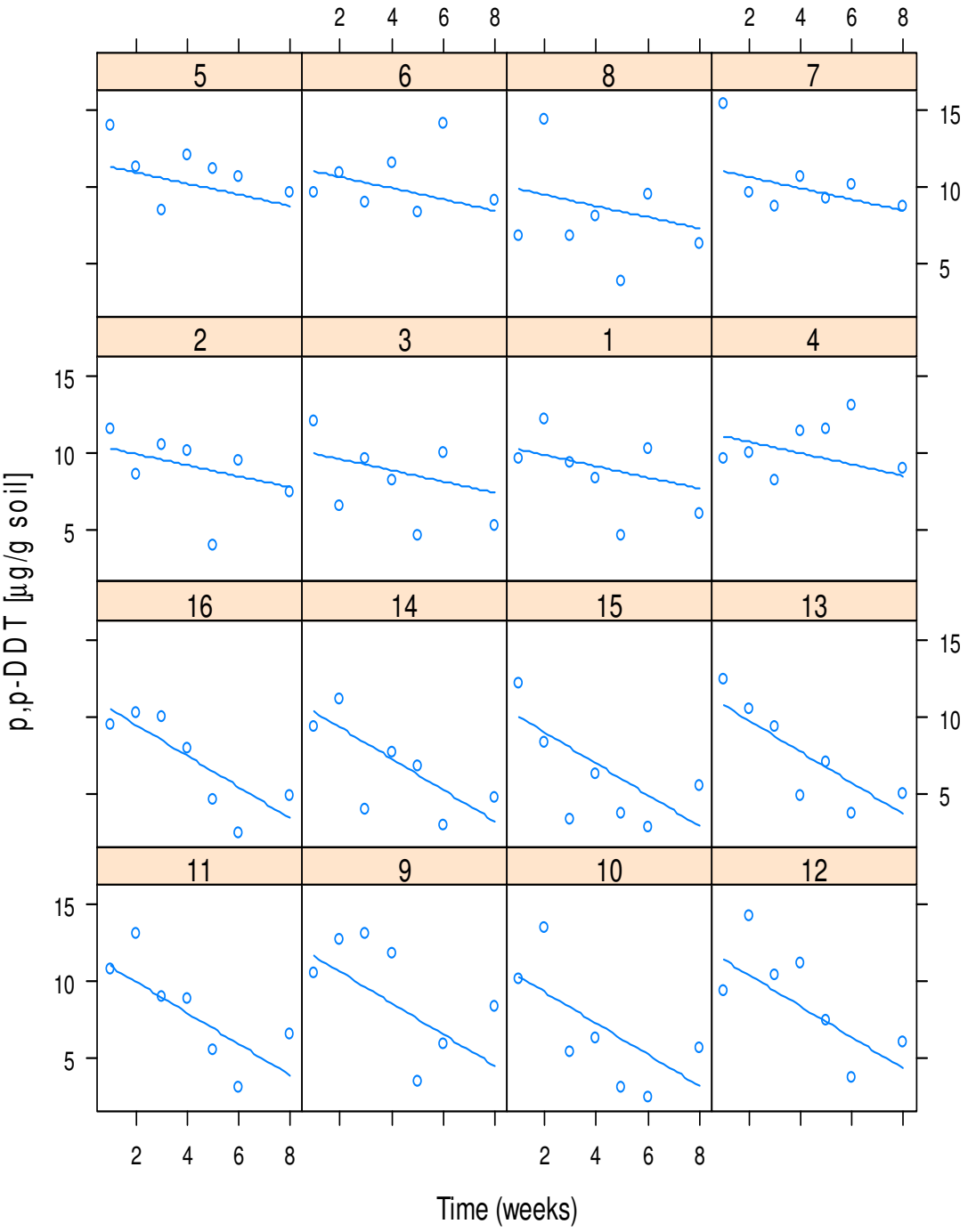

Fig. 65: LME model fitting for DDT degradation (y-axis = p,p-DDT concentration) in the paddy and field soils under anaerobic conditions.

1-4 = Paddy soil replicates; 5-8 = Paddy soil+compost replicates; 9-12 = Field soil replicates; 13-16 = Field soil+compost replicates

Table 22: Slopes {(µg/g soil)/day} and intercepts (µg/g soil) for the LME model fitting of p,p-DDT degradation of DDT in the paddy and field soils under anaerobic conditions

group	Intercept	Slope
Field soil	11.73	-1.012
Field soil + compost	11.73	-1.012
Paddy soil	10.95	-0.363
Paddy soil + compost	10.95	-0.363

To better appreciate the differences in formation of metabolites between the groups, a PRC analysis of the data was done. The first principle component showed clear differences between the two soils after week 5 (Fig. 66). The paddy soil had higher amounts of DDT and most of the metabolites as shown by the loadings. The second component did not show clear differences between the groups (Fig. 67), though there was a tendency towards separation according to soil type in the last two time points. The first component (vertical axis in scores and classes/classes sections of Fig. 68) of the analysis using group information separated the groups into two classes according to soil type. The presence of PSt1 in the field soil class and FSt2 in the paddy soil class (Fig. 68) can be attributed to the lack of clear separation between the soils in the first five weeks (Fig. 66). The compounds had higher concentrations in the paddy soil except for o,p-DDE and o,p-DDT (canonical weights/variables sections of Fig. 68). This was consistent with the loadings of the 1st component PRC curve (Fig. 66). The second component (horizontal axis in the scores and classes/classes sections of Fig. 68) of analysis using group information did not show further separation.

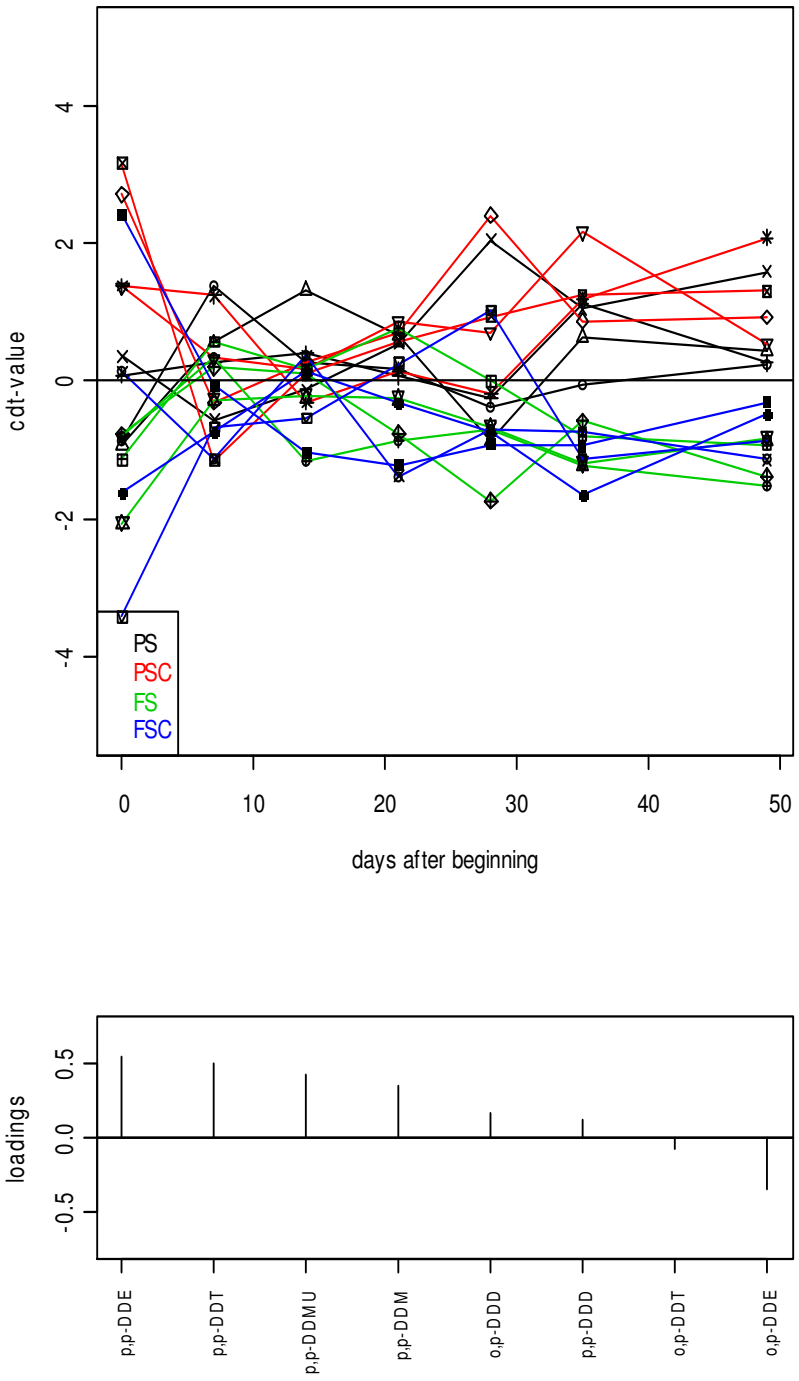

Fig. 66: PRC-curve (component 1: declared variance = 25.1 %) for p,p-DDT and its metabolites during the anaerobic degradation of DDT in the paddy and field soils.

PS = Paddy soil (4 replicates), PSC=Paddy soil+compost (4 replicates), FS=Field soil (4 replicates), FSC=Field soil+compost (4 replicates).

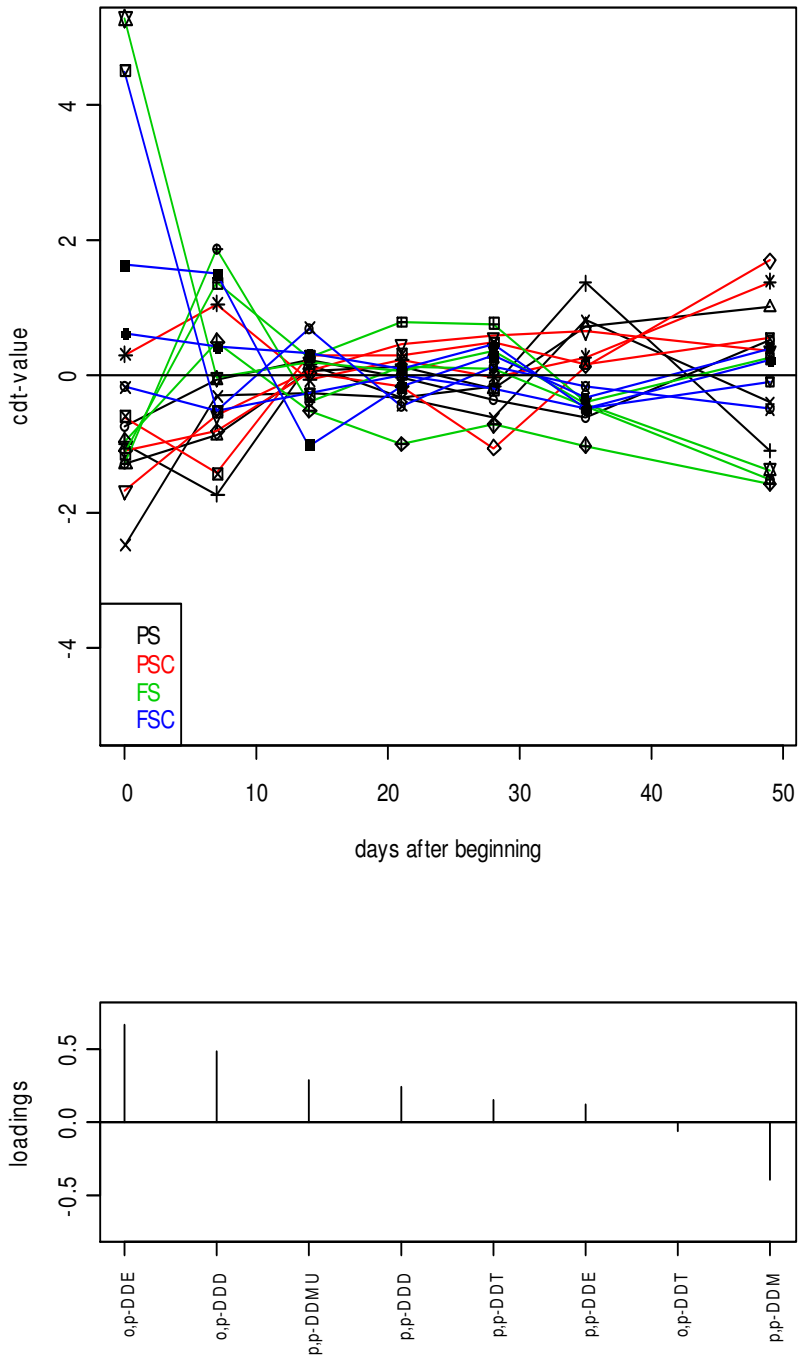

Fig. 67: PRC-curve (component 2**:** declared variance = 22.5 %) for p,p-DDT and its metabolites during the anaerobic degradation of DDT in the paddy and field soils.

PS = Paddy soil (4 replicates), PSC=Paddy soil+compost (4 replicates), FS=Field soil (4 replicates), FSC=Field soil+compost (4 replicates).

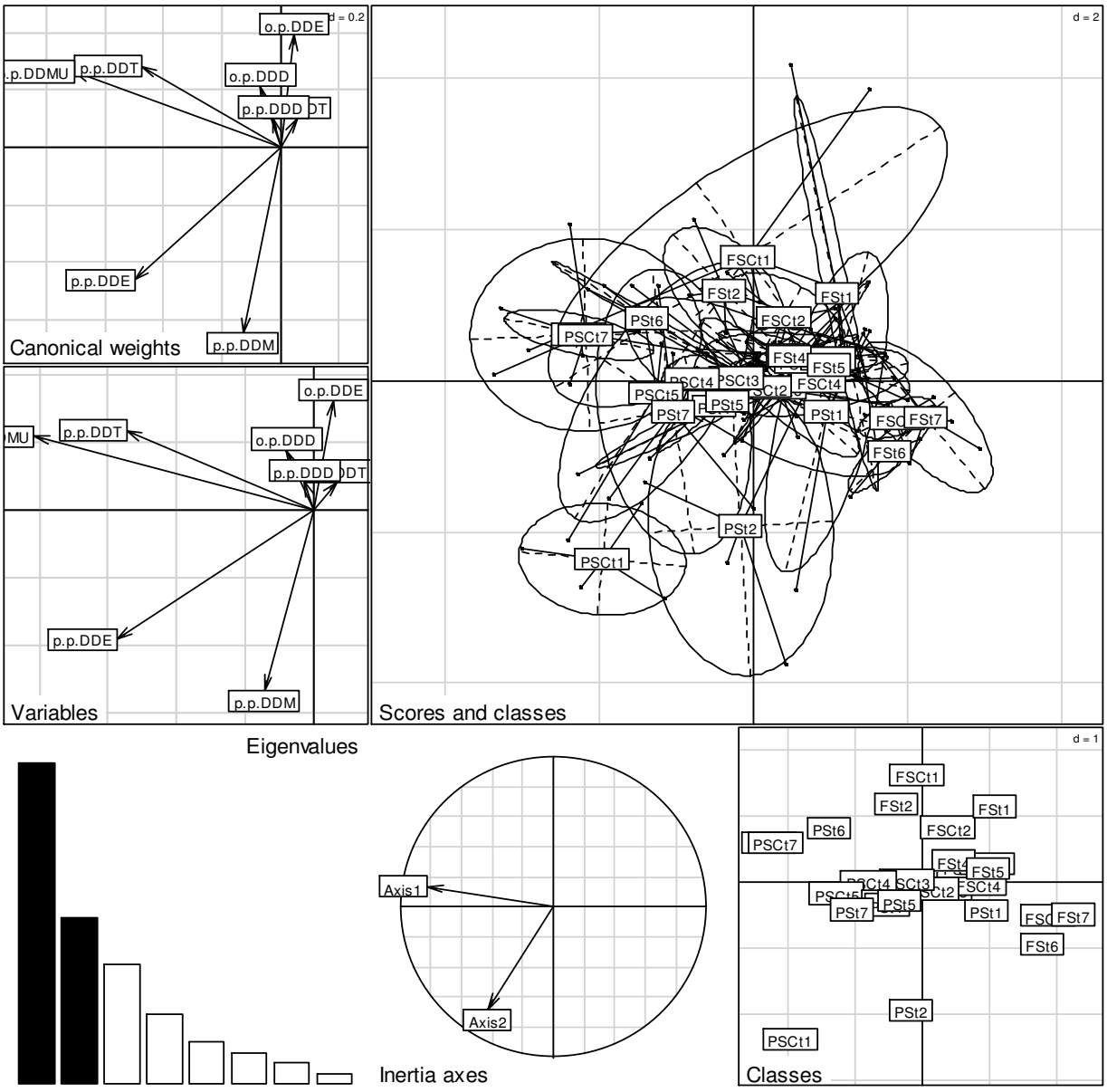

Fig. 68: Results of data analysis using group information (ade4-package, between function), based on components 1 and 2, showing the distribution of p,p-DDT and its metabolites in the field and paddy soils during the incubation experiment under anaerobic conditions. 'Scores and classes' is a 3-D presentation of the data separation by the two components/axes, while 'Classes' is a simple 2-D presentation of the same; 'Canonical weights' shows the loading of each metabolite; 'Variables' shows the extent and direction of each metabolite; 'Eigenvalues' shows the contribution of the components/axes in explaining the data: the two dark axes have been used to separate the groups.

PS = Paddy soil, PSC=Paddy soil+compost, FS=Field soil, FSC=Field soil+compost

3.4.2 Changes in soil properties during the anaerobic degradation of DDT

To appreciate the effect of soil type and compost amendment on soil chemistry during the anaerobic degradation of DDT, a PRC analysis of some measured soil parameters was done The first component clearly separated the two soils, and further separated the two groups within each soil (Fig. 69). Factor 4 (F4), NH_4^+, DOC, K^+, CO_2 and Fe (II) were higher in the field soil, while the other parameters were higher in the paddy soil as shown by the loadings. The second component separated the groups into compost-amended and un-amended soils (Fig 70). DOC, ESP, SAR, N_2O, F5 and Fe(III) were higher in the un-amended soils, while the other parameters were higher in the amended soils.

Analysis using group information, and based on the first two components, distinctly separated the treatments into the four classes (Fig. 71). The first component (vertical axis in scores and classes/classes sections of Fig. 71) of the analysis using group information separated the groups into two classes according to soil type. The second component (horizontal axis in the scores and classes/classes sections of Fig. 71) further separated the groups within each soil according to compost amendment. DOC was highest in the field soil (canonical weights/variables sections of Fig. 71); F4, NH_4^+, Fe(II), CO_2 and CO_2:CH_4 ratio were highest in the field soil with compost; N_2O, ESP and SAR were highest in the paddy soil; while F1, F2, F3, F5, salinity, CH_4, reducible Fe, SO_4^{2-}, NO_2^- and NO_3^- were highest in the paddy soil with compost.

3.4.3 Changes in soil anions during the anaerobic degradation of DDT

3.4.3.1 Changes in concentrations of the anions

Figure 72 shows the changes in nitrate, sulphate, nitrite, bromide, hydrogen phosphate, chloride and salinity concentrations with time in the paddy and field soils. There were rapid decreases of nitrate and sulphate in the amended and unamended paddy soils in the first one week. The sulphate concentrations in the paddy soil samples increased slightly in week 2 and remained fairly constant for the rest of the experimental period. The compost-amended field soil had high nitrate content and this decreased rapidly in the first week. The nitrate content remained low in all samples after the first week.

The nitrite content decreased rapidly in the first week in the paddy soil samples, and then gradually to a minimum in week 8. The nitrite content in the field soils was lower and decreased gradually over the 8 weeks. The bromide content increased gradually in all samples over the experimental period, while hydrogen phosphate content was low and did not change

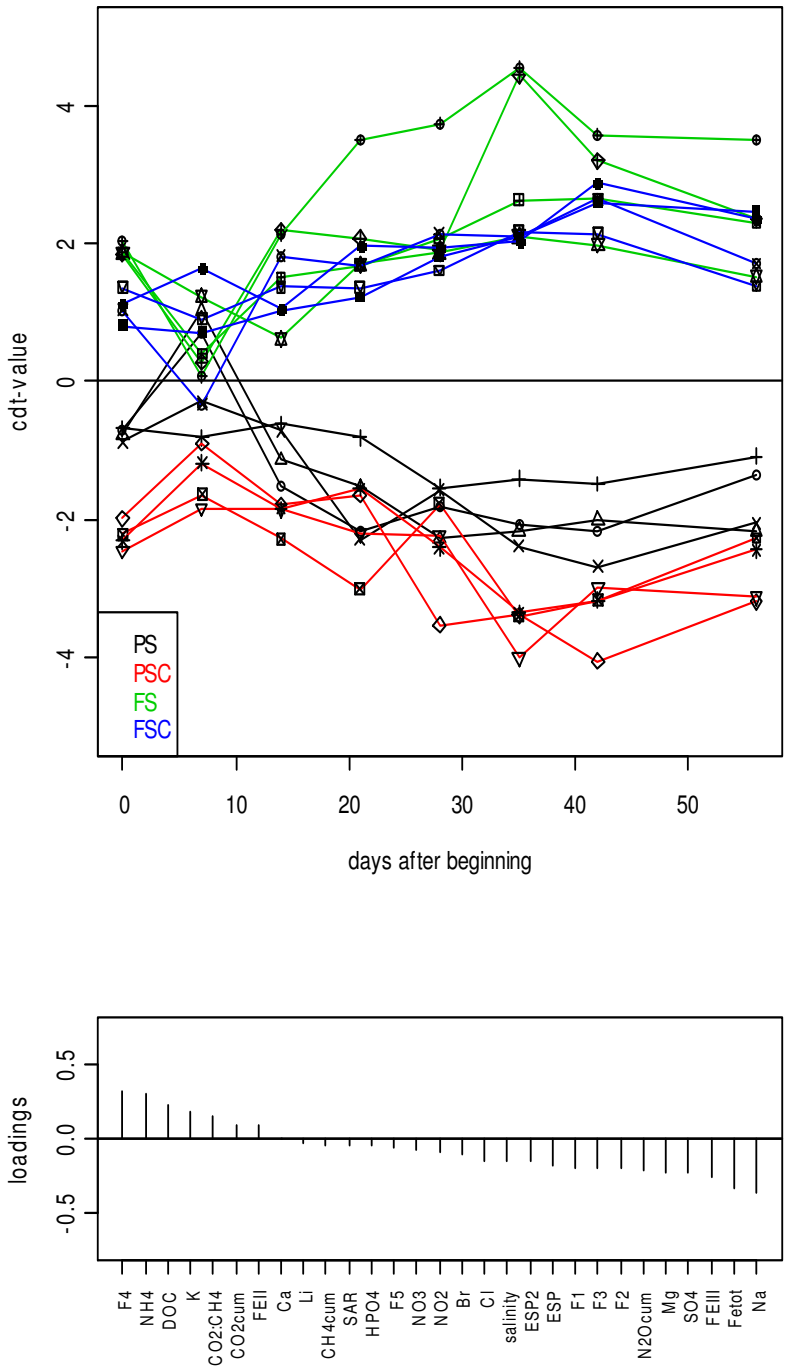

Fig. 69: PRC-curve (component **1)** for changes in soil parameters in the paddy and field soils during the anaerobic degradation of DDT (declared variance = 29.4 %).

PS = Paddy soil (4 replicates), PSC=Paddy soil+compost (4 replicates), FS=Field soil (4 replicates), FSC=Field soil+compost (4 replicates).

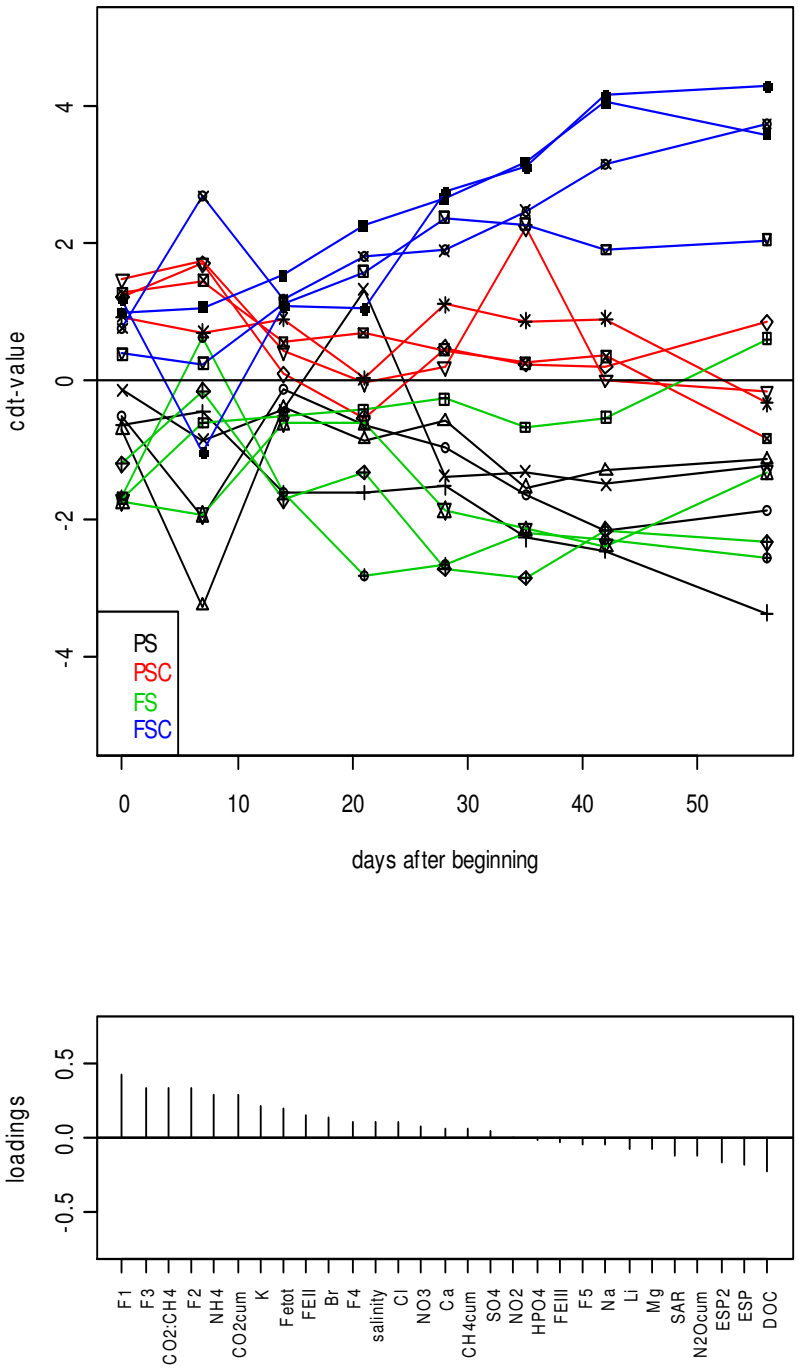

Fig. 70: PRC-curve (component **2)** for changes in soil parameters in the paddy and field soils during the anaerobic degradation of DDT (declared variance = 19.1 %).

PS = Paddy soil (4 replicates), PSC=Paddy soil+compost (4 replicates), FS=Field soil (4 replicates), FSC=Field soil+compost (4 replicates).

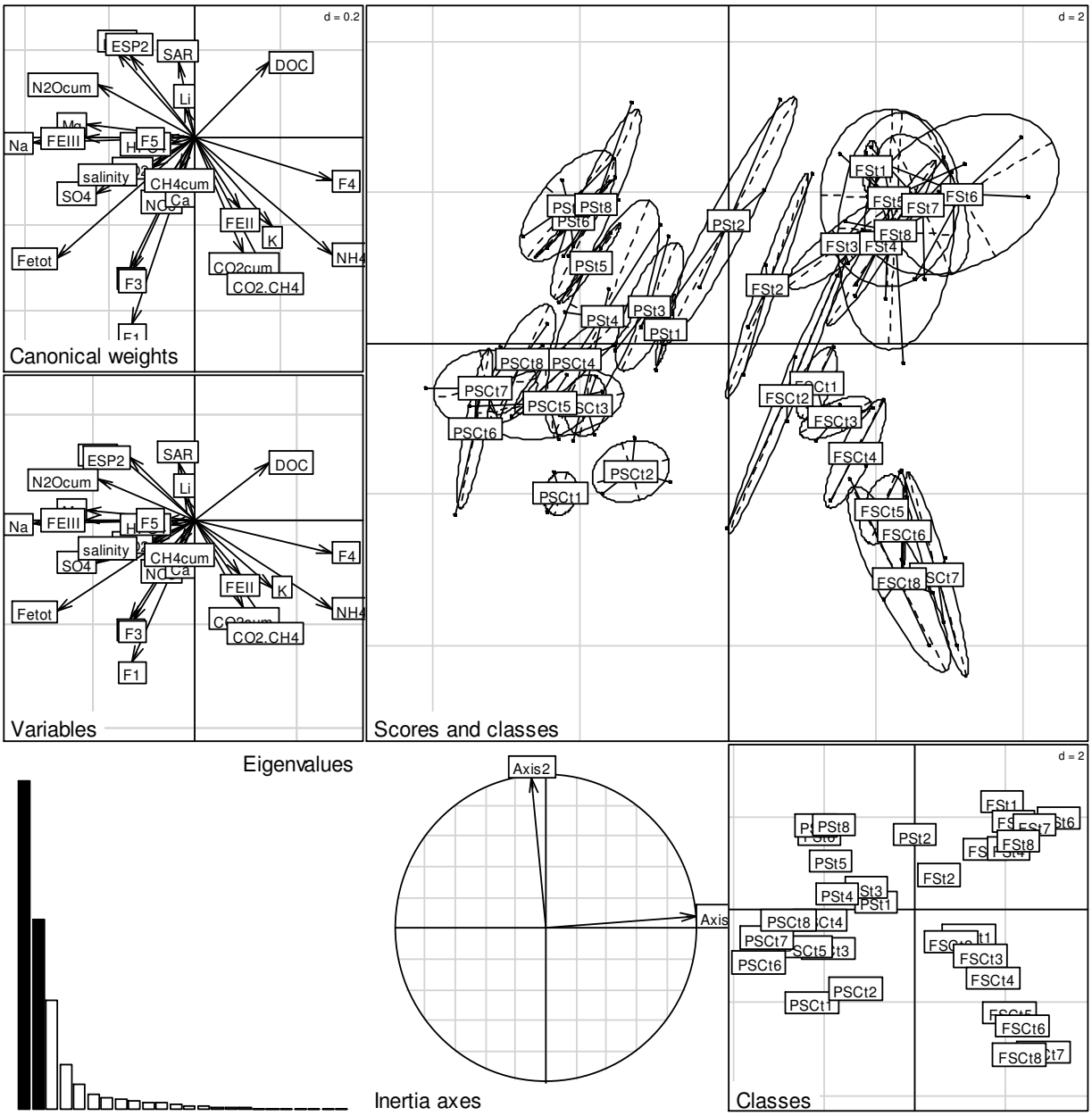

Fig. 71: Results of data analysis using group information (ade4-package, between function), based on components 1 and 2, showing the distribution of soil parameters in the field and paddy soils during the incubation experiment under anaerobic conditions. 'Scores and classes' is a 3-D presentation of the data separation by the two components/axes, while 'Classes' is a simple 2-D presentation of the same; 'Canonical weights' shows the loading of each metabolite; 'Variables' shows the extent and direction of each metabolite; 'Eigenvalues' shows the contribution of the components/axes in explaining the data: the two dark axis have been used to separate the groups.

PS = Paddy soil, PSC=Paddy soil+compost, FS=Field soil, FSC=Field soil+compost

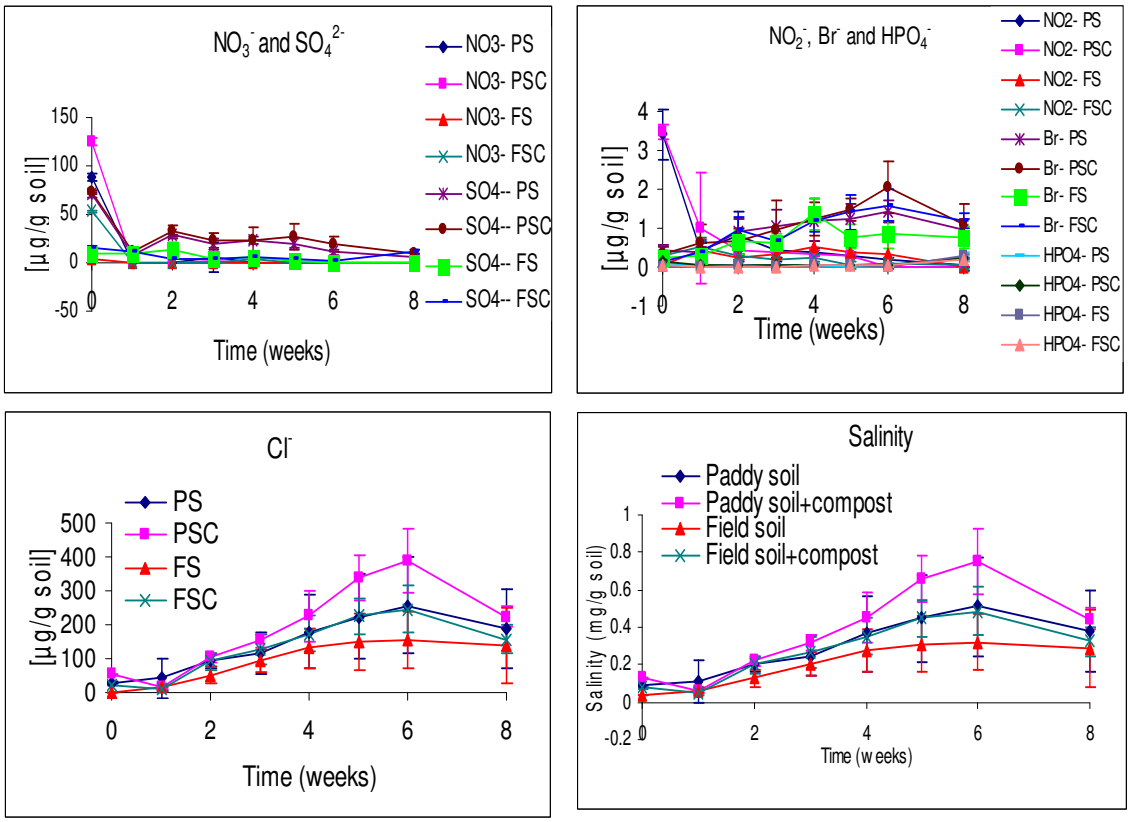

Figure 72: Changes in nitrate, sulphate nitrite, bromide, hydrogen phosphate, chloride and salinity concentrations in the paddy and field soils during the anaerobic degradation of DDT.

PS=Paddy soil; PSC=Paddy soil+compost; FS=Field soil; FSC=Field soil+compost

Table 23: Significant test p-values (p = 0.05) for anions in the paddy and field soils during the anaerobic degradation of DDT.

group	Cl^-	NO_2^-	Br^-	NO_3^-	HPO_4^-	SO_4^{2-}	Salinity
Intercept (FS)	<0.0001	<0.0001	<0.0001	<0.0001	<0.0001	<0.0001	<0.0001
Slope (FS)	<0.0001	<0.0001	<0.0001	<0.0001	<0.0001	<0.0001	<0.0001
Intercept (PS)	0.0618	0.0005	0.0675	0.0327	0.0900	<0.0001	0.0615
Intercept (CE)	0.1186	0.5778	0.057	0.1350	0.7805	0.0476	0.118
Slope (PS)	0.051	<0.0001	0.7032	0.0010	0.3002	<0.0001	0.0515
Slope (CE)	0.0877	0.3806	0.0124	0.0196	0.1774	0.4080	0.0866

FS = Field soil; PS = Paddy soil; CE = compost effect

much over the 8 weeks. The chloride content increased gradually to a maximum on week 6 followed by a slight decrease. The significance test p-values are shown in Table 23.

3.4.3.2 Salinity

Salinity (mg/g soil) was calculated using the formula

Salinity = (1.85 x Chlorinity) + 0.03……1 (Forch et al., 1902)

Where chlorinity = [Cl-] + [Br-]

To test whether a relationship existed between soil properties and DDT degradation, correlation coefficients between p,p-DDT, p,p-DDD, p,p-DDMU and different soil parameters were determined (Tables 24, 25, 26 and 27). The correlations of some of these parameters with p,p-DDT and p,p-DDD were plotted to illustrate the correlations. The four tables (Tables 24, 25, 26 and 27) were used to present the rest of the correlations.

Fig. 73 shows the correlation of salinity with p,p-DDT and p,p-DDD. There were no significant correlations between p,p-DDT and salinity in the paddy soils sets. However, there were good inverse correlations of salinity with p,p-DDT in the field soil sets, and strong positive correlations with p,p-DDD in all the sets (Fig. 73). There was a positive correlation between salinity and p,p-DDMU in the paddy soil (Table 24), but not in the compost-amended paddy soil (Table 25). There was no correlation between salinity and p,p-DDMU in the field soil samples (Tables 26 and 27). There were significant correlations between salinity and other soil properties such as Fe, CH_4, CO_2 and N_2O in both the paddy and field soils (Tables 24, 25, 26 and 27).

3.4.4 Changes in soil cations during the anaerobic degradation of DDT

3.4.4.1 Changes in concentrations of cations

Figure 72 shows the changes in Na^+, K^+, Li^+, Mg^{2+}, Ca^{2+}, SAR and ESP concentrations with time in the paddy and field soils. All the cations increased gradually with time over the period except for Li^+ whose concentration remained constant. The concentrations of Na^+, Mg^{2+} and Ca^{2+} decreased at the last sampling point. The significance test p-values are shown in Table 28.

3.4.4.2 Sodicity

Exchangeable sodium percentage (ESP) and sodium absorption ratio (SAR) are measures of sodicity (Sumner et. al, 1998). Sodicity describes the swelling and dispersion of soils. This is normally caused where the concentration of sodium reaches a level where it causes the

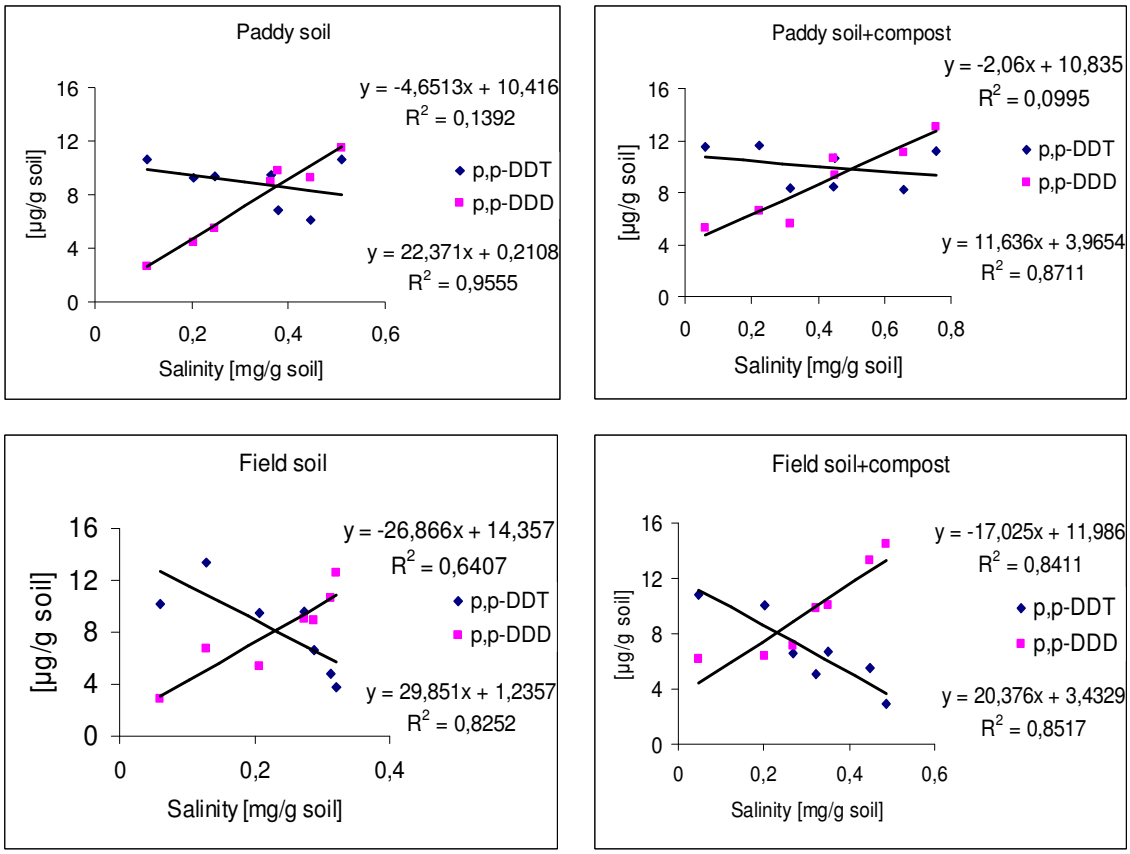

Figure 73: Correlations of salinity with p,p-DDT and p,p-DDD (n = 7, df = 5, Pearson R^2 critical value = 0.4476 (p=0.05)) in the paddy and field soils during the anaerobic degradation of DDT.

weakening of bonds between soil particles upon wetting (Rangsamy, 1984).

The results of the cation measurements were used to determine the Exchangeable sodium percentage (ESP). The alkali and alkaline earth metals, as well as NH_4^+, were used in determining the total cation concentration (TCC).

ESP = $[Na^+]*100/[TCC]$……2 (Sumner et. al, 1998).

Where TCC (total cation concentration) = sum of Li^+, Na^+, K^+, NH_4^+, Mg^{2+} and Ca^{2+} concentrations.

ESP is usually determined using only Na^+, K^+, Mg^{2+} and Ca^{2+}. This was also calculated and is hereafter refered to as ESP2, viz:

ESP2 = $[Na^+]*100/([\ Na^+]+[\ K^+]+[\ Mg^{2+}]+[\ Ca^{2+}]$……...2 (Sumner et. al, 1998).

Table 24: Correlation co-efficients for p,p-DDT, p,p-DDD, p,p-DDMU and various soil parameters in the paddy soil during the anaerobic degradation of DDT (n = 7, df = 5, critical value for Pearson r = 0.669 (p = 0.05)).

	p,p-DDT	p,p-DDD	p,p-DDMU	ESP	SAR	Salinity	Fe (II)	Fe (III)	CH_4	N_2O	CO_2	F1	F2	F3	F4	F5	DOC	NH_4^+
p,p-DDT	1																	
p,p-DDD	-0.357	1																
p,p-DDMU	-0.372	0.815	1															
ESP	0.525	-0.730	-0.904	1														
SAR	0.508	-0.807	-0.915	0.985	1													
Salinity	-0.373	0.978	0.713	-0.616	-0.700	1												
Fe (II)	-0.490	0.980	0.841	-0.766	-0.843	0.946	1											
Fe (III)	0.489	-0.982	-0.842	0.771	0.846	-0.948	-0.100	1										
CH_4	-0.503	0.920	0.957	-0.868	-0.911	0.853	0.955	-0.955	1									
N_2O	-0.536	0.918	0.931	-0.866	-0.913	0.868	0.947	-0.947	0.986	1								
CO_2	-0.494	0.854	0.987	-0.910	-0.932	0.769	0.895	-0.895	0.986	0.972	1							
F1	-0.492	0.252	0.266	-0.488	-0.54	0.200	0.337	-0.334	0.339	0.433	0.350	1						
F2	-0.194	-0.195	-0.24	-0.009	-0.058	-0.207	-0.132	0.136	-0.173	-0.066	-0.167	0.862	1					
F3	-0.577	0.432	0.486	-0.678	-0.727	0.349	0.529	-0.526	0.55	0.613	0.562	0.962	0.704	1				
F4	-0.191	0.674	0.651	-0.659	-0.755	0.597	0.688	-0.686	0.692	0.748	0.681	0.762	0.469	0.820	1			
F5	-0.254	-0.339	-0.181	-0.006	-0.022	-0.372	-0.231	0.238	-0.173	-0.082	-0.123	0.801	0.920	0.661	0.371	1		
DOC	0.166	-0.568	-0.069	0.236	0.32	-0.618	-0.497	0.503	-0.259	-0.301	-0.143	-0.289	-0.196	-0.297	-0.360	0.182	1	
NH_4^+	-0.283	0.519	0.573	-0.710	-0.734	0.356	0.576	-0.576	0.570	0.499	0.568	0.395	0.090	0.585	0.496	-0.0003	-0.360	1

Table 25: Correlation co-efficients for p,p-DDT, p,p-DDD, p,p-DDMU and various soil parameters in the compost-amended paddy soil during the anaerobic degradation of DDT (n = 7, df = 5, critical value for Pearson r = 0.669 (p = 0.05)).

	p,p-DDT	p,p-DDD	p,p-DDMU	ESP	SAR	Salinity	Fe (II)	Fe (III)	CH_4	N_2O	CO_2	F1	F2	F3	F4	F5	DOC	NH_4^+
p,p-DDT	1																	
p,p-DDD	-0.173	1																
p,p-DDMU	-0.231	0.742	1															
ESP	0.1604	-0.441	-0.77	1														
SAR	0.1648	-0.488	-0.752	0.9915	1													
Salinity	-0.315	0.933	0.562	-0.189	-0.26	1												
Fe (II)	-0.186	0.968	0.733	-0.537	-0.578	0.856	1											
Fe (III)	0.4272	-0.929	-0.716	0.4644	0.5205	-0.922	-0.931	1										
CH_4	-0.532	0.878	0.827	-0.557	-0.588	0.847	0.88	-0.968	1									
N_2O	-0.52	0.895	0.861	-0.594	-0.62	0.844	0.884	-0.949	0.991	1								
CO_2	-0.437	0.818	0.957	-0.703	-0.701	0.698	0.824	-0.856	0.947	0.962	1							
F1	-0.43	-0.081	-0.001	-0.531	-0.55	-0.148	0.036	-0.032	0.061	0.097	0.059	1						
F2	-0.289	-0.377	-0.406	-0.121	-0.138	-0.359	-0.306	0.3183	-0.323	-0.28	-0.35	0.887	1					
F3	-0.505	-0.021	0.121	-0.6	-0.606	-0.105	0.092	-0.092	0.154	0.197	0.179	0.988	0.836	1				
F4	-0.788	0.376	0.292	-0.345	-0.371	0.419	0.505	-0.649	0.669	0.612	0.527	0.445	0.163	0.486	1			
F5	-0.445	0.115	0.654	-0.765	-0.691	-0.096	0.228	-0.221	0.425	0.45	0.623	0.419	0.083	0.537	0.444	1		
DOC	-0.388	-0.023	0.516	-0.213	-0.118	-0.082	-0.076	-0.005	0.243	0.28	0.449	-0.171	-0.287	-0.03	0.023	0.669	1	
NH_4^+	-0.100	0.463	0.845	-0.601	-0.538	0.249	0.521	-0.477	0.616	0.61	0.787	-0.229	-0.602	-0.11	0.265	0.724	0.623	1

Table 26: Correlation co-efficients for p,p-DDT, p,p-DDD, p,p-DDMU and various soil parameters in the field soil during the anaerobic degradation of DDT (n = 7, df = 5, critical value for Pearson r = 0.669 (p = 0.05)).

	p,p-DDT	p,p-DDD	p,p-DDMU	ESP	SAR	Salinity	Fe (II)	Fe (III)	CH_4	N_2O	CO_2	F1	F2	F3	F4	F5	DOC	NH_4^+
p,p-DDT	1																	
p,p-DDD	-0.751	1																
p,p-DDMU	0.004	0.309	1															
ESP	0.802	-0.805	-0.400	1														
SAR	0.770	-0.836	-0.338	0.986	1													
Salinity	-0.800	0.908	0.297	-0.943	-0.973	1												
Fe (II)	-0.732	0.906	0.442	-0.862	-0.886	0.956	1											
Fe (III)	0.7397	-0.902	-0.444	0.829	0.847	-0.931	-0.995	1										
CH_4	-0.802	0.827	0.571	-0.915	-0.875	0.889	0.923	-0.924	1									
N_2O	-0.763	0.731	0.632	-0.894	-0.820	0.791	0.805	-0.805	0.969	1								
CO_2	-0.757	0.743	0.640	-0.905	-0.839	0.812	0.827	-0.825	0.977	0.999	1							
F1	0.2842	-0.72	-0.141	0.596	0.692	-0.69	-0.575	0.517	-0.388	-0.300	-0.330	1						
F2	0.3941	-0.814	-0.274	0.711	0.789	-0.791	-0.703	0.652	-0.550	-0.470	-0.490	0.982	1					
F3	0.416	-0.839	-0.139	0.597	0.674	-0.710	-0.626	0.591	-0.466	-0.380	-0.400	0.952	0.957	1				
F4	-0.701	0.714	0.141	-0.861	-0.906	0.927	0.859	-0.822	0.749	0.629	0.654	-0.616	-0.692	-0.558	1			
F5	-0.112	-0.157	0.641	-0.228	-0.085	-0.007	0.085	-0.106	0.397	0.539	0.524	0.501	0.362	0.503	-0.027	1		
DOC	-0.426	0.756	-0.064	-0.584	-0.704	0.771	0.688	-0.645	0.420	0.254	0.284	-0.906	-0.894	-0.874	0.769	-0.597	1	
NH_4^+	-0.773	0.756	0.602	-0.929	-0.867	0.838	0.834	-0.827	0.972	0.991	0.992	-0.381	-0.54	-0.443	0.707	0.486	0.340	1

Table 27: Correlation co-efficients for p,p-DDT, p,p-DDD, p,p-DDMU and various soil parameters in the compost-amended field soil during the anaerobic degradation of DDT (n = 7, df = 5, critical value for Pearson r = 0.669 (p = 0.05)).

	p,p-DDT	p,p-DDD	p,p-DDMU	ESP	SAR	Salinity	Fe (II)	Fe (III)	CH_4	N_2O	CO_2	F1	F2	F3	F4	F5	DOC	NH_4^+
p,p-DDT	1																	
p,p-DDD	-0.863	1																
p,p-DDMU	-0.141	-0.088	1															
ESP	0.9483	-0.809	-0.361	1														
SAR	0.9632	-0.823	-0.16	0.968	1													
Salinity	-0.917	0.923	-0.048	-0.869	-0.914	1												
Fe (II)	-0.859	0.842	0.288	-0.951	-0.922	0.894	1											
Fe (III)	0.8485	-0.803	-0.304	0.9369	0.9124	-0.904	-0.989	1										
CH_4	-0.924	0.777	0.391	-0.978	-0.934	0.883	0.947	-0.958	1									
N_2O	-0.837	0.719	0.594	-0.916	-0.793	0.708	0.845	-0.826	0.915	1								
CO_2	-0.861	0.718	0.586	-0.938	-0.828	0.734	0.865	-0.852	0.939	0.997	1							
F1	-0.244	0.098	0.578	-0.429	-0.263	0.052	0.374	-0.317	0.411	0.558	0.539	1						
F2	0.3692	-0.44	0.318	0.2198	0.3547	-0.556	-0.267	0.337	-0.26	-0.06	-0.09	0.772	1					
F3	-0.199	0.011	0.481	-0.377	-0.244	0.033	0.329	-0.288	0.374	0.444	0.438	0.972	0.776	1				
F4	-0.916	0.722	0.088	-0.895	-0.923	0.868	0.832	-0.84	0.906	0.731	0.766	0.384	-0.202	0.422	1			
F5	0.0118	-0.178	0.85	-0.177	0.0436	-0.285	0.064	-0.018	0.153	0.467	0.433	0.779	0.704	0.665	-0.051	1		
DOC	-0.186	0.093	0.715	-0.285	-0.056	0.054	0.215	-0.226	0.375	0.617	0.578	0.632	0.378	0.529	0.174	0.7459	1	
NH_4^+	-0.898	0.847	0.429	-0.968	-0.895	0.845	0.951	-0.93	0.955	0.96	0.966	0.43	-0.217	0.332	0.791	0.2525	0.406	1

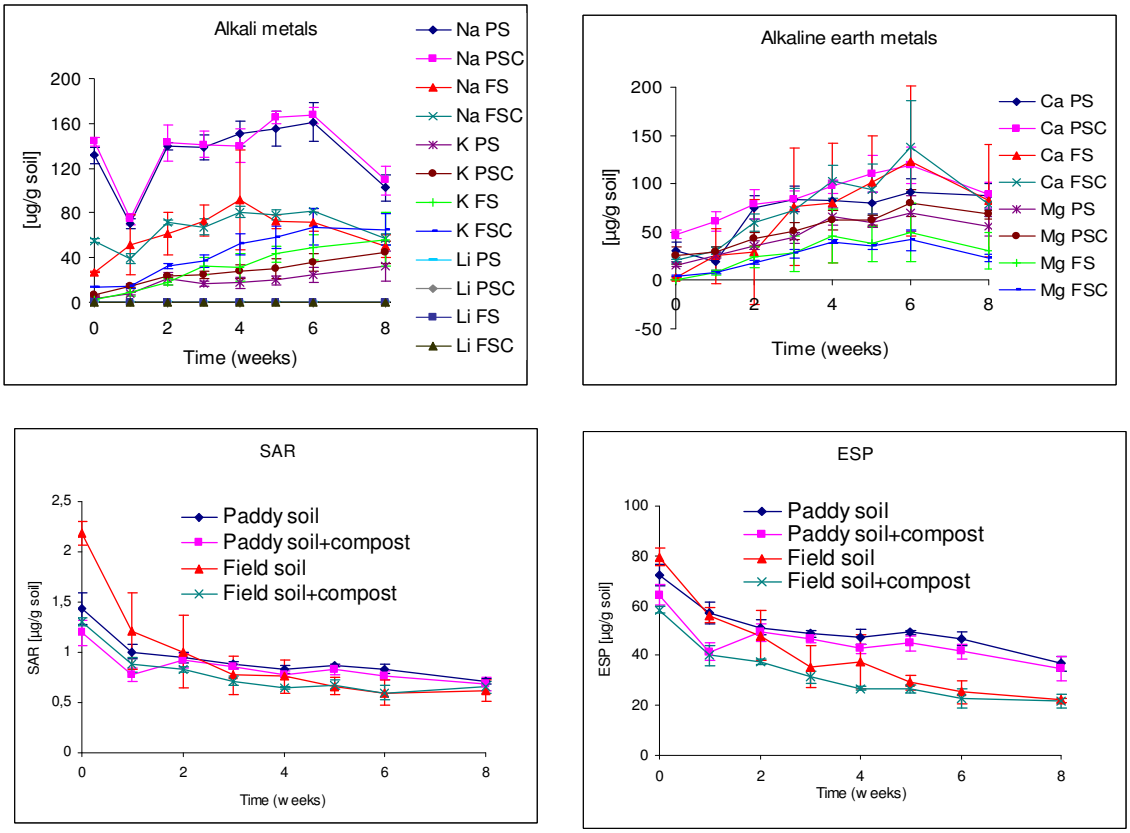

Figure 74: Changes in Na^+, K^+, Li^+, Ca^{2+}, Mg^{2+}, SAR and ESP concentrations in the paddy and field soils during the anaerobic degradation of DDT.

PS=Paddy soil; PSC=Paddy soil+compost; FS=Field soil; FSC=Field soil+compost

Table 28: Significant test p-values (p = 0.05) for cations in the paddy and field soils during the anaerobic degradation of DDT.

group	NH_4^+	Li^+	Na^+	K^+	Mg^{2+}	Ca^{2+}
Intercept (FS)	<0.0001	<0.0001	<0.0001	<0.0001	<0.0001	<0.0001
Slope (FS)	<0.0001	0.0002	0.0069	<0.0001	<0.0001	<0.0001
Intercept (PS)	<0.0001	0.3119	<0.0001	0.0026	0.0001	0.5463
Intercept (CE)	0.0084	0.1523	0.4041	0.0238	0.5485	0.2904
Slope (PS)	<0.0001	0.5238	0.8910	<0.0001	0.0352	0.0232
Slope (CE)	<0.0001	0.3615	0.8552	0.1422	0.5348	0.3985

FS = Field soil; PS = Paddy soil; CE = compost effect

ESP was shown to have higher loading values than ESP2 in the PRC curves (Figs. 69, 70, 71) and thus had a higher influence on the differences between the groups. Therefore, further

presentation of the results is based on ESP.

ESP decreased gradually over the experimental period (Fig. 74). The ESP data was fitted into the LME model (Fig. 75) and showed greater slopes for the field soil samples (Table 29), indicating faster changes in ESP.

The sodium absorption ratio (SAR) was determined using the equation

SAR = (([Na^+]/([Mg^{2+}]+[Ca^{2+}])/2)^0.5……..3 (Sumner et. al, 1998).

To allow comparision with other soil parameters, the concentrations were expressed as µg/g soil. It has been argued that SAR is a good measure of dispersion for water-logged soils (Rengasamy, 1984). SAR decreased gradually over the experimental period (Fig. 74). The SAR data was fitted into the LME model (Fig. 75). The LME model fitting showed differences between the soils, with the field soil having higher absolute slope values relative to the paddy soil (Fig. 76 and Table 29). This indicated a higher rate of decrease of ESP in the field soil. The compost-amended soils also had higher absolute slope values relative to the unamended soils. This meant that there was a higher rate of decrease in the compost-amended soils compared to the un-amended ones.

Table 29: Slopes {(µg/g soil)/day} and intercepts (µg/g soil) for the LME model fitting of ESP and SAR in the paddy and field soils under anaerobic conditions.

Sample	ESP intercept	ESP slope	SAR intercept	SAR slope
Paddy soil	67.0	-3.7	1.28	-0.08
Paddy soil + compost	52.3	-1.9	0.90	-0.02
Field soil	65.2	-6.4	1.44	-0.14
Field soil + compost	50.5	-4.6	1.06	-0.08

To test the influence of sodicity on DDT degradation, the SAR and ESP values were correlated to p,p-DDT, p,p-DDD, p,p-DDMU and other soil factors (Tables 24, 25, 26 and 27). The correlations of SAR with p,p-DDT and p,p-DDMU were also plotted (Fig. 77). SAR and ESP did not have any significant correlation with p,p-DDT in the paddy soil samples (Tables 24, 25 and Fig. 77), but had positive correlations in the field soil samples (Tables 26, 27 and Fig. 77). There were significant inverse correlations between p,p-DDD and SAR/ESP

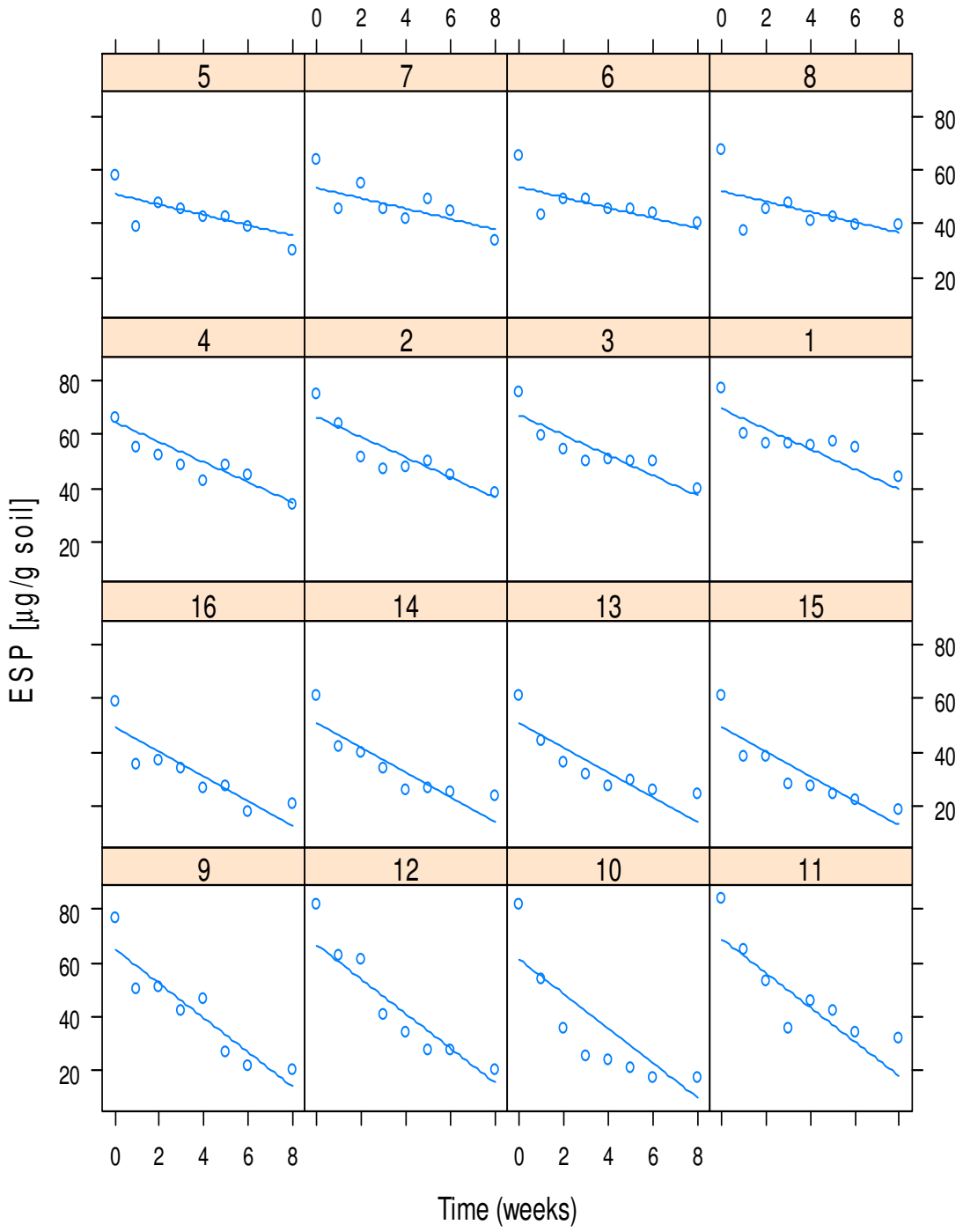

Fig. 75: LME model fitting for exchangeable sodium percentage (ESP) changes in the field and paddy soils during the anaerobic degradation of DDT.

1-4 = Paddy soil; 5-8 = Paddy soil+compost; 9-12 = Field soil; 13-16 = Field soil+compost

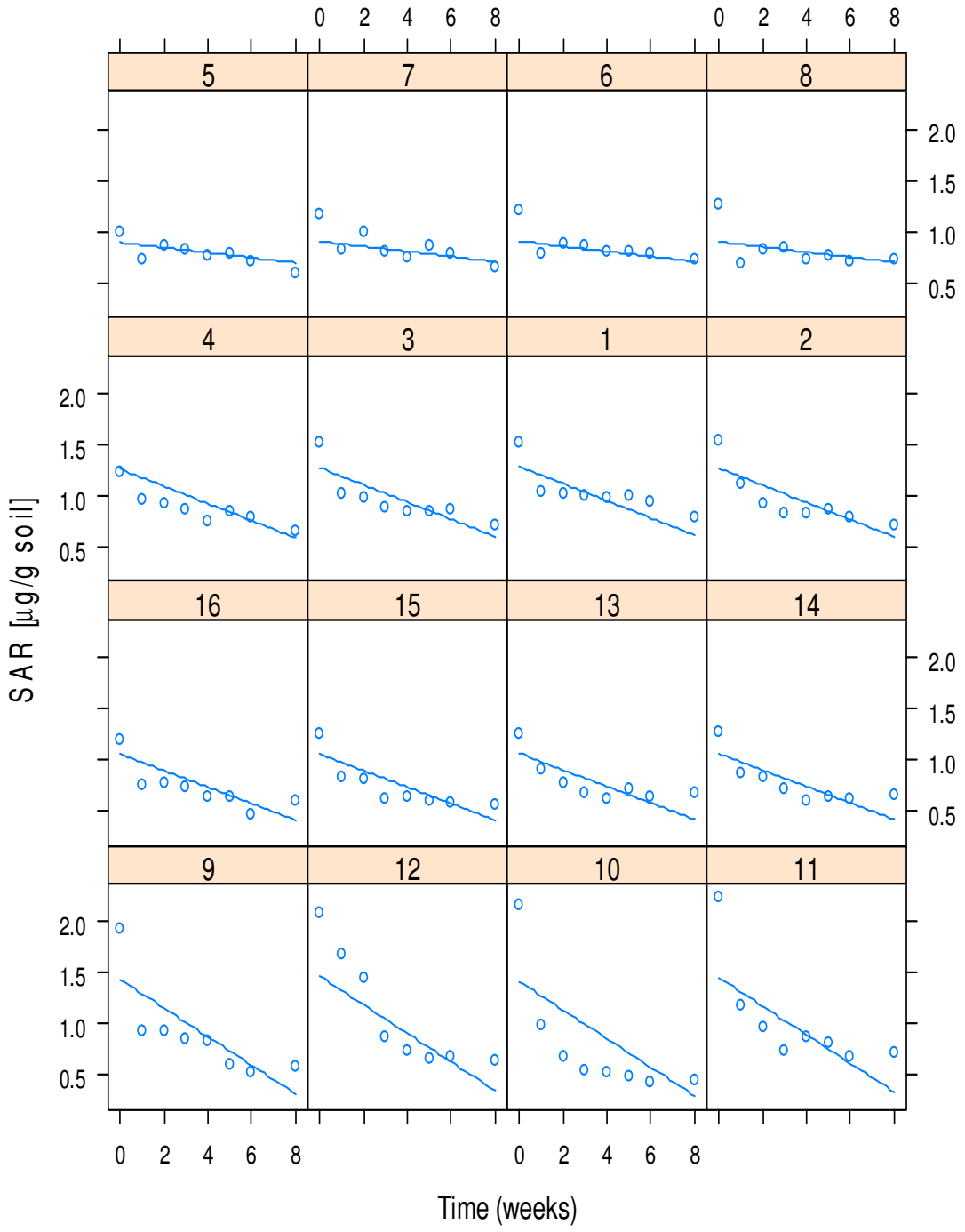

Fig. 76: LME model fitting for sodium absorption ratio (SAR) changes in the field and paddy soils during the anaerobic degradation of DDT.

1-4 = Paddy soil; 5-8 = Paddy soil+compost; 9-12 = Field soil; 13-16 = Field soil+compost

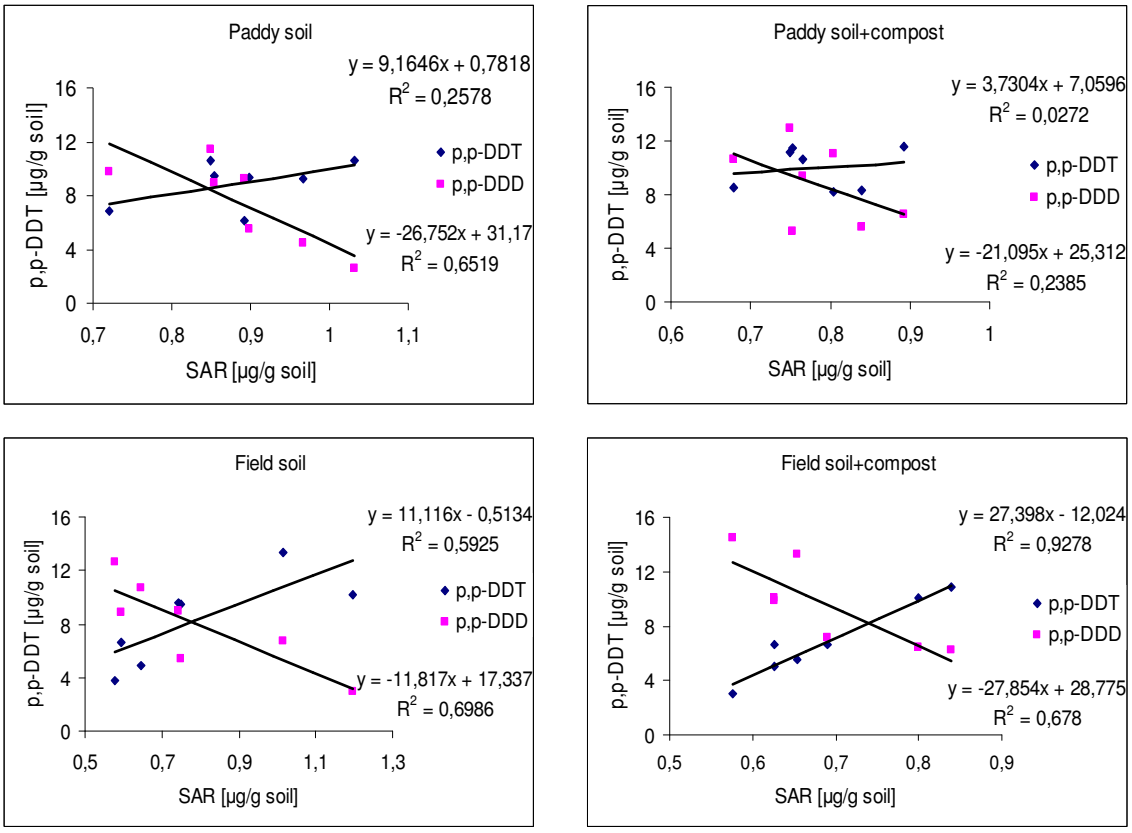

Figure 77: Correlations of SAR with p,p-DDT and p,p-DDD (n = 7, df = 5, Pearson R^2 critical value = 0.4476 (p=0.05)) during the anaerobic degradation of DDT in the paddy and field soils

Table 30: Significant test p-values for ESP, SAR and Fe species in the paddy and field soils during the anaerobic degradation of DDT.

group	ESP (TCC)	ESP (Mg & Ca)	SAR	Fe^{2+}	Fe^{3+}	Reducible Fe (total)
Intercept (FS)	<0.0001	<0.0001	<0.0001	<0.0001	<0.0001	<0.0001
Slope (FS)	<0.0001	<0.0001	<0.0001	<0.0001	<0.0001	0.9265
Intercept (PS)	<0.0001	0.0011	0.3433	<0.0001	<0.0001	<0.0001
Intercept (CE)	0.0006	0.0028	0.0013	0.0001	0.0295	<0.0001
Slope (PS)	<0.0001	<0.0001	0.0002	0.0177	0.0738	0.8515
Slope (CE)	0.0004	0.0003	0.0001	0.0004	0.0126	0.5392

FS = Field soil; PS = Paddy soil; CE = compost effect

in the various sets except for the compost-amended paddy soil (Tables 24, 25, 26, 27 and Fig. 77). SAR/ESP had inverse correlations with p,p-DDMU in the paddy soil samples only (Tables 23, 24, 25 and 26). SAR/ESP had significant correlations with CO_2 in all the sets. There were more correlations of SAR/ESP with other soil properties in the filed soil relative to the paddy soil (Tables 23, 24, 25 and 26).

3.4.5 Changes in reducible Fe during the anaerobic degradation of DDT

Iron has been shown to be the dominant alternative electron acceptor in waterlogged soils (Jäckel et al., 2005). Fe (II) concentration increased to a maximum in week 4, and remained fairly constant thereafter, with higher concentrations in the field soil samples (Fig. 78). As expected, Fe (III) concentrations decreased, reaching a minimum in week 4, and remained fairly constant thereafter (Fig. 78). Reducible Fe remained fairly constant in all sets over the 8 week experimental period (Fig. 78).

To test for the influence of Fe on DDT degradation, Fe (II) concentrations were correlated with p,p-DDT, p,p-DDD, p,p-DDMU and other soil properties (Tables 24, 25, 26 and 27). The correlations of Fe (II) with p,p-DDT and p,p-DDMU were plotted and are shown in Fig. 79. Fe (II) did not have any significant correlation with p,p-DDT in the paddy soil samples (Fig. 79), but had significant inverse correlations with p,p-DDT in the field soil samples. There were significant positive correlations between p,p-DDD and Fe (II) in all the samples (Fig. 79). Fe (II) had positive correlations with p,p-DDMU in the paddy soil samples only (Tables 24, 25, 26 and 27).

Fe (II) had significant correlations with methane, N_2O and CO_2 in all the samples; with F4 in all the samples except for the compost-treated paddy soil; and with NH_4^+ in the field soil samples only (Tables 24, 25, 26 and 27). Fe also correlated significantly with sodicity (ESP/SAR) in all the soil samples except the compost-amended paddy soil. There were more significant correlations of Fe with other soil properties in the field soil relative to the paddy soil (Tables 24, 25, 26 and 27).

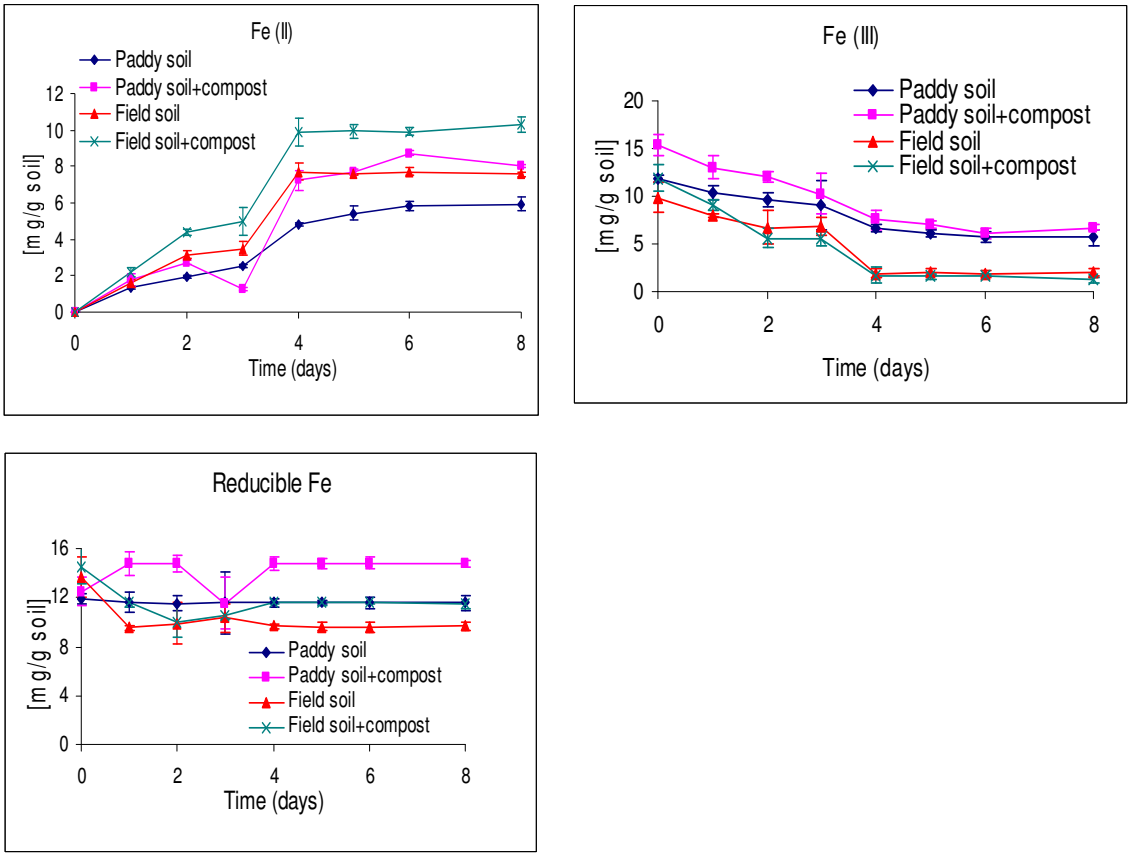

Figure 78: Changes in Fe(II), Fe(III) and reducible Fe in the field and paddy soils during the anaerobic degradation of DDT.

3.4.6 Dissolved organic matter

3.4.6.1 Quality and spectroscopic properties of DOM

3.4.6.1.1 PARAFAC model and characterization of of the fluorophore groups in DOC

The PARAFAC model quality parameters are shown in Fig. 81. The core consistency decreased gradually up to 56.7 % at factor 5, after which it decreased sharply to 24.15 at factor 6. A core consistency value may not be mathematically perfect but can be accepted based on other quality parameters (Bro & Kiers, 2003). Considering the sum of squared errors, the plots of the residuals and the number of iterations as well, the five-factor PARAFAC model was selected as being the most suitable. Fluorescence spectra of the five factors (fluorophore groups) contributing to the sample spectra are shown in Figures 82, 84, 86, 88 and 90, while the underlying PARAFAC loading vectors for each factor are shown in figures 83, 85, 87, 89 and 91. Vector multiplication of emission and excitation loading vectors results in the normalized spectra.

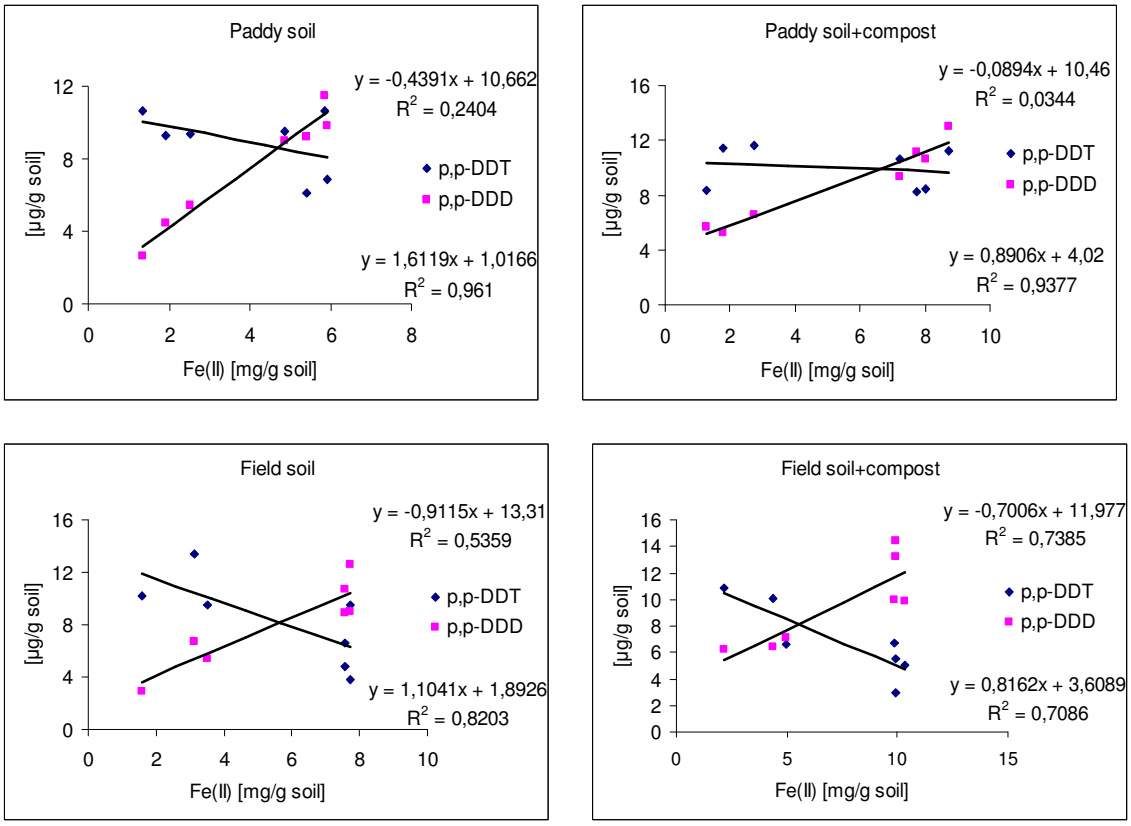

Figure 79: Correlations of Fe(II) with p,p-DDT and p,p-DDD in the paddy and field soils during the anaerobic degradation of DDT (n = 7, df = 5, Pearson R^2 critical value = 0.4476)

3.4.6.1.2 Identification of the fluorophore groups present in the DOC

The factors were identified by comparing with previously identified fluorophores. The excitation and emission wavelengths of the five factors, and those of fluorophores in literature, are shown in table 31.

Comparing the two sets of fluorophores (Table 31), Factor 1 corresponds to two previously identified humic like fluorophores (Components 1 and 2) of terrestrial origin; factor 2 corresponds to the previously identified component 3, a fulvic acid fluorophore group present in all environments, both terrestrial and aquatic; factor 3 corresponds to previously identified component 6, a humic fluorophore correlated to DOM exported from agricultural catchments possibly due to the spreading of animal waste on fields as fertilizer (Steadmon and Markager, 2005); factor 4 corresponds to previously identified components 7 and 8, tryptophan-like and tyrosine-like fluorophores respectively, which have been correlated to terrestrial fluorescent materials (Steadmon and Markager, 2005). Fluorescence measurement of standards showed that it corresponded most closely to tyrosine, phenol, 3-hydroxybenzaldehyde and gallic acid

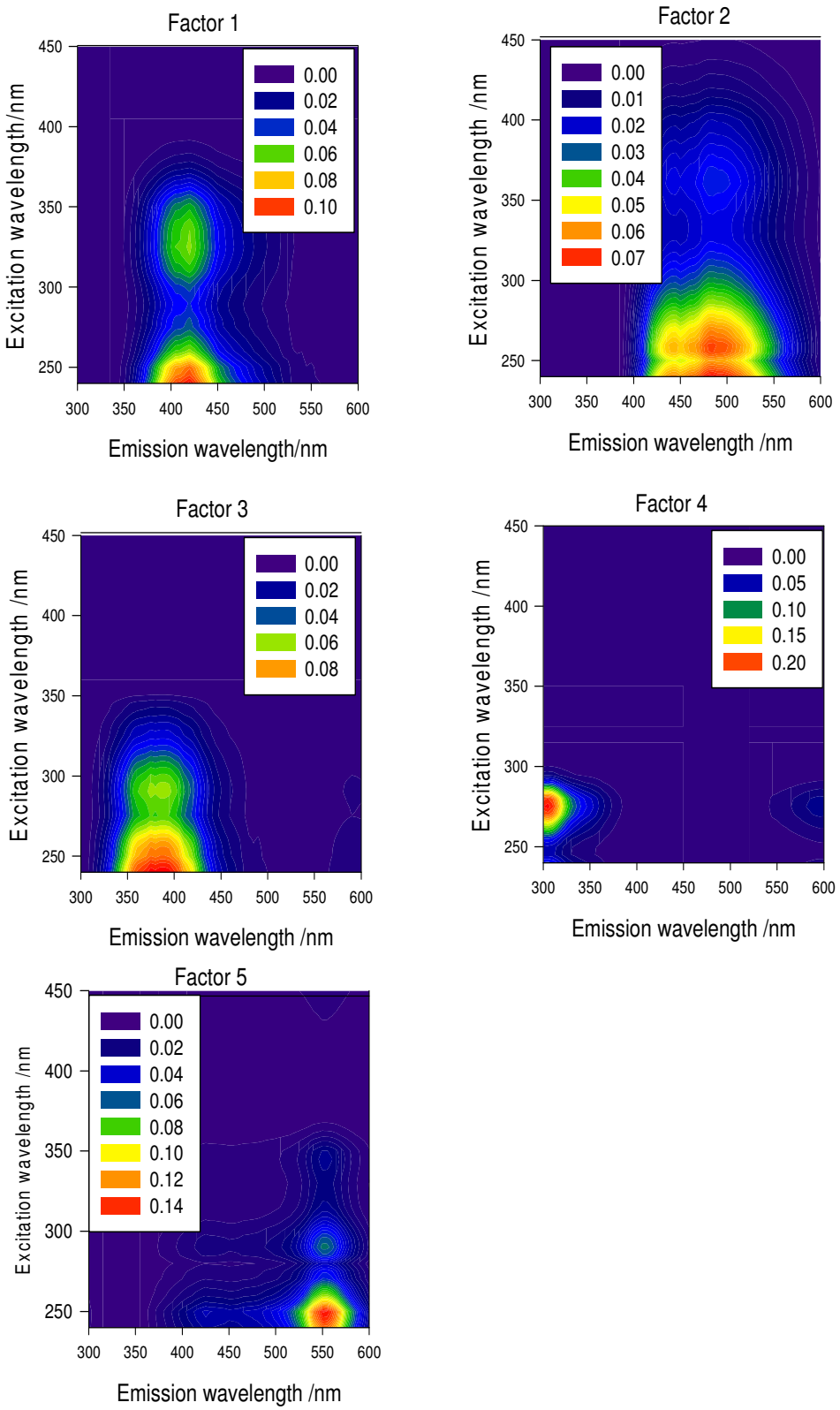

Figure 80: Fluorophore groups contained in DOC of the field and paddy soils during the anaerobic degradation of DDT, characterized using PARAFAC analysis.

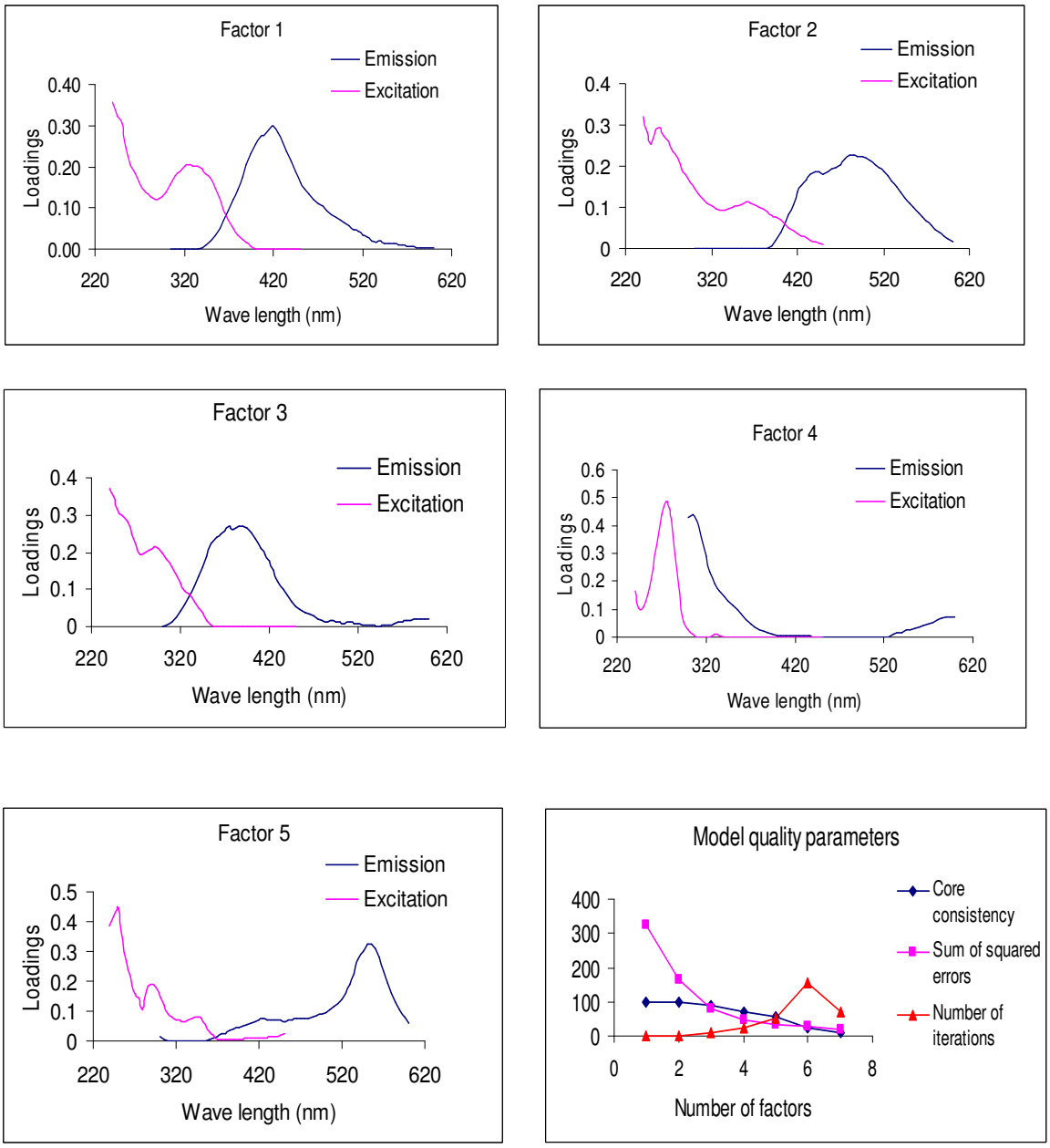

Figure 81: Factor loadings for the fluorophore spectra and PARAFAC model quality parameters

(Appendix). Tryptophan and hydroquinone were also within the same excitation and emission range. Factor 5 could correspond to the microbially derived components 2 and 3, and has only been reported in the Great Lakes (Hiriat-Baer et al., 2008). However, this factor is in an area that is heavily influenced by second-order Raman-scatter and could easily be missed out by fluorescence measurements.

Table 31: Positions of the fluorescence maxima of the five factors identified by the PARAFAC model

This study

Factor number	Excitation max (nm)	Emission max (nm)	Possible identity
1	260 (325)	390 - 440	Humic-like authochthonous
2	280 (360)	425 - 545	Fulvic-like authochthonous
3	260 (290)	350 - 430	Humic-like anthropogenic
4	275	330	Tryptophan/tyrosine/phenolic-like authochthonous
5	260 (290)	540 - 570	Microbial derived authochthonous

Compared to previously identified fluorophores

Factor	Excitation max (nm)	Emission max (nm)	Description/origin	Previously identified
1.	<250	430 - 450	UVC humic terrestrial	Comp. 1 [a]
2.	<250 (305)	380 - 460	UVC humic terrestrial	Comp. 2 [a]
3.	270 (360)	478	UVA fulvic acid terrestrial/authochthonous	Comp. 3 [a]
4.	<250 (320)	400	UVA humic terrestrial/anthropogenic	Comp. 6 [b]
5.	280	330-340	UVB tryptophan-like authochthonous	Comp. 7 [b]
6.	275	304-306	UVB tyrosine-like authochthonous	Comp. 8 [b]
7.	270	544	Microbial derived autochthonous	Comp. 2 [c]
8.	260	522	Microbial derived autochthonous	Comp. 3 [c]

UVA (long wave) = 400 nm – 315 nm; UVB (medium wave) = 315 – 280 nm; UVC (short wave) = 280 nm – 100 nm

a. Steadmon and Markager, 2003
b. Steadmon and Markager, 2005
c. Hiriat-Baer et al., 2008

3.4.6.1.3 Changes in the fluorophore groups with time

The five factors were present in both soils. However, factors 4 and 5 were present in negligible amounts at the beginning (Fig. 82). There were no significant changes ($p = 0.05$) with time in the paddy soil except for factor 4 (Table 32). However, there were notable changes in the field soil: factor 2 decreased while factor 4 and 5 increased with time in the field soil. Compost did not significantly affect the rate of change of any of the five factors

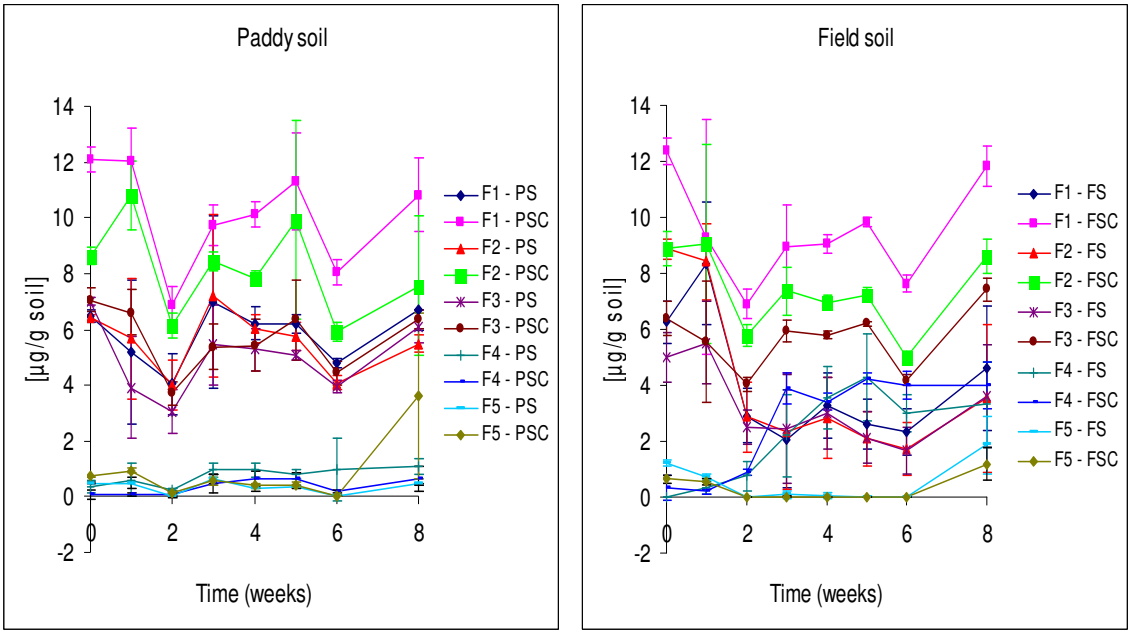

Figure 82: Changes in DOC quality in the paddy and field soils during the anaerobic degradation of DDT.

F1 to F5 = Factor 1 to Factor 5; PS = Paddy soil; PSC = Paddy soil+compost; FS = Field soil; FSC = Field soil+compost

Table 32: Significance test p-values (p = 0.05) for DOC factors and quantity in the paddy and field soils during the anaerobic degradation of DDT.

group	Factor 1	Factor 2	Factor 3	Factor 4	Factor 5	DOM
Intercept (FS)	<0.0001	<0.0001	<0.0001	<0.0001	<0.0001	<0.0001
Slope (FS)	0.1425	0.0001	0.2813	<0.0001	0.0361	0.0247
Intercept (PS)	0.0113	0.0145	0.0238	<0.0001	0.2153	0.1080
Intercept (CE)	<0.0001	<0.0001	0.0003	0.8863	0.3284	0.1508
Slope (PS)	0.2830	0.0592	0.4835	<0.0001	0.2884	0.0123
Slope (CE)	0.4672	0.1227	0.1498	0.7151	0.0726	0.4046

FS = Field soil; PS = Paddy soil; CE = compost effect

(Table 32). However, it caused significant increases at the beginning for factors 1, 2 and 3 in both soils.

To test for the influence of organic matter quality on DDT degradation, the five factors were correlated with p,p-DDT, p,p-DDD, p,p-DDMU and other soil properties (Tables 24, 25, 26 and 27). The correlations of F4 with p,p-DDT and p,p-DDMU were plotted (Fig. 83).

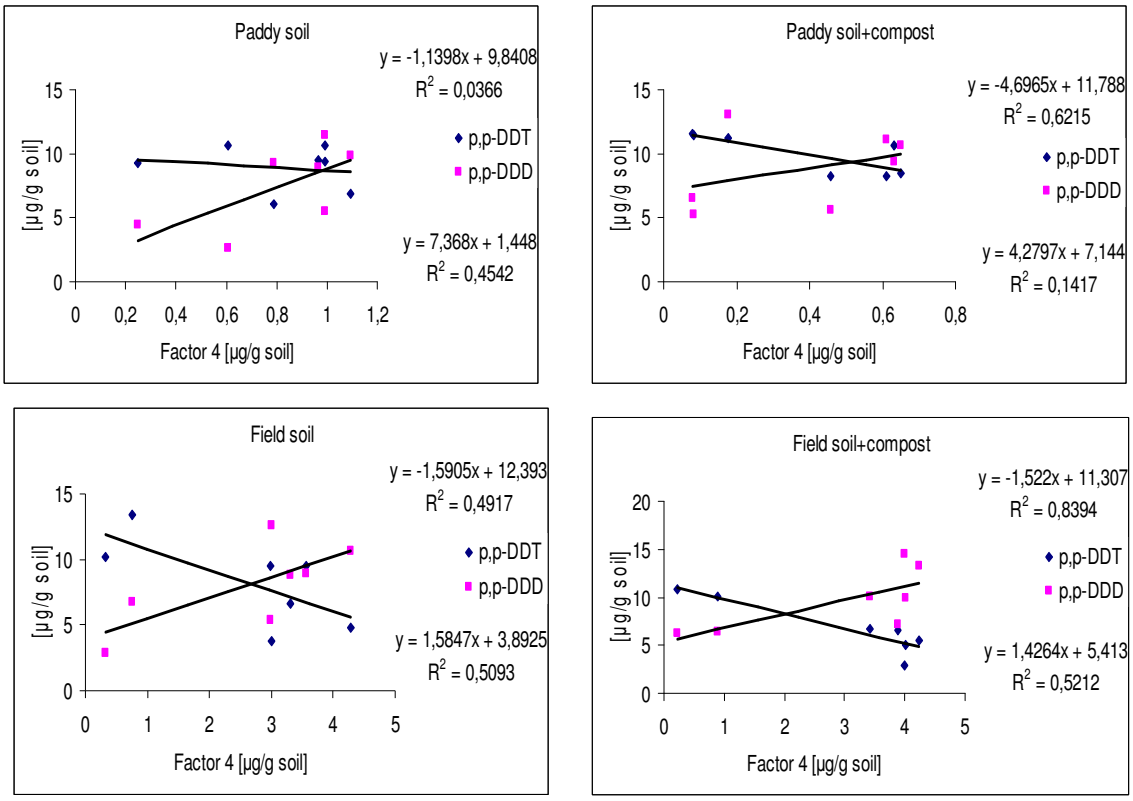

Figure 83: Correlations of Factor 4 with p,p-DDT and p,p-DDD in the paddy and field soils during the anaerobic degradation of DDT (n = 7, df = 5, Pearson R^2 critical value = 0.4476 (p=0.05))

p,p-DDT had significant inverse correlations with F4 in all the sets except for the paddy soil (Fig. 83). p,p-DDD had a significant positive correlation with F4 all the sets except for the paddy soil with compost, and significant negative correlations with F1, F2 and F3 in the field soil only (Fig. 83). p,p-DDMU had a significant positive correlation with F5 in the compost-amended field soil (Tables 24, 25, 26 and 27).

F4 had significant positive correlations with methane in all samples, with N_2O and CO_2 in all samples except for the compost-amended paddy soil (Tables 24, 25, 26 and 27). F4 had a positive correlation with NH_4^+ in both the field soil samples, and an inverse correlation with F2 in the field soil only (Tables 24, 25, 26 and 27). The untreated field soil had the most correlations between flouorophores and other soil properties. There were significant correlations with: salinity and SAR in all the fluorophores except F5; Fe(II)/Fe(II) with F2, F3 and F4; and inverse correlations of p,p-DDD with F1, F2 and F3 (Tables 24, 25, 26 and 27).

3.4.6.2 Changes in DOC quantity with time

Fig. 84 shows the changes in DOC concentrations with time. There were significant differences (p = 0.05) in the rates of change (slopes) with time of DOC concentrations in both soils (Table 32). There was no significant effect of compost on either the slope or intercept of both soils. There was great variability in the un-amended field soil (Fig. 84).

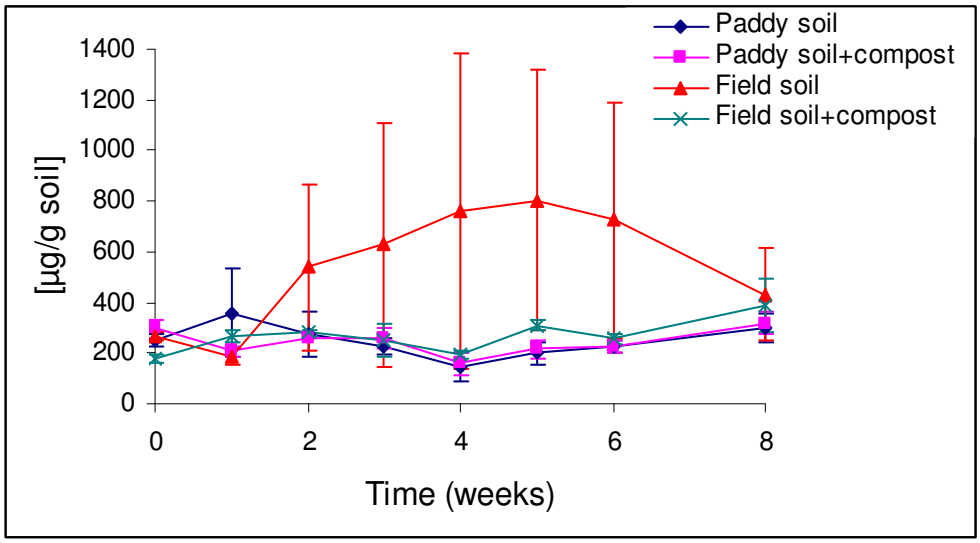

Figure 84: Changes in DOC quantity in the paddy and field soils during the anaerobic degradation of DDT.

3.4.7 Carbon and nitrogen mineralization during the anaerobic degradation of DDT

3.4.7.1 Carbon mineralization (CH_4 and CO_2 formation)

3.4.7.1.1 Methane formation

Methane production reached a peak faster for the compost-amended samples (Fig. 85), with the field soil peaking after two weeks and the paddy soil after 3 weeks. Both the un-amended soils reached a peak after 4 weeks. After methane production reached its peak, there was a decrease up to week 5 after which the concentrations remained fairly constant for all the sets. There were significant differences (p = 0.05) in the rate of methane production over time in both soils, and compost increased the rate of methane production in both soils (Table 33). The cumulative methane production with time is also shown in Fig. 85.

To test for the influence of methanogenesis on DDT degradation, cumulative methane production was correlated with p,p-DDT, p,p-DDD, p,p-DDMU and other soil properties (Tables 24, 25, 26 and 27). The correlations of methane with p,p-DDT and p,p-DDMU were plotted and are shown in Fig. 86. p,p-DDT had significant negative correlations with CH_4 in the field soil samples, but none in the paddy soil samples (Fig. 86). p,p-DDD had significant

positive correlations with CH_4 in all the samples (Fig. 86). p,p-DDMU had significant positive correlations with CH_4 in the paddy soil samples, but none in the field soil samples (Tables 24, 25, 26 and 27).

Table 33: Significant test p-values (p = 0.05) for CH_4, CO_2 and N_2O in the paddy and field soils during the anaerobic degradation of DDT.

group	CH_4	CO_2	CO_2:CH_4	N_2O
Intercept (FS)	<0.0001	<0.0001	<0.0001	<0.0001
Slope (FS)	0.0042	<0.0001	<0.0001	<0.0001
Intercept (PS)	0.1120	0.0680	0.0057	<0.0001
Intercept (CE)	0.6902	0.0153	0.0131	0.0798
Slope (PS)	0.0435	0.4392	0.0030	0.0279
Slope (CE)	0.0003	0.0006	<0.0001	0.4349

FS = Field soil; PS = Paddy soil; CE = compost effect

3.4.7.1.2 CO_2 formation

CO_2 production increased gradually with time (Fig. 85). There were no significant differences (p = 0.05) between the two soils (Table 33). Compost had no effect on CO_2 production in the paddy soil, but caused a significant increase in CO_2 production the field soil (Fig. 85 and Table 33). The cumulative CO_2 production is also shown in Fig. 85.

To test for the relationship of CO_2 production on DDT degradation, cumulative CO_2 values were correlated with p,p-DDT, p,p-DDD, p,p-DDMU and other soil properties (Tables 24, 25, 26 and 27). The correlations of CO_2 with p,p-DDT and p,p-DDMU were plotted and are shown in Fig. 87. p,p-DDT had significant negative correlations with CO_2 in the field soil samples, but none in the paddy soil samples (Fig. 87). p,p-DDD had strong positive correlations with CO_2 in all the samples (Fig. 87). In the paddy soil the correlations were stronger in the un-amended soil, while in the field soil the correlations were stronger in the compost-amended soil (Fig. 87). p,p-DDMU had significant positive correlations with CO_2 in the paddy soil samples, but none in the field soil samples (Tables 24, 25, 26 and 27).

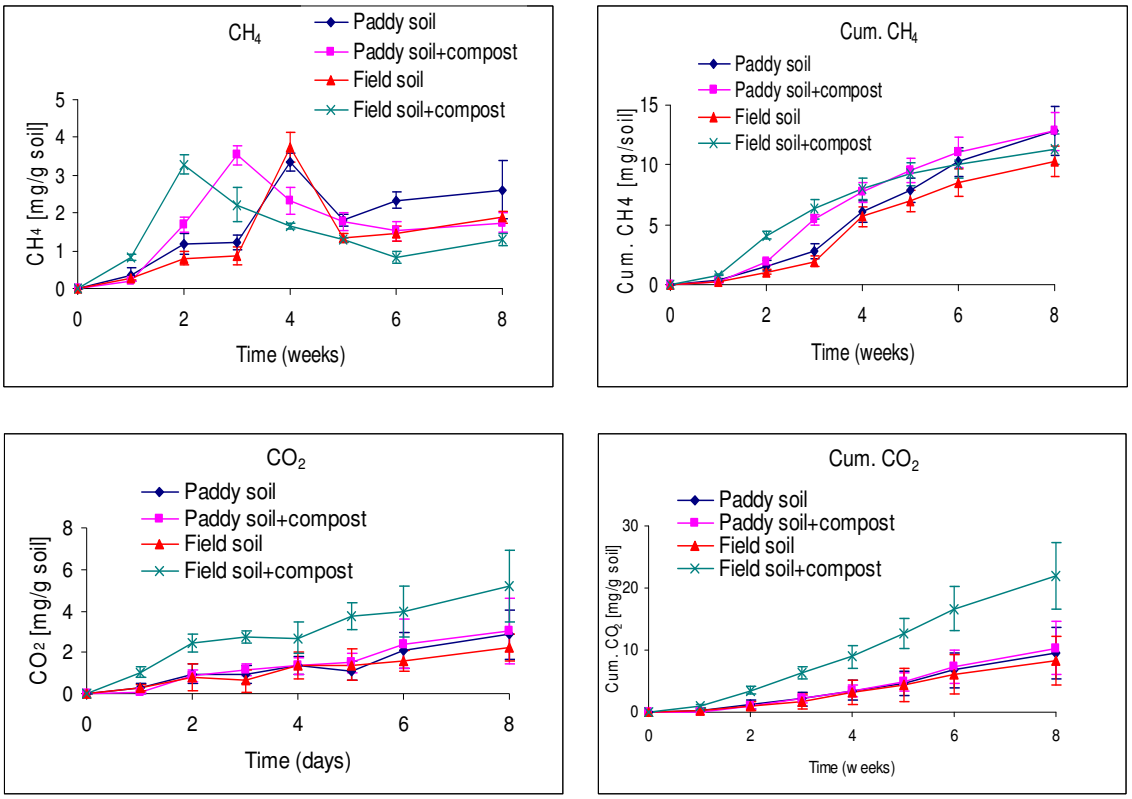

Fig. 85: CH_4 (rate), cumulative CH_4, CO_2 (rate), and cumulative CO_2 production in the field and paddy soils during the anaerobic degradation of DDT.

4.7.1.3 CO_2:CH_4 ratio

The ratio of the two terminal products of anaerobic decomposition – CO_2 and CH_4 – provides useful information on the dominant processes contributing to anaerobic decomposition (Keller et al., 2009). Under methanogenic conditions (i.e. once more thermodynamically favorable terminal electron acceptors have been consumed), CO_2 and CH_4 are produced in equal amounts resulting in a 1:1 ratio of CO_2: CH_4 (Conrad, 1999). This ratio was achieved in only a few incidences (Fig. 88). There were higher ratios in the field soil than in the paddy soil. In the paddy soil, the ratio was higher in the un-amended samples up to week 4, after which the ratio was higher in the amended samples. In the field soil, the ratio was generally higher in the amended sets over the entire experimental period. The differences in the ratios were significant for both the two soils and the compost-amended soils (Table 33)

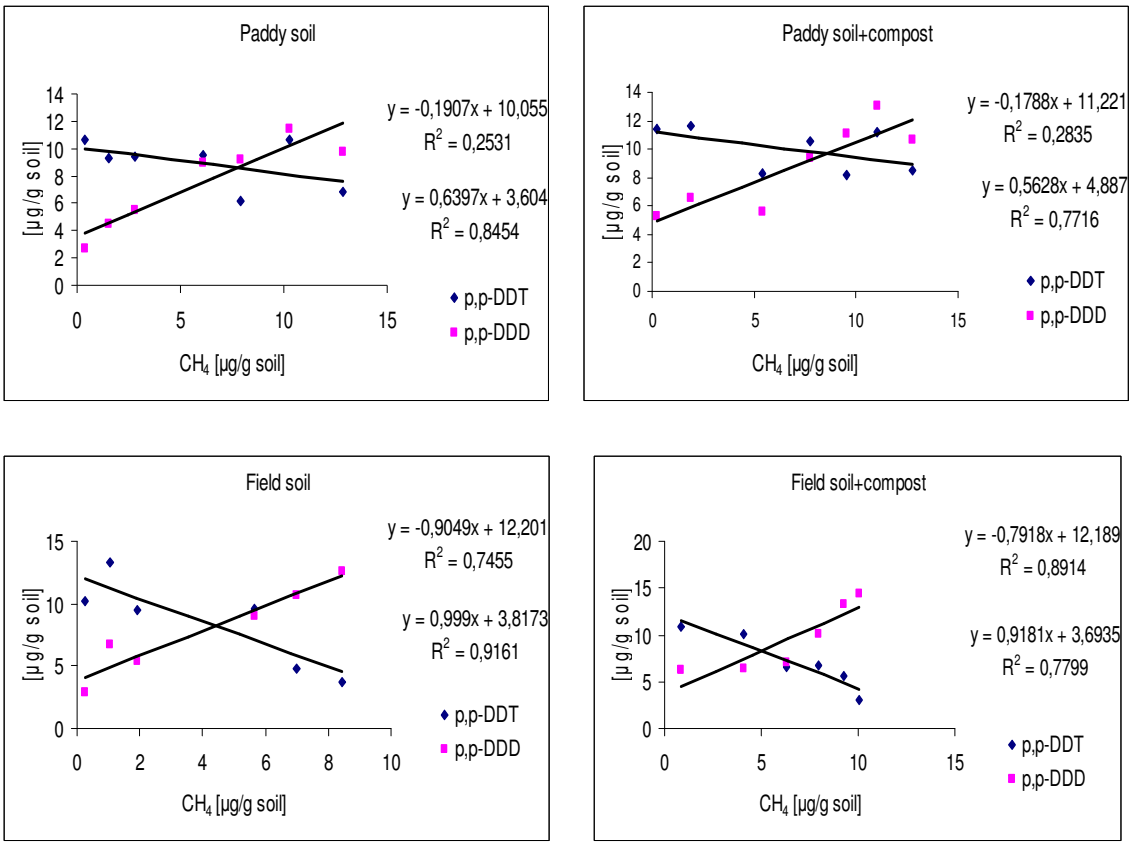

Figure 86: Correlations of methane with p,p-DDT and p,p-DDD in the paddy and field soils during the anaerobic degradation of DDT (n = 7, df = 5, Pearson R^2 critical value = 0.4476 (p=0.05))

3.4.7.2 Nitrogen mineralization (N_2O and NH_4^+ formation)

There was a gradual increase in N_2O production with time for the field soil samples (Fig. 89). However, there was high variability over time in paddy soil samples. There were significant differences (p = 0.05) between the two soils over time, but no significant compost effect (Table 33). Fig 89 shows the cumulative N_2O production over time.

There was higher NH_4^+ production in the field soil relative to the paddy soil (Fig. 89). The compost-amended paddy and field soils had significantly (p = 0.05) higher NH_4^+ production rates relative to the un-amended ones (Tables 28 and 33).

To test for the relationship of N_2O production on DDT degradation, cumulative N_2O values were correlated with p,p-DDT, p,p-DDD, p,p-DDMU and other soil properties (Tables 24, 25, 26 and 27). The correlations of N_2O with p,p-DDT and p,p-DDMU were plotted and are shown in Fig. 90. p,p-DDT had significant negative correlations with N_2O in the field soil samples, but none in the paddy soil samples (Fig. 90). p,p-DDD had strong positive correlations with N_2O in all the samples (Fig. 90). In the paddy soil the correlations were

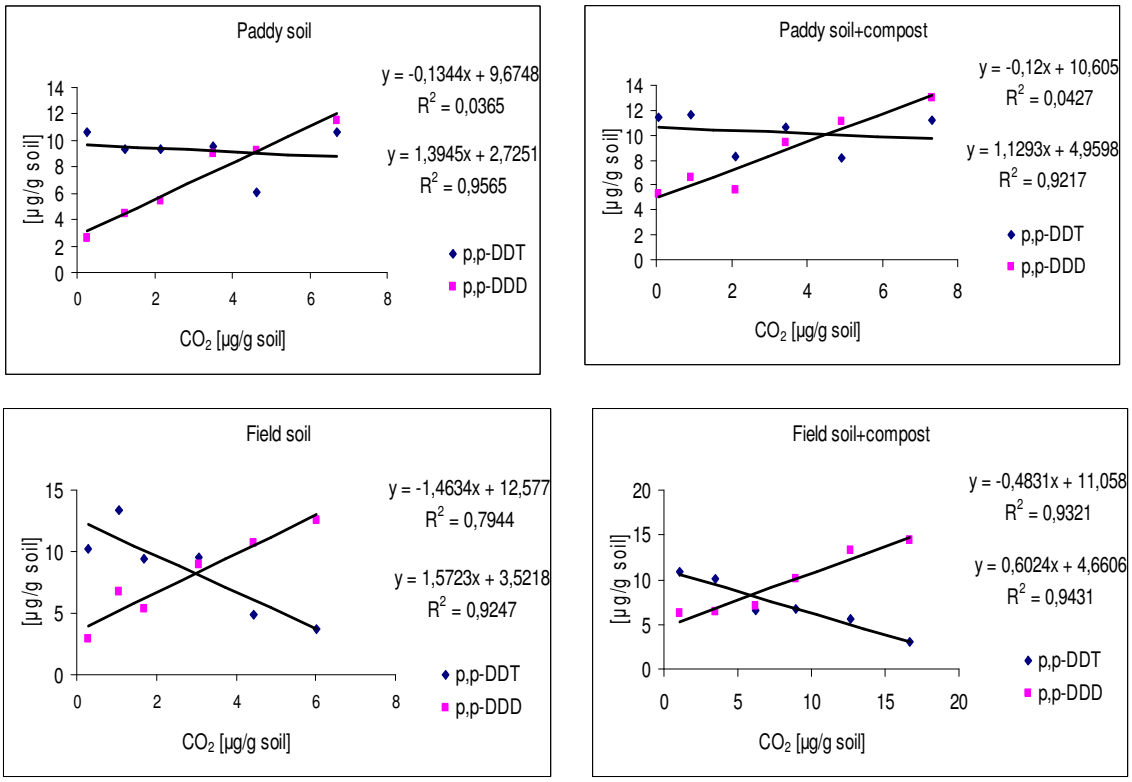

Figure 87: Correlations of carbon dioxide with p,p-DDT and p,p-DDD in the paddy and field soils during the anaerobic degradation of DDT (n = 7, df = 5, Pearson R^2 critical value = 0.4476 (p=0.05))

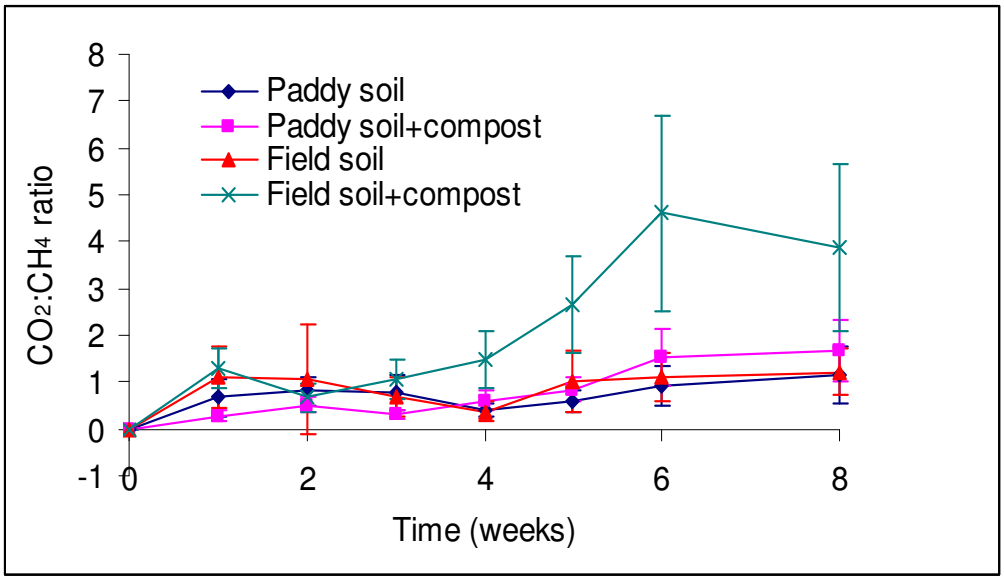

Figure 88: CO_2:CH_4 ratio changes in the field and paddy soils during the anaerobic degradation of DDT

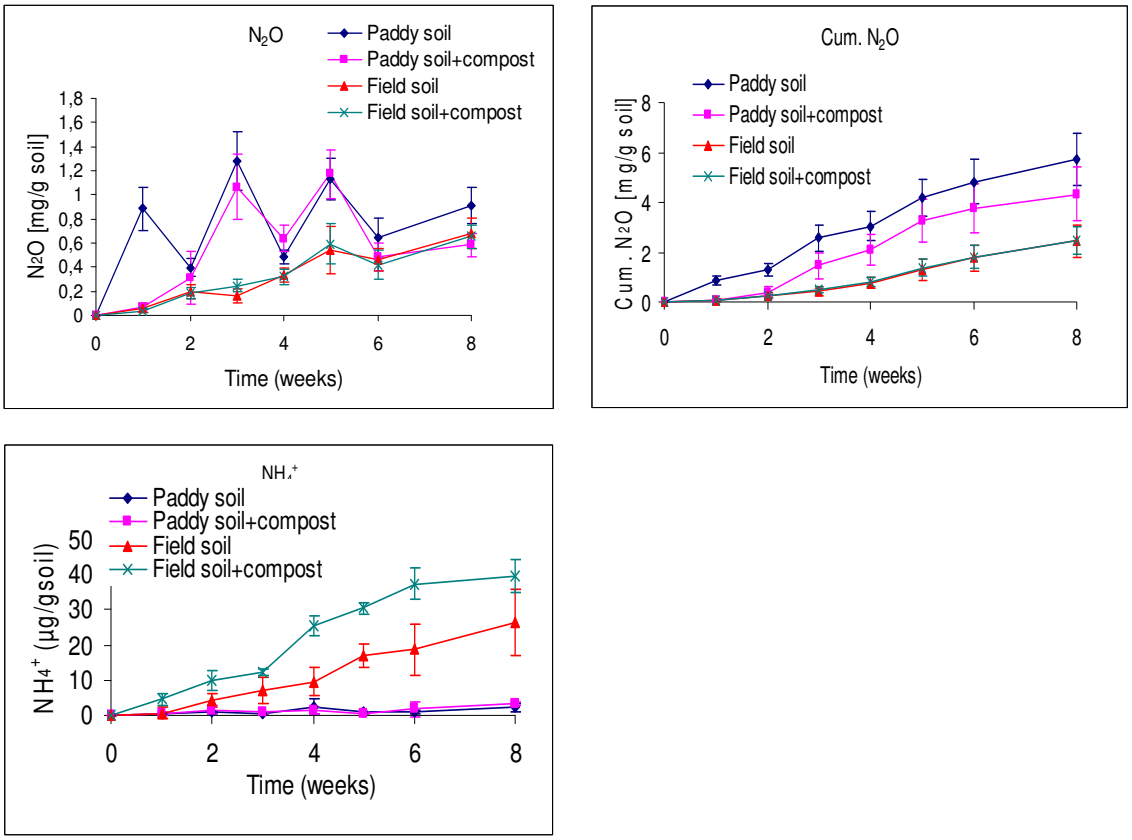

Figure 89: N_2O (rate), cumulative N_2O and NH_4^+ formation in the field and paddy soils during the anaerobic degradation of DDT.

stronger in the un-amended soil, while in the field soil the correlations were stronger in the compost-amended soil (Fig. 90). p,p-DDMU had significant positive correlations with N_2O in the paddy soil samples, but none in the field soil samples (Tables 24, 25, 26 and 27). N_2O had strong positive correlations with CH_4 and CO_2.

To test for the relationship of NH_4^+ production on DDT degradation, cumulative NH_4^+ values were correlated with p,p-DDT, p,p-DDD, p,p-DDMU and other soil properties (Tables 24, 25, 26 and 27). The correlations of N_2O with p,p-DDT and p,p-DDMU were plotted and are shown in Fig. 91. p,p-DDT had significant negative correlations with NH_4^+ in the field soil samples, but none in the paddy soil samples (Fig. 91). p,p-DDD had strong positive correlations with NH_4^+ in all the samples (Fig. 91). In the paddy soil the correlations were stronger in the un-amended soil, while in the field soil the correlations were stronger in the compost-amended soil (Fig. 90). p,p-DDMU had significant positive correlations with NH_4^+ in the paddy soil samples, but none in the field soil samples (Tables 24, 25, 26 and 27). NH_4^+ had significant correlations with CH_4, CO_2 and N_2O in the field soil samples.

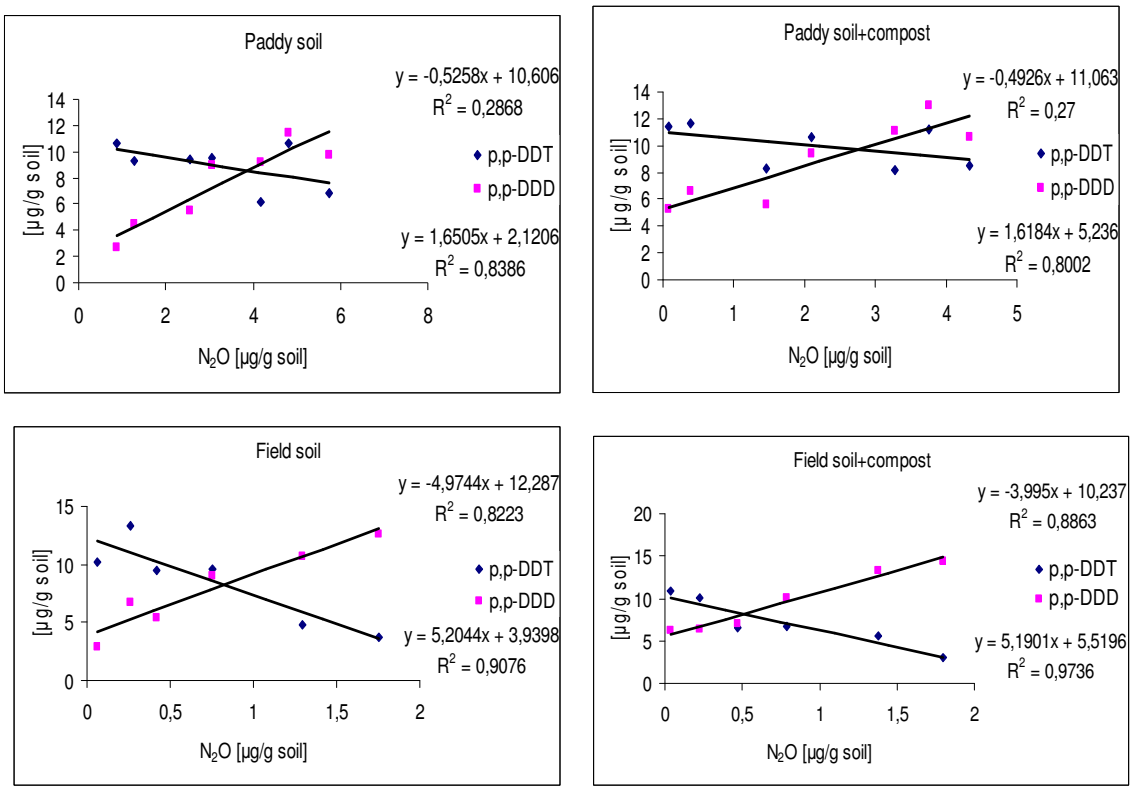

Figure 90: Correlations of N_2O with p,p-DDT and p,p-DDD in the field and paddy soils during the anaerobic degradation of DDT (n = 7, df = 5, Pearson R^2 critical value = 0.4476 (p=0.05))

3.4.8 Redox potential changes during the anaerobic degradation of DDT

Fig. 92 shows the redox potential of the soil systems over time. The result confirms that anaerobic conditions were achieved and maintained. The pH was stable over time, and therefore there was no adjustment of redox potential with respect to pH.

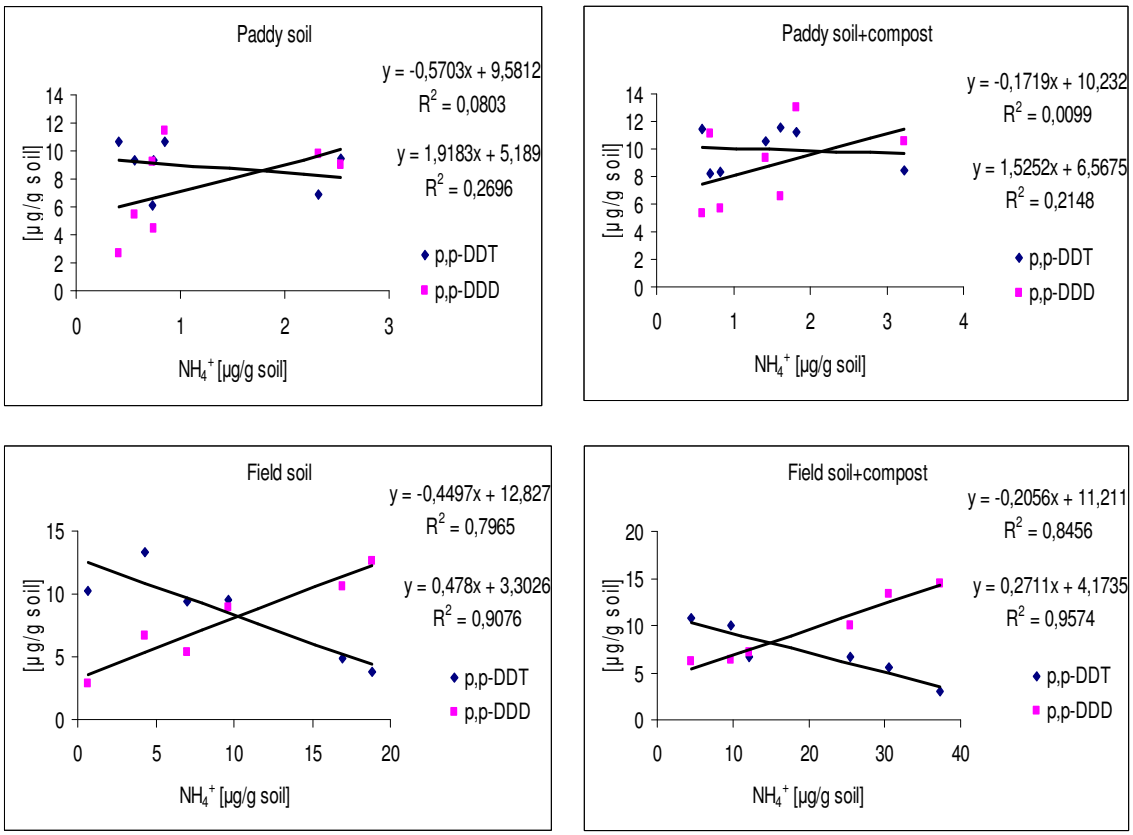

Figure 91: Correlations of NH_4^+ with p,p-DDT and p,p-DDD in the field and paddy soils during the anaerobic degradation of DDT (n = 7, df = 5, Pearson R^2 critical value = 0.4476 (p=0.05))

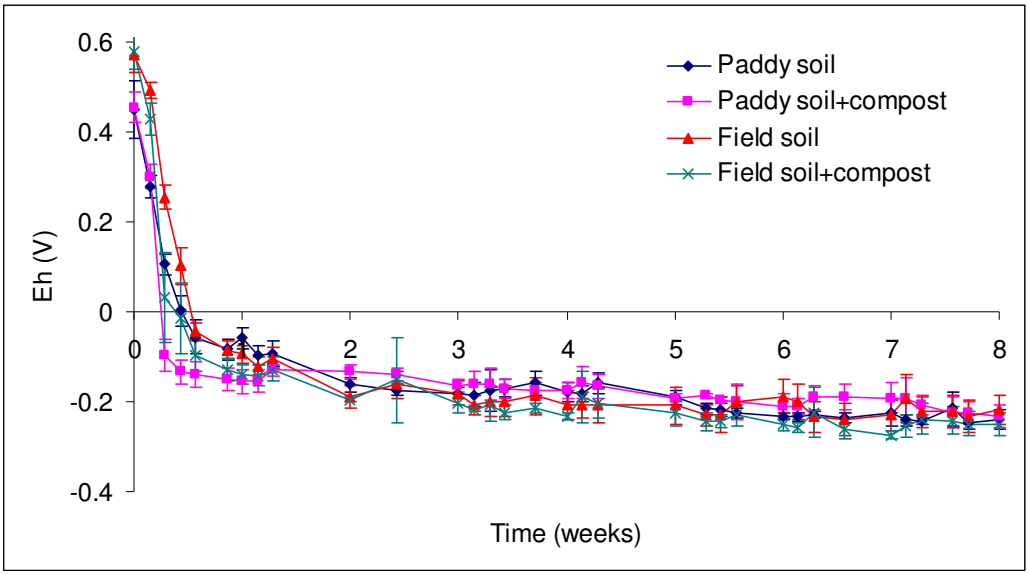

Figure 92: Redox potential in the field and paddy soils during the anaerobic degradation of DDT.

3.5 Degradative capacity of a 1,2,4-TCB degrading community on an OCPs cocktail

3.5.1. Ability of the microbial community to mineralize ^{14}C-1,2,4-TCB

The mineralization and volatilization of ^{14}C-1,2,4-TCB in liquid culture was monitored over the 30 week period the OCPs degradation experiment lasted (Fig. 93). The results show that the community could remain active over the entire study period without changing the liquid culture media. Up to 20 mg (corresponding to 88% of the applied 22.5 mg ^{14}C) was mineralized. Volatilization of up to 1.82 mg (corresponding to about 8% of the applied ^{14}C) was observed.

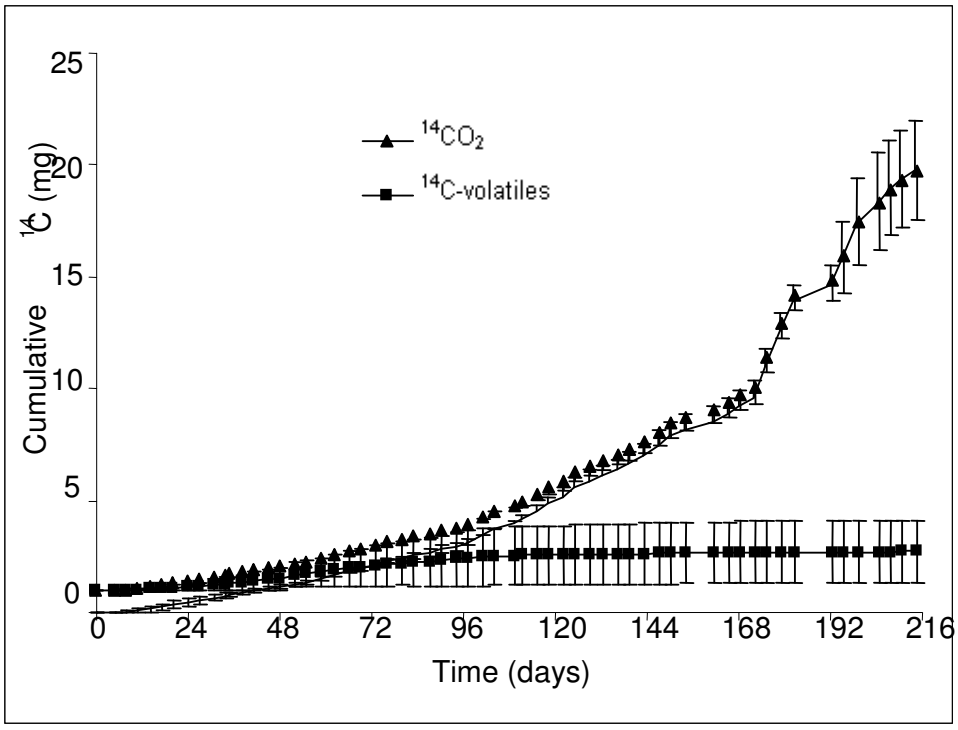

Figure 93: Mineralization and volatilization of ^{14}C-1,2,4-TCB during the entire period of the OCPs degradation experiment

3.5.2. Ability of the microbial community to degrade OCPs

All the data of the OCPs degradation experiment were analyzed statistically to enable an evaluation of the results.

Figure 94 shows the principal response curve for the dissipation of the OCPs with time during the first phase of the experiment and the loadings for the PRC. The multivariate method used in the data analysis shows the tendency of all the chemicals in the experiment to follow a given trend. It takes into account the contribution of each individual component (in this case

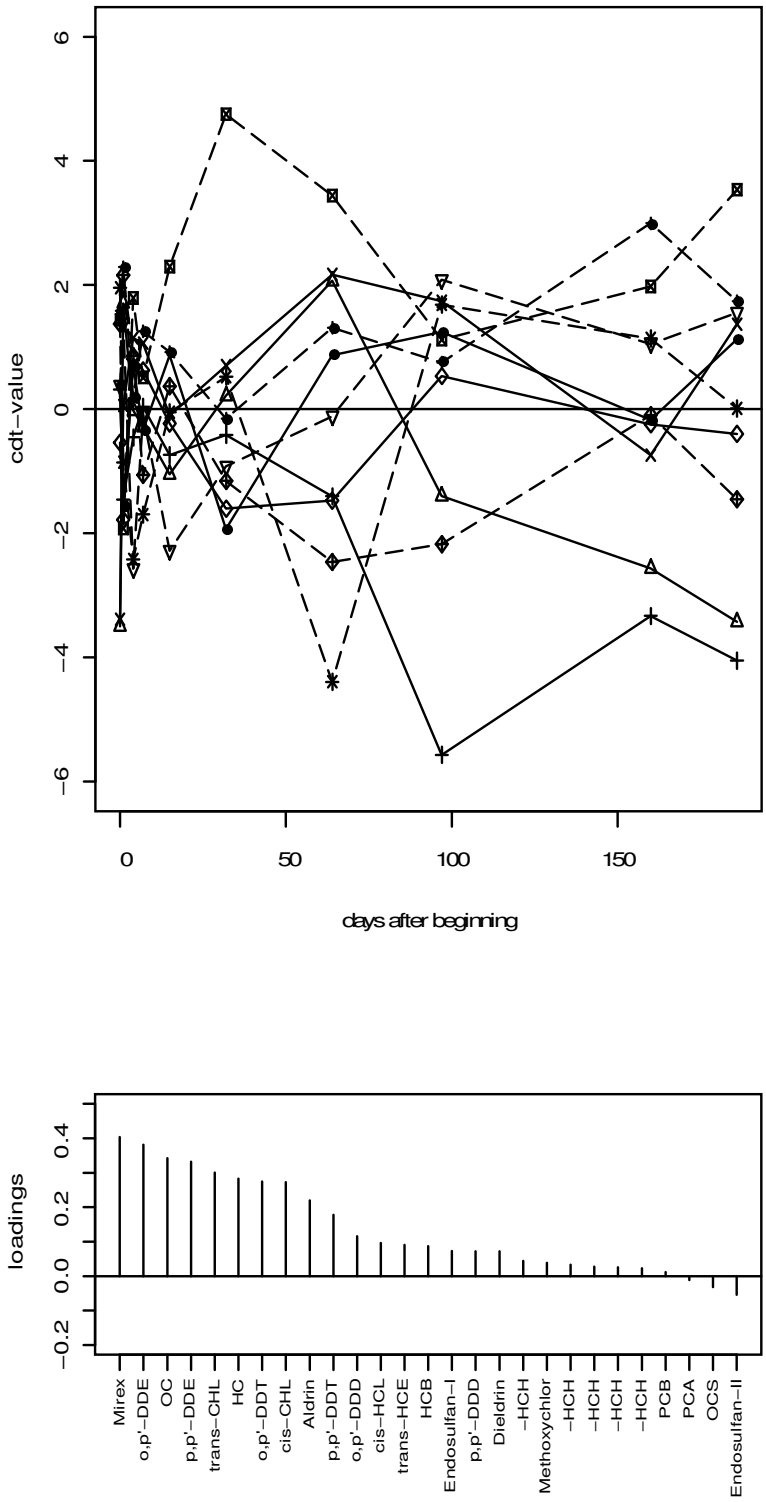

Fig. 94: Principal response curve (Component 1) and loadings for the OCPs during the first phase of the experiment (declared variance = 36.5 %).

Continuous line = control (5 replicates), Dotted line = Samples treated with microbes (5 replicates).

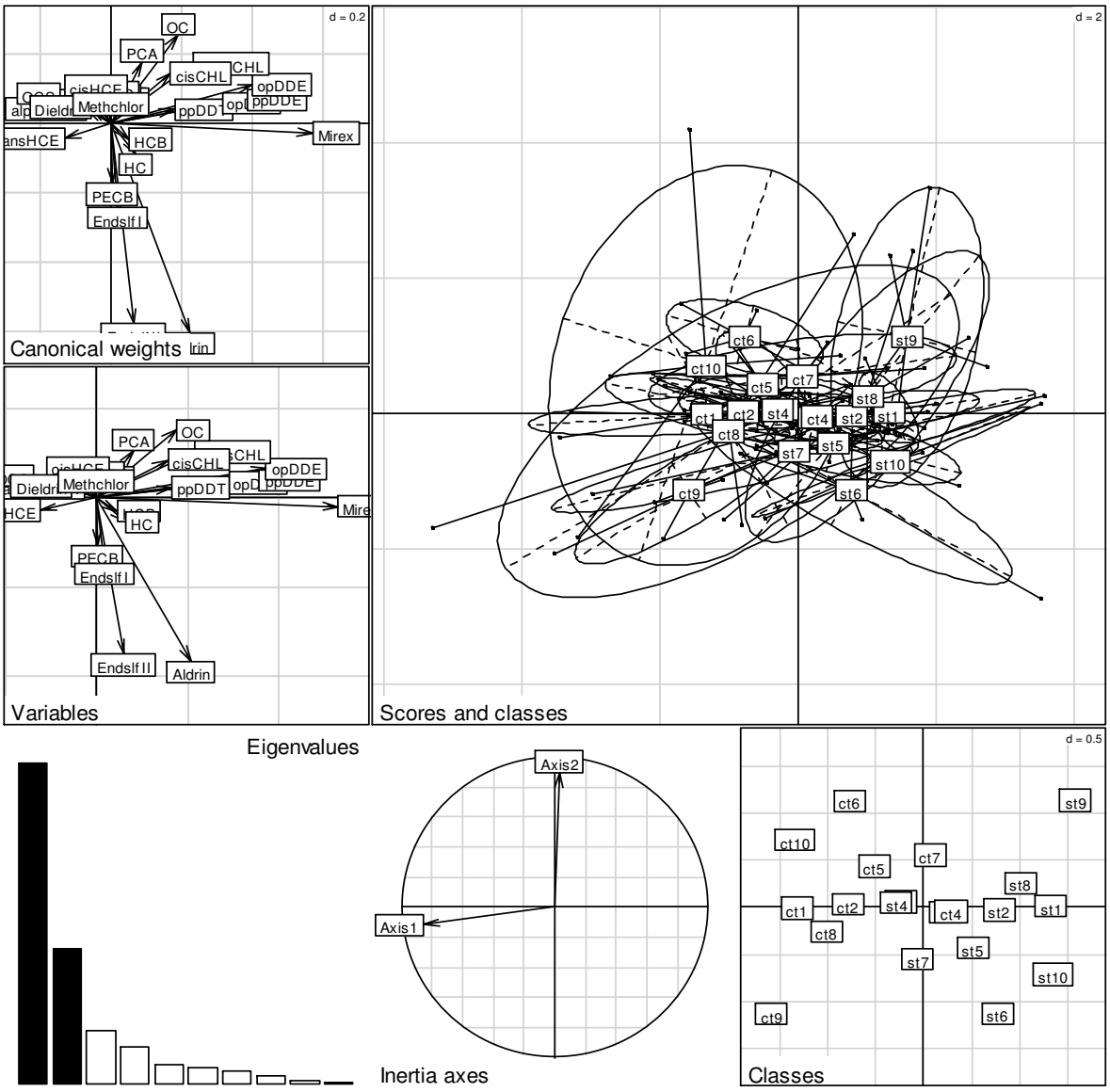

Fig. 95: Results of data analysis using group information (ade4-package, between function), based on components 1 and 2, showing the distribution of OCPs in the control and microbial treated sets during the first phase of the experiment. 'Scores and classes' is a 3-D presentation of the data separation by the two components/axes, while 'Classes' is a simple 2-D presentation of the same; 'Canonical weights' shows the loading of each metabolite; 'Variables' shows the extent and direction of each metabolite; 'Eigenvalues' shows the contribution of the components/axes in explaining the data: the two dark axes have been used to separate the groups.

c = controls; s=samples treated with microbes

Note: The digits after the letter signify the sampling point. There were 10 sampling points in the first phase i.e. 1-10. Therefore Ct9 means control at sampling point 9.

individual OCPs) to the observed trend. This individual contribution is called loading or weight (Fig. 94 and Fig. 98), and is factored in when plotting the PRC. As can be seen from Fig. 94, there was no significant difference in response between the samples treated with microbes and the controls during the whole experimental period ($p = 0.37$). However, beginning around day 60, there seemed to be a tendency towards separation between the two sets. This tendency increased with time, and was strongest on day 164 with the controls tending towards lower chemicals concentrations – but it remained a tendency at the end of this phase on day 186. The second component explained much less variance (declared variance = 13.4) and the PRC is not shown. Analysis of the data using group information showed a strong tendency towards complete separation of the groups (Fig. 95). The first component separated most of the group data into controls and treatments (Scores and classes in Fig. 95). The few which were not separated were nevertheless close to the principal component (Classes in Fig. 95).

The second phase of the experiment was necessitated by two reasons: (i) to confirm the results observed during the first phase - especially the first days where no difference in response was observed, and (ii) to find out whether the tendency in response witnessed at the end of the first phase would continue. To achieve conditions similar to the initial conditions in the first phase the OCPs were respiked and the microbial community was reapplied to the liquid cultures. As can be seen from Figure 96, there was a clear difference between the two experimental phases ($p < 0.001$). The tendency that was witnessed at the end of the first phase of the experiment became a clear trend in the second part of the experiment (Fig. 94 and Fig. 96). Aldrin and heptachlor had the highest concentrations in the treatments, while PCA was higher in the controls (loadings in Fig. 96). The first component was adequate to explain the data (declared variance = 78.4 %). The first component of analysis using group information separated the data into two distinct classes, viz: controls and treatments (Classes in Fig. 97). Like in the PRC, aldrin and heptachlor and aldrin had the highest values in the treatments while PCA was higher in the controls (Canonical weights and variables in Fig. 97).

The second experimental phase showed a trend where the controls had lower concentrations relative to the microbially treated samples (Fig. 96). To further evaluate this result, the loadings were compared with the log Kow and log K_H of the OCPs (Fig. 98 and Fig. 99). It was hypothesized that compounds with a high log Kow would partition more into the microbial phase while those with high log K_H would dissipate more because of volatilization. Therefore it would be expected that compounds with low log Kow and low log K_H would also have low loadings because such compounds could not volatilize to a high extent, nor be

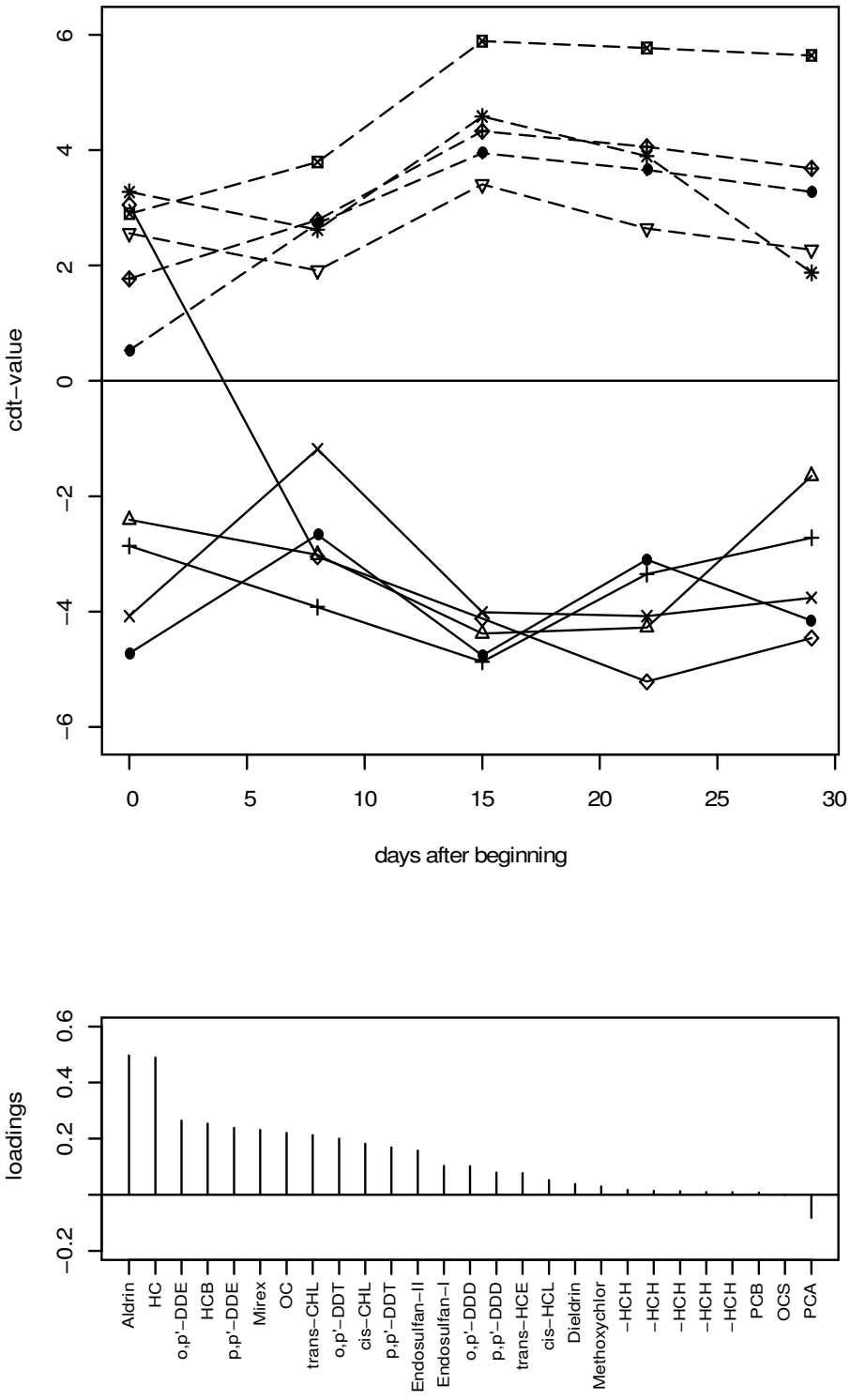

Fig. 96: Principal response curve and loadings for the OCPs during the second phase of the experiment (declared variance = 78.4%).

Continuous line = control (5 replicates), Dotted line = Samples treated with microbes (5 replicates).

.

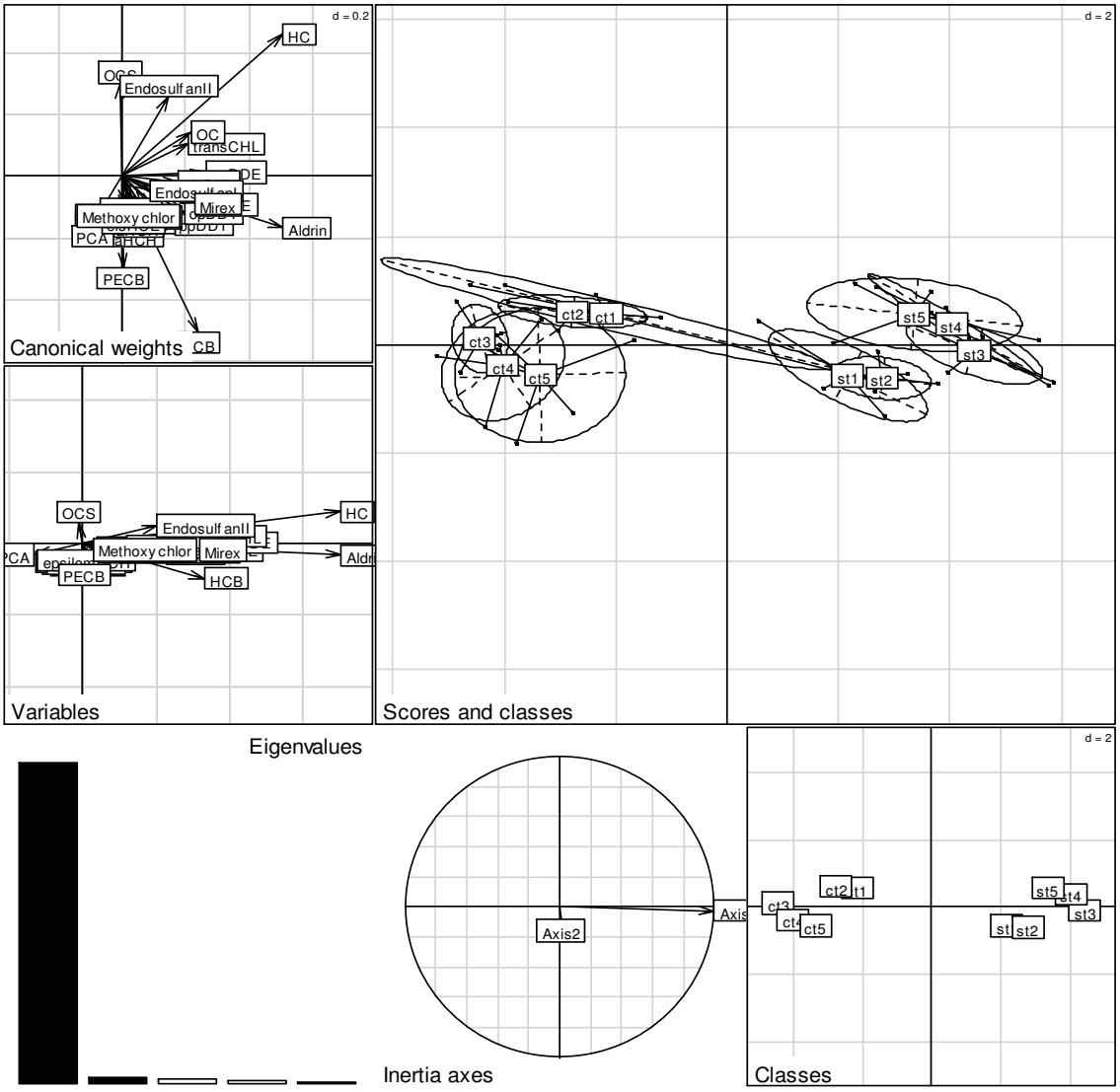

Fig. 97: Results of data analysis using group information (ade4-package, between function), based on components 1 and 2, showing the distribution of OCPs in the control and microbial treated sets during the second phase of the experiment. 'Scores and classes' is a 3-D presentation of the data separation by the two components/axes, while 'Classes' is a simple 2-D presentation of the same; 'Canonical weights' shows the loading of each metabolite; 'Variables' shows the extent and direction of each metabolite; 'Eigenvalues' shows the contribution of the components/axes in explaining the data: the two dark axes have been used to separate the groups.

c = controls, s=samples treated with microbes.

The digits after the letter signify the sampling point. There were 5 sampling points in the second phase i.e. 1-5. Therefore ct5 means control at sampling point 5.

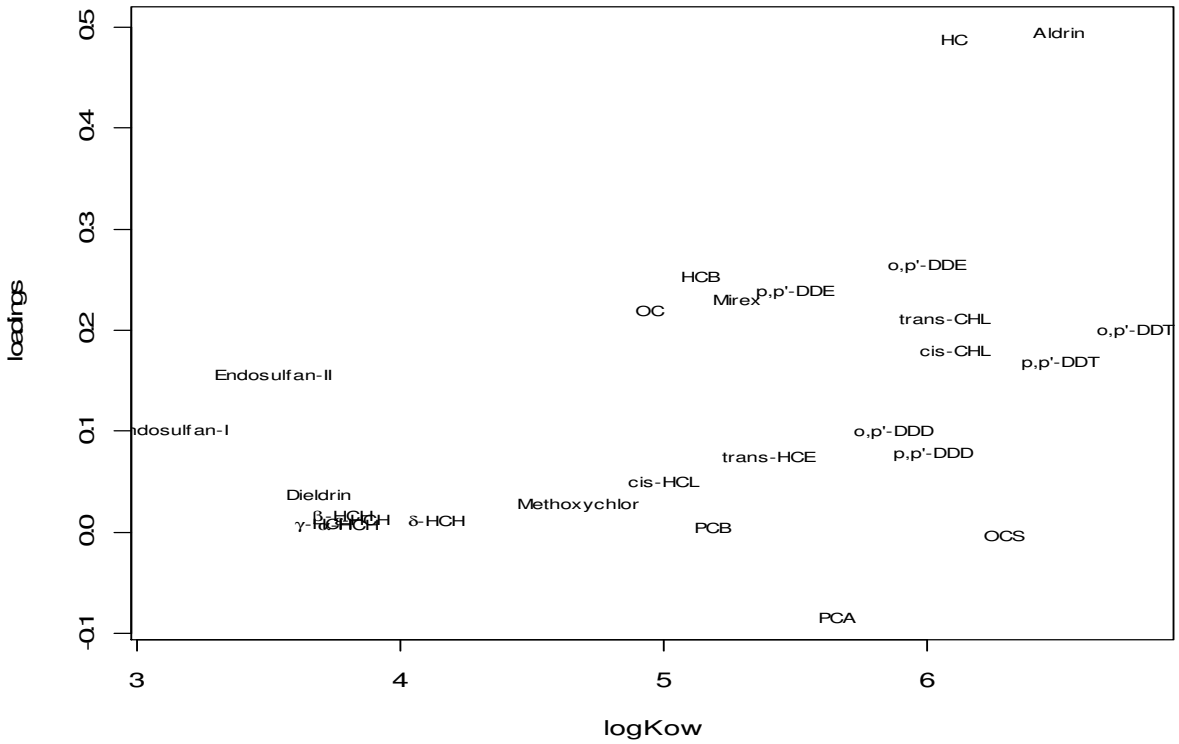

Fig. 98: Correlation of LogKow and the loadings of the second phase of the experiment

adsorbed considerably by the microbial phase – and therefore could not contribute much to the observed trend. The loadings would thus be expected to increase with increasing log Kow and log K_H values, with compounds having the highest log Kow and log K_H values also having the highest loadings – and therefore contributing the most to the observed trend. It could also be hypothesized that compounds with a low log Kow are more hydrophilic and soluble and, if such compounds also have a low K_H, they would volatilize less. The overall effect is that such compounds would be more bioavailable for microorganisms and should thus be degraded more relative to the other compounds in the cocktail. Such compounds would thus not contribute to the observed trend and, accordingly, their loadings would be negative or zero.

Figure 98 shows that there was a general increase in loadings with increasing log Kow, with aldrin and heptachlor showing the highest effect. The correlation was significant ($r = 0.44$ and $p = 0.019$). The endosulfans, with low log Kow showed higher loadings relative to other compounds with similar log Kow values. The HCHs, dieldrin and methoxychlor had low loadings consistent with their Kow values. PCB, PCA and OCS, however, had low loadings in

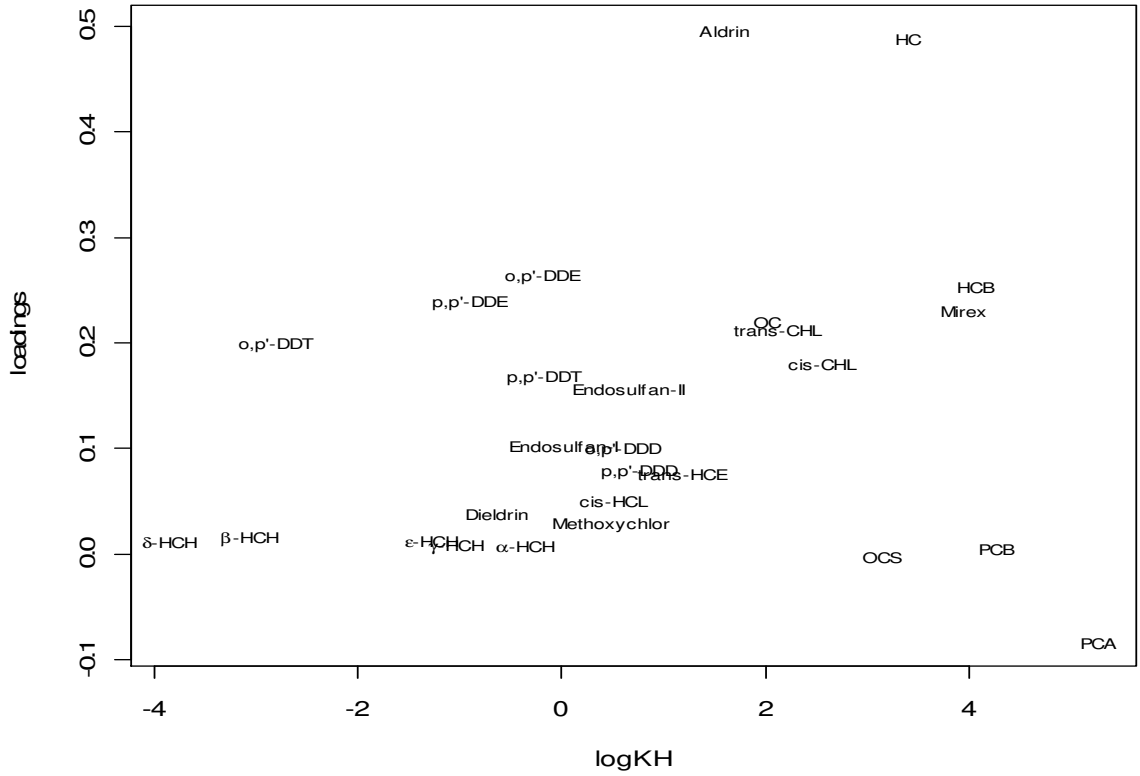

Fig. 99: Correlation of $LogK_H$ and the loadings of the second phase of the experiment

spite of their high log Kow values. These facts can account for the lack of a higher correlation coefficient. Figure 99 shows a similar trend as figure 98: increasing loadings with increasing log K_H values. However, there was no significant correlation ($r = 0.18$ and $p = 0.38$). This could indicate that there was no monotonic linear relationship for most of the chemicals. Heptachlor and aldrin again had the highest loadings, while PCB, PCA and OCS had low loadings despite their high log K_H values.

Fig. 100 shows the univariate curve of the log transformed data for heptachlor concentrations during the two experimental phases. It illustrates the general trend shown by most of the chemicals i.e. no clear differences between the controls and treated samples during the first experimental phase but clear differences during the second experimental phase, with the treatments having higher concentrations relative to the controls. This is the same trend that was observed in the PRC curves (Fig. 94 and Fig. 96). Since heptachlor showed the same trend as that of the PRC curves, it means that it contributed strongly to the overall trend of the PRC curves. Accordingly it had a high loading during both experimental phases (Fig. 94 and Fig. 96).

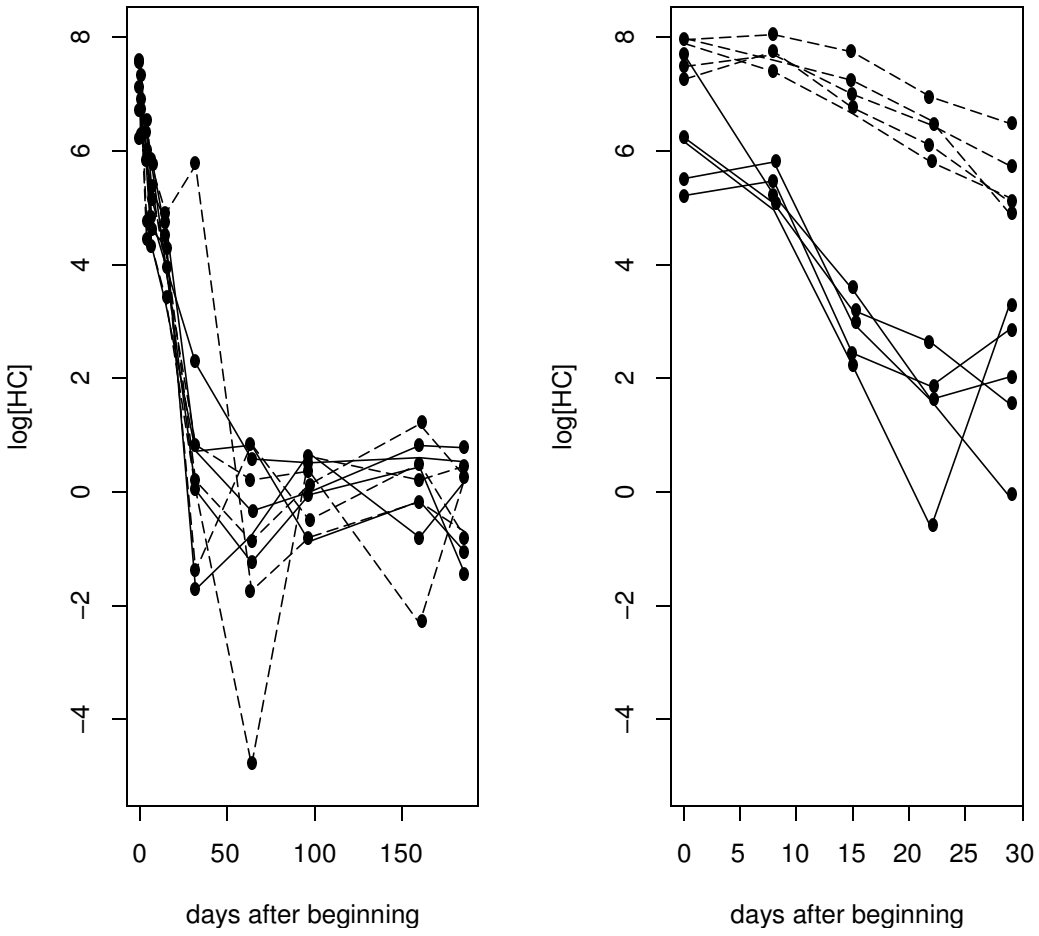

Fig. 100: Univariate curve for the dissipation of heptachlor in the first and second phases of the OCPs degradation experiment.

Continuous line = control (5 replicates), Dotted line = Samples treated with microbes (5 replicates).

3.5.3. Growth of the microbial community

After the first application of OCPs, microbes grew rapidly to a maximum after 8 days (Fig. 101). Thereafter there was a continuous decrease to a minimum on day 186. The slight increase observed on day 64 could be an artifact because no further increase was noted on the next sampling point. After day 186 there was a respiking of the liquid culture with the OCPs. Since the microbial population had decreased considerably to levels far below the initial microbial concentration, it was necessary to add the microbial culture, to achieve microbial concentrations similar to those at the start of the first phase. As can be seen from Figure 101, there was once again a sharp increase in population in the first days after respiking followed by a decrease in population. This is the same trend that had been witnessed at the beginning of

the first spiking (Fig. 101). There was no growth of microbes in the controls. This confirmed that sterile conditions were maintained throughout the experimental period.

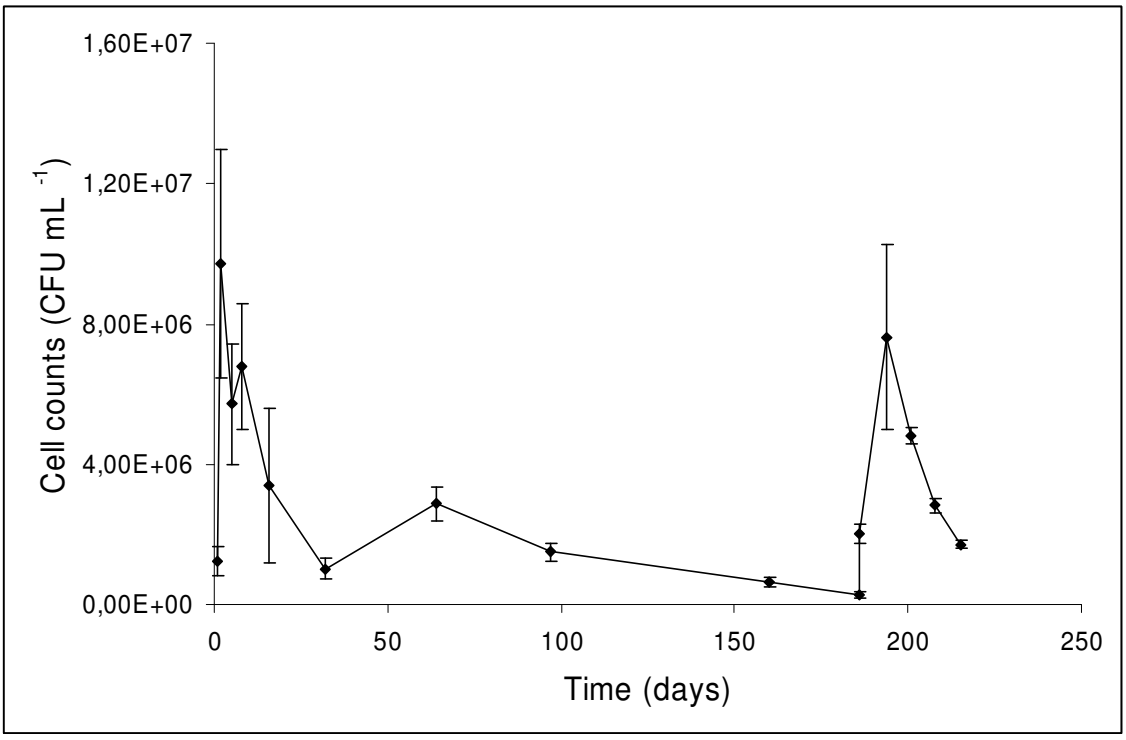

Fig 101: Cell counts during the first and second phases of the OCPs degradation experiment.

4.0: Discussion

The overall objective of the study was to induce or enhance the degradation and mineralization of HCB and DDT in two tropical clay soils. The general working hypothesis of the study was that steering ecological conditions would enhance the degradation of HCB and DDT in soil, by activating the biotic and abiotic pathways necessary for the degradation of chlorinated compounds. Experiments were carried out under aerobic, anaerobic and anaerobic-aerobic cycles conditions. The ability of 1,2,4-TCB mineralizing comminty to degrade OCPs was also tested.

4.1 Transformation of HCB and DDT under aerobic conditions

4.1.1 Mineralization and volatilization of ^{14}C-DDT and ^{14}C-HCB in field and paddy soils under aerobic conditions

The higher mineralization of DDT relative to HCB shows that the two soils have a higher innate ability to mineralize DDT relative to HCB. The fact that there was no difference in ^{14}C-DDT mineralization and volatilization in the two soils, could indicate similarity in DDT dissipation in the soils. The differences in HCB mineralization and volatilization (Fig. 18, Fig. 19, Table 7 and Table 8) in the two soils, shows that the paddy soil had higher innate ability to degrade HCB.

HCB is highly chlorinated while DDT is low chlorinated. Mineralization involves cleavage of the aromatic ring (Aislabie, 1997). Whereas this is feasible for the lower-chlorinated DDT, it is difficult for the highly chlorinated HCB - not only because of the sterric hindrance caused by the chlorides, but also because of the high energy requirements that the process would demand (Aislabie et al., 1997; Zhao et al., 2003). This accounted for the low HCB mineralization (Fig. 14) and degradation (Table 9). This is consistent with other research findings which show that both HCB and PCB do not degrade under aerobic conditions (Isensee et al, 1976; Beall, 1976; Griffin and Chou, 1981; Howard, 1991; Meijer et al, 2001). This is supported by the fact that there were high amounts of extractable residues (Fig. 20) indicating little, if any, microbial activity. There was, however, a significantly higher build-up of non-extractable residues in the paddy soil relative to field soil (Fig. 20). This hinted at greater microbial activity in the paddy soil because abiotic sorption would be expected to be greater in the field soil, given that it had higher organic carbon content of 2.25 % compared to 2.07 % for the paddy soil. It also hinted that there could be anaerobic spots in the paddy soil, even under ostensibly aerobic conditions, given that HCB is mainly degraded anaerobically

(Meijer et al, 2001). This phenomenon occurs in soils (Sextone et al, 1985) and should be greater in clay soils.

There was very low volatilization in both soils and for both compounds, at below 0.5 %. This is in agreement with Isensee et al. (1976) who showed that in covered containers there is no loss of HCB. This confirms other findings which show that it is the lower-chlorinated metabolites of HCB that are responsible for the volatilization of HCB, rather than the parent compound (Brahushi et. al., 2004; Rosenbrock et al., 1997; Ramanand et al., 1993; Yuan et al, 1999; Zhao et al., 2003; Fathepure and Vogel, 1991). There were significant differences in volatilization, however, between the two soils (Fig. 19, Table 7 and Table 8) with the paddy soil showing higher volatilization for both HCB and DDT ($p<0.05$). This shows that the field soil is better able to retain the compounds hence lowering volatilization. This can be explained by the higher organic carbon content of the field soil relative to the paddy soil. Organic matter has been shown to be the major parameter that influences the fate of chloroaromatic compounds in soil (Bradley et al. 1998; Field, 2004)

This experiment showed that both soils were capable of mineralizing DDT (a low-chlorinated aromatic compound), but only the paddy soil showed indications of being able to mineralize HCB (a highly- chlorinated aromatic compound) under aerobic conditions.

4.1.2 Effect of organic matter addition on the mineralization and volatilization of aged DDT residues

On day 84, compost was added to the DDT-spiked soils. The differences in volatilization and mineralization of DDT after the addition of compost could partly be attributed to the disturbance of the soil systems by mixing. However, both amended and un-amended soils were treated in the same way hence the increased aeration and dispersion was uniform The significantly higher mineralization in the field soil (Fig. 21 and Table 10), can be attributed to the higher carbon content in the field soil relative to the paddy soil (Table 3) because DDT has been shown to undergo co-metabolic degradation (Aislabie, 1997). The significantly lower volatilization in the field soil relative to the paddy soil (Fig. 22 and Table 10) can also be attributed to the higher organic carbon content of the field soil (Table 3). Organic matter has been shown to decrease the volatilization of chlorinated aromatics in soils (Field, 2004). The metabolite pattern showed that p,p-DDD and p,p-DDE were formed in equal amounts in the paddy soil (Fig. 23). This is contrary to expectations because DDE usually forms in higher amounts relative to DDD under aerobic conditions (Zhou et al., 2003). This would mean that the paddy clay achieves anaerobic conditions or that anaerobic sites exist within the soil, even

under aerobic conditions. This is consistent with the results of the HCB experiment discussed above. There was higher p,p-DDE formation relative to p,p-DDD in the field soil (Fig. 23), as expected for DDT degradation under aerobic conditions. The similarity in CO_2 production in the two soils during the incubation of DDT (Fig. 14 and Fig. 16), in spite of differences in metabolite formation, indicates that DDT - and not its metabolites – was mineralized. This is consistent with findings which show that DDD is not degraded under aerobic conditions (Foght et. al., 2001), while DDE is persistent under both aerobic and anaerobic conditions (Strompl and Thiele 1997). It also confirms reports that DDT is degraded aerobically in tropical soils (Wandiga, 2001).

4.2 Mineralization, volatilization and degradation of ^{14}C-HCB under anaerobic-aerobic cycles

After the first anaerobic phase, there was higher mineralization of HCB in the paddy soil relative to the field soil (Fig. 25). This was because of higher degradation of HCB in the paddy soil during the first anaerobic phase to yield lower chlorinated products (Figures 37, 38 and 39). The higher volatilization in the paddy soil (Fig. 28) supports this assertion and the metabolite results confirm it (Figures 37 and 39). This is consistent with other reports that it is the lower chlorinated metabolites of HCB that are subject to mineralization and volatilization (Brahushi et. al., 2004; Rosenbrock et al., 1997; Ramanand et al., 1993; Yuan et al, 1999; Zhao et al, 2003; Fathepure and Vogel, 1991).

However, whereas the cumulative mineralization of the treated paddy soil increased appreciably, that of the field soils did not (Fig. 25). This indicated that the paddy soil had a higher degradation capacity relative to the field soil, probably due to the presence of aerobic degraders for lower chlorinated benzenes. Studies have shown that CB, 1,3-DCB, 1,4-DCB, 1,2,4-TCB, 1,2,3,4-TeCB and 1,2,4,5-TeCB are biodegradable in soil under aerobic conditions (Feidieker et al., 1994; Marinucci and Bartha, 1979; Schroll et al., 2004). Therefore compost provided a supplementary carbon source for these degraders leading to increased mineralization of the HCB metabolites in the compost-amended paddy soil (Fig. 26, Fig. 27 and Table 13).

The high volatilization in all sets during the second aerobic phase (Fig. 28) could account for the lack of more appreciable mineralization. Mineralization of HCB and its metabolites has been shown to be limited by high volatilization (Meijer *et al.,* 2001). Wang and Jones (1994) have shown that high volatilization of 1,3-DCB, 1,2,3-TCB, 1,2,3,5-TeCB and PCB resulted in minimal mineralization. Brahushi et al. (2002) have shown the same for CB. The

volatilization was higher in the paddy soil relative to the amended paddy soil throughout the experimental period (Fig. 28). This indicates that compost led to decreased volatilization and increased mineralization in the paddy soil. Using mineralization as a measure of microbial activity (Sims and Cupples, 1999), this would mean that compost led to increased microbial activity. This is consistent with the findings of Wang et al. (2007) who showed that increased 1,2,4-TCB mineralization, caused by the application of an adapted 1,2,4-TCB degrading microbial community, led to decreased volatilization of 1,2,4-TCB.

As expected, the increase in non-extractable residues was accompanied by a decrease in extractable residues (Fig. 31, Fig. 32 and Table 16). The assertion that there were degraders in the paddy soil is supported by the higher formation of non-extractable residues in the paddy soil sets relative to the field soil samples (Fig. 32). The significant correlations of ^{14}C-non-extractable residues with both $^{14}CO_2$ and ^{14}C-volatilization (Fig. 33 and Fig. 34) indicate that the formation of non-extractable residues was mediated by microbes. Reports in literature have indicated that non-extractable residues, especially the bound residues portion, are an indicator of microbial activity (Kastner et al., 1999).

The mineralization rates were higher in the compost-amended samples relative to the untreated ones in both soils and in both aerobic phases (Fig. 26, Fig. 27 and Table 13).This was due to the higher formation of metabolites in the compost-treated soils (Fig. 41 and Fig. 43). This showed a positive compost effect in line with the hypothesis and objective of this work. This is contrary to the findings of Brahushi et al. (2004) who showed that supplementary carbon sources caused reduced degradation of HCB under anaerobic conditions. However, the higher production of metabolites in compost-treated samples in this study occurred in the second anaerobic phase, while Brahushi's experiment was only a single-phase anaerobic experiment.

The volatilization rates decreased over time for all sets, with the compost-treated samples having higher absolute slopes in both soils during the first aerobic phase (Fig. 29, Fig. 30 and Table 14). This means that there were greater losses via volatilization in the untreated soils relative to the treated ones. This is in line with the observation made in the HCB aerobic experiment, that the field soil - with higher organic matter content - showed lower volatilization relative to the paddy soil (Fig. 15). Thus the field soil (with higher organic content than the paddy soil) had lower volatilization (Figures 15, 17, 28, 29 and Table 8), while the compost-treated samples (with higher organic content the unamended samples) also had lower volatilization (Fig. 28, Fig. 29 and Table 14). This is consistent with the findings of other authors who have shown that organic matter greatly influences the fate of

chloroaromatic compounds in soil (Bradley et al., 1998; Field, 2004). However, in the second aerobic phase, the treated and untreated samples of each soil had the same volatilization rate with the same amount of volatilization (Fig. 30, Fig. 31 and Table 14). This was because extensive degradation of HCB had taken place in all samples (Figures 37, 38 and 41). However, the rate and amount of volatilization was higher in the paddy soil relative to the field soil (Figures 28, 29, 30 and Table 14).

The high formation of 1,3,5-TCB in both paddy and field soil samples (Figures 36 and 37), is consistent with the reports of other authors (Yuan et al., 1999; Brahushi et al., 2004) who have shown 1,3,5-TCB to be the major metabolite of HCB anaerobic degradation.

There was no dramatic compost effect in redox potential reduction as expected during the first anaerobic phase (Fig. 45). This could indicate that there were enough carbon sources in the soil for anaerobiosis, hence precluding the need for supplementary sources. The drop in redox potential on addition of yeast extract on day 256 during the second anaerobic phase, was a further indication that anaerobic processes in these soils were driven by microbial activity as has been reported by several authors (Heron & Christensen, 1994; Field, 2004; Bradley et al., 1998; Curtis and Reinhard, 1994; Perlinger et al., 1996).

In summary, the purpose of the whole experiment was to induce the degradation and mineralization of HCB in the paddy and field soils. The first anaerobic-aerobic cycle degraded HCB to a modest extent (Figures 36, 37, 38 and 39), and induced mineralization in the paddy soil but had no profound effect on the field soil (Fig. 24). The second anaerobic-aerobic phase caused extensive degradation of HCB in both soils (Figures 35, 37, 38 and 39), enhanced mineralization in the paddy soil samples (Fig. 24), but minimal mineralization was induced in the field soil. However the enhanced degradation in the second anaerobic-aerobic phase also caused increased volatilization (Figures 27 and 29) because of the lower-chlorinated metabolites (Figures 37, 38 and 39). The probable degradation pattern of HCB (Figures 37 and 38) in the soils is

HCB→ PCB →1,2,3,4-TeCB + 1,2,3,5 → TeCB → 1,3,5-TCB + 1,2,4-TCB +1,2,3-TCB → *1,4-TCB+1,2-TCB →CB.

* The 1,3-DCB standard was not available and therefore it was not analyzed

This is different from the pathway proposed by Fathepure and Vogel (1991) for HCB anaerobic-aerobic degradation, but similar to that proposed by Yuan et al.(1999).

Compost caused increased degradation in both soils (Figures 37, 38, 41 and 43) and mineralization (Figures 25, 26, 27 and Table 13). The greater mineralization in the paddy soil during the second aerobic phase showed that supplementary carbon sources are important if and when degradable forms of the contaminant (in this case lower chlorinated HCB metabolites) are present in the soil. Compost caused reduced volatilization of HCB during the first anaerobic-aerobic phase (Figures 28, 29 and Table 14), but had no effect during the second anaerobic-aerobic phase after HCB had been degraded to lower-chlorinated compounds (Figures 28, 30, 37, 38 and Table 14).

4.3 Mineralization, volatilization and degradation of ^{14}C-DDT under anaerobic-aerobic cycles

The higher mineralization of DDT in the field soil in the first aerobic phase (Fig. 46, Fig. 47 and Table 19), can be attributed to higher levels of DDT in the field soil relative to the paddy soil (Fig. 55, Fig. 56 and Fig. 58). The lack of rapid formation of p,p-DDE in both soils after the first anaerobic phase, can also be attributed to the reduced levels of DDT because there was less DDT available for transformation to DDE. It also indicates that after DDD is formed, it is not readily transformed to DDE. Hence one of the objectives of the experiment of preventing DDE formation was achieved. However, the formation of DDD presented a problem because it is not readily amenable to mineralization. The lack of degradation and mineralization of p,p-DDD during the aerobic phase is not surprising because DDD is mainly produced under anaerobic conditions (Kale et al., 1999). It is therefore unlikely that microbes capable of degrading DDD aerobically exist in soils. However, degradation during the second anaerobic phase resulted in greatly reduced quantities of DDD (Fig. 55 and Fig. 56), hence illustrating the effectiveness of the anaerobic-aerobic cycles in DDT degradation.

After the second anaerobic phase, there was minimal $^{14}CO_2$ production in both the field and paddy soils (Fig. 46). This coincided with low levels of DDT in both soils, with higher levels of p,p-DDD and p,p-DDMU (Fig. 55 and Fig. 56). This provided further evidence that high mineralization in the soils was dependent on the availability of DDT. The decrease in mineralization of ^{14}C-DDT during the second aerobic phase (Fig. 48 and Table 19) supports reports in literature that it is not DDT itself that is persistent in tropical soils, but rather its transformation products (Wandiga, 2001).

The higher dissipation of DDT in the field soil relative to the paddy soil (Fig. 57 and Table 20), in spite of higher metabolite formation in the latter (Fig. 55, Fig. 56 and Fig. 58), indicates that processes other than transformation to metabolites were responsible for the

increased DDT dissipation in the field soil. Of all the dissipation and degradation processes, only $^{14}CO_2$ formation was significantly different between the groups (Table 18). Therefore it is mineralization $^{14}CO_2$ that was responsible for the higher dissipation of DDT in the field soil relative to the paddy soil (Fig. 57 and Table 20). .

The increase in p,p-DDD and p,p-DDMU at the end of the second anaerobic phase (Fig. 55 and Fig. 56) coincided with an increase in non-extractable residues (Fig. 51). This could indicate microbial mediation in the formation of non-extractable residues (Boul, 1995).

Though there were metabolites that were higher in the field soil, namely: o,p-DDT, p,p-DDT and p,p-DDM (Fig. 58), the concentrations of these compounds were very low (Fig. 55 and Fig. 56).

Compost led to increased mineralization of DDT in both soils (Fig. 46). In the first aerobic phase, the mineralization of DDT was almost doubled in compost-amended samples. There were no major differences in the amounts of metabolites (Figures 55, 56 and 58), extractable and non-extractable residues between the two soils or between the compost-amended and un-amended samples (Fig. 50, Fig. 51, Fig. 52, Fig. 53, Fig. 54 and Table 18) to account for this difference. Therefore, the increased mineralization can be attributed to increased microbial activity due to compost amendment.

The low volatilization in these soils (Fig. 49) contradicts the assertion by Racke et al. (1997) that higher dissipation of DDT in tropical soils is mainly due to volatilization. There was also no evidence of increased volatilization of DDT and its metabolites as a result of water-logging, as reported by some authors (Boul et al., 1994; Spencer et al., 1996).

Therefore in summary, the paddy soil was the more efficient degrader of DDT (Fig. 55, Fig. 56 and Fig. 58), but the field soil dissipated DDT faster (Fig. 57 and Table 20). Mineralization accounted for the higher dissipation of DDT in the field soil, and compost enhanced mineralization in both soils during the first aerobic phase (Fig. 57 and Table 20). However, compost had no effect on DDT dissipation (Fig. 57 and Table 20) or metabolite formation (Fig. 55, Fig. 56 and Fig. 58).

4.4 Factors influencing the anaerobic degradation of DDT in tropical clay soils

4. 4.1 Degradation of DDT

The degradation of DDT yielded p,p-DDD and p,p-DDMU as the major metabolites (Fig. 63 and Fig. 64). This is in line with other reports on the anaerobic degradation of DDT (You et al., 1996, Aislabie et al., 1997). Higher metabolite concentrations were detected in the paddy soil (Fig. 66), but the DDT dissipation rate was higher in the field soil (Fig. 65 and Table 22).

This difference in DDT dissipation can be attributed to various soil factors (Fig. 69). In particular, fluorophore 4, NH_4^+, DOC, K, CO_2 and Fe (II) were higher in the field soil as shown by the loadings of figure 69. Therefore these would be the parameters that were mainly responsible for the higher DDT dissipation in the field soil. On the other hand, the paddy soil had higher amounts of Na^+, Mg^{2+}, Cl^-, Br^-, Li^+ and the other four fluorophores (Fig. 69). The roles that different soil properties could have played in the degradation of DDT are discussed in the sections that follow.

4.4.2 The role of salinity in the anaerobic degradation of DDT

The significantly higher salinity with time in the paddy soil relative to the field soil ($p = 0.05$) indicates higher dehalogenation (Fig. 72). This is not surprising given that the paddy soil is adapted to anaerobic conditions. The high correlation between salinity and p,p-DDD in both soils (Fig. 73), shows that increasing salinity is an indicator of increasing dehalogenation. p,p-DDD is the first metabolite in the anaerobic dechlorination of p,p-DDT (Zook and Feng, 2008). The significant correlation of p,p-DDT with salinity in the field soil, and lack of correlation in the paddy soil (Fig. 73), shows that prevailing salinity conditions had greater influence on DDT degradation in the field soil relative to the paddy soil.

The decrease in salinity after week 6 (Fig. 75), accompanied by a decrease in p,p-DDD (Fig. 63 and Fig. 64), showed that salinity was a limiting factor in DDT dechlorination. Dechlorination has been shown to be a reversible process in naturally occurring organochlorines (Field, 2004), and reversible processes are always dependent on prevailing system conditions such as concentration. Increasing salinity has been shown to reduce microbial activity and carbon mineralization (Pankhurst et al., 2001). The lower correlation of salinity with p,p-DDMU relative to p,p-DDD (Tables 24, 25, 26 and 27) could be due to the fact that p,p-DDMU is a secondary metabolite of DDT dechlorination (Zook and Feng, 2008). In the field soil, there was higher correlation of salinity with p,p-DDT and p,p-DDD in the compost-amended soil (Fig. 73). However, the opposite was noted in the paddy soil i.e. lower correlation in the compost-amended soil (Fig. 73). The paddy soil had high initial chloride content, the field soil had lower initial chloride content, while the added compost had the highest chloride content of the three (Table 3). Thus addition of compost led to greater salinity in the compost-amended paddy soil (Fig. 75), which could have limited the degradation and dissipation processes of DDT (Pankhurst et al., 2001).

4.4.3 The role of sodicity in the anaerobic degradation of DDT

Results based on values of SAR, ESP and TCC of the soils used in this study indicate that the soils could be regarded as potentially dispersive (Rengasamy et al., 1984). The greater decrease in SAR and ESP over time in the field soil relative to the paddy soil (Figures 74, 75, 76 and Table 29), indicates a greater reduction in swelling and dispersion of the field soil (Nelson and Oades, 1998). This means that there was greater dispersion and swelling in the paddy soil over the experimental period. This could explain the higher formation of metabolites in the paddy soil (Figures 37, 38 and 39) because greater dispersion and swelling of clays leads to greater availability of DDTr (Nelson and Oades, 1998).

The significant positive correlations of p,p-DDT concentrations with ESP and SAR in the field soil (Fig. 77), show that DDT degradation in the field soil was influenced by sodicity. This means that DDT degradation decreased as the soil sodicity decreased. In a preliminary work examining DDT transformation in soil amended with green waste and/or manure, a significant correlation was observed between soil Na^+ levels and DDT transformation (Kantachote, 2001). Na^+ is known to cause soil dispersion and increase in DOC levels (Nelson and Oades, 1998; Wood, 1995; White, 1997) and both mechanisms could potentially increase the bioavailability of DDT residues (DDTr) in the soil environment by either releasing DDTr from soil particles/colloids or exposing DDTr that were previously physically protected from degrading microbes. The lack of correlation between sodicity (SAR) and p,p-DDT in the paddy soil (Fig. 77) means that DDT dissipation was independent of the decreasing soil sodicity. However, the significant correlations between SAR and p,p-DDD in the un-amended field and paddy soils (Fig. 77) shows the dependence of DDT dechlorination on soil sodicity.

There was a significant correlation of SAR with p,p-DDD in the compost-amended field soil but not in the compost-amended paddy soil (Fig. 77). This can easily be explained by the effect of compost on soil sodicity. Whereas compost caused increased initial SAR/ESP in the field soil, it caused decreased initial SAR/ESP in the paddy soil (Fig. 74). This means that compost addition caused increased clay dispersion and swelling in the field soil, effectively availing more DDTr for degradation (Nelson and Oades, 1998; Wood, 1995; White, 1997). On the other hand, compost addition caused decreased dispersion and swelling – probably through clay flocculation - in the paddy soil, effectively decreasing the amount of DDTr available for degradation.

Therefore the overall effect is that higher sodicity in the paddy soil resulted in greater dispersion and availability of DDT, leading to higher metabolite formation in the paddy soil

relative to the field soil. Compost addition led to increased dispersion and availability of DDTr in the field soil, but decreased dispersion and availability in the paddy soil.

4.4.4 The role of reducible Fe in the anaerobic degradation of DDT

Due to a high abundance of iron, microbial reducible Fe (III) is normally the dominant alternative electron acceptor (AEA) in paddy soil (Yao et al., 1999). The strong correlations between Fe (II) and p,p-DDD in all the soil samples (Fig. 79), show that Fe played a major role in the dechlorination of DDT. The significant correlation of p,p-DDT with Fe (II) in the field soil, and lack of correlation in the paddy soil (Fig. 79), shows that reducible Fe had greater influence on DDT dissipation in the field soil relative to the paddy soil. The high correlations between Fe (II)/Fe (III) and cumulative CH_4 in all soil samples (Tables 24, 25, 26 and 27) show that Fe had a great influence on soil methanogenic processes (Huang et al., 2009). Studies have shown that Microbial Fe (III) reduction regulates CH_4 emission from flooded rice fields (Frenzel et al., 1999; Huang et al., 2009; Wang et al., 1993). The significantly ($p = 0.05$) higher formation of Fe (II) in the compost treated samples (Fig. 78 and Table 28) indicates that increased organic matter led to increased reducible Fe activity. The significant correlations of Fe (II)/Fe (III) with other soil properties (Tables 24, 25, 26 and 27) underscore the dominant role of reducible Fe in the processes of the studied clays.

4.4.5 The role of DOC in the anaerobic degradation of DDT

The DOC quality consisted of commonly reported fluorophores 1, 2, 3 and 4 (Fellman et al., 2008, Stedmon et al., 2003, 2005) and the seldom reported fluorophore 5 (Hiriat-Baer et al., 2008). These fluorophores have commonly been reported in the aquatic and marine environments (Coble et al., 1996; Cory and Mcknight, 2005; Luciani et al., 2008; Stedmon et al., 2003, 2005), and also in the terrestrial soil environment (Fellman et al., 2008; Junko and Zsolany, 2008; Zsolany et al., 1999; Zsolany et al., 2003). Though fluorophores 1 and 2 have been commonly reported in the marine and aquatic environments, their origin has always been attributed to the terrestrial environment (Coble et al., 1996; Cory and Mcknight, 2005; Fellman et al., 2008; Luciani et al., 2008; Stedmon et al., 2003, 2005). The fact that these components were dominant in both soils (Fig. 92 and Fig. 93) corroborates these claims. The presence of high amounts of fluorophore 3 in these soils, a fluorophore attributed to agricultural activities such as manure application (Stedmon et al., 2005), is not surprising given that the soils were picked from agricultural farms. The significant correlation between protein-like fluorophore 4 and NH_4^+ ((Tables 24, 25, 26 and 27), a product of protein

metabolism, confirms previous reports that it is of microbial origin (Coble et al., 1996; Cory and Mcknight, 2005; Fellman et al., 2008; Luciani et al., 2008; Stedmon et al., 2003, 2005). Given that fluorophore 5 increased only towards the end of the experimental period in both soils (Fig. 92 and Fig. 93), it could mean that it is also a product of microbial metabolism as shown by Hiriat-Baer et al. (2008).

The significant inverse correlations of F4 with p,p-DDT in all the soil samples, except the paddy soil (Fig. 83), shows that F4 was produced as p,p-DDT dissipated. The significant positive correlations of F4 with p,p-DDD in all the soil samples, except the paddy soil with compost (Fig. 83), indicates that F4 was produced during the dechlorination of DDT.

The presence of tryptophan and tyrosine-like fluorophores has been used to predict the biodegradability of DOC (Fellman et al., 2008). Thus the higher formation of F4 over time in the field soil indicates that more organic matter was degraded in the field soil than in the paddy soil (Fig. 82). This means that humic substances acted as direct food sources for microbes (oxidative mode), to provide energy for anaerobic processes such as dechlorination, in the field soil (Fig. 3; Bradley et al., 1998; Field et al., 2004). This is further supported by the inverse significant correlation between F4 and F2 in the field soil (Table 26). This means that the increase in F4 was due to the degradation of F2 (Fig. 82).

The relative stability of the DOC fractions in the paddy soil (Fig. 82) could preclude the oxidative mode, at least for the analyzed fluorophores. This could mean that dechlorination involved the reductive mode of humus in the paddy soil – both biotic and abiotic (Fig. 4). The high amounts of reducible Fe in the soils (Fig. 78), and the strong correlations between p,p-DDD and Fe (II), are indicators of the abiotic mode, with Fe playing an electron shuttling role for humic substances in the reductive dechlorination of DDT (Curtis and Reinhard 1994; Perlinger et al., 1996). It has been shown that quinones and hydroquinones, the major players in DOC electron-shuttling role (Field 2004), are the major constituents of fluorophores 1 and 2 (Cory and Mcknight, 2005).

However, the changes in redox status of the soil (NO_3^-, SO_4^{2-} and Eh) and mineralization (N_2O, CO_2 and CH_4) indicated microbial activity (Figures 72, 85, 89 and 92). Further, the positive significant correlations between p,p-DDD and F4 in the paddy soil (Fig. 83) support the idea of the involvement of humic substances in DDT dechlorination. This is especially so because no correlation could be shown between F4 and p,p-DDT in the paddy soil, hence precluding an oxidative mode of degradation. Thus the biotic mode of humus also played a role in dechlorination of DDT in the paddy soil (Field 2004).

The stability of some fluorophores (F1 and F3) in the field soil (Fig. 82) could indicate that

the reductive mode of dechlorination was also at play (Fig. 4). The inverse correlations of F1 and F3 with p,p-DDD in the field soil (Table 26), coupled with a lack of correlation with p,p-DDT, indicates for a reductive mode of humic substances in dechlorination (Fig. 3; Bradley et al., 1998; Field et al., 2004).

Thus both oxidative and reductive dechlorination took place in the field soil, while only reductive dechlorination took place in the paddy soil.

4.4.6 Carbon and nitrogen transformation during the anaerobic degradation of DDT

4.4.6.1 Carbon mineralization

The strong inverse correlations of p,p-DDT with cumulative CH_4 and CO_2 in the field soil (Figures 86 and 87), strong positive correlations with p,p-DDMU in the paddy soil (Tables 24 and 25), and excellent positive correlations with p,p-DDD in all the soil samples (Figures 86 and 87), show that CH_4 and CO_2 production can be used as indicators of DDT degradation.

The lack of correlation of CH_4 and CO_2 with p,p-DDT in the paddy soil is not surprising because DDT dissipation was mainly via reductive dechlorination as shown by the higher amounts of major metabolites when compared to the field soil (Fig. 58 and Fig. 66). The strong correlation of CO_2 with p,p-DDT in the field soils (Fig. 87), on the other hand, indicates that p,p-DDT underwent direct mineralization as organic matter was mineralized (Fig. 3, Bradley et al., 1998; Field et al., 2004). This is a strong indicator for co-metabolic breakdown, in line with other studies which show that DDT and other POPs mainly undergo co-metabolic degradation (Aislabie, 1997; Foght et al., 2001; Zhao et al., 2003).

The strong positive correlations of CH_4 and CO_2 with p,p-DDD in all the samples (Figures 86 and 87) indicate involvement of organic matter in the dechlorination of DDT (Field et al., 2004). This is supported by the significant positive correlations between F4 and CH_4 in both field and paddy soil samples (Tables 24, 25, 26 and 27). Thus in the paddy soil there was low direct mineralization of DDT, but high co-metabolic dechlorination to p,p-DDD and p,p-DDMU (Perlinger et al., 1998). In the field soil there was direct mineralization of p,p-DDT and co-metabolic degradation to p,p-DDD.

Compost caused increased CO_2 production in the field soil (Fig. 85). This showed that compost caused increased mineralization in the field soil, and in the process caused increased DDT mineralization. This is indicated by the strong correlation between p,p-DDT and CO_2 in the compost-amended field soil (Fig. 87). However, this compost effect on CO_2 production

was not noted in the paddy soil, further precluding oxidative breakdown of humic substances in this soil.

The paddy soil CO_2:CH_4 ratio of < 1 for most of the experimental period (Fig. 88) indicates that methanogenesis was the dominant process in this soil (Conrad, 1999). The slightly > 1 ratio in both amended and un-amended paddy soils in weeks 6 and 8 (Fig. 88) could be attributed to CO_2 produced directly during fermentation (Vile et al., 2003, Schink, 1997). Many fermentation reactions produce CO_2 in the processing of organic molecules (Schink, 1997). The ratio of about 1 for the un-amended field soil for most of the period (Fig. 88) concurred with the theoretical value of 1 for methanogenic systems (Keller et al., 2009). The high CO_2:CH_4 ratio in the compost-amended field soil (Fig. 88) can be attributed to the utilization of humic substances as terminal electron acceptors, TEAs (Segers, 1998; Neubauer et al., 2005; Heitmann et al., 2007; Keller and Bridgham, 2007). Dissolved organic matter is an important electron acceptor, contributing directly (through humic reduction) or indirectly to high CO_2:CH_4 ratios (Heitmann and Blodau, 2006; Heitmann et al., 2007). Therefore the high ratio could be as a result of a shift in the dominant pathway of anaerobic decomposition from methanogenesis to the utilization of the more thermodynamically favorable DOM as TEAs (Keller et al., 2009). The time when there is a shift to lower ratios in the time course e.g. week 4 for the un-amended paddy and field soil samples (Fig. 88), could indicate a predominance of methanogenesis over utilization of DOM - resulting in larger production of CH_4 relative to CO_2 (Conrad, 1999).

Hence in some cases organic matter yielded an electron donor-like response in which both CO_2 and CH_4 production were stimulated resulting in a final CO_2:CH_4 ratio near 1 (Fig. 88). In other cases, there was an electron acceptor-like response in which CO_2 production increased while CH_4 production decreased, resulting in increased CO_2:CH_4 ratios. In cases with a CO_2:CH_4 ratio >2, the predominance of humic substances as TEAs may have strongly limited the production of CH_4 (Keller et al., 2009).

4.4.6.2 Nitrogen transformation

Soil micro-organisms demand carbon as well as nitrogen for their growth (Nordin, 2004). Therefore nitrogen influences the breakdown of organic matter and contaminants in soil. Anaerobic transformation processes can lead to an overall depletion or build-up of nitrogen. Denitrification is assumed to be the major nitrate removal pathway in many anoxic ecosystems (Jetten, 2008). However, there are increasing reports of nitrate reduction to ammonium (Christensen et al., 2000; Strohm et al., 2007; Tomaszek and Gruca-Rokosz,

2007; Mazeas et al., 2008). These two forms of nitrate reduction occurred in this study, and can be presented as (Tiedje, 1988):

1. Denitrification

$NO_3^- \rightarrow NO_2^- \rightarrow N_2O/N_2$

2. Disimilatory nitrate reduction to ammonium

$NO_3^- \rightarrow NO_2^- \rightarrow NH_4^+$

However, the denitrification process is more efficient in that it yields more ATP:

$2\ NO_3^- + 2H^+ + 5\ H_2 \rightarrow N_2 + 6\ H_2O$ $\quad dG° = -1120.5$ KJ per reaction

$NO_3^- + 2H^+ + 4\ H_2 \rightarrow NH_4^+ + 3\ H_2O$ $\quad dG° = -599.6$ KJ per reaction

The high N_2O production in the paddy soil, with negligible NH_4^+ production (Fig. 89), indicates that denitrification was the major mechanism of NO_3^- reduction (in the paddy soil). Conversely, the low N_2O production coupled with high NH_4^+ production in the field soil (Fig. 89) could indicate that disimilatory nitrate reduction was the predominant mechanism of nitrate reduction in the field soil, though NH_4^+ is also formed by other microbial processes. This is not surprising given that the paddy soil is waterlogged most of the time and has therefore adapted efficient means of anaerobic energy production. This higher ATP production could account for the higher dechlorination in the paddy soil because the dechlorination process requires energy (Zhao et al., 2003). Secondly, whereas there was an overall depletion of nitrogen with time in the paddy soil, there was overall build-up of nitrogen (NH_4^+) in the field soil (Fig. 89). Therefore at the end of the anaerobic period, there was higher nitrogen content in the field soil relative to the paddy soil. In anaerobic-aerobic cycles, this means higher amounts of nitrogen for the subsequent aerobic phase.
Taking N_2O as an indicator of efficient anaerobic processes, and NH_4^+ as a possible indicator of inefficient anaerobic processes (Tiedje, 1988), it is possible to explain the differences in DDT degradation between the soils. The strong correlation of N_2O with p,p-DDD in the paddy (Fig. 90), indicates the dominance of the efficient reductive dechlorination process. The strong correlation of p,p-DDD with N_2O in the field soil also indicates the presence of the efficient reductive dechlorination process. However, since the amounts of N_2O formed were low (Fig. 89), it also means that reductive dechlorination was low in the field soil. This would explain the higher formation of p,p-DDD in the paddy soil relative to the field soil (Figures

63, 64 and 66).

The strong correlation of NH_4^+ with both p,p-DDT and p,p-DDD in the field soil (Fig. 91) indicates inefficient processes in DDT degradation. The high amounts of NH_4^+ produced indicate that the inefficient processes were dominant in the field soil (Fig. 89). The strong significant correlation between F4 and NH_4^+ in both field soil samples (Tables 26 and 27) can be used as a further indication that degradation in the field soil was less efficient and thus more energy was required for the process (Tiedje, 1988). The lack of correlation of NH_4^+ with p,p-DDT and p,p-DDD in the paddy soil (Fig. 91) indicates the absence of inefficient processes. Thus only the energy efficient reductive dechlorination took place in the paddy soil.

4.5 The degradative capacity of a 1,2,4-TCB mineralizing community for an OCPs cocktail.

The fact that the community remained active in the same 1,2,4-TCB spiked liquid culture over the whole experimental period (Fig. 93) confirmed that it could survive for long periods. Wang et al. (2007) had shown that the same community could mineralize 1,2,4-TCB in liquid culture, but the experiments typically lasted two to four weeks in the same media. Unlike the 1,2,4-TCB experiment, the OCPs experiment was carried out at low and realistic ambient concentrations. Though this was in part due to the solubility limitation of the compounds, the primary motivation was the desire to find out if the microbes could degrade environmentally relevant OCPs by utilizing them as the sole carbon sources at the low concentrations found in environmental waters and soil solution. The hypothesis was that since the community has the ability to degrade 1,2,4-TCB, a chlorinated compound, it could be able to degrade other chlorinated compounds even at low concentrations.

There was a decrease in concentrations of OCPs with time in both the controls and treated samples (illustrated in Fig. 100). To appreciate the differences in trend between the two groups, PRC analysis was done. This showed a clear difference in response between the treatments and the controls in the second phase (Fig. 96), with the controls having lower chemical concentrations relative to the treatments. This was contrary to the expected results based on the experimental hypothesis: that the microbes would utilize the OCPs as carbon sources and therefore lower concentrations would be measured in the treated samples relative to the controls.

The findings to the contrary could be due to the low concentrations used, because it has been shown that low concentrations may hamper biodegradation (Gianfreda and Rao, 2008;

Johnsen et al., 2005); the use of a complex mixture, because complex phenomena inhibiting the degradation of xenobiotics may arise when more polluting compounds are simultaneously present (Gianfreda and Rao, 2008); the high volatilization and high Kow values of these compounds (Table 2), because the presence of microbes could have stemmed the tide of volatilization in the treated samples by providing sorption sites for the OCPs. The high Kow values (Table 2) commend this line of reasoning because of partitioning into the organic (microbial) phase. This is consistent with the findings of Wang et al. (2007) who showed that in a liquid culture inoculated with the same community, the volatilization of 1,2,4-TCB decreased from 45.38% in the control to only 0.73% in the inoculated samples. Rapp and Timmis (1999) had earlier shown that 1,2,4,5-TeCB adsorbed to *Burkholderia* sp. strain PS14 in liquid culture, with a sorption co-efficient (Kp) that was approximately 4 orders of magnitude stronger than adsorption to a soil used in the same study. Secondly, the fact that the microbes were not filtered off prior to extraction could also explain the higher concentrations noted in the treated samples. It means that the amounts sorbed by the microbes, though removed from the aqueous media, were nevertheless analyzed as present in the treated samples. Wang et al. (2007) showed that the concentration of ^{14}C in ^{14}C-1,2,4-TCB-spiked liquid media decreased from 14.38% to 2.36% after the microbes were filtered off.

The loadings reveal the contribution of the individual compounds to the observed trend. Based on these loadings and the properties of the compounds, it is possible to explain the influence of individual compounds to the trend and categorize the OCPs into three broad groups. Group 1 contains those compounds which are more soluble relative to the other compounds in the cocktail, have relatively low logKow values and low K_H values. The behaviour of these compounds was similar in the controls and in the treated sets. Accordingly, the loading values for these compounds were zero or close to zero in both experimental phases. The HCH isomers are the main compounds in this group. Dieldrin and methoxychlor do not have the relatively high solubilities of the HCHs (Table 2). However, based on the loadings and their properties, they had little influence on the observed trend and can therefore be placed in the first group.

The second group of compounds is the major contributor to the observed trend. These have low solubility and high Kow values. Therefore these compounds volatilized considerably, with volatility increasing with increasing K_H values. The high Kow values caused partitioning of the compounds to the microbial phase hence reducing their dissipation in the treated sets relative to the controls. Most of the compounds fall into this category (Fig. 94, 96, 98 and 99)

with the main contributors being heptachlor and aldrin. Others in the group are the DDTs, the chlordanes, mirex, HCB, the endosulfans and the heptachlor epoxides.

The third group is interesting because it consists of compounds with high Kow and high K_H values. However their loadings are around or below zero (Fig. 94, 96, 98 and 99). These compounds are PCA, PCB and OCS. This means that these compounds acted against the observed trend. Given their high K_H values one would expect greater losses in the controls, as was the case with the compounds discussed in group 2 above. This indicates that the microbes did act on these compounds to the extent that the concentrations in the treated samples were as low as those in the controls, in spite of the higher volatilization in the latter. Therefore these are the compounds that were most probably responsible for the microbial growth noted at the beginning of the experiments in both phases (Fig. 101), besides the nutrients introduced by the repetition of inoculation. *Bordetella Petrii* has also been shown to possess a large number of genes coding for enzymes of chloroaromatic metabolism and also complete pathways for the degradation of these compounds (Gross et al., 2008).

The compounds in group 3 have one property in common: they all contain a single aromatic ring. This explains the observed results, because the community used mineralizes 1,2,4-TCB, a lower-chlorinated mono-aromatic compound. Furthermore, this community was isolated from a site polluted with chlorobenzenes (Schroll et al., 2004). From all these facts it was expected that the community is adapted to degrading chlorobenzenes and that it could also degrade higher chlorinated mono-aromatic compounds as used in the cocktail. This is also supported by the fact that related microbes have the ability to degrade aromatic compounds (Bianchi et al., 2005; Ericksson et al., 2003; Gross et al., 2008) and that other microbes have been shown to degrade some chlorobenzenes at low concentrations (Van der Meer et al., 1987; Rapp and Timmis, 1999).

4.6 General discussion

Contaminant degradation processes, whether aerobic or anaerobic, have to be understood in the light of two critical factors, namely: availability of energy for the process and availability of electron acceptors. Under aerobic conditions, O_2 is the most thermodynamically favourable electron acceptor. Aerobic respiration is highly efficient as it yields high amounts of ATP. Oxidizable organic matter is broken down in this process by donating electrons to O_2. Some contaminants can also be broken down by acting as electron donors so long as the process is thermodynamically feasible. However, some contaminants cannot be broken down because the energy requirements make the reactions thermodynamically unfavourable. This is the

basis of inducing anaerobic conditions. Whereas anaerobic processes yield less energy than aerobic processes, the absence of O_2 means that other compounds can act as electron acceptors. Depending on which electron donors and acceptors are at play, the anaerobic processes can be efficient or inefficient.

DDT could be mineralized aerobically because the breakdown of the mono-chlorinated aromatic rings is a thermodynamically feasible process. However, the three aliphatic chlorines make DDT a persistent compound because aerobic dechlorination is thermodynamically unfavourable (Racke, 1997). Therefore anaerobic conditions were required to enhance dechlorination.

The production of NH_4^+ in the field soil can be used as an indicator of energy inefficient anaerobic processes (Tiedje, 1988). This is not surprising given that the field soil is usually under aerobic conditions. This inefficiency would result in a higher energy demand for anaerobic processes such as dehalogenation. This would mean greater depletion of available carbon sources to provide the required ATP. Therefore carbon sources such as humic substances would be used as food sources for microbes – hence acting as electron acceptors (Field 2004). The build-up in the field soil of F4, a product of microbial metabolism of organic matter, is an indicator of this organic matter oxidation (Fellman et al., 2008). The fact that the organic matter quality was initially similar in the two soils (Fig. 9) means that the higher production of F4 in the field soil was as a result of this demand for higher energy, rather than availability of easily degradable organic matter. The significant correlation between the formation of F4 and NH_4^+ in the field soil supports this view (Tables 26 and 27). This greater degradation of organic matter to yield more energy would inadvertently lead to greater direct degradation of DDT, given that POPs are usually degraded co-metabolically (Aislabie, 1997). This means that DDT would end up undergoing direct mineralization (Field, 2004) as evidenced by the strong significant correlations between p,p-DDT and CO_2 in the field soil (Fig. 88). The direct breakdown of DDT via ring-cleavage is feasible given that it is a low-chlorinated compound, and therefore the aromatic rings are accessible to microbes. Humic substances can mediate this process (Fig. 3). While the humic substances act as electron acceptors, DDT can act as an electron donor and be oxidized, ending up in the formation of an aliphatic chain and CO_2 (Field 2004). DDT therefore undergoes oxidative dechlorination (Bradley, 1998).

On the other hand, reductive dechlorination results in removal of a chlorine atom without affecting the aromatic ring (Zhao et al., 2003). With DDT, it begins with the removal of an aliphatic chloride to form p,p-DDD. This happens because the chlorine atom on DDT acts as a

terminal electron acceptor resulting in the formation of a chloride ion and the metabolite. Subsequent dechlorination results in the formation of lower-chlorinated metabolites. Therefore, whereas oxidative dechlorination results in the mineralization of DDT, reductive dechlorination results in the formation of diphenyl metabolites.

Reductive dechlorination is thermodynamically more favourable than oxidative dechlorination under anaerobic conditions (Holliger et al., 1999). The paddy soil had more efficient anaerobic processes as indicated by the higher N_2O and negligible NH_4^+ (Fig. 89) production (Tiedje, 1988). This higher efficiency is attributed to the fact that the paddy soil is usually waterlogged and has therefore better anaerobic mechanisms relative to the field soil. This energy efficiency could explain why reductive dechlorination was more predominant in the paddy soil resulting in higher formation of DDT metabolites (Figures 63, 64 and 66).

The low formation of F4 and stability of all the fluorophores in the paddy soil (Fig. 82) precludes the oxidation of humic substances. A role of DOM in the soil processes can, however, be inferred by the fact that other redox players such as $NO_3^-$and SO_4^{2-} were rapidly depleted in the first three days (Fig. 72). Reducible Fe and humic substances are the only redox players that were present in substantial amounts throughout the experimental period (Figures 72, 78 and 82). Humic substances and Fe have been shown to mediate reductive dechlorination (Field, 2004). Humic substances act as electron donors to DDT, while Fe (II) donates electrons to the humic substances (Fig. 4) or DDT. Thus the two are involved in electron shuttle reactions which ensure continuous dechlorination, while their concentrations remain fairly constant. In this sense, humic substances played a reductive role in the degradation of DDT (Perlinger et al., 1996).

The fact that DDT metabolites were formed in the field soil (Fig. 64) means that reductive dechlorination also took place. The presence of stable fluorophores and Fe in the field soil (Figures 78 and 82) indicate a reductive role for humic substances in the degradation of DDT. This is evidenced by the significant correlations of p,p-DDD with F1, F2, F3, F4 and DOC in the field soil (Table 26 and Fig. 83).

Therefore, reductive dechlorination of DDT took place in the paddy soil while both reductive and oxidative dechlorination took place in the field soil. The higher reductive dechlorination of DDT in the paddy soil resulted in the higher formation of metabolites compared to the field soil (Figures 63, 64 and 66). However, because DDT degradation in the field soil was through both reduction and oxidation, there was an overall greater dissipation of DDT in the field soil relative to the paddy soil (Fig. 65 and Table 22).

HCB is highly chlorinated hence making its aerobic degradation thermodynamically unfavourable. This accounts for the negligible mineralization and degradation of HCB in the two soils under aerobic conditions (Fig. 14 and Table 8). Therefore anaerobic conditions were required to induce dechlorination. Only reductive dechlorination, and not oxidative dechlorination, of HCB could take place because of the sterric hindrance of the aromatic ring by the chlorine atoms. Therefore greater HCB degradation resulted in greater metabolite formation. Not surprisingly, the paddy soil - which was better at reductive dechlorination – had higher dissipation of HCB and higher metabolite formation, compared to the field soil (Figures 36, 37, 38 and 39).

Compost mainly contained FI, F2 and F3 (Table 9). Therefore compost amendment led to an increase of these factors in both soils (Fig. 82 and Table 32. The significant inverse correlations of p,p-DDD with these factors (Table 26), shows that they were necessary in the dechlorination process. However, the decrease in these factors was highest in the first two weeks after which the concentrations remained fairly constant (Fig. 82). This indicates that these factors were not limiting in the soils, and so the addition of compost did not significantly enhance the degradation and dechlorination processes, as evidenced by similar amounts of p,p-DDT and p,p-DDD in the amended and un-amended field samples (Figures 63 and 64).

However, addition of compost led to increased microbial activity as evidenced by the increased production of CO_2 in the compost-amended field soil (Fig. 85). CO_2 production is an indicator of oxidative dechlorination with humic substances as food sources for microbes (Fig. 3 and Bradley et al., 1998). Given that p,p-DDT is mineralized along with the humic substances, which are always in high amounts compared to the contaminant, the amount of pesticide broken down is low. So there can be a significant difference in CO_2 production without a corresponding significant difference in pesticide degradation. This was shown to be the case in the degradation of ^{14}C-DDT using anaerobic-aerobic cycles, where there were significant differences in $^{14}CO_2$ production but no significant differences in DDT dissipation in both soils (Fig. 57 and Table 20).

In the case of HCB, only reductive dechlorination could take place. Therefore microbial activity as a result of compost amendment could only increase the extent of reductive dechlorination. This is indeed what happened, as evidenced by the higher formation of metabolites in the compost-amended paddy and field soils (Figures 37, 38, 41 and 43). This increased dechlorination therefore resulted in lower amounts of HCB in the compost-amended paddy and field soils (Fig. 36 and Table 17). Increased anaerobic degradation of HCB, as a

result of compost amendment, led to increased $^{14}CO_2$ production in the subsequent aerobic phase (Figures 25, 26, 27 and Table 13). Aerobic degradation of lower chlorinated HCB metabolites can take place because the process is thermodynamically feasible (Meijer et al., 2001). Aerobic mineralization can take place because removal of the chlorine atoms exposes the aromatic ring to microbes. The 1,2,4-TCB degrading community used in this study is an exemplification of this fact (Wang, 2007). The community could thus be utilized for enhancing the degradation of HCB metabolites in remediation processes, if volatilization of the lower-chlorinated benzenes could be controlled. Furthermore, given the indications of the community's ability to degrade mono-aromatic chlorinated compounds (Figures 94, 96, 98 and 99), further research would reveal its remediation potential for contaminated sites.

5.0: Conclusion and recommendations

5.1 Conclusion

The results showed that there was hardly any mineralization or degradation of HCB under aerobic conditions in the two tropical clay soils. The anaerobic-aerobic cycles were successful in inducing and enhancing the degradation and mineralization of HCB in both soils. There was higher mineralization and degradation of HCB in the paddy soil relative to the field soil. However, the increased HCB degradation resulted in increased volatilization due to formation of lower-chlorinated metabolites. Organic matter was shown to reduce the volatilization of HCB but not of its metabolites.

There was higher DDT mineralization and degradation, relative to HCB, in both soils under aerobic conditions. The anaerobic-aerobic cycles were successful in enhancing the degradation and mineralization of DDT in both soils. There was greater formation of DDT metabolites in the paddy soil, but higher DDT dissipation and mineralization in the field soil. Reductive dechlorination was the main DDT anaerobic degradation process in the paddy soil, while both oxidative and reductive dechlorination of DDT took place in the field soil. Sodicity was higher in the paddy soil and resulted in higher metabolite formation, possibly because clay dispersion caused increased bioavailability. Fe affected processes in both soils including DDT degradation and methane formation. Salinity limited the anaerobic degradation of DDT in both soils, and was higher in the paddy soil. The results showed that the quality of organic matter is critical in determining the efficacy of amendments in remediation. Five fluorophores were identified in the soils and compost, and the build up of fluorophore 4 was associated with greater microbial degradation of organic matter.

Compost amendment resulted in increased clay dispersion in the field soil, but decreased clay dispersion in the paddy soil. Compost resulted in increased mineralization of HCB and DDT in both soils, but had no effect on the degradation rate. Compost also affected the quantities and dynamics of other soil properties during the degradation of DDT under anaerobic conditions including Fe, salinity, carbon and nitrogen transformation.

The results showed that steering ecological conditions is a feasible approach for enhancing degradation and mineralization of DDT and HCB in the two tropical clay soils.

The microbial consortium could not degrade most of the compounds in the OCPs cocktail such as the DDTs, Chlordanes and Heptachlors. However, there were indications that the community could be able to degrade mono-aromatic OCPs like PCA, PCB and OCS.

5.2 Recommendations

The experiments can be carried out using different concentrations and qualities of compost to see if this would induce a significant effect in the degradation of DDT. The field soil is a good candidate for bioaugmentation to enhance the degradation of HCB, especially during the second aerobic phase when lower-chlorinated compounds are present. The 1,2,4-degrading community, which showed indications that it could degrade chlorinated monoaromatic compounds, could be used for such bioaugmentation. Further studies of this community with monoaromatic OCPs are needed to verify the findings of this study.

Further studies can be carried out under field conditions – especially with DDT which did not show high volatilization - to see if the results of the model experiments can be replicated in agricultural soils. More anaerobic-aerobic cycles could be used to further accelerate the degradation process. Further studies of these compounds could also be carried out with more soils.

6.0: References

Adrian L. & Gorisch H. (2002). Microbial transformation of chlorinated benzenes under anaerobic conditions. *Re Microbio,* **153**, 131-137.

Adrian L., Manz W., Szewzyk U. & Gorisch, H. (1998). Physiological characterization of a bacterial consortium reductively dechlorinating 1,2,3- and 1,2,4-trichlorobenzene. *Appl Environ Microbio,* **64**, 496-503.

Aigner E.J., Leone A.D. & Falconer R.L. (1998). Concentrations and enantiomeric ratios of organochlorine pesticides in soils from the U.S. Corn Belt. *Environ. Sci Technol,* **32**, 1162–1168.

Aislabie J.M., Richards N.K. & Boul H.L. (1997). Microbial degradation of DDT and its residues - a review. *New Zeal J Agr Res*, **40**, 269-282.

Andersson C.A. & Bro R. (2000). The N-way Toolbox for MATLAB. *Chemometrics and Intelligent Laboratory Systems*, **52,** 1-4.

Arisoy M. (1998). Biodegradation of chlorinated organic compounds by white-rot fungi. *Bull Environ Contam Toxicol*, **60**, 872-876.

ARS - Agricultural Research Service, U.S. Department of Agriculture. Pesticide Properties Database. Accessed in August 2009 at http://www.ars.usda.gov/Services/docs.htm?docid.

ATSDR - Agency for Toxic Substances and Disease Registry. Accessed in August 2009 at http://www.atsdr.cdc.gov/.

Bahram M., Bro R., Stedmon C. & Afkhami A. (2006). Handling of Rayleigh and Raman scatter for PARAFAC modeling of fluorescence data using interpolation. *Journal of Chemometrics,* **20,** 99-105.

Baraldi E.A., Damianovic M., Manfio G.R., Foresti E. & Vazoller R.F. (2008). Performance of a horizontal-flow anaerobic immobilized biomass (HAIB) reactor and dynamics of the microbial community during degradation of pentachlorophenol (PCP). *Anaerobe*, **14**, 268–274.

Barcelona M.J., Holm T.R., Schock M.R. & George G.K. (1989). Spatial and Temporal Gradients in Aquifer Oxidation-Reduction Conditions. *Water Resour Res*, **25**, 991-1003.

Bartholomew G.W. & Pfaender F.K. (1983). Influence of spatial and temporal variations on organic pollutant biodegradation rates in an estuarine environment. *Appl Environ Microbiol,* **45**, 103-109.

Bartlett R.J. & James B.R. (1995). System for categorizing soil redox status by chemical field testing. *Geoderma*, 68, 211-218.

Beall, M.L. (1976). Persistence of aerially applied hexachlorobenzene on grass and soil. *J Environ Qual*, **5**, 367-369.

Beck J. & Hansen K.E. (1974). The degradation of quintozene, pentachlorobenzene, hexachlorobenzene and pentachloroaniline in soil. *Pestic Sci*, **5**, 41-48.

Beunink J. & Rehm H-J. (1988). Synchronous anaerobic and aerobic degradation of DDT by an immobilized mixed culture system. *Appl Microbiol Biotechnol*, **29**, 72-80.

Bhatnagar A. & Bhatnagar M. (2005). Microbial diversity in desert ecosystems. *Curr Sci*, **89**, 1.

Bianchi F., Careri M., Mustat L., Malcevschi A. & Musci M. (2005). Bioremediation of toluene and naphthalene: development and validation of a GC-FID method for their monitoring. *Ann Chim-Rome,* **95**, 515-524.

Bignert A., Olson M., Persson W., Jensen S., Zakrison S., Litzen K., Häggberg L. & Alsberg T. (1998). Temporal trends of organochlorines in northern Europe, 1967-1995. Relation to global fractionation, leakage from sediments and international measures. *Environ Pollut,* **99**, 177-198.

Boul H.L. (1995). DDT residues in the environment—a review with a New Zealand perspective. *New Zealand J Agric Res,* **38**,257–277.

Boul M.L., Garnham M.L., Hucker D., Baird D. & Aislabie J. (1994). Influence of agricultural practices on the levels of DDT and its residues in soil. *Environ Sci Technol*, **28**, 1397-1402.

Bradley P.M., Chapelle F.H. & Lovley D.R. (1998). Humic acids as electron acceptors for anaerobic microbial oxidation of vinyl chloride and dichloroethene. *Appl Environ Microbio,* **64**, 3102-3105

Brahushi F., Dorfler U., Schroll R., Feicht E. & Munch J.C. (2002). Environmental behaviour of monochlorobenzene in an arable soil. *Fresenius Environ Bull*, **11**, 599-604.

Brahushi F., Dorfler U., Schroll R., Munch J.C. (2004). Stimulation of reductive dechlorination of hexachlorobenzene in soil by inducing the native microbial activity. *Chemosphere*, **55**, 1477-1484.

Beurskens J.E.M., Dekker C.G.C., Vandenheuvel H., Swart M. & Dewolf J. (1994). Dechlorination of chlorinated benzenes by an anaerobic microbial consortium that selectively mediates the thermodynamic most favourable reactions. *Environ Sci Technol*, **28**, 701-706.

Bro R. (1998). Multi-way analysis in the food industry - models, algorithms, and applications. *Doctoral dissertation*, University of Amsterdam, Amsterdam.

Bro R. & Kiers H.A.L. (2003). A new efficient method for determining the number of components in PARAFAC models. *Journal of Chemometrics*, **17,** 274-286.

Cao B., Nagarajan K. & Loh K-C (2009). Biodegradation of aromatic compounds: current status and opportunities for biomolecular approaches. *Appl Microbiol Biot,* **85**, 207–228.

Carroll J. & Chang J.J. (1970). Analysis of individual differences in multidimensional scaling via an n-way generalization of "Eckart-Young" decomposition. *Psychometrika*, **35,** 283-319.

Chang B.V., Su C.J. & Yuan S.Y. (1998). Microbial hexachlorobenzene dechlorination under three reducing conditions. *Chemosphere*, **36**, 2721-2730.

Chen I.M., Chang B.V., Yuan S.Y. & Wang Y.S. (2002). Reductive dechlorination of hexachlorobenzene under various additions. *Water Air Soil Pollut*, **139**, 61-74.

Chisholm A. and Dumsday R. (Eds.) (1987). Land degradation: problems and policies. Cambridge University Press

Christensen T.H., Kjeldsen P., Albrechsten H.J., Heron G., Nielsen P.H., Bjerg P.L. & Holm P.E. (1994): Attenuation of pollutants in landfill leachate polluted aquifers. *Crit Rev Environ Sci Technol*, **24**, 119-202.

Christensen P.B., Rysgaard S., Sloth N.P., Dalsgaard T. & Schwaerter S. (2000). Sediment mineralization, nutrient fluxes, denitrification and dissimilatory nitrate reduction to ammonium in an estuarine fjord with sea cage trout farms. *Aquat Microb Ecol,* **21,** 73–84.

Coble P.G., Green S.A., Blough N.V. & Gagosian R.B. (1990). Characterization of dissolved organic matter in the Black Sea by fluorescence spectroscopy. *Nature*, **348,** 432-435.

Conrad R. (1999). Contribution of hydrogen to methane production and control of hydrogen concentrations in methanogenic soils and sediments. *FEMS Microbiol Ecol*, **28**, 193–202.

Corona-Cruz A., Gold-Bouchot G., Gutierrez-Rojas M., Monroy-Hermosillo O., Favela E. (1999). Anaerobic-aerobic biodegradation of DDT (Dichlorodiphenyl Trichloroethane) in soils. *Bull Environ Contam Toxicol*, **63**, 219-225.

Cory R.M. & McKnight D.M. (2005). Fluorescence spectroscopy reveals ubiquitous presence of oxidized and reduced quinones in dissolved organic matter. *Environ Sci Technol,* **39**, 8142–8149.

Cuppen J.G.M., Van den Brink P.J., Camps E., Uil K.F. & Brock T.C.M. (2000). Impact of the fungicide carbendazim in freshwater microcosms. I. Water quality, breakdown of particulate organic matter and responses of macroinvertebrates. *Aquat Toxicol*, **48**, 233–250.

Curtis G.P. & Reinhard M. (1994). Reductive dehalogenation of hexachloroethane, carbon-tetrachloride, and bromoform by anthrahydroquinone disulfonate and humic-acid. *Environ Sci Technol,* **28**, 2393-2401.

Demidenko E. (2004). Mixed models: theory and applications. *John Wiley & Sons Inc*. Hoboken, New jersey USA. 704 pp.

Dermietzel J. & Vieth A. (2002). Chloroaromatics in groundwater: chances of bioremediation. *Environ Geol*, **41**, 683-689.

Diabaté L., Blanc Ph., Wald L., Solar radiation climate in Africa (2004). Solar radiation climate in Africa. *Solar Energy*, **76**, 733-744.

Dimond J.B. & Owen R.B. (1996). Long-term residue of DDT compounds in forest soils in Maine. *Environ Pollut*, **92**, 227-230.

Diaz E. (2004). Bacterial degradation of aromatic pollutants: a paradigm of metabolic versatility. *Int Microbiol*, **7**, 173–180.

DiGioia D., Sciubba L., Bertin L., Barberio C., Salvadori L., Frassinetti S. & Fava F. (2009). Nonylphenol polyethoxylate degradation in aqueous waste by the use of batch and continuous biofilm bioreactors. *Water Res,* **43**, 2977–2988.

Edgehill R.U. & Finn R.K. (1983). Microbial treatment of soil to remove pentachlorophenol. *Appl Environ Microb,* **45**, 1122-1125.

Edwards C.A. (1996). Insecticide residues in soils. *Residue Rev*, **13**, 82-132.

EPA – United States Environmental Protection Agency, office of solid waste and emergency response (1997). Use of monitored natural attenuation at superfund, RCRA corrective action, and underground storage tank sites. *Draft interim final OSWER directive 9200*. 4-17, 25 pp.

Eriksson M., Sodersten E., Yu Z.T., Dalhammar G. & Mohn W.W. (2003). Degradation of polycyclic aromatic hydrocarbons at low temperature under aerobic and nitrate-reducing conditions in enrichment cultures from northern soils. *Appl Environ Microb*, **69**, 275–284.

Fellman J.B., D'Amore D.V., Hood E. and Boone R.D. (2008). Fluorescence characteristics and biodegradability of dissolved organic matter in forest and wetland soils from coastal temperate watersheds in southeast Alaska. *Biogeochemistry*. DOI 10.1007/s10533-008-9203-x.

Field J. (2004). The role of humic substances in the anaerobic degradation of chlorinated solvents. Euro Chlor workshop on soil chlorine chemistry: workshop proceedings. Can be accessed at www.eurochlor.org

Fathepure B.Z., Tiedje J.M. & Boyd S.A. (1988). Reductive dechlorination of hexachlorobenzene to trichlorobenzenes and dichlorobenzenes in anaerobic sewage sludge. *Appl Environ Microbiol*, **54**, 327-330.

Fathepure B.Z. & Vogel T.M. (1991). Complete Degradation of polychlorinated hydrocarbons by a 2- stage biofilm reactor. *Appl Environ Microbiol*, **57**, 3418-3422.

Foght J., April T., Biggar K. & Aislabie J. (2001). Bioremediation of DDT: a review. *Bioremediation Journal,* **5**: 3, 225 – 246.

Forch, C, Knudsen, M. & Serensen, S. P. L. (1902). Berichte über die Konstantenbestimmungen zur Aufstellung der hydrographischen Tabellen. K. danske Vidensk. Selsk. Skr., Raekke 6, *Nat Og Math*., **12**: 1, 151 pp.

Frenzel, P., Bosse, U., Janssen, P.H. (1999). Rice roots and methanogenesis in a paddy soil: ferric iron as an alternative electron acceptor in the rooted soil. *Soil Biol Biochem*, **31**, 421–430.

Gianfreda L. & Rao M.A. (2008). Interactions between xenobiotics and microbial and enzymatic soil activity. *Crit Rev in Environ Sci Technol*, **38**, 269-310.

Gribble G.W. (2003). The diversity of naturally occurring organohalogen compounds. *Chemosphere*, **52**, 289-297.

Gribble G.W. (2004). Amazing organohalogens. *Am Sci*, **92**, 342-349.

Griffin R.A. & Chou S.F.J. (1981). Movement of PCBs and other persistent organic compounds through soil. *Water Sci Technol*, **13**, 1153-1163.

Gross R., Carlos A.G., Mohammed S., Vítor A.P., Martins D.S., Dietmar H.P., Ralf K., Melanie L., Daniela B., Jens B., Jomuna V.C., Thomas E., Lars G., Stefanie H., Amit N.K., Christof L., Stefanie L., Burkhard L., Folker M., Sascha M., Diana N., Christian R., Susanne S.B., Kai S., Frank-Jörg V., Tetyana Y., Jacquelyn T.E., William E.G., Alfred P., Ulf B.G., Alexander G., Helmut B., Olaf K. & Rosa M.A. (2008). The missing link: *Bordetella petrii* is endowed with both the metabolic versatility of environmental bacteria and virulence traits of pathogenic Bordetellae. *BMC Genomics,* **9**, 20.

Harshman R.A. (1970). Foundations of the PARAFAC procedure: model and conditions for an 'explanatory' multi-mode factor analysis. *UCLA Working Papersin phonetics*, **16**.

Hay A.G. & Focht D.D. (1998). Co-metabolism of 1,1-Dichloro-2,2-Bis(4-Chlorophenyl)Ethylene by *Pseudomonas acidovorans* M3GY Grown on Biphenyl. *Applied Environ Microbio*, **64**:6, 2141 – 2146.

Heberer T. & Dunnbier U. (1999). DDT metabolite bis(chlorophenyl) acetic acid: the neglected environmental contaminant. *Environ Sci Technol*, **33**, 2346–2361.

Heitmann T., Goldhammer T., Beer J. & Blodau C. (2007). Electron transfer of dissolved organic matter and its potential significance for anaerobic respiration in a northern bog, *Global Change Biology,* **13**, 1771–1785.

Heitmann T. & Blodau C**.** (2006). Oxidation and incorporation of hydrogen sulfide by dissolved organic matter, *Chemical Geology*, **235**, 12-20.

Hense B.A., Welzl G., Severin G.F. & Schramm K-W. (2005). Nonylphenol induced changes in trophic web structure of plankton analysed by multivariate statistical approaches. *Aquat Toxicol*, **73**, 190–209.

Hense B.A., Jaser W., Welzl G., Pfister G., Woehler-Moorhoff G.F. & Schramm K-W. (2008). Impact of 17α-ethinylestradiol on the plankton in freshwater microcosms—II: Response of zooplankton and abiotic variables. *Ecotox Environ Safe,* **69**, 453–465.

Heron G. & Christensen T.H. (1995). Impact of sediment-bound iron on the redox buffering in a landfill leachate polluted aquifer (Vejen, Denmark). *Environ Sci Technol*, **29**, 187-192.

Hiriat-Baer V.P., Diep N. and Smith R.E.H. (2008). Dissolved organic matter in the Great Lakes: Role of allochthonous material. *J. Great Lakes Res* 34: 383 – 394.

Hitch R.K. & Day H.R. (1992). Unusual persistence of DDT in some western USA soils. *Bull Environ Contam Toxicol*, **48**, 259-264.

Holliger C., Schraa G., Stams A.J.M. and Zehnder A.J.B. (1992). Enrichment and properties of an anaerobic mixed culture reductively dechlorinating 1,2,3-trichlorobenzene to 1,3-dichlorobenzene. *Appl Environ Microbiol*, **58**, 1636-1644.

Holliger C., Wohlfarth G. & Diekert G. (1999). Reductive dechlorination in the energy metabolism of anaerobic bacteria. *FEMS Microbiology Reviews*, **22**, 383-398.

Hostettler J.D. (1984). Electrode electrons, aqueous electrons and redox potentials in natural waters. *Am J Sci*, **284**, 734-759.

Howard P.H. (1991). Hexachlorobenzene. In: Handbook of environmental fate and exposure for organic chemicals. Vol. I. Large production and priority pollutants. *Lewis Publishers Inc.*, Chelsea, Michigan, pp. 351-359.

HSDB - Hazardous Substances Data Bank, National Library of Medicine. Accessed in August 2009 at http://toxnet.nlm.nih.gov/cgi-bin/sis/htmlgen?HSDB.

Huang B., Yu K. & Gambrell R.P. (2009). Effects of ferric iron reduction and regeneration on nitrous oxide and methane emissions in a rice soil. *Chemosphere*, **74**, 481–486.

Iwamoto T. & Nasu M. (2001). Current bioremediation practice and perspective. *J Biosci Bioeng,* **92**, 1-8.

Isensee A.R., Holden E.R., Woolson E.A. & Jones G.E. (1976) Soil persistence and aquatic bioaccumulation potential of hexachlorobenzene (HCB). *J Agr Food Chem*, **24**, 1210-1214.

Jaeckel U., Russo S. & Schnell S. (2005). Enhanced Fe reduction by Fe supplement: a strategy to reduce methane emission from paddies. *Soil Biol Biochem*, **37**, 2150–2154.

Jetten M.S.M. (2008). The microbial nitrogen cycle. *Environ Microbio*, **10**: 11, 2903-2909.

Johnsen A.R., Wick L.Y. & Hams H. (2005). Principles of microbial PAH degradation in soil. *Environ Pollut*, **133**, 71-84.

Juang R.S. & Kao H.C. (2009). Estimation of the contribution of immobilized biofilm and suspended biomass to the biodegradation of phenol in membrane contactors. *Biochem Eng J*, **43**, 122–128.

Juang R.S. & Wu C.Y. (2007). Microbial degradation of phenol in high salinity solutions in suspensions and hollow fiber membrane contactors. *Chemosphere*, **66**, 191–198.

Junko A. and Zsolany A. (2008). Effects of long-term de-vegetation on the quantity and quality of water extractable organic matter (WEOM): Biogeochemical implications. *Chemosphere*, **72**, 1462-1466.

Kale S.P., Murthy N.B.K., Raghu K., Sherkhane P.D. & Carvalho F.P. (1999). Studies on degradation of ^{14}C-DDT in the marine environment. *Chemosphere*, **39**, 959–968.

Kantachote D., Naidu R., Williams B., McClure N., Megaharaj M., Singleton I. (2004). Bioremediation of DDT-contaminated soil: enhancement by seaweed addition. *J Chem Technol Biotechnol*, **79**, 632–638.

Kastner M., Streibich M., Beyrer M., Richnow H.H. & Fritsche W. (1999). Formation of bound residues during microbial degradation of [^{14}C]anthracene. *Appl Environ Microbiol*, **65**, 1834–1842.

Kazman Z., Shainberg I. & Gal M. (1983). Effect of low levels of exchangeable sodium and applied phosphogypsum on the infiltration rate of various soils, *Soil Sci,* **135**, 184–192.

Keller J. K. and Bridgham S.D. (2007). Pathways of anaerobic carbon cycling across an ombrotrophic-minerotrophic peat land gradient. *Limnology and Oceanography*, **52**, 96-107.

Keller J.K., Weisenhorn P.B.J. & Megonigal P. (2009). Humic acids as electron acceptors in wetland decomposition. *Soil Biol Biochem*, **41**, 1518–1522.

Lichtenstein E. P. & Schulz K. R. (1959). Persistence of some chlorinated hydrocarbon insecticides as influenced by soil types, rate of application and temperature. *Journal of Economic Entomology,* **52**, 124-131.

Lindberg R.D. & Runnels D.D. (1984). Groundwater redox reactions: an analysis of equilibrium state applied to Eh measurements and geochemical modeling. *Science*, **225**, 925-927.

Loftfield N., Brumme R. & Beese F. (1992). Automated monitoring of nitrous oxide and carbon dioxide flux from forest soils. *Soil Science Society of America*, **56**, 1147–1150.

Luciani X., Mounier S., Paraquetti H.H.M., Redon R., Lucas Y., Bois A., Lacerda L.D., Raynaud M. & Ripert M. (2008). Tracing of dissolved organic matter from the SEPETIBA Bay (Brazil) by PARAFAC analysis of total luminescence matrices. *Marine Environmental Research*, **65**, 148–157

Mackay D., Shiu W-Y., & Ma K-C. (1997). Illustrated handbook of physical-chemical properties and environmental fate for organic chemicals. *Pesticide Chemicals*, **5**, Lewis Publishers, New York, 812 pp.

Marinucci A.C. & Bartha R. (1979). Biodegradation of 1,2,3-trichlorobenzene and 1,2,4-trichlorobenzene in soil and in liquid enrichment culture. *Appl Environ* Microbiol, **38**, 811-817.

Mazeas L., Vigneron V., Le-Menach K., Budzinski H., Audic J.M., Bernet N. & Bouchez T. (2008). Elucidation of nitrate reduction pathways in anaerobic bioreactors using a stable isotope approach. *Rapid Comm Mass Spec,* **22**, 1746–1750.

McKnight D.M., Boyer E.W., Westerhoff P.K., Doran P.T., Kulbe T. & Andersen D.T. (2001). Spectrofluorometric characterization of dissolved organic matter for indication of precursor organic material and aromaticity. *Limnology and Oceanography*, **46,** 38-48.

McTainsh G. & Boughton W.C. (Eds.) (1993*).* Land degradation processes in Australia. *Longman,* Cheshire.

Middeldorp P.J.M., deWolf J., Zehnder A.J.B., Schraa G. (1997). Enrichment and properties of a 1,2,4-trichlorobenzene dechlorinating methanogenic microbial consortium. *Appl Environ Microbiol*, **63**, 1225-1229.

Meijer S.N., Halsall C.J., Harner T., Peters J., Ockenden W.A., Johnston A.E. & Jones K.C. (2001). Organochlorine pesticide residues in archived UK soil. *Environ Sci Technol*, **35**, 1989-1995.

Menzie C. M. (1980). Metabolism of Pesticides: Update III. USDI-FWS, *Spec. Sci. Rpt.-Wildl*, **232**, Washington, D.C., 214-226.

Miguel A., Providenti H.L., Jack T.T. (1993). Selected factors limiting the microbial degradation of recalcitrant compounds. *J Ind Microbiol,* **12**, 379 – 395.

Moser T., Roembke J., Schallnass H-J., Van Gestel C.A.M (2007). The use of the multivariate principal response curve (PRC) for community level analysis: a case study on the effects of carbendazim on enchytraeids in terrestrial model ecosystems (TME). *Ecotoxicology,* **16**, 573-583.

National Irrigation Board (NIB). Mwea Irrigation Scheme. Accessed in January 2009 at, http://www.nib.or.ke/index.php?option=com_content&task=view&id=34&Itemid=47

Nelson, P. N. & Oades, J. M. (1998). 'Organic matter, sodicity, and soil structure', in M. E. Sumner and R. Naidu (eds), Sodic soils: distribution, properties, management, and environmental consequences, *Oxford*, pp. 51–75.

Neubauer S.C., Givler K., Valentine S.K. & Megonigal J.P. (2005). Seasonal patterns and plant-mediated controls of subsurface wetland biogeochemistry. *Ecology*, **86**, 3334–3344.

Nicolella C., Zolezzi M., Furfaro M., Cattaneo C. & Rovatti M. (2007). High-rate degradation of aromatic sulfonates in a biofilm airlift suspension reactor. *Ind Eng Chem Res,* **46**, 6674–6680.

Nishino S.F., Spain J.C., Belcher L.A., Litchfield C.D. (1992). Chlorobenzene degradation by bacteria isolated from contaminated groundwater. *Appl Environ Microbiol*, **58**, 1719-1726.

Nishino S.F., Spain J.C., & Pettigrew C.A. (1994). Biodegradation of chlorobenzene by indigenous bacteria. *Environ Toxicol Chem*, **13**, 871-877.

Nordin A., Schmidt I.K. & shaver G.R. (2004). Nitrogen uptake by arctic soil microbes and plants in relation to soil nitrogen supply. *Ecology*, **85**: 4, 955-962.

Nyer E.K. and Duffin M.E. (1997). The state of the art of bioremediation. *Groundwater Monitoring and Remediation,* **17,** 2, 64-69.

Oliver B.G. (1985). Desorption of chlorinated hydrocarbons from spiked and anthropogenically contaminated sediments. *Chemosphere*, **14**:8, 1087-1106.

Onjala J. (2001). Water pricing options in Kenya: cases of Mwea and West Kano irrigation schemes. CDR Working Paper 01.9. Centre for Development Research Copenhagen. Accessed in January 2009 at http://www.diis.dk/graphics/CDR_Publications/cdr_publications/working_papers/wp-01-9.pdf

Paasivirta J., Sinkkonen S., Mikkelson P., Rantio T. & Wania F. (1999). Estimation of vapour pressures, solubilities and Henry's law constants of selected persistent Organic Pollutants as functions of temperature. *Chemosphere*, **39**, 5.

Pankhurst C.E., Yu S., Hawke B.G. & Harch B.D. (2001). Capacity of fatty acid profiles and substrate utilization patterns to describe differences in soil microbial communities associated with increased salinity or alkalinity at three locations in South Australia. *Biol Fertil Soils,* **33,** 204-217.

Perlinger J.A., Angst W. & Schwarzenbach R.P. (1996). Kinetics of the reduction of hexachloroethane by juglone in solutions containing hydrogen. *Environ Sci Techno,* **30**, 3408-3417.

PPDB - Pesticide properties database. Accessed in July 2009 at

http://sitem.herts.ac.uk/aeru/iupac/.

Quensen III J.F., Mueller S.A., Jain M.K. & Tiedje J.M. (1998). Reductive dechlorination of DDE to DDMU in marine sediment microcosms. *Science,* **280**, 722 – 724.

Quensen III J.F., Tiedje J.M., Jain M.K. & Mueller S.A. (2001). Factors controlling the rate of DDE to DDMU in Palos Verdes Margin under anaerobic condition. *Environ Sci Techno*, **35**, 286–291.

Racke K.D., Skidmore M.W., Hamilton D.J., Unsworth J.B., Miyamoto J., and Cohen S.Z. (1997). Pesticide fate in tropical soils (technical report). *Pure Appl Chem*, **69**, 1349–1371.

Ramanand K., Balba M.T. & Duffy J. (1993). Reductive dehalogenation of chlorinated benzenes and toluenes under methanogenic conditions. *Appl Environ Microbiol*, **59**, 3266-3272.

Rapp P. & Timmis K.N. (1999). Degradation of chlorobenzenes at nanomolar concentrations by *Burkholderia* sp. strain PS14 in liquid cultures and in soil. *Appl Environ Microb,* **65**, 2547-2552.

Rengasamy P., Greene R. S. B., Ford G.W. & Mehanni A. H. (1984). Identification of dispersive behaviour and the management of red-brown earths. *Aust J Soil Res,* **22**, 413–431.

Rengasamy P. & Churchman G.J. (1999). Cation exchange capacity, exchangeable cations and sodicity. In Peverill K.I., Sparrow L.A. & Reuter D.J. (eds): Soil analysis: an interpretation manual. *CSIRO Publishing*, Collingwood, 147-157.

Rijnaarts H.H.M., Van Aalst-Van Leeuwen M.A., Van Heiningen E., Van Buyzen H., Sink A., Van Liere H.C., Harkes M., Baartmans R., Bosma T.N.P. & Dod-Dema H.J. (1998). Intrinsic and enhanced bioremediation in aquifers contaminated with chlorinated and aromatic hydrocarbons in the Netherlands. *Contaminated Soil*, **'98**:1, 109-112.

Rosenbrock P., Martens R., Buscot F., Munch J.C. (1997). Initiation of [$^{36}Cl^-$] hexachlorobenzene dechlorination in three different soils under artificially induced anaerobic conditions. *App. Microbiol Biotechnol*, **48**, 115-120.

Schink B. (1997). Energetics of syntropic cooperation in methanogenic degradation. *Microbiol Mol Biol Rev*, **61**, 262–280.

Schramm K-W., Jaser W., Welzl G., Pfister G., Woehler-Moorhoff G.F., Hense B.A. (2008). Impact of 17α-ethinylestradiol on the plankton in freshwater microcosms—I: Response of zooplankton and abiotic variables. *Ecotox Environ Safe,* **69**, 437–452.

Schroll R., Brahushi F., Doerfler U., Kuehn S., Fekete J. & Munch J.C. (2004). Biomineralization of 1,2,4-Trichlorobenzene in soils by an adapted microbial population. *Environ Pollut*, **127**, 395-401.

Schroll R., Becher H.H., Doerfler U., Gayler S., Grundmann S., Hartmann H.P. & Ruoss J. (2006). Quantifying the effect of soil moisture on the aerobic microbial mineralization of selected pesticides in different soils. *Environ Sci Technol*, **40**, 3305–3312.

Segers R. (1998). Methane production and consumption: A review of processes underlying wetland methane fluxes. *Biogeochemistry*, **41**, 23–51.

Shen H., Henkelmann B., Levy W., Zsolnay A., Weiss P., Jakobi G., Kirchner M., Moche W., Braun K. & Schramm K-W. (2009). Altitudinal and chiral signature of persistent organochlorine pesticides in air, soil, and spruce needles (*Picea abies*) of the Alps. *Environ Sci Technol*, **43**, 2450-2455.

Shen L., Wania F., Lei Y.D., Teixeira C., Muir D.C.G., Bidleman T.F. (2005). Atmospheric distribution and long-range transport behaviour of organochlorine pesticides in North America. *Environ Sci Technol,* **39**, 409–420.

Shiu W-Y. & Mackay D. (1997). Henry's law constants of selected aromatic hydrocarbons, alcohols, and ketones. *J Chem Eng Data*, ***42***:1, 27–30.

Sims Gerald K and Cupples Alison M (1999). Factors controlling degradation of pesticides in soil. *Pestic Sci,* **55**, 566-614.

Singh D.K. (2007). Biodegradation and bioremediation of pesticides in soil: concept, method and recent developments. *Indian J Microbiol,* **48**, 35-40.

Spencer W.F., Singh G., Taylor C.D., LeMert R.A., Cliath M.M. & Farmer W.J. (1996). DDT persistence and volatility as affected by management practices after 23 years. *J Environ Qual,* **25**, 815–821.

Stedmon C.A., Markager S. & Bro R. (2003). Tracing dissolved organic matter in aquatic environments using a new approach to fluorescence spectroscopy. *Marine Chemistry*, **82,** 239-254.

Stedmon, C.A., Markager, S. (2005). Resolving the variability in dissolved organic matter fluorescence in a temperate estuary and its catchment using PARAFAC analysis. *Limnol Oceanogr,* **50**: 2, 686–697.

Stephenson J. & Warnes A. (1996). Release of genetically modified micro-organisms into the environment. *J Chem Technol Biot,* **65**, 5–14.

Stewart D.K.R. & Chisholm D. (1971). Long-term persistence of BHC, DDT and Chlordane in a sandy loam soil. *Can J Soil Sci*, **51**, 379–383.

Stockholm convention on persistent organic pollutants. Accessed in August 2009 at http://chm.pops.int/.

Stocking M.A. (2003). Tropical soils and food security: the next 50 years. *Science,* **302**: 5649, 1356 – 1359.

Stookey L.L. (1970). Ferrozine - a new spectrophotometric reagent for iron. *Anal Chem*, **42**, 779-781.

Stroempl C. & Thiele J. H. (1997). Comparative fate of 1,1-Diphenylethylene (DPE), 1,1-Dichloro-2,2-bis(4-chlorophenyl)-ethylene (DDE), and pentachlorophenol (PCP) under alternating aerobic and anaerobic conditions. *Arch Environ Contam Toxicol*, **33**, 350–356.

Strohm T.O., Griffin B., Zumft W.G. & Schink B. (2007). Growth yields in bacterial denitrification and nitrate ammonification. *Appl Environ Microbiol,* **73**, 1420–1424.

Su Y., Hayley H., Pierrette B., Gregory P., Roland K., Alexei K., Phil F., Henrik L., Charles G., Gary S., Bruno R. and Leonard B. (2008). A circumpolar perspective of atmospheric organochlorine pesticides (OCPs): results from six Arctic monitoring stations in 2000-2003. *Atmos Environ*. **42**, 4682-4698.

Sumner M.E., Rengasamy P. & Naidu R. (1998). Sodic soils: a reappraisal. In Sumner M.E. & Naidu R. (eds): Sodic soils - distribution, properties, management and environmental consequences. *Oxford University Press*, New York, 3-17.

Tiedje J.M. (1988). Ecology of denitrification and dissimilatory nitrate reduction to ammonium. In. Zehnder A.J.B (ed), Environmental microbiology of anaerobes. *John Wiley and Sons*, New York, 179-244.

Tomaszek J.A., & Gruca-Rokosz R. (2007). Rates of dissimilatory nitrate reduction to ammonium in two polish reservoirs: impacts of temperature, organic matter content, and nitrate concentration. *Environ Technol,* **28**, 771–778.

Tonnaer H., Otten A., Alphenaar A. & Roovers C. (1998). Natural attenuation: a basis for developing extensive remediation concepts. *Contaminated Soil*, **'98**:1, 191-196.

UNEP – United Nations Environmental Program. Action plans and studies to replace/reduce release of POPs. Accessed in October 2009 at http://www.chem.unep.ch/pops/actplan.html.

UNEP – United Nations Environmental Program (2002). State of the environment and policy retrospective: 1972 – 2002. Accessed in January 2010 at http://www.unep.org/geo/geo3/english/pdfs/chapter2-2_land.pdf

US EPA. Natural attenuation: Toxic compounds hydrology program. Accessed in January 2010 at http://toxics.usgs.gov/definitions/natural_attenuation.html

Van den Brink P.J. & Ter Braak C.J.F. (1998). Multivariate analysis of stress in experimental ecosystems by Principal Response Curves and similarity analysis. *Aquat Ecol*, **32**, 163–178.

Van den Brink P.J. and Ter Braak C.J.F. (1999). Principal response curves: analysis of time-dependent multivariate responses of a biological community to stress. *Environ Toxicol Chem*, **18**, 138-148.

Van der Meer J.R., Roelofsen W., Schraa G., & Zehnder A.J.B. (1987). Degradation of low concentrations of dichlorobenzenes and 1,2,4-trichlorobenzenes by *Pseudomonas* sp. P51 in non sterile soil columns. *FEMS Microbiol Ecol,* **45**, 333-341.

Van der Meer J.R., Werlen C., Nishino S.F. & Spain J.C. (1998). Evolution of a pathway for chlorobenzene metabolism leads to natural attenuation in contaminated groundwater. *Appl Environ Microbiol*, **64**, 4185-4193.

Verma A. & Pillai M. K. K. (1991). Bioavailability of soil bound residues of DDT and HCH to certain plants. *Soil Biol Biochem,* **23**, 347-51.

Vile M. A., Bridgham S.D., Wieder R.K. and Nova´ k M. (2003). Response of anaerobic carbon mineralization rates to sulfate amendments in a boreal peatland. *Ecol Appl*, **13**, 720–734.

Wandiga S.O. (2001). Use and distribution of organochlorine pesticides. The future in Africa. *Pure Appl Chem*, **73**: 7, 1147–1155 © 2001 IUPAC.

Wang F., Grundmann S., Schmid M., Doerfler U., Roehrer S., Munch J.C., Hartmann A., Jiang X. & Schroll R. (2007). Isolation and characterization of 1,2,4-trichlorobenzene mineralizing *Bordetella* sp. and its bioremediation potential in soil. *Chemosphere*, **67**, 896-902.

Wang F., Dörfler U., Schmid M., Fischer D., Kinzel L., Scherb H., Munch J.C., Jiang X. and Schroll R. (2010). Homogeneous inoculation vs. microbial hot spots of isolated strain and microbial community: What is the most promising approach in remediating 1,2,4-TCB contaminated soils? *Soil Biol Biochem*, **42**, 331-336.

Wang J., Bi Y., Pfister G., Henkelmann B., Zhu K. & Schramm K-W. (2009). Determination of PAH, PCB, and OCP in water from the three gorges reservoir accumulated by semi-permeable devices (SPMD). *Chemosphere*, **75**, 1119-1127.

Wang M.J. & Jones, K.C. (1994). Behaviour and fate of chlorobenzenes in spiked and sewage sludge-amended soil. *Environ Sci Technol*, **28**, 1843-1852.

Wang Z.P., Lindau C.W., Delaune R.D. & Patrick W.H. (1993). Methane emission and entrapment in flooded rice soils as affected by soil properties. *Biol Fert Soils*, **16**, 163–168.

Wania F. & Mackay D. (1993). Global fractionation and cold condensation of low volatility organochlorine compounds in polar regions. *Ambio,* 22-27.

Wania F. & Mackay D. (1996). Tracking the distribution of persistent organic pollutants. *Environ Sci Technol*, **30**, 390-396.

Ware G.W., Crosby D.G. & Giles J.W. (1980). Photodecomposition of DDA. *Arch Environ Contamin Toxicol*, **9**, 135–146.

Wawire N.W., Jamoza J.E, Shiundu R., Kipruto K. B. & Chepkwony P. (2006). Identification and ranking of zonal sugarcane production constraints in the Kenya sugar industry. *Kenya Sugar Research Foundation Technical Bulletin no. 1*.

White R. E. (1997). Principles and Practice of Soil Science: The soil as a natural resource, 3rd ed., *Blackwell Science Ltd*., Carlton, 348 pp.

WHO - World Health Organization (2007). The use of DDT in malaria vector control: WHO position statement, Global Malaria Programme.
http://apps.who.int/malaria/ddtandmalariavectorcontrol.html

Wood M. (1995). Environmental Soil Biology, 2nd ed., *Chapman & Hall*, Tokyo, 150 pp.

Wu F.C., Tanoue E. & Liu C.Q. (2003). Fluorescence and amino acid characteristics of molecular size fractions of DOM in the waters of Lake Biwa. *Biogeochemistry,* **65**, 245–257.

Wu Q.Z., Milliken C.E., Meier G.P., Watts J.E.M., Sowers K.R. & May H.D. (2002). Dechlorination of chlorobenzenes by a culture containing bacterium DF-1, a PCB dechlorinating microorganism. *Environ Sci Technol,* **36**, 3290-3294.

Yao H., Conrad R., Wassmann R. & Neue H.U. (1999). Effect of soil characteristics on sequential reduction and methane production in sixteen rice paddy soils from China, the Philippines and Italy. *Biogeochemistry,* **47**, 269–295.

You G., Sayles G.D., Kupferle M.J., Kim I.S. and Bishop P.L. (1996). Anaerobic DDT biotransformation: enhancement by application of subsurfactants and low oxidation reduction potential. *Chemosphere,* **32**:11, 2269-2284.

Yuan S.Y., Su C.J. & Chang B.V. (1999). Microbial dechlorination of hexachlorobenzene in anaerobic sewage sludge. *Chemosphere,* **38**, 1015-1023.

Zehnder A.J.B., Huser B.A., Brock T.D. & Wuhrmann K. (1980). Characterization of an acetate decarboxylating nonhydrogen-oxidizing methane bacterium. *Arch Microbiol,* **124**, 1-11.

Zhao X., Quan X., Zhao H.M., Chen J.W., Chen S. & Zhao Y.Z. (2003). Effects of natural organic matters and hydrated metal oxides on the anaerobic degradation of lindane, p, p -DDT and HCB in sediments. *J Environ Sci China,* **15**, 618-621.

Zook C. & Feng J. (2008). Biocatalysis/Biodegradation database, University of Minnesota. http://umbbd.msi.umn.edu/ddt/ddt_map.html Accessed in October 2009

Zook C. & Feng J.(2009). Biocatalysis/Biodegradation database, University of Minnesota. http://umbbd.msi.umn.edu/ddt2/ddt2_map.html Accessed in October 2009

Zsolnay Á., Baigar E., Jimenez M., Steinweg B. & Saccomandi F. (1999). Differentiating with fluorescence spectroscopy the sources of dissolved organic matter in soils subjected to drying. *Chemosphere,* **38**, 45–50.

Zsolany Á. (2003). Dissolved organic matter: artifacts, definitions, and functions. *Geoderma*, **113**, 187-209.

Appendix

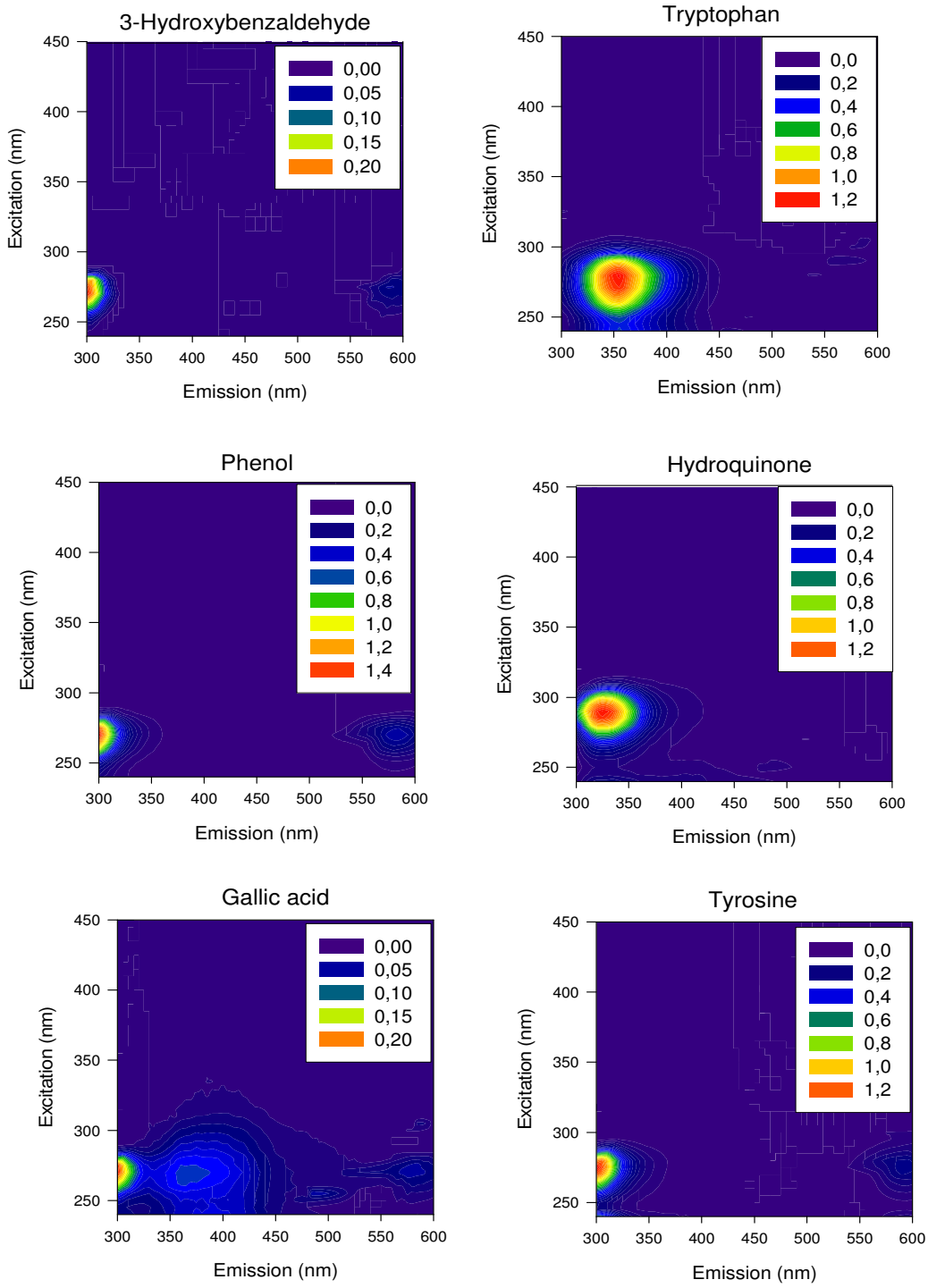

Figure A1: Fluorophore spectra of some standards, characterized using PARAFAC analysis.

Presented with gratitude courtesy of Dr. Roland Fuß, Institute of Soil Ecology, HelmholtzZentrum München – National Center for Environmental Health.

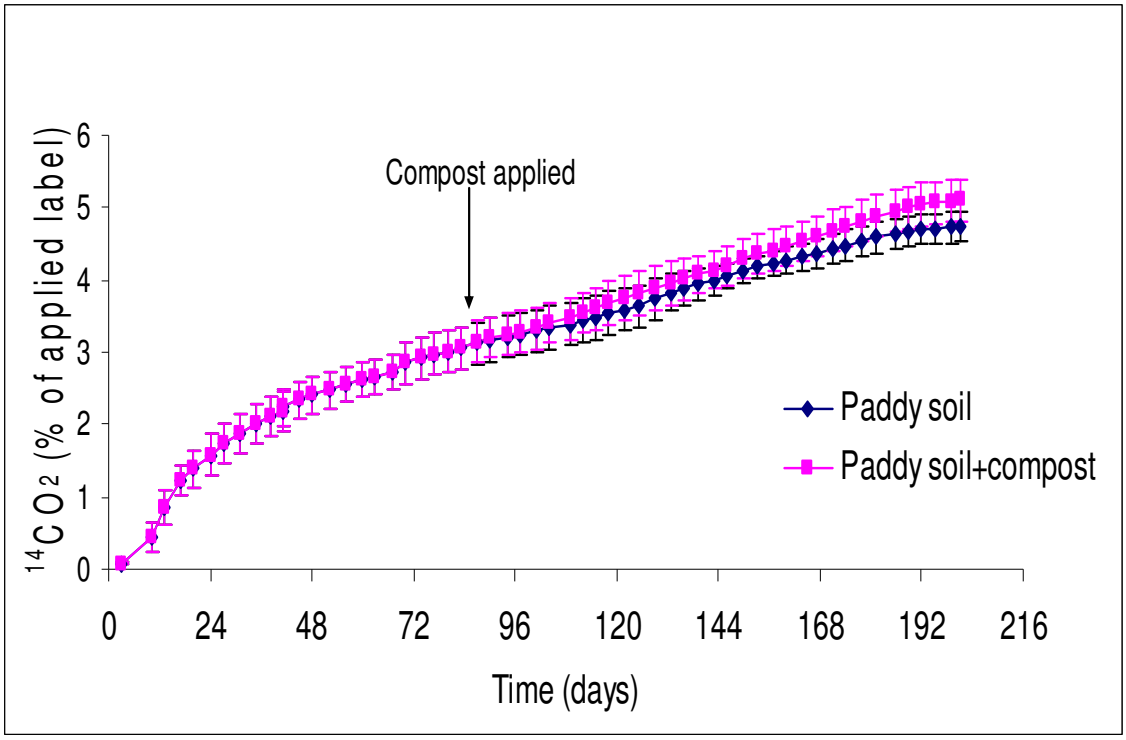

Figure A2: ^{14}C-DDT cumulative mineralization with time in the paddy soil under aerobic conditions

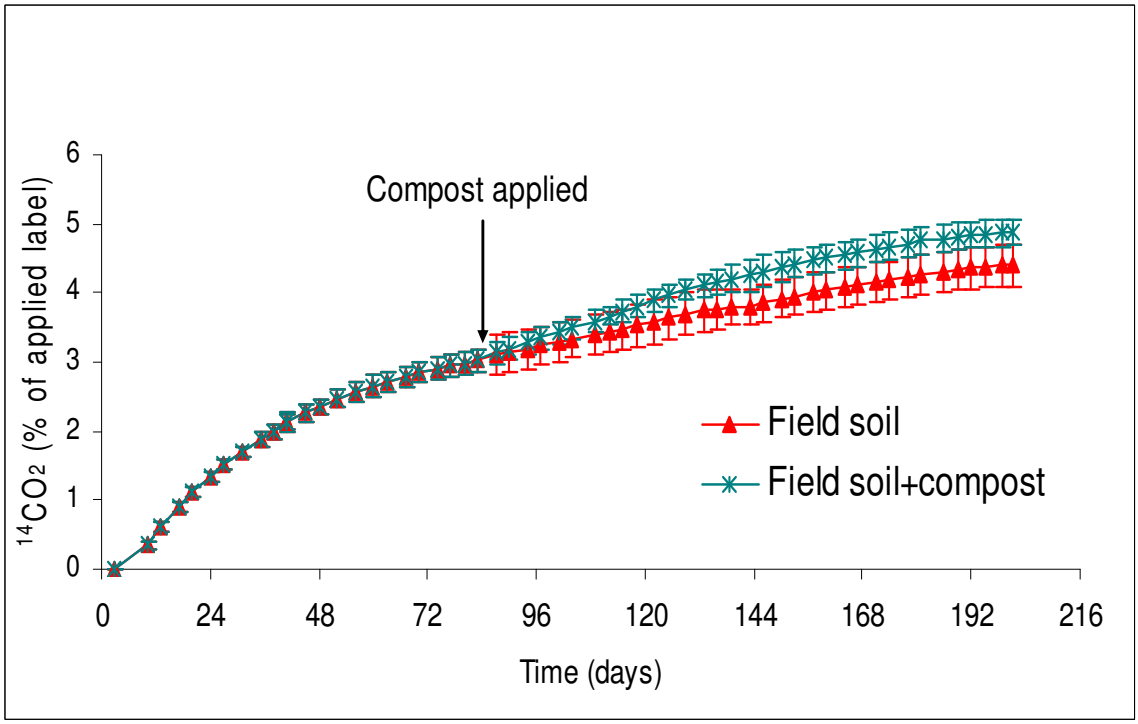

Figure A3: ^{14}C-DDT cumulative mineralization with time in field soil under aerobic conditions

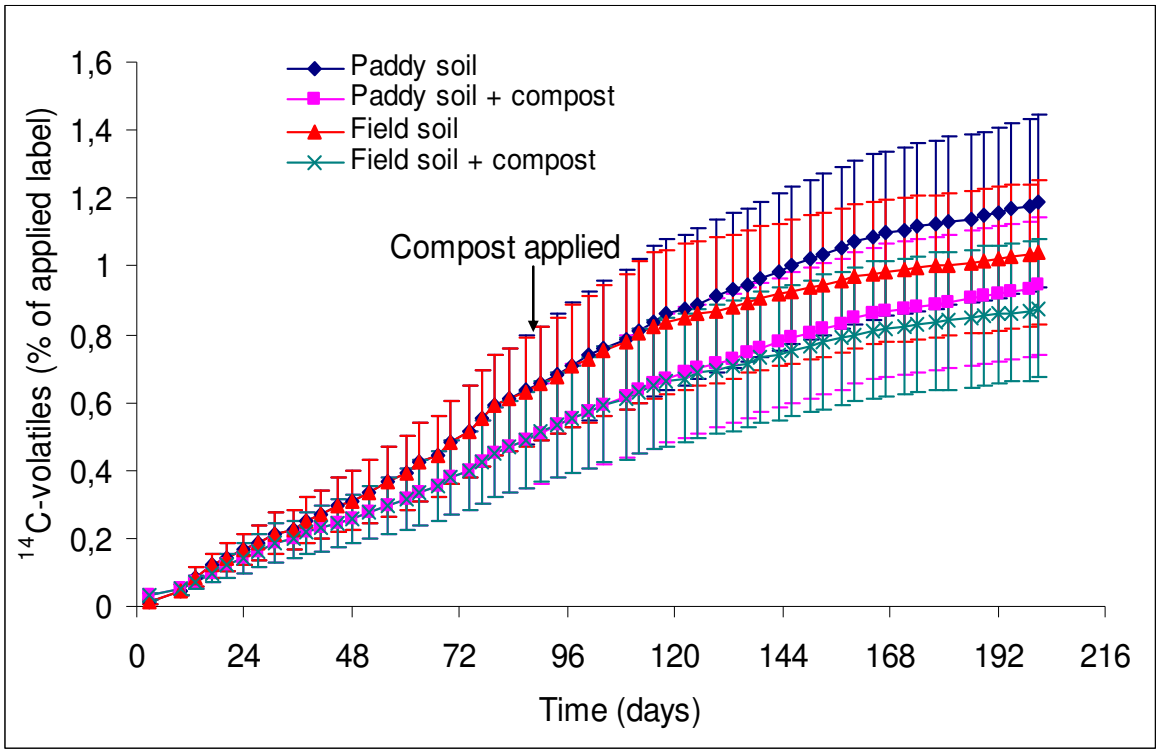

Figure A4: ^{14}C-DDT cumulative volatilization with time in the paddy and field soils during the aerobic degradation of DDT.

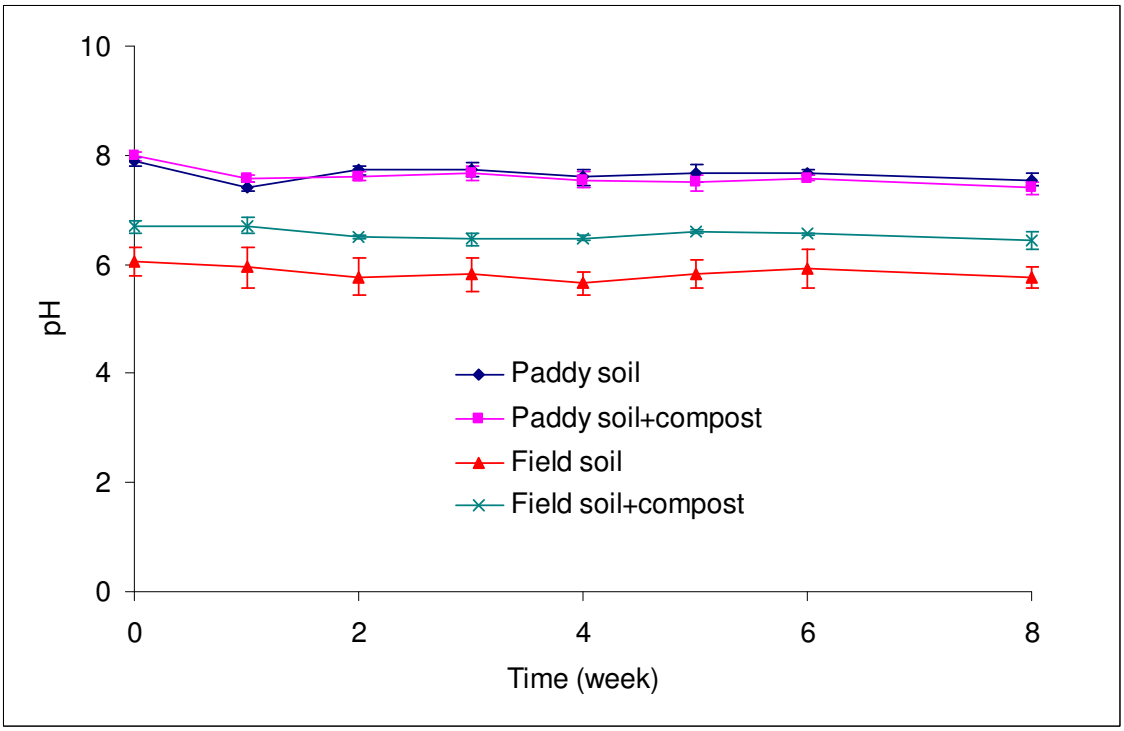

Figure A5: pH values with time during the anaerobic degradation of DDT.

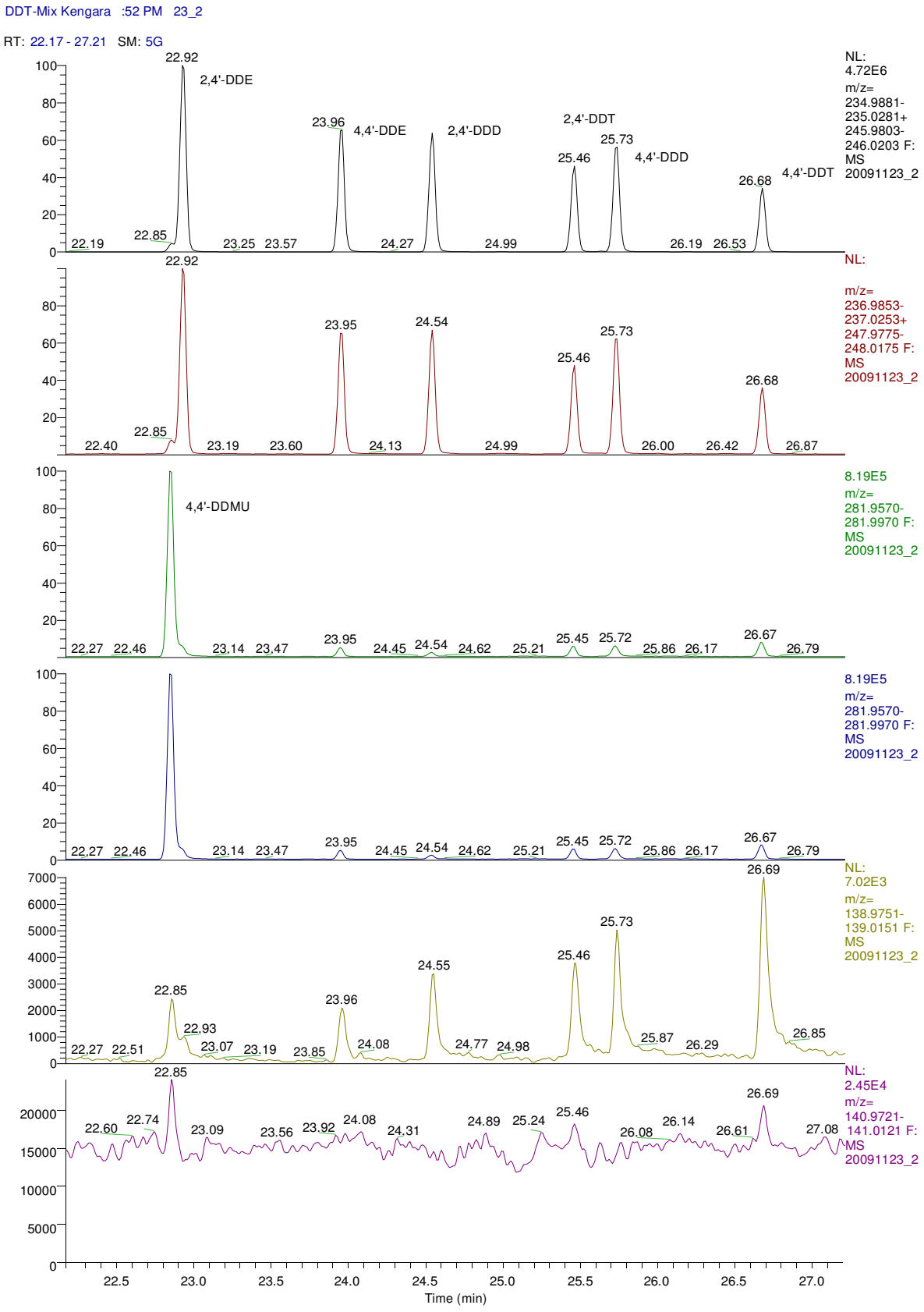

Figure A6: GC-MS full scan of a DDTr standard mixture

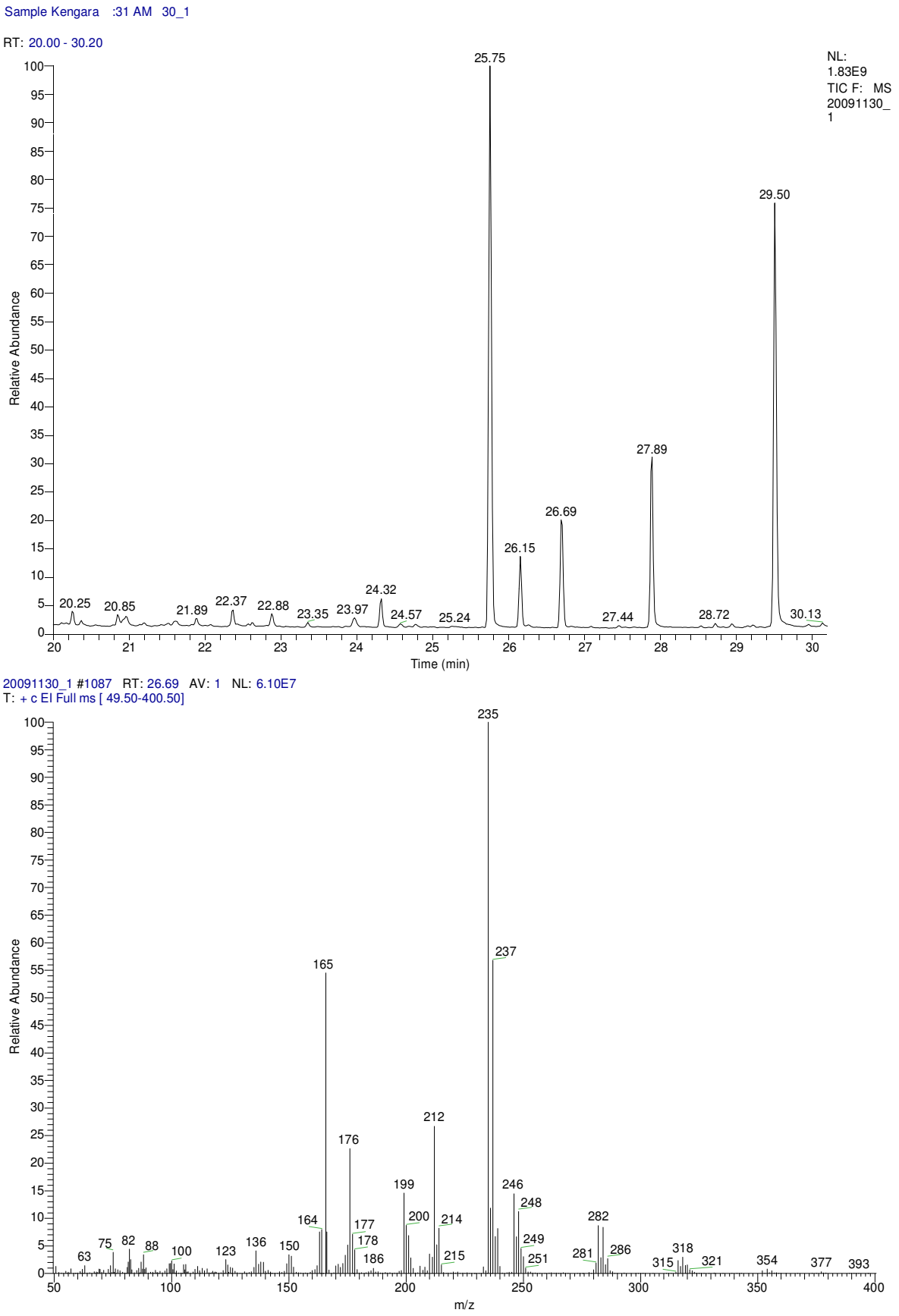

Figure A7: GC-MS analysis of p,p-DDT standard in SIM mode

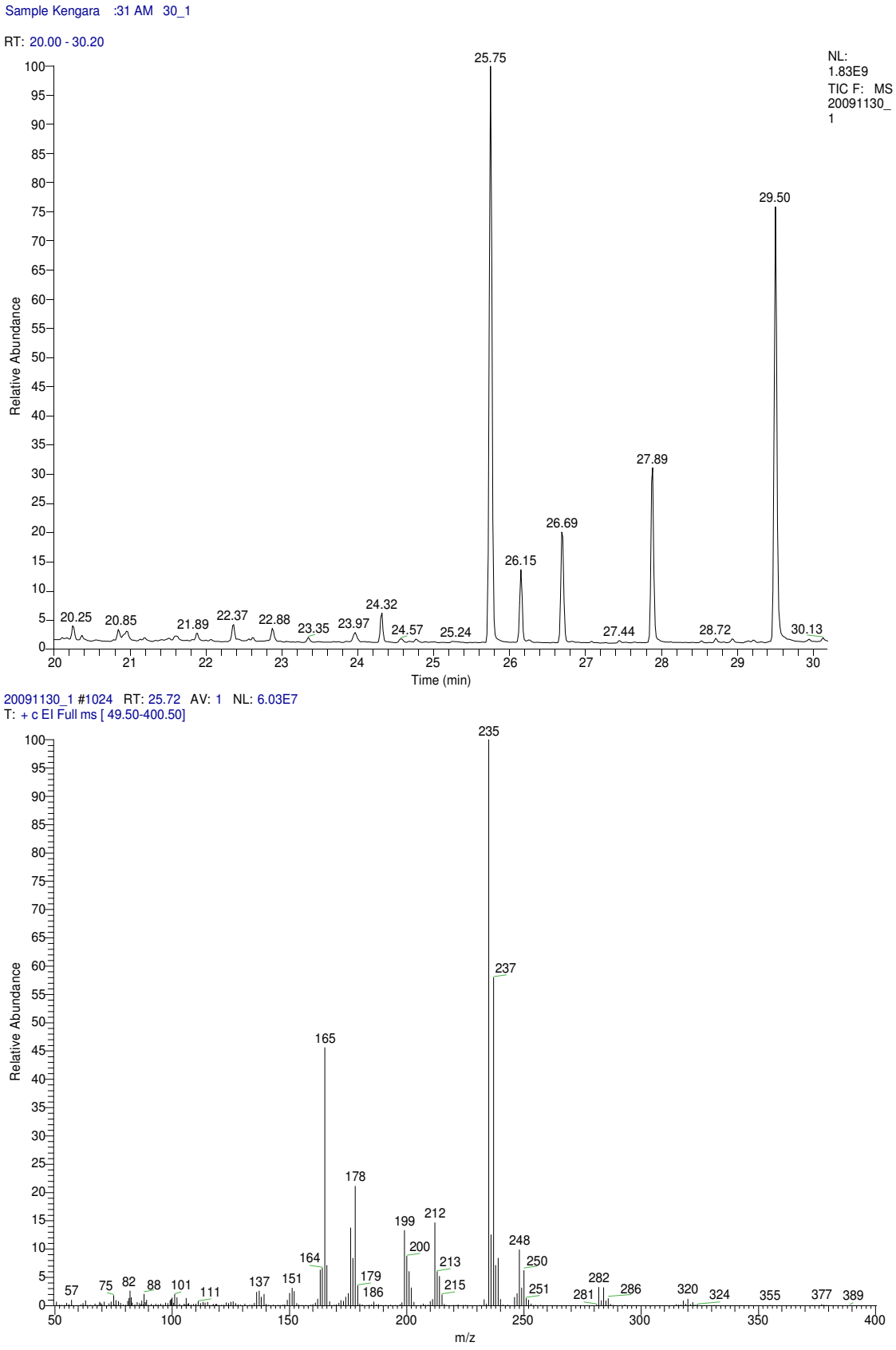

Figure A8: GC-MS analysis of p,p-DDD standard in SIM mode

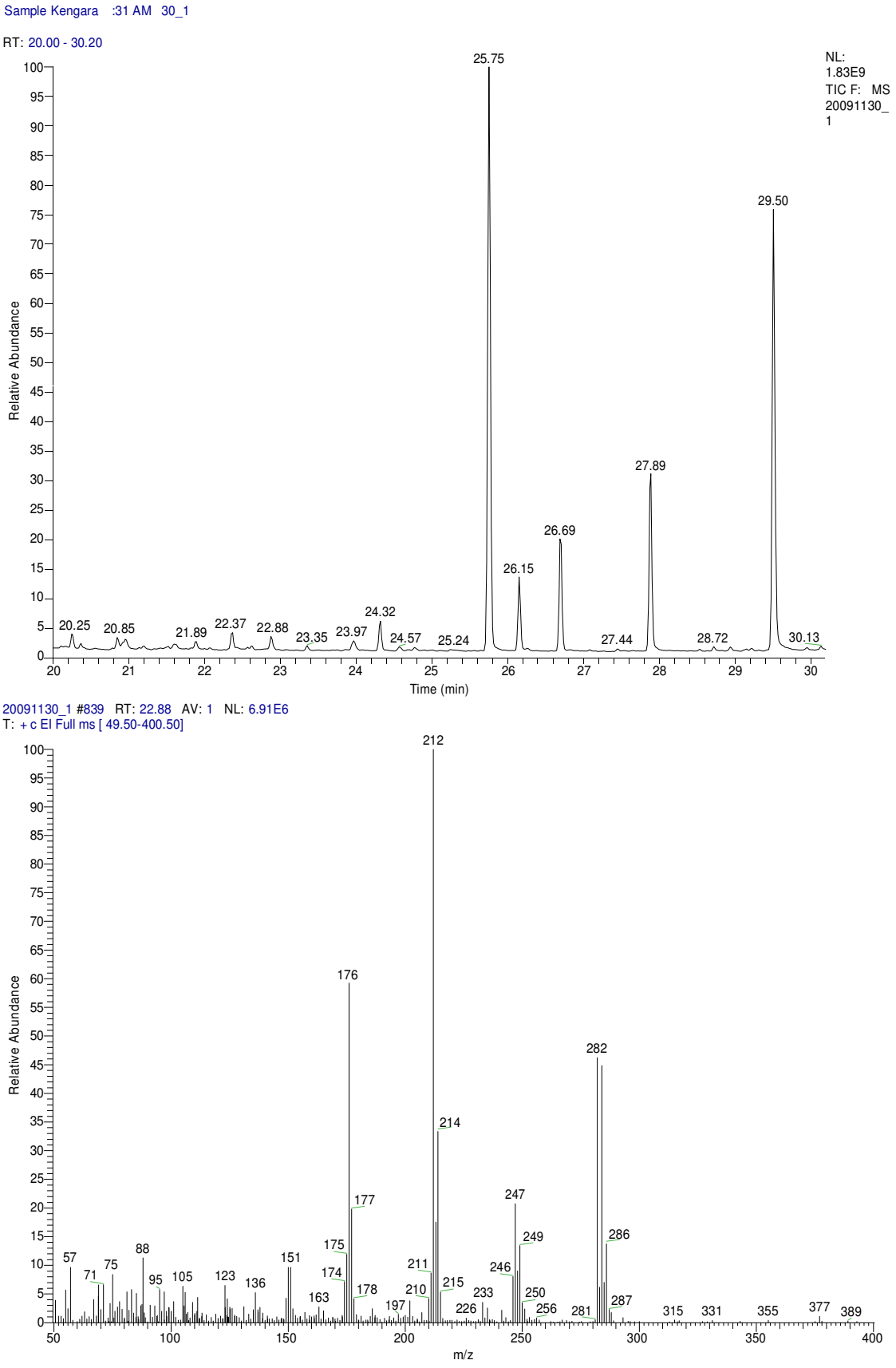

Figure A9: GC-MS analysis of p,p-DDMU standard in SIM mode

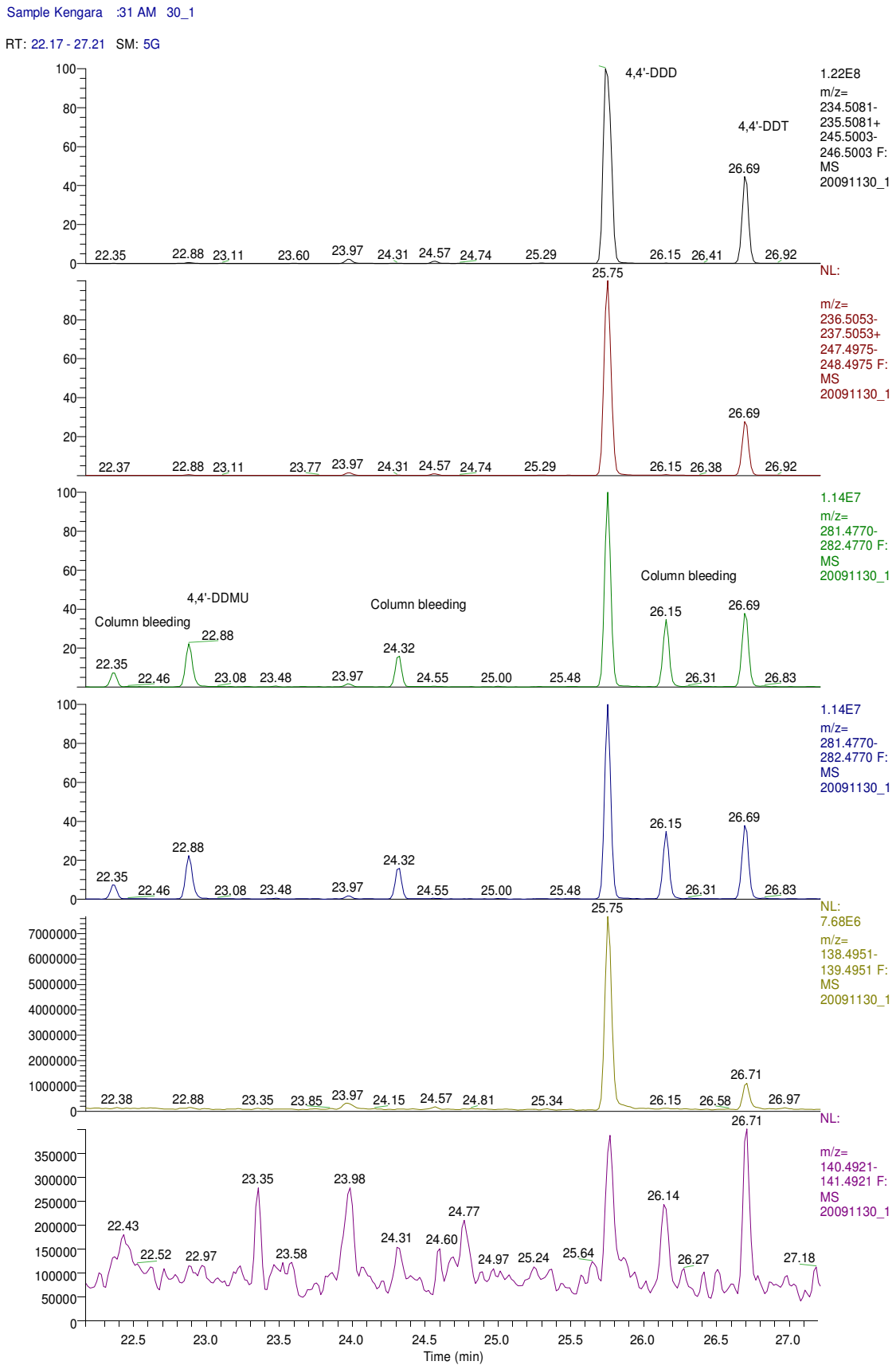

Figure A10: GC-MS full scan of a sample from the DDT anaerobic degradation experiment.

Table A1: Data used to generate Fig. 37 {HCB metabolites concentrations (µg/g soil) in the paddy soil samples during the anaerobic-aerobic cycles incubation experiment}

Day	0	38	86	109	253	356	405	461
PCB_PS	0	0.38±0.068	6.94±3.785	11.20±5.945	4.04±2.014	7.73±4.014	9.06±5.303	4.10±2.197
PCB_PSC	0	0.40±0.058	12.00±1.118	12.70±0.977	4.75±1.253	9.19±1.847	13.10±3.855	6.37±2.096
1,3,5-TCB_PS	0	0	0.41±0.120	1.27±1.120	1.79±1.036	7.75±1.295	7.89±1.442	2.43±0.405
1,3,5_TCB-PSC	0	0	0.54±0.374	0.56±0.518	0.95±0.659	7.32±1.118	9.39±2.315	2.86±0.531
CB_PS	0	0	0	0	0	0.69±0.115	2.11±0.162	0.46±0.123
CB_PSC	0	0	0	0	0	0.87±0.076	2.81±0.240	0.78±0.166
1,4-DCB_PS	0	0	0	0	0	0.49±0.593	0.32±0.263	0.18±0.185
1,4_DCB-PSC	0	0	0	0.63±1.018	0	1.51±0.421	0.33±0.349	0.11±0.020
1,2-DCB_PS	0	0	0	0	0	2.66±0.763	0.07±0.044	0.03±0.012
1,2_DCB-PSC	0	0	0	0	0	2.11±0.385	0.06±0.065	0.02±0.010
1,2,4-TCB_PS	0	0	0.06±0.003	0.11±0.049	0.10±0.024	0.28±0.060	0.24±0.058	0.13±0.057
1,2,4_TCB-PSC	0	0	0.05±0.008	0.09±0.043	0.08±0.026	0.34±0.092	0.47±0.036	0.19±0.111
1,2,3-TCB_PS	0	0	0	0.03±0.010	0.01±0.001	0.07±0.012	0.05±0.021	0.01±0.005
1,2,3_TCB-PSC	0	0	0	0.03±0.014	0.01±0.002	0.10±0.042	0.05±0.008	0.04±0.003
1,2,3,5-TCB_PS	0	0	0.22±0.050	0.43±0.076	0.24±0.051	0.28±0.044	0.36±0.081	0.14±0.051
1,2,3,5-TCB_PSC	0	0	0.21±0.047	0.29±0.071	0.24±0.030	0.20±0.024	0.35±0.075	0.20±0.048
1,2,3,4-TCB_PS	0	0	0.14±0.031	0.23±0.032	0.10±0.034	0.08±0.023	0.07±0.038	0.03±0.013
1,2,3,4-TCB_PS	0	0	0.10±0.035	0.18±0.037	0.17±0.019	0.18±0.036	0.19±0.053	0.08±0.033

PS = Paddy soil, PSC = Paddy soil + compost

Table A2: Data used to generate Fig. 38 {HCB metabolites concentrations (µg/g soil) in the field soil samples during the anaerobic-aerobic cycles incubation experiment}

	0	38	86	109	253	356	405	461
CB_FS	0	0	0	0	0	0.42±0.027	1.00±0.096	0.52±0.299
CB_FSC	0	0	0	0	0	0.48±0.072	1.29±0.136	0.91±0.161
1,4-DCB_FS	0	0	0	0	0	0.09±0.045	1.93±0.360	1.12±0.494
1,4_DCB-FSC	0	0	0	0	0	0.18±0.099	3.75±1.020	3.06±0.389
1,2-DCB_FS	0	0	0	0	0	0.09±0.073	0.03±0.018	0.05±0.050
1,2_DCB-FSC	0	0	0	0	0	0.16±0.068	0.38±0.143	0.06±0.022
1,3,5-TCB_FS	0	0	0	0	0	1.49±0.132	0.89±0.611	0.26±0.081
1,3,5_TCB-FSC	0	0	0	0	0	2.83±1.114	1.53±1.233	0.94±1.381
1,2,4-TCB_FS	0	0	0.05±0.009	0.06±0.008	0	0.03±0.003	0.07±0.083	0.01±0.003
1,2,4_TCB-FSC	0	0	0.06±0.009	0.06±0.013	0	0.32±0.062	0.27±0.144	0.11±0.023
1,2,3-TCB_FS	0	0	0	0	0.10±0.064	0.15±0.061	0.01±0.002	0.02±0.003
1,2,3_TCB-FSC	0	0	0	0.02±0.028	0	0.15±0.023	0.02±0.003	0.02±0.006
1,2,3,5-TCB_FS	0	0	0	0	0.01±0.007	0.07±0.051	0.09±0.060	0.03±0.048
1,2,3,5-TCB_FSC	0	0	0	0	0.01±0.013	0.11±0.032	0.14±0.051	0.04±0.04
1,2,3,4-TCB_FS	0	0	0	0	0	0.02±0.014	0.07±0.030	0.01±0.006
1,2,3,4-TCB_FS	0	0	0	0	0	0.06±0.015	0.03±0.007	0.02±0.013
PCB_FS	0	0.14±0.083	0.21±0.079	0.28±0.094	0.30±0.219	1.29±0.955	1.12±1.011	1.35±1.195
PCB_FSC	0	0.07±0.035	0.27±0.154	1.30±0.982	0.83±0.491	1.77±1.412	1.45±0.718	1.51±0.964

FS = Field soil, FSC = Field soil + compost

Table A3: Data used to generate Fig. 55 {Concentrations of DDT and its metabolite (µg/g soil) in the paddy soil samples during the anaerobic-aerobic cycles incubation experiment}

	0	32	70	98	229	319	384	440
p,p-DDT-PS	30.00±0	13.7±2.153	2.67±0.314	6.22±0.924	3.75±0.991	1.17±1.210	1.04±0.616	2.25±0.449
p,p-DDT-PSC	30.00±0	12.3±0.518	2.24±0.389	5.38±0.939	4.74±0.634	1.00±1.112	0.50±0.489	0.69±0.776
o,p-DDT-PS	0	0	0.01±0.000	0	0	0.01±0.001	0.01±0.003	0
o,p-DDT-PSC	0	0	0.01±0.000	0	0	0.01±0.001	0.01±0.003	0
p,p-DDD-PS	0	8.11±1.266	10.20±0.751	6.97±3.790	3.09±0.173	13.8±02.555	10.50±3.645	7.01±1.759
p,p-DDD-PSC	0	6.80±0.510	9.94±1.551	9.43±1.120	3.75±0.352	16.40±3.737	11.30±2.048	5.78±1.442
o,p-DDD-PS	0	0.08±0.021	0.10±0.009	0.15±0.025	0.11±0.014	0.13±0.051	0.10±0.042	0.08±0.029
o,p-DDD-PSC	0	0.07±0.005	0.09±0.006	0.15±0.048	0.16±0.056	0.15±0.065	0.09±0.004	0.06±0.024
p,p-DDE-PS	0	0.12±0.024	0.17±0.011	0.11±0.049	0.12±0.005	0.20±0.044	0.14±0.051	0.25±0.019
p,p-DDE-PSC	0	0.11±0.022	0.16±0.005	0.12±0.038	0.16±0.050	0.21±0.078	0.12±0.021	0.24±0.022
o,p-DDD-PS	0	0	0.18±0.035	0	0.01±0.015	0	0.13±0.038	0.05±0.033
o,p-DDD-PSC	0	0	0.14±0.006	0	0.01±0.015	0	0.07±0.043	0
p,p-DDMU-PS	0	1.87±0.477	1.03±0.123	4.17±0.863	5.10±0.259	9.20±4.720	5.68±2.688	5.53±1.834
p,p-DDMU-PSC	0	1.43±0.247	1.28±0.244	3.93±1.263	7.14±2.696	10.00±4.630	5.00±2.270	5.15±1.713
p,p-DDM-PS	0	0.10±0.097	0.03±0.005	0.13±0.047	0.10±0.017	0.02±0.002	0.08±0.074	0.04±0.009
p,p-DDM-PSC	0	0.03±0.005	0.03±0.006	0.13±0.034	0.10±0.011	0.07±0.036	0.04±0.004	0.05±0.029

PS = Paddy soil, PSC = Paddy soil + compost

Table A4: Data used to generate Fig. 56 {Concentrations of DDT and its metabolite (µg/g soil) in the field soil samples during the anaerobic-aerobic cycles incubation experiment}

	0	32	70	98	229	319	384	440
p,p-DDT-FS	30.00±0	19.9±0.677	16.10±0.461	11.80±0.993	6.77±0.722	0.62±0.746	0.88±0.384	0.80±1.088
p,p-DDT-FSC	30.00±0	19.50±0.501	9.59±0.496	9.39±0.755	5.14±0.711	0.26±0.855	0.73±0.159	1.81±1.080
o,p-DDT-FS	0	0.02±0.000	0.01±0.001	0.02±0.000	0	0.01±0.001	0.01±0.001	0
o,p-DDT-FSC	0	0.03±0.000	0.01±0.001	0.01±0.000	0	0.01±0.001	0.01±0.000	0
p,p-DDD-FS	0	3.00±0.255	4.94±2.302	4.03±2.924	1.64±0.247	9.11±6.911	5.40±3.686	5.42±1.616
p,p-DDD-FSC	0	2.56±0.133	4.95±0.461	4.98±3.313	1.45±0.497	4.64±1.641	6.43±1.613	8.24±1.079
o,p-DDD-FS	0	0.03±0.000	0.09±0.005	0.04±0.021	0.03±0.005	0.11±0.036	0.07±0.016	0.06±0.019
o,p-DDD-FSC	0	0.03±0.002	0.08±0.003	0.08±0.019	0.05±0.007	0.06±0.014	0.06±0.008	0.06±0.014
p,p-DDE-FS	0	0.51±0.068	0.66±0.133	0.79±0.156	0.90±0.084	1.23±0.466	0.97±0.414	2.50±0.391
p,p-DDE-FSC	0	0.42±0.065	0.34±0.034	0.42±0.213	0.48±0.193	0.44±0.238	0.68±0.172	2.17±0.474
o,p-DDD-FS	0	0	0.12±0.010	0	0	0	0	0
o,p-DDD-FSC	0	0	0.10±0.006	0	0	0	0	0
p,p-DDMU-FS	0	0.88±0.179	1.15±0.386	2.82±0.924	6.78±0.800	20.20±4.630	9.90±2.119	9.29±3.079
p,p-DDMU-FSC	0	0.82±0.157	0.95±0.037	3.10±0.449	4.09±1.297	5.92±1.941	7.20±1.513	10.20±3.398
p,p-DDM-FS	0	0	0	0.44±0.059	0.03±0.004	0.03±0.010	0.04±0.003	0.02±0.028
p,p-DDM-FSC	0	0.01±0.013	0	0.42±0.113	0.03±0.005	0.05±0.030	0.04±0.003	0

FS = Field soil, FSC = Field soil + compost

Table A5: Data used to generate Fig. 63 {Concentrations of DDT and its metabolite (µg/g soil) in the paddy soil samples during the incubation experiment under anaerobic conditions}

	0	1	2	3	4	5	6	8
p,p-DDT-PS	30.00±0	10.64±1.268	9.29±2.380	9.36±0.936	9.50±1.534	6.11±3.557	10.60±1.614	6.85±1.629
p,p-DDT-PSC	30.00±0	11.47±3.933	11.60±1.966	8.30±0.972	10.60±1.761	8.22±3.134	11.20±2.065	8.49±1.434
o,p-DDT-PS	0	0	0.25±0.064	0.24±0.174	0.02±0.008	0	0	0
o,p-DDT-PSC	0	0	0.67±0.473	0.25±0.257	0.01±0.011	0.01±0-014	0	0
p,p-DDD-PS	0	2.63±1.289	4.44±2.344	5.46±1.804	8.97±1.298	9.23±1.254	11.50±5.171	9.79±0.942
p,p-DDD-PSC	0	5.29±3.098	6.55±2.560	5.62±0.474	9.36±1.385	11.10±1.329	13.00±1.44	10.60±0.912
o,p-DDD-PS	0	0.04±0.039	0.05±0.017	0.04±0.018	0.06±0.012	0.05±0.004	0.08±0.013	0.14±0.023
o,p-DDD-PSC	0	0.07±0.035	0.06±0.053	0.04±0.006	0.07±0.018	0.06±0.010	0.07±0.003	0.18±0.040
p,p-DDE-PS	0	0.26±0.166	0.72±0.219	0.23±0.082	0.38±0.076	0.19±0.119	0.20±0.074	0.69±0.044
p,p-DDE-PSC	0	0.92±0.059	0.42±0.183	0.18±0.039	0.42±0.059	0.26±0.083	0.22±0.056	0.77±0.114
o,p-DDE-PS	0	0.01±0.027	0.01±0.030	0	0	0.04±0.049	0.07±0.047	0.05±0.063
o,p-DDE-PSC	0	0.02±0.038	0	0	0	0.02±0.043	0	0.07±0.050
p,p-DDMU-PS	0	1.27±0.162	2.29±0.981	2.70±0.471	3.99±0.199	4.03±0.512	7.45±1.824	9.83±1.321
p,p-DDMU-PSC	0	2.94±0.590	2.98±1.540	2.90±0.852	3.94±0.487	4.66±0.099	9.23±0.880	11.60±2.939
p,p-DDM-PS	0	0.43±0.454	0.56±0.202	0.25±0.145	0.21±0.057	0.46±0.276	0.21±0.026	0.67±0.466
p,p-DDM-PSC	0	0.72±0.214	0.44±0.143	0.15±0.049	0.13±0.025	0.52±0.412	0.30±0.038	0.49±0.206

PS = Paddy soil, PSC = Paddy soil + compost

Table A6: Data used to generate Fig. 64 {Concentrations of DDT and its metabolite (µg/g soil) in the field soil samples during the incubation experiment under anaerobic conditions}

	0	1	2	3	4	5	6	8
p,p-DDT-FS	30.00±0	10.20±0.594	13.40±0.744	9.46±3.873	9.55±3.014	4.84±2.395	3.77±1.697	6.62±1.462
p,p-DDT-FSC	30.00±0	10.80±1.690	10.00±1.235	6.63±3.535	6.68±1.415	5.52±1.604	2.97±0.545	5.03±0.292
o,p-DDT-FS	0	0	0.45±0.022	0.69±0.090	0.03±0.024	0.05±0.115	0	0
o,p-DDT-FSC	0	0	0.35±0.310	0.73±0.760	0.01±0.018	0	0	0
p,p-DDD-FS	0	2.91±0.706	6.72±2.788	5.35±2.249	8.97±4.045	10.7±4.513	12.60±3.126	8.87±0.776
p,p-DDD-FSC	0	6.21±2.499	6.42±2.156	7.12±0.859	10.00±1.361	13.30±1.906	14.50±1.368	9.88±0.364
o,p-DDD-FS	0	0.06±0.008	0.11±0.036	0.04±0.021	0.08±0.054	0.06±0.034	0.07±0.024	0.13±0.051
o,p-DDD-FSC	0	0.08±0.069	0.06±0.066	0.04±0.029	0.07±0.023	0.07±0.030	0.08±0.011	0.18±0.019
p,p-DDE-FS	0	0.32±0.043	0.51±0.116	0.12±0.055	0.21±0.180	0.17±0.043	0.23±0.102	0.26±0.114
p,p-DDE-FSC	0	0.48±0.352	0.37±0.170	0.21±0.023	0.21±0.104	0.17±0.035	0.15±0.031	0.38±0.071
o,p-DDE-FS	0	0.28±0.033	0.04±0.051	0	0	0.10±0.110	0	0.06±0.022
o,p-DDE-FSC	0	0.40±0.568	0.05±0.062	0	0.02±0.033	0.05±0.057	0	0.07±0.046
p,p-DDMU-FS	0	1.21±0.345	2.87±0.903	1.22±0.474	2.60±1.256	1.56±0.917	2.09±0.380	4.31±1.527
p,p-DDMU-FSC	0	2.73±1.411	3.77±0.908	2.22±0.428	3.04±0.736	1.91±0.722	2.81±0.327	7.58±0.835
p,p-DDM-FS	0	0.11±0.003	0.10±0.014	0.14±0.074	0.12±0.016	0.28±0.178	0.21±0.010	0.78±0.195
p,p-DDM-FSC	0	0.11±0.020	0.13±0.049	0.18±0.122	0.16±0.109	0.31±0.358	0.16±0.108	0.61±0.091

FS = Field soil, FSC = Field soil + compost